University of Nottingham

Institute of Engineering Surveying and Space Geodesy

Advantages and Problems of Combining GPS with GLONASS

by

John W. Swann, B.Sc.(Hons.)

Thesis submitted to the University of Nottingham

for the degree of Doctor of Philosophy

October 1999

Table of Contents

4 Satellite Observables, Positioning Principles and Techniques

5 Software Development and Validation

6 Applications of GPS/GLONASS Positioning

7 Real Time Kinematic Positioning for Setting Out

Appendix C Satellite Availabilities

Appendix D Traverse Computation

List of Figures

5 Software Development and Validation

6 Applications of GPS/GLONASS Positioning

7 Real Time Kinematic Positioning for Setting Out

List of Tables

2 The GPS and GLONASS Systems

5 Software Development and Validation

List of Plates

6 Applications of GPS/GLONASS Positioning

7 Real Time Kinematic Positioning For Setting Out

Abstract

The Global Positioning System (GPS) has been an undoubted success and a great many applications have benefited from it. It does however have limitations, which make its use in certain environments, and for certain tasks, difficult or indeed impossible. In recent years a second satellite based navigation system, the Global'naya Navigatsionnaya Sputnikov Sistema (GLONASS) has become increasingly available. A great deal of interest has been expressed in combining both these systems, in the hope that combined GPS/GLONASS technology will present significant benefits under conditions where GPS alone has struggled.

The research described in this thesis was undertaken to examine the potential benefits and problems of such a combination. This has been primarily achieved through the modification of the existing GPS processing software of the Institute of Engineering Surveying and Space Geodesy (IESSG) to accept GLONASS observations.

The analysis of data collected under controlled conditions and processed through this software has highlighted biases in the pseudorange measurements from the GLONASS satellites. This is due to the fact that each GLONASS satellite broadcasts on a different frequency, which is then delayed by slightly different amounts through the Radio Frequency (R/F) section of the receiver. If these R/F sections were identical in each receiver, this error source would cancel, but this has not been found to be the case with the receivers used in this research. Interestingly, no such biases have found to be present in the GLONASS carrier phase observations.

Various tests have been performed and the data processed through both IESSG and commercially available software. These have highlighted that there are undoubted potential benefits of using combined GPS/GLONASS receivers in environments where visibility is restricted. Under ideal conditions however,

the effect of any benefit is reduced, and indeed the biases present in the GLONASS pseudoranges may slightly degrade the accuracy of differential positioning.

The software developed has already been used in other research projects within the IESSG. Although the future of the GLONASS system is somewhat uncertain, any future changes to it should be easily accounted for within the code. There is however a real need to further develop and incorporate cycle slip detection software, especially for GLONASS observations, and to investigate the possibility of solving for the biases in the GLONASS pseudoranges.

Acknowledgements

The research that lead to the production of this thesis was undertaken within the Institute of Engineering Surveying and Space Geodesy (IESSG), which is part of the School of Civil Engineering at The University of Nottingham. The Engineering and Physical Science Research Council (EPSRC) funded the work.

I would like to thank both the past and present Directors of the IESSG, Professors V. Ashkenazi and A.H. Dodson for the opportunity of performing this research. I would also like to thank my supervisor Dr. T. Moore, for his continued help and advice throughout this project.

The development of existing software was a major part of this project and I would therefore like to thank the original authors of this code. Special thanks are also due to Dr. W. Chen, Dr. N. Penna, Dr. G. Ffoulkes-Jones and Dr. M. Stewart for their advice on software development.

It would have been impossible to perform the field trials without the help of Mr. K. Gibson, Mr. A. Nesbitt and Mr. D. Russell, for which I am grateful. I would also like to thank Dr. G. Roberts for the data collected at the Humber Bridge. Many thanks to Dr. T. Moore, Dr. N. Penna, Dr. M. Aquino and Mr. K. Gibson for the proof reading of this thesis.

I would also like to say a special thankyou to the friends I have made in Nottingham - they have made the last three years an enjoyable experience. I must also apologise to those whom have been the recipients of the occasional and completely accidental miss-timed tackles, which I have been known to commit, in our many *friendly* games of football.

Finally, I would like to thank my mother and father for their help and encouragement over the years, and to mention Lesta Swann who unfortunately

passed away in the summer of 1998. She was much more than an aunt to my brother, sister and myself, and is greatly missed by us all.

"Nothing in the world can take the place of persistence.
Talent will not: nothing is more common than unsuccessful men with talent.
Genius will not: unrewarded genius is almost a proverb.
Education will not: the world is full of educated derelicts.
Persistence and determination alone are omnipotent."

Chay Blyth (First man to row the Atlantic).

Chapter 1

Introduction

The Global Positioning System (GPS) has, since its inception in 1978, been the subject of intensive research and development by numerous academic and commercial organisations throughout the world. As a result of this work, an almost unlimited number of previously unthought of applications have found uses for this technology. For example, mariners can use GPS to navigate both in the open ocean and confined harbour environments, surveyors can measure positions to millimetre accuracies, and farmers can use it to guide their machinery. However, in recent years the pace of this development has slowed as the potential of the GPS system as it stands is reached. Restrictions on the availability, accuracy, and integrity of position solutions limit the sole use of GPS, and in scenarios such as aircraft landings, make it an unacceptable proposition.

Interestingly, a second satellite based navigation system called the 'Global'naya Navigatsionnaya Sputnikova Sistema' (GLONASS) has, since the

mid 1990's, become increasing available for commercial use. If used alone, as a rival to GPS, then GLONASS would suffer from the same limitations as mentioned above, as it shares a number of the characteristics of GPS. However, when both systems are combined, a great many of these problems are overcome, or at least their effects greatly reduced.

The first area of potential improvement is that of solution availability. As will be explained in Chapter 4, the minimum requirement of simultaneously visible satellites, using GPS, to obtain an autonomous three-dimensional position is four, and for real-time on-the-fly centimetre accuracy positioning, this rises to five. Now, under ideal conditions for satellite positioning i.e. unobstructed views of the sky, this is not a problem, as there are usually seven or more GPS satellites visible at any one time. However, in a great many environments this is not always the case. For example, in open cast mines, urban environments, forested areas and valleys, large parts of the sky may be obscured, and thus the number of in-view satellites will be reduced. If the number of satellites falls below the numbers outlined above, the result will be an inability to compute a position. Clearly, the addition of the extra satellites, which the GLONASS constellation offers, will significantly increase the availability of the system, even though there is the need for an additional satellite in a combined solution (Chapter 4). In all environments these extra satellites will also strengthen the geometry of the visible constellation, and position accuracy, which is a function of geometry, should also be improved. Finally, when considering centimetre level positioning, the time taken to reach this level is again dependent on the number of visible satellites, so a combined GPS/GLONASS system should reach these higher accuracies more quickly than GPS alone.

Integrity is the term given to the ability of the system to warn the user that the derived position is in error. While this is no doubt of benefit, it would be more desirable that the system could not only warn the user, but also provides the correct solution. With GPS it takes a minimum of five satellites to detect a potential problem, and a sixth satellite to be able to isolate and remove a single satellite failure. Even with its full design specification of twenty-four satellites,

GPS cannot fulfil this requirement at all points on the Earth's surface, twenty-four hours a day. As with the issue of availability, extra GLONASS satellites will improve this situation, and in addition will bring an added advantage of being a totally independent system, providing a check of the GPS system as a whole.

The final issue is that of the position accuracy achievable using the systems. GPS is capable of a stand-alone (autonomous) position accuracy in the region of 20 metres, but this is denied to all but a few authorised/military users by a processes called Anti-Spoofing (A/S) and Selective Availability (S/A) (Chapter 2). A civilian user, using authorised codes, can expect to obtain a stand-alone position accurate to within 100 metres of the true position 95% of the time. Because GLONASS is not subjected to the same restrictions, combining the observations of both systems with appropriate weighting returns accuracies to the 20 metre level. While this represents a significant improvement, it still remains unacceptable for applications such as hydrographic surveying, which requires accuracies under 5 metres. Differential GPS and differential GPS/GLONASS have been designed to meet this requirement by calculating a set of corrections at a receiver located over a known point, and broadcasting them to the user. However, as S/A is a rapidly varying error source, these corrections need to be updated regularly if this level of positioning is to be maintained. Again, this is not the case with GLONASS.

With potential benefits such as these, and with an ever increasing number of GPS/GLONASS receivers becoming available, research ranging from hardware design and fabrication, through to algorithm development, has been undertaken by numerous research institutions, many of which have a history of work with other satellite based positioning systems.

The IESSG (Institute of Engineering Surveying and Space Geodesy) of the University of Nottingham, has been involved in various aspects of satellite based positioning and navigation, dating back to the days of the Transit system. However, up until the commencement of this project in October 1996, it had

no experience with the GLONASS system. The aim of this research was therefore to ascertain the potential advantages, problems and issues affecting GLONASS, and more particularly combined GPS/GLONASS positioning. Over the previous decade a comprehensive suite of GPS processing software, collectively called GPS Analysis Software (GAS), had been developed within the University as a result of previous research projects and dedicated programming. It was decided that the bulk of the project time available should be allocated to the alteration of this processing suite to accept combined GPS and GLONASS data. This process would highlight any difficulties in combining the systems, enable different and novel processing strategies to be investigated and validated, allow peculiarities of the GLONASS system to be examined, and create a means by which the potential benefits of the combined system could be quantified. Future research projects could also possibly benefit from the ability to freely process both GPS and GLONASS observations. The objectives of the research can be summarised as:

- Modify existing software, and where necessary develop new software and processing strategies to enable combined GPS/GLONASS data to be processed within GAS.

- Validate the alterations made to the software through controlled tests, and quantify the relative performance of the systems for various means of positioning.

- Evaluate the potential benefits of combining GPS with GLONASS in actual applications.

In addition to this, the data gathered during these experiments has also been processed with the latest processing packages developed by the receiver manufacturers. This not only serves as a check on the results obtained using the modified software, but also quantifies the achievable benefits that can be

expected if combined GPS/GLONASS receivers are used in commercial environments.

Throughout the project L1 only data has been used (Chapter 2), as it is all that has been available from the two Ashtech GG-24 receivers that the University of Nottingham presently owns. However further modifications necessary for L1/L2 GPS/GLONASS processing are minimal and thus, should the University acquire in the future, dual frequency GPS/GLONASS receivers, data from these should still be able to be processed. The achievements and main conclusions of the project can be summarised as follows:

- The GAS software has been successfully altered to process combined GPS/GLONASS data to give stand-alone pseudorange, differential pseudorange, float carrier phase and fixed carrier phase solutions.

- Difficulties with the GLONASS pseudorange data were discovered, explained, and accounted for in the processing strategies.

- The potential benefits of combined GPS/GLONASS use, for various applications, have been quantified. From this it can be seen that there are undoubted benefits with combined solutions for autonomous positioning and all forms of positioning in areas of restricted visibility. However, for static, geodetic type surveying it appears that the benefits are less apparent. Indeed much better results were achieved in these environments using GPS L1/L2 observations.

Chapter 2 outlines the concepts and history of both the GPS and GLONASS systems, and reference is also made to forthcoming changes. This is followed in Chapter 3 by a detailed description of the differences existing between the systems that must be accounted for if successful combination is to be achieved. A short description of the International GLONASS EXperiment (IGEX-98)

campaign, which was implemented to provide some solutions to these problems, is also given. Chapter 4 then presents a review of error sources, measurements, observables and different positioning techniques, optimised for GPS/GLONASS where necessary. The development and validation of a combined GPS/GLONASS software suite is discussed in Chapter 5. Trials to quantify the potential benefits of GPS/GLONASS in both a Kinematic and Static application have been performed and are detailed in Chapter 6, with results obtained from both commercially available software, and that developed in Nottingham given. Chapter 7 presents the results of a series of tests performed specifically to look at potential benefits in Real Time Kinematic (RTK) applications. Finally, Chapter 8 summarises the research work carried out by the author, with the presentation of conclusions and suggestions for future work on the subject.

Chapter 2

The GPS and GLONASS Systems

2.1 Introduction to Navigation

Records dating back as far as 1100 BC detail the importance of navigation in the exploration of new worlds, as the Phoenicians sailed through the Straits of Gibraltar to Cornwall and Madeira by means of the stars [ETG, 1998]. Some 900 years later Greek mathematicians approximated the Earth's radius from solar readings, and in so doing introduced the concept of latitude. Over the centuries a great deal of effort was made to further improve and refine these navigational techniques which still held as a basis celestial observations. While perfectly able to determine latitude from such measurements, accurate longitude calculation was not possible, and so throughout the great ages of exploration it could be said that sailors were quite literally lost at sea. With thousands of lives and the increasing fortunes of nations dependent on a successful resolution, 'the Longitude Problem' quickly became the scientific Holy Grail [Sobel, 1996]. Finally, in 1761 a

successful solution was reached when a clock maker called Harrison invented the 'Chronometer'. Position could now finally be determined anywhere on the planet with some degree of accuracy, some 3000 years after the first crude attempts were made.

Thankfully the pace of advancement since the turn of the century has been somewhat more rapid. Opportunities created by scientific breakthroughs have been adapted to fulfil various navigational requirements, especially those of warfare. The most notable of these is the use of developments made in the fields of electronics and electromagnetics, which has opened up a whole new field of navigation since 1930, when the first local radio positioning system became operational. The concept is simple, with electromagnetic waves being emitted from antennas at known positions and then being received and evaluated at the unknown location. Successive systems brought improvements in accuracy and range. With the launch of the space age and the requirement for global positioning the obvious step was to use highly visible artificial satellites as beacons, and hence the era of satellite navigation was born.

2.2 The History of Satellite Navigation

Shortly after the launch of the first artificial satellite, the soviet 'Sputnik I', in 1957, scientists at the Applied Physics Laboratory of the Johns Hopkins University quickly found that the position of the satellite could be determined by measuring the Doppler shift of its signals at ground points with known coordinates. Inverting this principle meant that it would also be possible to coordinate a point on the ground by receiving satellite signals, provided that the position of the satellite was known.

The first worldwide navigation satellite system was 'Transit', which became operational in 1964 and was released for civilian use in 1967. Although developed by the United States Department of Defense (USDoD) to position its 'Polaris'

submarines, it quickly became popular amongst surveyors and geodesists for the establishment of widely spaced network stations. In 1965 the Soviet equivalent called 'Tsikada' was put into operation, but unsurprisingly did not gain any popularity in the West, as it was never formally released from military control, although its message structure was successfully decoded and published.

Both systems shared a great many similarities and therefore suffered from the same drawbacks. Firstly, they were inherently two-dimensional. Secondly, the velocity of the user had to be accounted for, and finally, mutual interference between satellites restricted their total number, and resulted in the satellite's only being visible for limited periods, giving discontinuous operation.

These systems marked the first generation of this new technology and proved the viability of the concept. However the problems outlined above placed a great many limitations on operational capabilities, especially for real time navigation, and heralded the design of new, improved systems.

2.3 The Global Positioning System

NAVSTAR GPS is an acronym for NAVigation Satellite Timing And Ranging Global Positioning System, and is commonly abbreviated to GPS. It is a space based radio navigation system developed by the USDoD to provide instantaneous, worldwide, all-weather single point positioning. Two positioning services are provided, the Precise and Standard Positioning Services (PPS and SPS respectively). The PPS is designated for military and authorised users only, with a 2drms (twice the distance root mean square) plan accuracy of 17.6 metres, whilst the SPS is available to all users with plan accuracies of 100 metres at 2drms [DoD/DoT, 1990].

Early satellite systems suffered from many limitations (Section 2.2), and it was with these in mind that development of the system began in 1972 with the creation

of the Joint Program Office (JPO). This brought together ideas from three existing satellite systems to match the positioning requirements of the USDoD outlined above. These systems were the US Navy's Transit, a Doppler positioning system, and two development projects: the Navy Research Laboratory's precise time and time transfer project Timation and the US Air Force's 621B project. Properties of all three of these systems were incorporated in the design of GPS.

GPS can conveniently be divided into three parts or segments: the space segment, the control segment and the user segment. These categories are used when describing the system in the following sections. Its signal structure and navigation message, are also examined and the current constellation detailed, as these are important areas when comparing GPS with GLONASS.

2.3.1 The Space Segment

Position is determined using GPS by a form of intersection, with the user measuring ranges to known points, the satellites themselves. In order to calculate a three-dimensional position, four unknowns must be solved for (Chapter 4). These unknowns are the three coordinate components and the error within the receiver's low-cost internal clock with respect to system time. It therefore follows that a minimum of four satellites must be observed simultaneously if a position is to be derived. The satellite constellation was designed to satisfy this requirement at any point on the Earth, at any time.

Initially the design specification of the system was for a constellation of twenty-four satellites plus three active spares orbiting the Earth at a nominal altitude of 20,200 km with a period of approximately 11 hours 58 minutes (2 orbits = 1 sidereal day). However budgetary restrictions produced a series of changes to this, finally leading to the present constellation specification of twenty-one plus three active spares. These satellites are placed in six orbital planes (four satellites

unevenly spaced in each plane), which are equally spaced around the equator and have an inclination of 55 degrees to the equatorial line.

The first GPS satellite was launched in February 1978 and was labelled to have 'research and development' status. Over the next seven years a further nine of these Block I satellites were successfully launched, and these were used to test and further develop the system. The second generation of satellites, called Block II, began being launched in February 1989, and unlike the earlier Block I satellites, these were deemed to be 'operational'. At present there are four different classifications of Block II satellites; II, IIA, IIR and IIF. Satellite numbers 13 to 21 are classified as II. Numbers 22 to 40 are IIA, and have an extended navigation capability. Block IIRs are numbered 41 to 60 and use UHF-Crosslinks for ranging and communication. This gives them the capability to navigate autonomously for up to 180 days after upload from the ground station. The first of these Block IIR (Replenishment) satellites was due to be placed into orbit on 17th January 1997, but blew up on launch. The first successful launch occurred on 22nd July 1997, and the satellite became operational on 31st January 1998. The specification for the next generation Block IIF (Follow-on) satellites has only recently been finalised, although the contract for the first six (phase 1) satellites has been completed, and construction started. These will offer improvements in areas such as life-span and integrity monitouring, but it is from satellite 07 in the potential series of thirty-three that the greatest benefits will occur. Two new civilian frequencies have been defined to be broadcast by these satellites. These are a C/A code signal at L2 and a new signal at 1176.45 MHz (Section 2.3.4) [The White House, 1999]. These will allow ionospheric corrections to be made and the use of wide-laning to directly acquire the carrier cycle count. The first launch of a Block IIF satellite is scheduled to occur some time in 2003/2004.

The GPS constellation achieved Initial Operational Capability (IOC) in December 1993 with twenty-four operational satellites (three Block I and twenty-one Block II). The full operational constellation of twenty-four Block II satellites was realised in March 1994 and Full Operational Capability (FOC) announced on 27th April 1995. The present status of the GPS constellation is detailed in Section 2.3.6.

2.3.2 The Ground Control Segment

The function of the Ground Based Control Segment (GBCS) is to calculate the satellite orbits, clock corrections and generally monitor the performance of the whole space segment. To do this it must be able to both transmit and receive data from each satellite.

The control segment consists of a Master Control Station (MCS) and four other monitoring stations distributed in such a way that each satellite is tracked for over 90% of its orbit. The MCS is located at 'Schriever Air Force Base', near Colorado Springs. The monitor stations are located approximately around the equatorial plane at Ascension Island, Diego Garcia, Hawaii and Kawajalein (Figure 2.1).

It is the MCS, which performs all necessary calculations, using the measurements made from all the stations. Predicted orbits and satellite clock corrections are then uploaded in a navigation message from either Ascension Island, Diego Garcia or Kwajalein to each satellite via an S-Band radio link.

As the coordinates of the monitor stations have been determined very precisely in the World Geodetic System 1984 (WGS 84) reference frame, the satellite orbits and all observations made using GPS are therefore with respect to this global datum. Further reference is made to this in Chapter 3.

Figure 2.1 Location of the GPS Control Segment's Tracking Network [ETG, 1998]

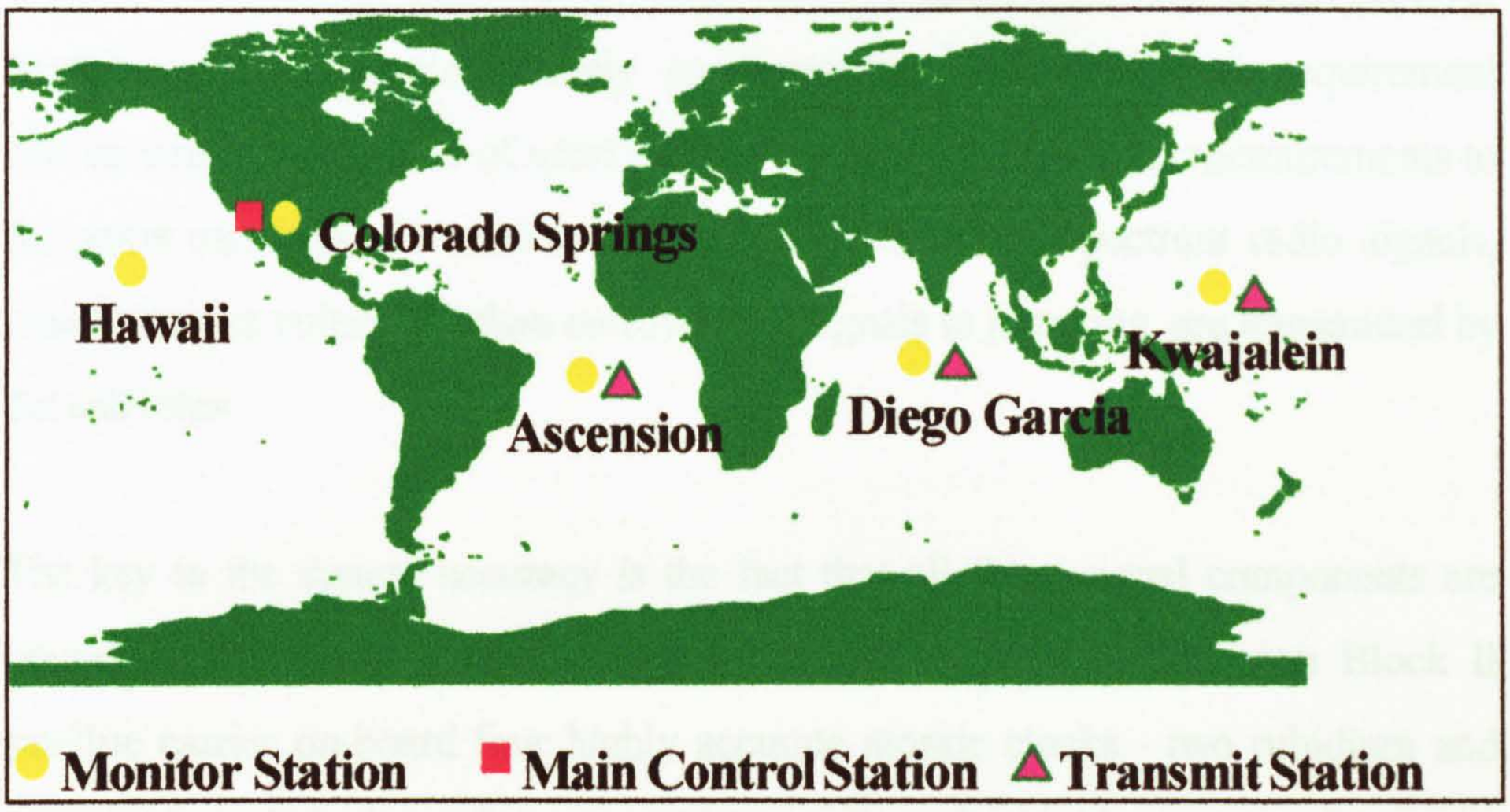

2.3.3 The User Segment

The user segment consists of the users of the system, and has an ever-expanding size as the classes and applications of equipment continually increase. Production of GPS user equipment now exceeds one million sets per year and the rate is accelerating. This kind of boom is possible as the system has been designed to be passive, with each user only receiving signals from the satellites.

To use the system each user requires at least one GPS receiver, which is basically a radio receiver, with an in-built data processor to calculate position. The type and cost of receiver is dependent on the accuracy requirement of the application and it can measure all or some of the observables available. For example, the most accurate geodetic sets used for surveying may measure both code and carrier observations on both wavelengths. They can give positioning accuracies of a few millimetres, and cost in the region of £10,000 - £15,000. By comparison, simple hand held sets used by hill walkers measure only single frequency code observations, are accurate to 100 metres, but can cost as little as £150.

2.3.4 Signal Structure

To achieve real time positioning, range measurements from satellite to receiver must be calculated instantaneously. As already mentioned, it is also a requirement that an unlimited number of users be able to make simultaneous measurements to the same satellites. To achieve this, continuous spread spectrum radio signals, which are less vulnerable than narrow band signals to jamming, are transmitted by the satellites.

The key to the system accuracy is the fact that all these signal components are precisely controlled by atomic clocks. This is reflected in that each Block II satellite carries on-board four highly accurate atomic clocks - two rubidium and two caesium. It is these that are used to produce the highly accurate frequency standard and derive the fundamental frequency of 10.23 MHz. Coherently derived from this fundamental frequency are two signals, the L1 and L2 carrier waves, are generated by multiplying the fundamental frequency by 154 and 120 respectively, thus yielding L1 = 1575.42 MHz (with a wavelength of 19.05 cm) and L2 = 1227.60 MHz (with a wavelength of 24.45 cm). This atomic frequency standard is however affected by the motion of the satellite and its lower gravitational potential. These are collectively referred to as *relativistic effects*, and are compensated for by altering the fundamental frequency of the signal to 10.2999999454 MHz [Leick, 1995].

Two pseudo/random noise (PRN) codes are modulated onto these carrier signals and it is these that act as the ranging codes, providing an instantaneous range. Figure 2.2 (A) shows a representation of the unmodulated carrier signal, onto which the PRN code depicted in Figure 2.2 (B) is imposed. This results in the signal depicted in Figure 2.2 (C), and shows how the carrier phase is multiplied by –1 for any change in the binary state, corresponding to a 180° change in carrier phase.

Figure 2.2 GPS Signal Structure

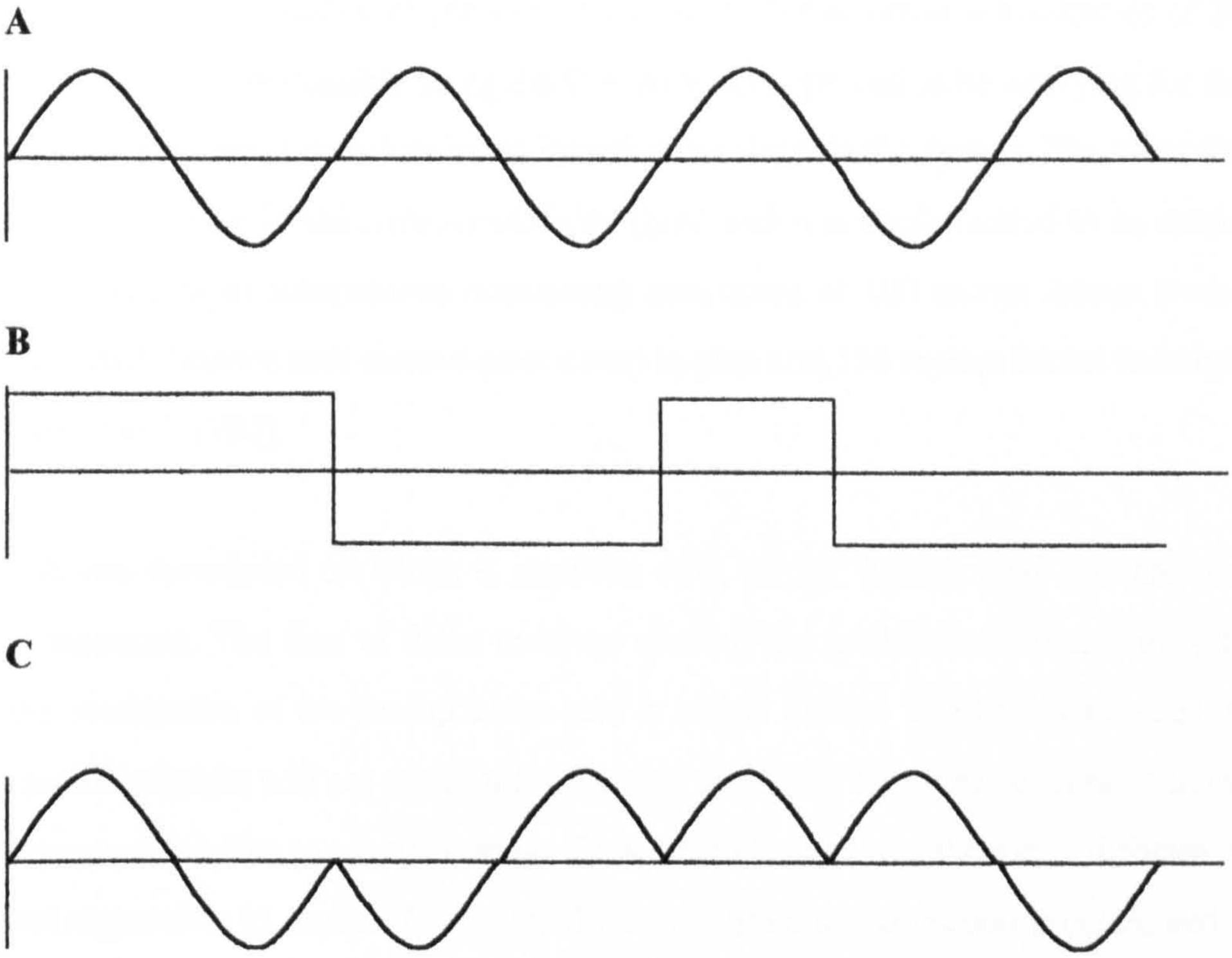

The L1 carrier is modulated with both the coarse acquisition (C/A) code and the precise (P) code, and the L2 carrier with just the P code. These consist of apparently random sequences of binary digits, which are in fact discrete and repeatable. In order for the receiver to distinguish between satellites, each satellite broadcasts its own unique C/A code sequence, and is referred to as Code Division Multiple Access (CDMA). The C/A code consists of a sequence, which is repeated every millisecond, equating to approximately 300 kilometres in distance terms. It is modulated onto the L1 carrier with a chipping rate of one tenth of the fundamental frequency (1.023 MHz) which gives a wavelength of approximately 300 metres. The P code has a period of 267 days and is modulated onto both L1 and L2 with a chip rate of 10.23 MHz, resulting in a spacing of approximately 30 metres. Each satellite transmits a different one-week portion of the P-code, which repeats every week. This P code is modulated by a third code, called the W code, to form the Y code which is made available to authorised users only. This process is known as *Anti Spoofing* (A/S).

The original intended available position accuracy for non-authorised users was to be in the region of 300 to 500 metres [Baker, 1986]. However, it quickly became apparent that the quality of the system was such that achievable accuracies of 20 to 30 metres were possible using the C/A code. This proved to be worrying for the USDoD and thus it was decided to intentionally degrade the system. The name for this degradation is *Selective Availability* (S/A) and it is implemented to an extent which results in autonomous positioning accuracies of 100 metres 2drms (twice the radial distance root mean square error) in plan and 156 metres 2drms in height [DoD/DoT, 1990].

S/A was introduced on Block II satellites only, on 25th March 1990 and has two components. The first of these involves altering the satellite's oscillator prior to the modulation of the timing codes and is called *Dither*. The broadcast satellite clock correction will not account for this and there will therefore be an error in the measured satellite to receiver range. This error changes rapidly and is difficult, if not impossible to model. *Epsilon* is the name given to the second process, and it involves introducing errors in the broadcast satellite position. The effect of this is to produce an error in the satellite to receiver range, which changes only very slowly with time. Although the Dither component has been implemented, Epsilon has not.

The effect of S/A varies in amplitude by up to 70 metres [Leick, 1995], and because it is a changing bias with low frequency terms in excess of a few hours, position solutions cannot be effectively averaged over periods shorter than a few hours. It is however possible to remove the vast majority of these effects by differencing the observations (Chapter 4). This fact, along with calls from the civilian community, led to a Presidential statement in 1996 that S/A would be discontinued within a decade, and that the situation would be reviewed annually from the year 2000 [The White House, 1996].

The original intended available position accuracy for non-authorised users was to be in the region of 300 to 500 metres [Baker, 1986]. However, it quickly became apparent that the quality of the system was such that achievable accuracies of 20 to 30 metres were possible using the C/A code. This proved to be worrying for the USDoD and thus it was decided to intentionally degrade the system. The name for this degradation is *Selective Availability* (S/A) and it is implemented to an extent which results in autonomous positioning accuracies of 100 metres 2drms (twice the radial distance root mean square error) in plan and 156 metres 2drms in height [DoD/DoT, 1990].

S/A was introduced on Block II satellites only, on 25th March 1990 and has two components. The first of these involves altering the satellite's oscillator prior to the modulation of the timing codes and is called *Dither*. The broadcast satellite clock correction will not account for this and there will therefore be an error in the measured satellite to receiver range. This error changes rapidly and is difficult, if not impossible to model. *Epsilon* is the name given to the second process, and it involves introducing errors in the broadcast satellite position. The effect of this is to produce an error in the satellite to receiver range, which changes only very slowly with time. Although the Dither component has been implemented, Epsilon has not.

The effect of S/A varies in amplitude by up to 70 metres [Leick, 1995], and because it is a changing bias with low frequency terms in excess of a few hours, position solutions cannot be effectively averaged over periods shorter than a few hours. It is however possible to remove the vast majority of these effects by differencing the observations (Chapter 4). This fact, along with calls from the civilian community, led to a Presidential statement in 1996 that S/A would be discontinued within a decade, and that the situation would be reviewed annually from the year 2000 [The White House, 1996].

2.3.5 GPS Navigation Message

Both the L1 and L2 carriers are also modulated at a rate of 50 bits per second (bps) with a navigation message. The aim of this is to provide the user with requisite data for positioning, timing and the planning of surveys. The full message consists of twenty-five 1500 bit long frames, taking 12.5 minutes to be fully transmitted. The information included in this message consists of satellite ephemerides (Section 2.3.5.1), ionospheric modelling coefficients, status information, system time, and satellite clock bias and drift information. The navigation message of the C/A code contains a further piece of information called the Hand-Over-Word (HOW), which tells the receiver which portion of the P code is being transmitted by each satellite, and hence where to start its search for signal matching.

2.3.5.1 GPS Broadcast Ephemeris

The GPS Broadcast Ephemeris is transmitted to the user as part of the data message and therefore has a practical limitation on its size. In terms of Cartesian coordinates, a GPS orbit varies enormously with time and cannot be stored efficiently. On the other hand however, a Keplerian format consisting of the six Keplerian elements in combination with correction terms, allows orbital information covering a long time-span to be stored. For this reason, the GPS Broadcast Ephemeris is described in Keplerian terms, although it is derived in a Cartesian framework. A full explanation of Kepler's Laws and Keplerian elements can be found in [Leick, 1995].

The GPS Broadcast Ephemeris consists of the sixteen elements listed in Table 2.1 [Whalley, 1990], and is valid for two hours either side of its reference time, the Time Of Ephemeris (TOE). It consists of the basic Keplerian elements together with correction terms to estimate the difference between the ideal Keplerian orbit and the true one, and terms to account for the behaviour of the satellite clock.

To compute Earth-centred, Earth-fixed Cartesian coordinates, the Cartesian coordinates in the orbital plane are first calculated, before two rotations are applied. The first rotation is through the inclination angle, resulting in the correct direction for the Z-axis, and the second rotation is about the new Z-axis so that the X-axis coincides with the Greenwich Meridian. This gives rise to the transformation equations (2.1) - (2.3), which are however simplified as they do not account for the correction terms also provided in the broadcast ephemeris. A full derivation can be found in [Ashkenazi and Moore, 1986].

$$X = r\cos u\cos\Omega - r\sin u\cos i\cos\Omega \qquad (2.1)$$

$$Y = r\cos u\sin\Omega + r\sin u\cos i\sin\Omega \qquad (2.2)$$

$$Z = r\sin u\sin i \qquad (2.3)$$

where:

r = the geocentric radius

Table 2.1 Elements of the GPS Broadcast Ephemeris

t_0	reference epoch for the ephemeris
M_0	mean anomoly at t_0
Δn	correction to the computed mean motion n_0
e	eccentricity of orbital ellipse
$a^{\frac{1}{2}}$	square root of the semi-major axis
Ω_0	right ascension of ascending node at t_0
i_0	inclination of orbital plane
w	argument of peregee
$\delta i / \delta t$	rate of change of the inclination with time
$\delta\Omega / \delta t$	rate of change of right ascension with time
C_{ue}, C_{us}	amplitude of cos and sin correction terms to the argument of latitude (u)
C_{re}, C_{rs}	amplitude of cos and sin correction terms to the geocentric radius (r)
C_{ie}, C_{is}	amplitude of cos and sin correction terms to the inclination of the orbital plane (i)
af_0	satellite clock offset
af_1	satellite clock drift term
af_2	satellite clock ageing term

2.3.6 Constellation Status

As already outlined in this chapter, the design specification for the GPS constellation is twenty-four satellites. However, as can be seen in Figure 2.3, the present constellation exceeds this by three satellites. The reasoning behind this is that the U.S. Government has indicated to the civilian community that it will maintain a minimum operational constellation of twenty-four satellites. As quite a few of the satellites, which presently make up the constellation, are nearing the end of their design life, two operational spares are already in orbit. The third spare is the first of the Block IIRs and has been launched to gain experience of the actual performance of the next generation of satellite.

Figure 2.3 Current GPS Constellation Status [MIT-1, 1999]

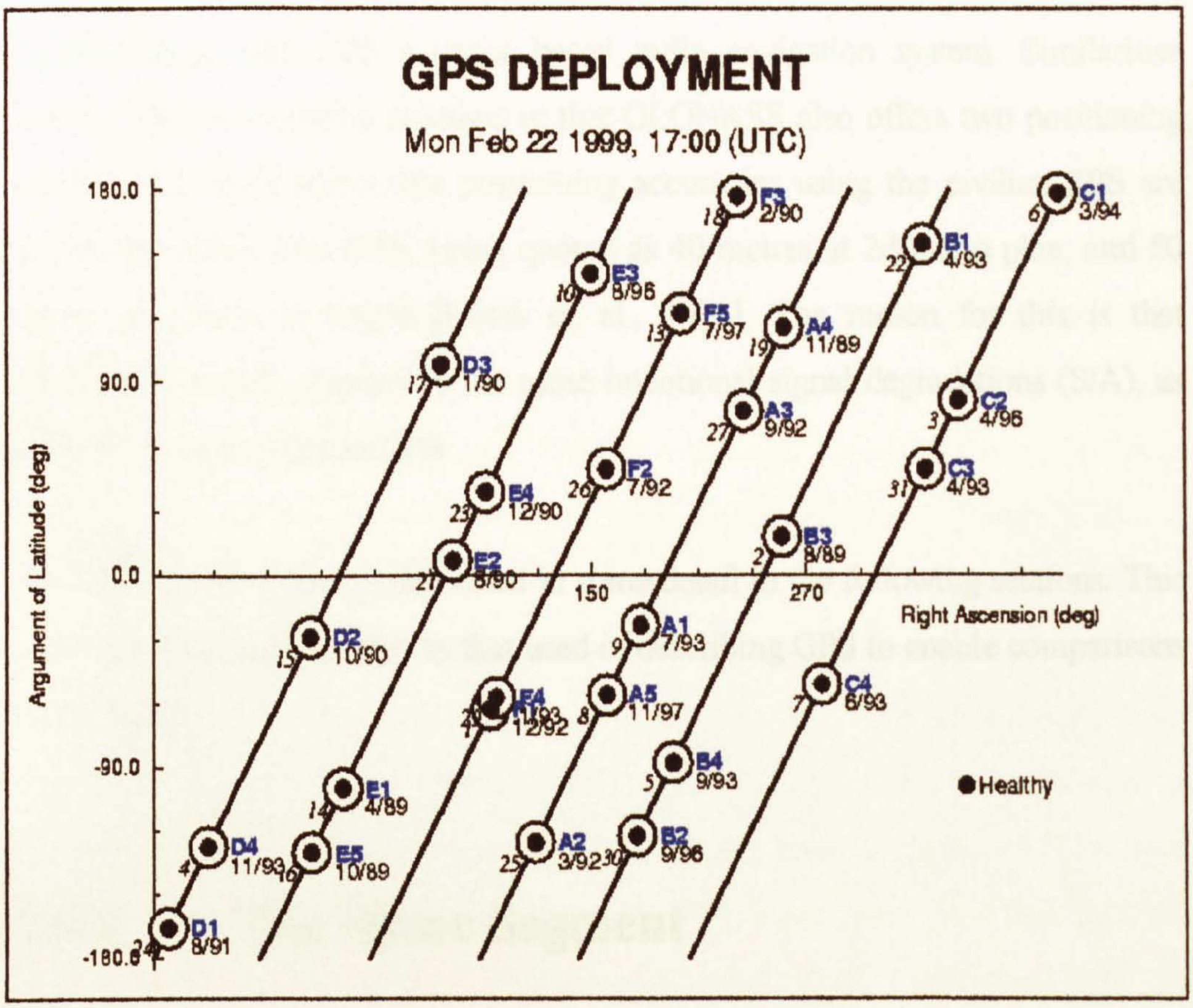

2.4 The Global'naya Navigatsionnaya Sputnikova Sistema

In the early 1970's, the former Soviet Ministry of Defence conceived the Global'naya Navigatsionnaya Sputnikova Sistema or the Global Navigation Satellite System - GLONASS [Langley, 1997]. The parties involved in its design were the NPO of Applied Mathematics, the Russian NII of Space Devices and the Russian Institute of Radio Navigation and Time. Its development has been less well publicised than that of GPS, although information outlining the intentions of the system was lodged with the International Frequency Registration Board in 1982.

GLONASS is, like GPS a space based radio navigation system. Similarities between the two systems continue in that GLONASS also offers two positioning services. However achievable positioning accuracies using the civilian SPS are somewhat higher than GPS, being quoted as 40 metres at 2drms in plan, and 50 metres at 2drms in height [Misra et. al., 1996]. The reason for this is that GLONASS is not subjected to the same intentional signal degradations (S/A), as currently implemented in GPS.

The GLONASS system is described in some detail in the following sections. This will follow the same pattern as that used in describing GPS to enable comparisons to be drawn.

2.4.1 The Space Segment

As with GPS, a minimum of four GLONASS satellites must be simultaneously visible to the user if a stand-alone three-dimensional position is to be calculated (Chapter 4). To fulfil this requirement a full constellation design of twenty-four satellites (twenty-one operational + three active spares) has been specified. These

satellites are placed in three orbital planes (eight satellites equally spaced in each plane) at an inclination of 64.8 degrees to the equator. The orbital planes are numbered 1, 2 and 3, with the first orbital plane containing slot numbers 1...8, the second orbital plane - slots 9...16, and the third orbital plane - slots 17...24 [CSIC 1995].

Nominally, the satellite orbits are circular and have an altitude of 19100 km, some 1000 km lower than GPS satellites. This shorter orbital radius yields a shorter orbital period of 8/17 of a sidereal day such that, after eight sidereal days the GLONASS satellites will have completed seventeen orbital revolutions. This design means that, in an eight-day period, all the satellites in the constellation pass through the same azimuth and elevation. Therefore, a regional ground segment can monitor/control all the satellites in the constellation while maintaining a global navigation capability [Basker et. al., 1998].

The first GLONASS launch occurred on 12th October 1982 when a Proton booster vehicle launched from Baikonur, Kazakhstan, placed three satellites in orbit. This ability to launch three satellites at a time is a common feature of almost all GLONASS launches and gives the potential for a rapid replenishment of the constellation. Between 1982 and 1985 the system was designated as 'Pre-operational', with a total of ten satellites being launched. These Block I development satellites were given COSMOS (K) space designator numbers between 1651 - 1780. The system was declared operational in 1985, with the launch of the first Block II production satellites. As with GPS there are different classifications of these satellites: IIA, IIB and IIV (V is the Latin transliteration of the Cyrillic alphabet's third letter). A total of six IIAs (K 1651 - 1780) were launched between May 1985 and September 1986. From April 1987 to May 1988 twelve Block IIBs (K 1838 - 1948) were launched. From September 1988 the satellite development entered its latest phase, with a total of forty-six IIV satellites (K 1970 - 2364) being launched to date.

Each subsequent satellite generation has contained equipment enhancements and also achieved longer lifetimes. It is intended that the next GLONASS launch will

contain two Block IIV and one of the next generation Block II M (Modernisation) satellites. These are said to feature improved frequency and timing accuracies and to have expected lifetimes of five to seven years [Langley, 1997].

The first decree relating to the development of GLONASS was issued by President Yeltsin on 24th September 1993, declaring the system to be operational and gave approval for its continued development. A second decree, dealing specifically with civil use of GLONASS, was issued by Prime Minister Chernomyrdin on 7th March 1995 and reaffirmed plans to achieve a full constellation in 1995. This was achieved on 18th January 1996 with twenty-four operating satellites and one spare in orbit. However, there have been few occasions since when twenty-four satellites have been operational. This is discussed in more detail in Section 2.4.5. Finally, President Yeltsin issued the latest decree on 18th February 1999. In this, the GLONASS system and Russian experience and expertise in the space industry was basically offered to the Western Europe as the basis for their planned Satellite Navigation System, in return for foreign investment and funding. As yet it appears that no final decision as to whether or not to include GLONASS in any future European venture has been taken.

2.4.2 The Ground Control Segment

The GBCS controls the entire GLONASS system and fundamentally performs the same tasks in the same way as the corresponding segment of GPS. It consists of the System Control Centre (SCC) located in Moscow and several Command Tracking Stations (CTS), which are placed over a wide area of Russia (Figure 2.4).

The CTSs track the GLONASS satellites in view using two-way radio ranging, and telemetry control and navigation message data to the satellite. Again, this information is processed at the SCC to determine satellite clock and orbit states and to update the navigation message of each satellite. This updated information is

transmitted to the satellites via the CTSs, which are also used for transmitting control information.

The CTS's ranging data are periodically calibrated using laser-ranging devices at the Quantum Optical Tracking Stations, which are within the GLONASS Control Segment. Each satellite carries a laser reflector specifically for this purpose [ETG, 1998].

Figure 2.4 Location of the GLONASS Control Segments Tracking Network [ETG, 1998]

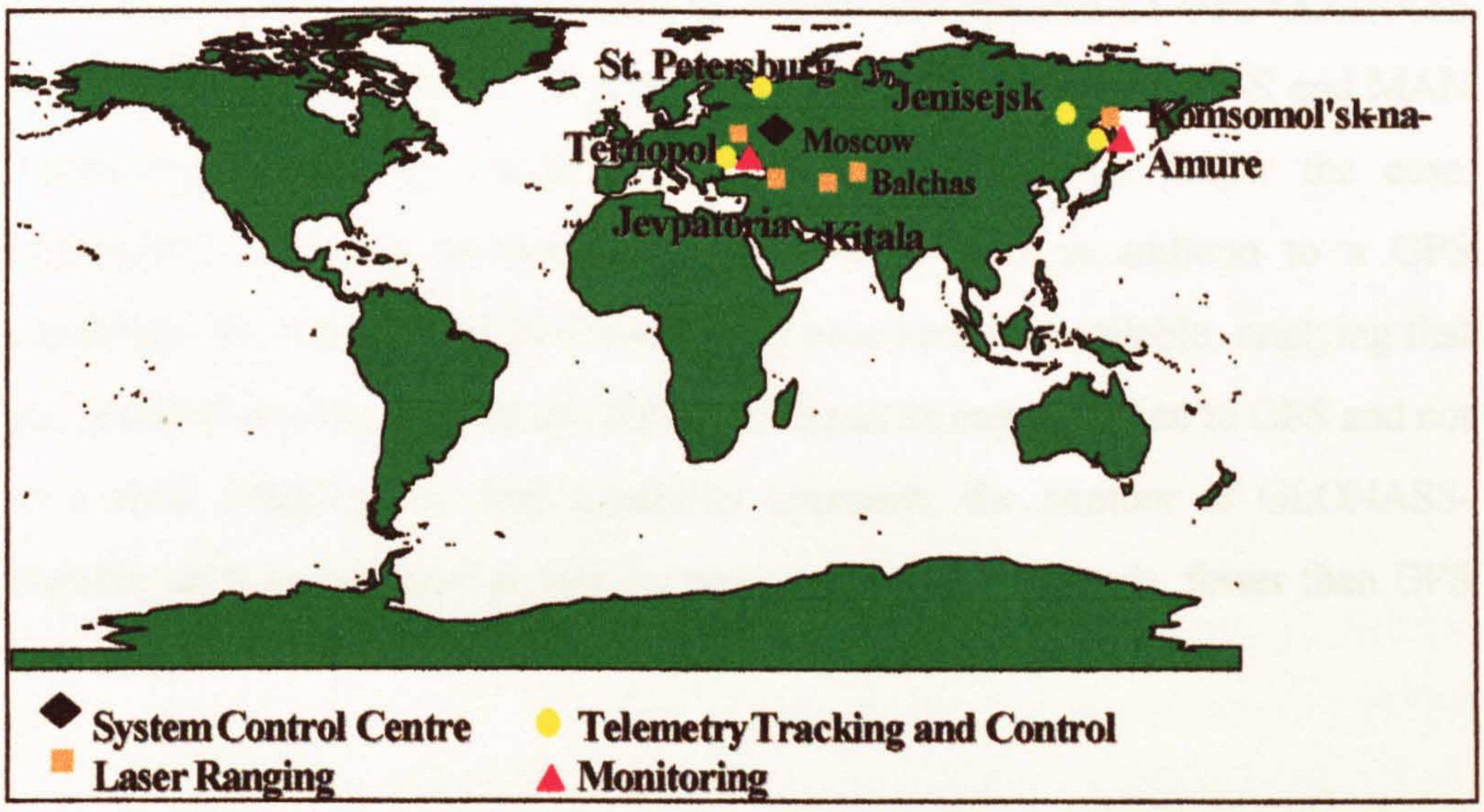

Unlike GPS, GLONASS does not use the WGS 84 reference frame for coordinate definition of its network of control stations. Instead these are referenced to the Parametry Zemli (PZ-90 or, in English translation, Parameters of the Earth 1990, PE-90) geodetic datum. PZ-90 replaced the Soviet Geodetic System SGS 85, used by GLONASS until 1993. Further reference to this is made in Chapter 3.

2.4.3 The User Segment

Until recently, the lack of available GLONASS receivers proved to be the major limiting factor to the widespread use and thus realisation of the Russian system. Outside Russia the manufacture of GLONASS receivers was for a great many years restricted to development units designed and built by research groups such as the University of Leeds, *Institute of Satellite Navigation* (ISN), in an attempt to gain experience with GLONASS.

However, in 1996 Ashtech launched its twenty-four channel L1 GPS/GLONASS receiver, and with a number of recognised manufacturers, such as 3S and MAN Technology producing similar equipment now, this is no longer the case. Interestingly all such receivers now offer GLONASS in addition to a GPS capability. No commercial GLONASS-only receivers are available, implying that the potential civilian benefits of GLONASS lie as an augmentation to GPS and not as a rival. Despite this dual capability approach, the number of GLONASS-capable units in existence is still, by some orders of magnitude, fewer than GPS only units.

2.4.4 Signal Structure

As both GPS and GLONASS basically provide the same capability, namely one-way passive ranging, it is unsurprising that GLONASS shares a very similar signal structure to that outlined previously for GPS, with each satellite broadcasting radio signals on two frequencies.

However the main difference between the two systems lies in the fact that each GLONASS satellite broadcasts the same modulated codes, and thus the GPS receiver technique of using individual codes to track each satellite is not possible. To overcome this, all visible GLONASS satellites transmit carrier signals at different L-band frequencies, allowing the receiver to separate the incoming

signals by assigning different frequencies to its tracking channels. This process is called Frequency Division Multiple Access (FDMA).

Initial specification for the ranges of these frequency bands were between 1602.0 MHz and 1615.5 MHz for L1 and 1246.0 MHz and 1256.5 MHz for L2, with the actual frequency of each satellite being governed by Equations (2.4) and (2.5) [CSIC, 1995].

For the L1 frequency

$$f = (1602 + n * 0.5625) \text{ MHz} \qquad (2.4)$$

For the L2 frequency

$$f = (1246 + n * 0.4375) \text{ MHz} \qquad (2.5)$$

where n is an integer number between 1 and 24, referred to as the frequency channel.

This specification provided twenty-five channels, so that each satellite in the full twenty-four satellite constellation could be assigned a unique frequency, with the remaining channel being reserved for testing. However some of these GLONASS signals were found to be interfering with radio astronomy observations which occupy frequency bands close to those of GLONASS. As the International Telecommunications Union (ITU) has granted primary user status to these astronomers and, in addition, allocated the 1610 - 1626.5 MHz band to low-earth-orbiting communication satellites, the GLONASS authorities were forced to reduce the number of frequencies used by the satellites and shift the bands to slightly lower frequencies. Following discussions in 1993, these authorities agreed to the following programme of changes. Since 1994, frequency channels 15 - 20 have not been used, whilst others have been used by satellite pairs. This sharing is possible by selecting antipodal satellites (diametrically opposite) which cannot be viewed simultaneously from the same point on the Earth's surface. Between 1998 and 2005 it is proposed to further downshift this range to channels -7 to +12, which equates to 1598.1 MHz to 1608.8 MHz. Finally, after 2005, channels -7 to + 6 will be used, further reducing the upper frequency limit to 1605.4 MHz. To

accomplish this it is proposed to use diametrically opposite satellites broadcasting on the same frequency.

In a similar fashion to GPS, GLONASS satellites transmit two PRN timing codes on the carrier frequencies. The C/A code is present on the L1 frequency only, whereas the P code is present on both the L1 and L2 frequencies, although it appears that GLONASS-M satellites will have the C/A code on the L2 frequency [Lowe and Daly, 1996]. The clock rates are 5.11 MHz, and 0.51 MHz for the P and C/A codes, respectively. This is approximately half of the corresponding values used for GPS and results in GLONASS observations having a slightly lower resolution and being more susceptible to multipath (Chapter 4).

The satellites in the constellation are referenced both by their slot number and by their frequency channel, which has been outlined already. The slot number refers to the position of the satellite in orbit, with slots 1-8 in plane I, slots 9-16 in plane II and slots 17-24 in plane III. Thus if a satellite is quoted as 20/01, it is in slot III and transmitting on frequency channel 01.

Finally, it is worth noting that GLONASS signals are subjected to neither the intentional restrictions, nor degradations (A/S and S/A), as experienced by GPS. This presents potential significant benefits for GLONASS, especially in terms of absolute positioning, and is examined in more detail in Chapter 5.

2.4.5 GLONASS Navigation Message

The navigation message is broadcast from GLONASS satellites at a rate of 50 bps, and serves the same purposes as outlined in Section 2.3.5. It includes satellite clock epoch and rate offsets from GLONASS time, the satellite ephemeris, satellite health information, data age, the offset of GLONASS time from Universal Coordinated Time (UTC) and almanacs (approximate

ephemerides) for all other GLONASS satellites. The full message lasts 2.5 minutes, but the ephemeris and clock information is repeated every 30 seconds.

2.4.5.1 GLONASS Broadcast Ephemeris

Like GPS, the GLONASS system also transmits its Broadcast Ephemeris as part of the data message. It has however adopted the policy of directly using Cartesian coordinates to describe satellite position. It overcomes the problems of variation with respect to time, and storage efficiency, as mentioned in Section 2.3.5.1, by limiting the period for which these values are valid to fifteen minutes either side of the Time Of Ephemeris (TOE).

The parameters of the satellite ephemeris are listed in Table 2.2 and show that the satellite position is described by its position in X, Y and Z at the TOE, and its velocities and accelerations in these three directions. To calculate an instantaneous position within +/- 15 minutes of this TOE, a quadruple Runge-Kutta integration of equations (2.6) – (2.8) [CSIC, 1995], is performed.

Table 2.2 Elements of the GLONASS Broadcast Ephemeris

t_0	Reference epoch for the ephemeris
X	Coordinate of satellite in X at reference epoch
Y	Coordinate of satellite in Y at reference epoch
Z	Coordinate of satellite in Z at reference epoch
VX	X velocity vector componentat reference epoch
VY	Y velocity vector component at reference epoch
VZ	Z velocity vector component at reference epoch
AX	Acceleration in X at reference epoch caused by effect of Sun and Moon
AY	Acceleration in Y at reference epoch caused by effect of Sun and Moon
AZ	Acceleration in Z at reference epoch caused by effect of Sun and Moon
af_0	satellite clock offset
af_1	satellite clock drift term

$$\delta V_x / \delta t = -\frac{u}{r^3}x + \frac{3}{2}C_{20}\frac{ua_e^2}{r^5}x[1-\frac{5z^2}{r^2}] + w_3^2 x + 2w_3 V_y \qquad (2.6)$$

$$\delta V_y / \delta t = -\frac{u}{r^3}y + \frac{3}{2}C_{20}\frac{ua_e^2}{r^5}y[1-\frac{5z^2}{r^2}] + w_3^2 x - 2w_3 V_x \qquad (2.7)$$

$$\delta V_z / \delta t = -\frac{u}{r^3}z + \frac{3}{2}C_{20}\frac{ua_e^2}{r^5}z[3-\frac{5z^2}{r^2}] \qquad (2.8)$$

where:

r = $\sqrt{x^2+y^2+z^2}$

u = 398600.44 km^3s^{-1} -Earth's universal gravitational parameter;

a_e = 6378.136 km -equatorial radius of Earth;

C_{20} = $-1082.63*10^{-6}$ -zonal geopotential coefficient of spherical harmonic expansion;

w_3 = $0.7292115*10^{-4}c^{-1}$ -Earth's rotation rate.

The values u, a_e, C_{20}, w_3 are given as in PZ-90.

2.4.6 Constellation Status

The current Russian economic situation has certainly been seen to have had an adverse effect on the GLONASS system in recent years. Its impact has hit all essential elements of the system, especially the space segment. Despite the fact that there are enough spare GLONASS satellites on the ground, and launch vehicles to put them into orbit, budgetary restrictions have seriously slowed down the support of the constellation. Indeed, until the most recent launch of three satellites into Plane I on 30th December 1998, there had not been a launch since 14th December 1995, some three years earlier. As a result, the constellation has, since briefly reaching its full design specification of twenty-four satellites in January 1996, experienced a steady decline.

Even with this most recent launch there still remains an urgent need for more satellites to be placed into orbit as at least six of the current operational satellites are reaching or have exceeded their design life. Figure 2.5 shows the constellation as it stood on 22nd February 1999 with 15 useable satellites. This still provides a useful augmentation to GPS, but the benefits and faith in the GLONASS system will be dramatically reduced if the present situation is allowed to further deteriorate.

Figure 2.5 Current GLONASS Constellation Status [MIT-2, 1999]

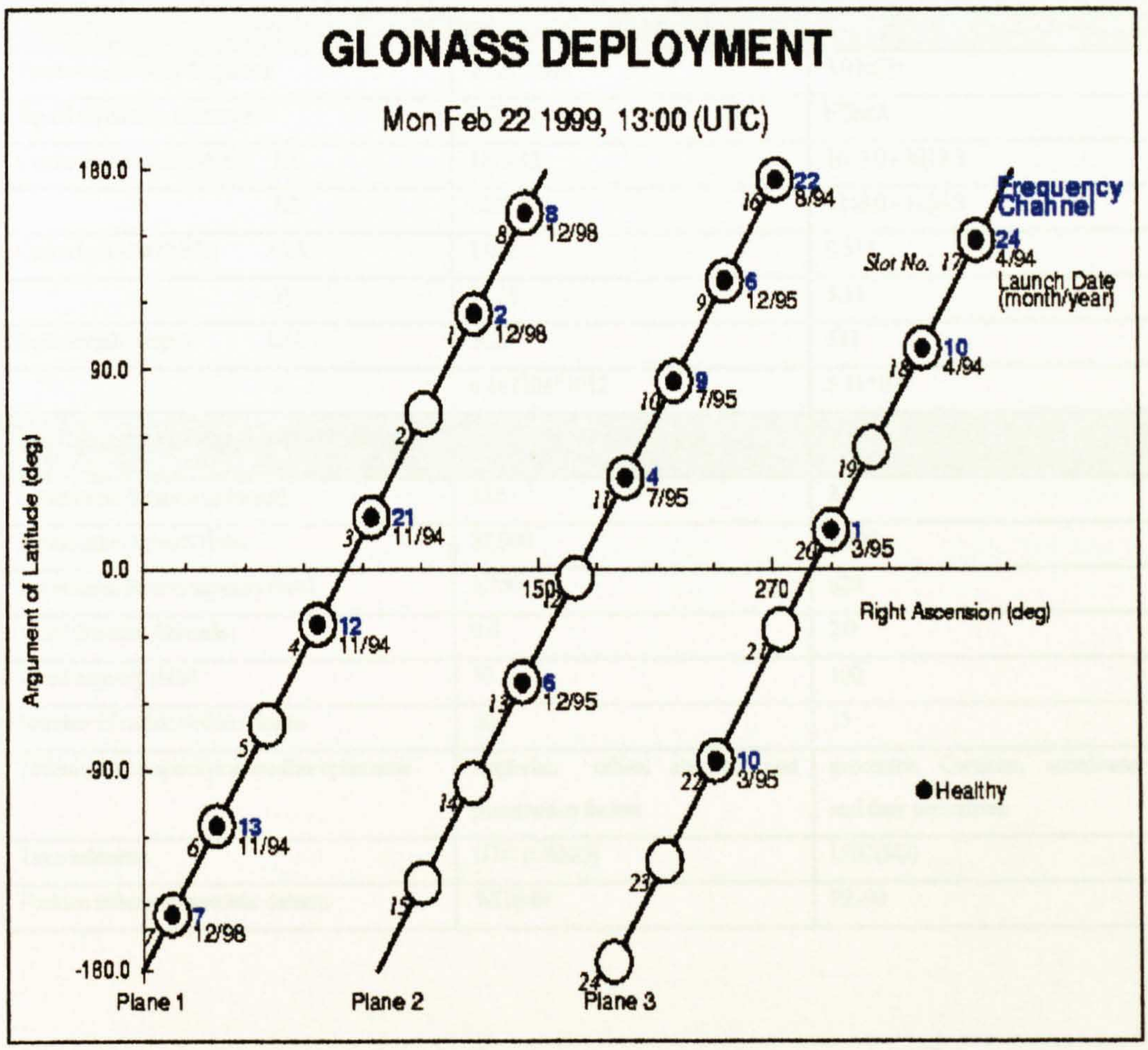

2.5 Summary

The major features of both GPS & GLONASS, which have been described above, are tabulated in Table 2.3. From this it is quite clear that both systems are conceptually very similar, but in their realisation have developed subtle but important differences.

Table 2.3 Comparison of GPS and GLONASS Nominal Characteristics [Langley, 1997]

Parameter/technique	GPS	GLONASS
Satellites		
Number of satellites	21 + 3 spare	21 + 3 spare
Number of orbital planes	6	3
Orbital plane inclination (degrees)	55	64.8
Orbital radius(kilometres)	26,560	25,510
Signals		
Fundamental clock frequency	10.23 MHz	5.0 MHz
Signal separation technique	CDMA	FDMA
Carrier frequencies (MHz) L1	1575.42	1602.0 - 1615.5
L2	1227.60	1246.0 - 1256.5
Code clock rate (MHz) C/A	1.023	0.511
P	10.23	5.11
Code length (chips) C/A	1023	511
P	6.187104*1012	5.11*106
C/A-code navigation message		
Superframe duration (minutes)	12.5	2.5
Superframe capacity (bits)	37,500	7,500
Superframe reserve capacity (bits)	2,750	620
Word duration (seconds)	0.6	2.0
Word capacity (bits)	30	100
Number of words within a frame	50	15
Techniques for specifying satellite ephemeris	Keplerian orbital elements and perturbation factors	geocentric Cartesian coordinates and their derivatives
Time reference	UTC (USNO)	UTC(SU)
Position reference (geodetic datum)	WGS-84	PZ-90

2.6 REFERENCES

Ashkenazi, V., Moore, T., 1986, *The Navigation of Navigation Satellites*, Journal of Navigation, 39(3), pp. 377-393.

Baker, P., 1986, *Global Positioning System Policy*, Proceedings of the 4th International Geodetic Symposium on Satellite Positioning, Austin, Texas, Vol. 1, pp51.

Basker, S., Holmes, D., Trethewey, M.L., 1998, *GLONASS: The System, Availability, and Issues*, Signal Computing Ltd., Guildford, United Kingdome.

CSIC, 1995, Coordinational Scientific Information Centre of the Russian Space Force, *GLONASS Interface Control Document*.

Department of Defence / Department of Transport [DoD/DoT], 1990, *Federal Radionavigation Plan*, Report No. DOD-4650.4, Report No. DPT-VNTSC-RSPA-90-3.

European Tripartite Group [ETG], 1998, Multi-Modal Education Workshop.

Langley, R.B., 1997, *GLONASS: Review and Update*, GPS World, July 1997, pp.46.

Leick, A., 1995, *GPS Satellite Surveying*, Second Edition, John Wiley & Sons, Inc.

Lowe, D., Daly, P., 1996, *GPS and GLONASS for Navigation Surveying*, Royal Institute of Chartered Surveyors, Land and Hydrographic Survey Division Biennial Conference, University of Nottingham, Nottingham, United Kingdom.

Misra, P., Pratt, M., Muchnik, B., Burke, B., Hall, T., 1996, *GLONASS Performance: Measurement Data Quality and System Upkeep*, Proceedings of ION GPS-96, Kansas City, Missouri, USA, pp.261-270.

MIT-1, 1999, Massachusetts Institute of Technology, URL http://satnav.atc.ll.mit.edu/gps/images/gg_gps_dep.gif accessed on 22nd February 1999.

MIT-2, 1999, Massachussetts Institute of Technology, URL http://satnav.atc.ll.mit.edu/glonass/images/deploy.gif accessed on 22nd February 1999.

Sobel, D., 1996, *Longitude*, Fourth Estate.

The White House, 1996, *U.S. Global Positioning System Policy*, Office of Science and Technology Policy, National Security Council.

The White House, 1999, *Initiative Would Make Global Positioning System More Accessible to Civilian Users*, Office of the Vice President.

Whalley, S., 1990, *Precise Orbit Determination for GPS Satellites*, PhD Thesis, University of Nottingham, Nottingham, United Kingdom.

Chapter 3

Significant Differences between the Systems

3.1 Introduction

As outlined in Chapter 2, there exist a number of differences between the GPS and GLONASS systems. Some of these, such as the orbital radius of the satellite and the number of orbital planes in each constellation, have absolutely no effect on the resultant position if both systems are combined. However, in the case of reference frames, time scales, and signal structure, this is not so. Therefore, if the receivers are to maximise the potential of both systems for hybrid positioning, the effect of these differences must be understood and some account made where possible. This Chapter examines each of these differences in turn, looking at their potential effect on the accuracy of a position solution, and methods that are available to overcome or at least reduce their impact.

3.2 Reference Frames

Before going into the details of the difference that exist between the GPS and GLONASS coordinate reference frames, it is felt appropriate at this stage to briefly describe them and the role they serve in satellite positioning.

As both GPS and GLONASS are global navigation systems, there is a fundamental requirement that every point on the surface of the Earth can be uniquely defined. This requirement, along with advances in computer technology, which enable easy processing of large numbers, have made the adoption of a three-dimensional Cartesian coordinate system the ideal choice [Methley, 1991]. The principle of giving a point *P* coordinate values in such a way is illustrated in Figure 3.1.

Figure 3.1 Three Dimensional Cartesian Coordinates

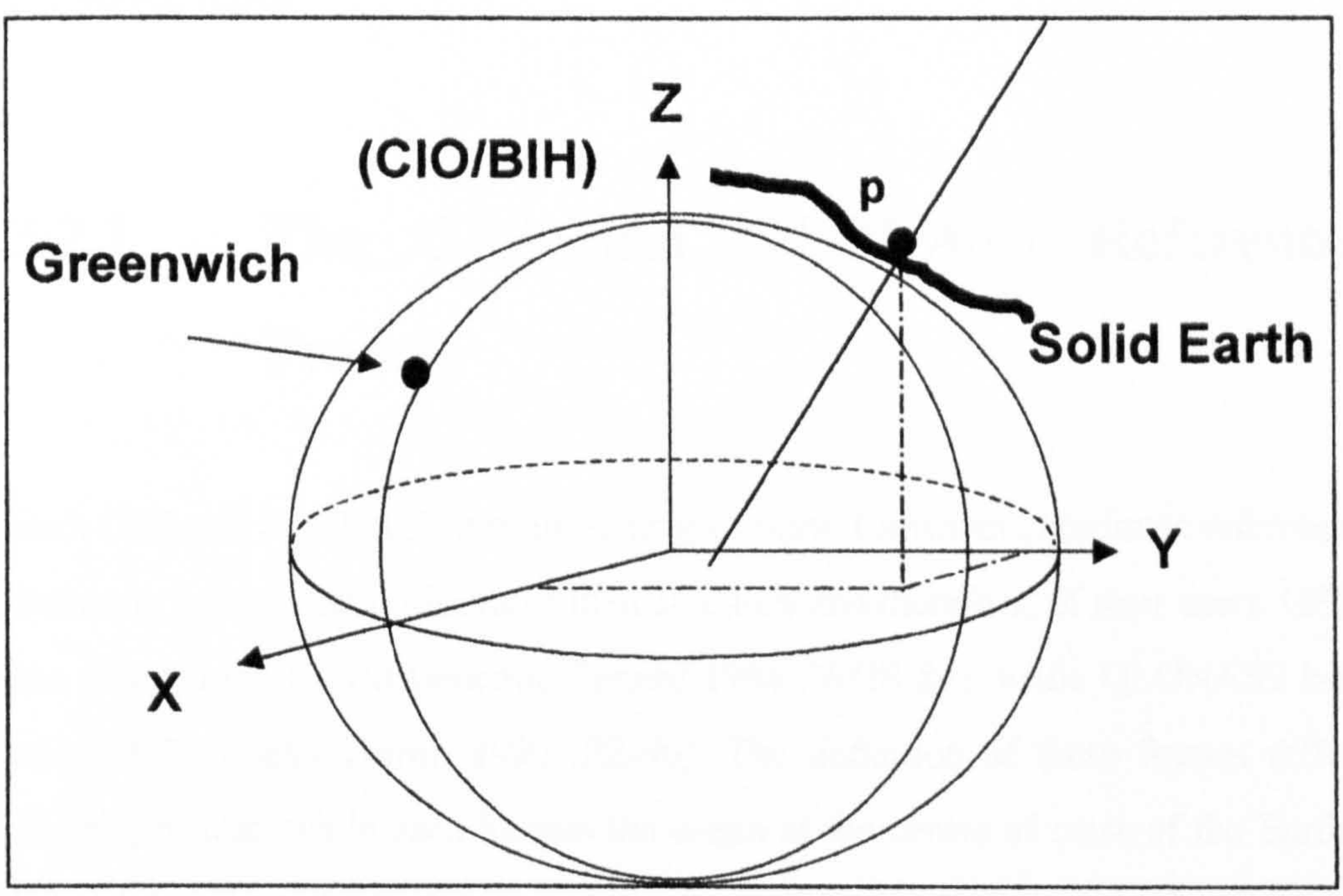

From examining Figure 3.1 it is clear that if such a system is to be adopted, then the location of an origin, a scale, and the direction of the axis need be defined. Being a global system, the obvious choice of origin is the centre of the Earth. As the Earth is spining, the system needs also to be *Earth fixed* to ensure that point

coordinates remain the same. The normal convention is to have the z axis parallel to the Earth's axis of rotation, and the x and y axis rotating with the Earth, the x-axis being parallel to the Grenwich meridian [Bomford, 1980]. In addition to these parameters, a reference ellipsoid, geoid and gravity model will also often be included in the reference system.

The definition of such systems is very easy, but much harder to realise e.g. it is simple to say that a coordinate system will have its centre at the centre of mass of the Earth, but how does one actually determine coordinates on such a system [Cross, 1990]. Realisation is achieved by assigning Cartesian coordinates to a number of points over the Earth's surface. In theory, three such points would be sufficient, but in practice many more are used. A consistent set of such coordinates defines implicitly the coordinate frame (i.e. an origin, a set of directions for the Cartesian axes, and a scale factor). Once a reference system is realised, it becomes a reference frame.

3.2.1 The GPS and GLONASS Reference Frames

Both GPS and GLONASS use different geocentric Cartesian coordinate reference frames to express the positions of their satellites and therefore, of their users. GPS has adopted the World Geodetic System 1984 (WGS 84), while GLONASS has adopted Parametry Zemili 1990 (PZ-90). The definition of these frames differ slightly, in that, while each locates the origin at the centre of mass of the Earth, WGS 84 defines the z-axis as passing through the instantaneous pole of 1984, while PZ-90 has instead adopted the average position of the pole between the years 1900 and 1905. Further information on the definition of each frame can be found for GPS in [DMA, 1997], and for GLONASS in [CSIC, 1997].

Even if their formal definitions were identical, it would not necessarily ensure that the coordinates of the same point in the two systems would be identical. This is

because, as detailed in Section 3.2, the coordinate frame of each system is realised by the adoption of coordinates of a set of reference stations. Thus, even if GPS and GLONASS had adopted the same definition, the autonomous implementation by each system would have kept the two from being coincident.

Therefore, if measurements from the two systems are to be combined, then transformation parameters are required between the two coordinate frames. Alternatively, if differential positioning is being used, and the application of a transformation is ignored, any resultant errors will appear as orbital errors, and so between satellites in common view, will cancel or be significantly reduced. The effectiveness of this technique does however decrease as the separation between receivers increases.

3.2.2 Transformation

Over the past few years, various studies (Hartmann 1991, Misra 1994, Misra 1996, Rossbach 1996, Bazlov 1999) have attempted to quantify and account for the differences between WGS 84 and PZ-90 as interest in combining the systems has grown. In the following sections the basic principle of defining a transformation is outlined. There are two principal techniques that can be adopted for defining coordinate values, which serve as the input to the transformation, and these along with their results will then be detailed. Before doing this however, it is perhaps useful at this stage to quantify the potential extent of this coordinate difference. Misra et. al. [1996] indicates it to be less than 15 metres for any point on the Earth, and on average is approximately 5 metres.

3.2.2.1 Transformation Model

The coordinates of a point in one Cartesian coordinate system may be linked to another by a seven parameter shift called a 'Helmert' transformation. This performs, where necessary, a translation of the origin, a rotation of the three axes and a scale change. Equation 3.1 describes the relationship of these parameters to coordinate values in each system, while Figure 3.2 gives a graphical representation of this transformation process.

$$\begin{bmatrix} X \\ Y \\ Z \end{bmatrix} = \begin{bmatrix} dX_0 \\ dY_0 \\ dZ_0 \end{bmatrix} + (1+dm)\begin{bmatrix} 1 & B_Z & -B_Y \\ -B_Z & 1 & B_X \\ B_Y & -B_X & 1 \end{bmatrix}\begin{bmatrix} U \\ V \\ W \end{bmatrix} \qquad (3.1)$$

where:

X,Y,Z	=	coordinates of point in one system
U,V,W	=	coordinates of same point in second system
dX_0, dY_0, dZ_0	=	the offset of the origins
B_X, B_Y, B_Z	=	differences in coordinate axes orientation
dm	=	scale difference

To determine all seven transformation parameters between two coordinate systems requires at least three points with known coordinates in each system. This is because, to solve for all seven, at least seven equations are needed. Now, two points provide only six equations – three coordinates in each system, but three points provide nine equations, thus surpassing the minimum requirement.

However, as these three points can never be perfectly determined in either frame, more points need to be included and their optimal geographical location, as well as their accuracy in each system, considered. A least-squares estimation method can then be employed to derive a set of values that meet the condition of minimal difference in coordinates after conversion. It should be noted, that if some of the parameters are highly correlated or insignificant, fewer than seven parameters may be estimated, and for the transformation to apply globally, the distribution of points used to derive the values should also be global [Bazlov et. al., 1999].

Figure 3.2 The Relationship between Two Reference Frames

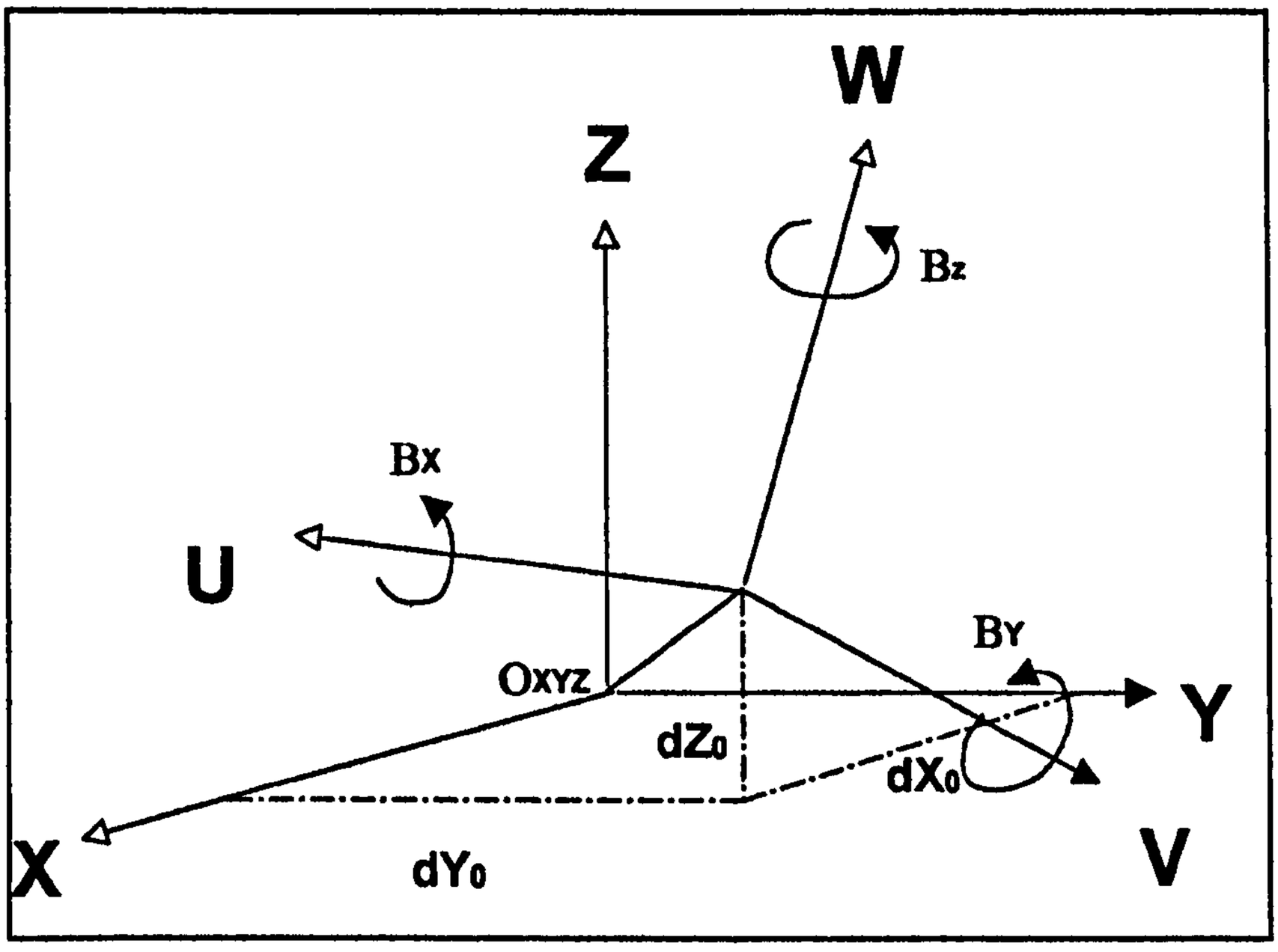

3.2.2.2 Satellite Orbits

One of the major problems to date with estimating a transformation between PZ-90 and WGS 84 has been the determination of precise position estimates of a common set of points in both coordinate frames. However, until very recently, there has not been a global network of precisely defined coordinates in the PZ-90 coordinate frame. Consequently, cumulative single point positioning has had to be used in a great many instances to define coordinates in PZ-90 and this is much less accurate than the relative positioning that can be employed when using WGS 84 coordinates. Furthermore, until the launch of Ashtech's GG-24 receiver in 1996, GLONASS receivers were scarce, and so it proved difficult to take observations at a great many points.

One way to overcome this lack of ground points coordinated in PZ-90 is to adopt the policy of using the GLONASS satellites themselves, which broadcast their positions in PZ-90. All that is now needed with this approach is to obtain their corresponding coordinates in WGS 84. This technique was adopted by [Misra et.

al., 1996] and used laser ranging and deep space radar tracking data from sites, who's coordinates were precisely known in WGS 84, for two GLONASS satellites to estimate their orbits in WGS 84. The data was recorded between September 1995 and March 1996 and split into ten data sets of nine days for each satellite. From each of these nine day sessions approximately 150 data points were derived in WGS 84 corresponding to the broadcast orbits in PZ-90. These were then used in a least squares estimation process to define the following transformation parameters between PZ-90 and WGS 84, which have been substituted into Equation 3.1.

$$\begin{bmatrix} X \\ Y \\ Z \end{bmatrix} = \begin{bmatrix} 0 \\ 2.5m \\ 0 \end{bmatrix} + (1+0) \begin{bmatrix} 1 & -1.9\times10^{-6} & 0 \\ 1.9\times10^{-6} & 1 & 0 \\ 0 & 0 & 1 \end{bmatrix} \begin{bmatrix} U \\ V \\ W \end{bmatrix} \qquad (3.2)$$

where:

X,Y,Z = coordinates in WGS 84

U,V,W = coordinates in PZ-90

As can be seen from Equation 3.2, there are two non-zero elements in the seven parameter transformation. A small clockwise rotation (0.4'') of the z-axis of PZ-90 brings the two frames substantially into coincidence, and the residuals are further, though only slightly reduced, by a 2.5 metre displacement of the origin along the y-axis [Misra et. al., 1996].

Undoubtedly the biggest error source with this experiment came from the fact that the broadcast ephemeris was used to define the PZ-90 coordinate values. The GLONASS Interface Control Document (ICD) [CSIC, 1997] lists the rms. error in position from the ephemeris to be approximately 23 metres. However, as these errors are referenced to a point some four Earth radii from the origin, the effect manifest on the transformation calculation is the same as that experienced by an error one quarter the size on the Earth's surface: rms. < 6 metres. Ideally precise ephemeris values would have been used, but in 1995/96 they were not available.

It is these transformation parameters that have been adopted by Ashtech as the

defaults in the combined GPS/GLONASS receivers. For further information see Ashtech [1997].

3.2.2.3 Ground Point Coordination

The difficulties of using a set of points on the ground, as outlined in Section 3.2.2.2, have diminished somewhat since 1996 with the launch of a number of GPS/GLONASS receivers from a number of manufacturers e.g. Ashtech, 3S and MAN. This has enabled a densification of the number of ground points coordinated in both systems, and perhaps explains why recent experiments to define transformation parameters between PZ-90 and WGS 84 have adopted the approach of using ground coordinated points. Indeed, this approach will be ideally suited for the analysis of the data collected from the recent International GLONASS EXperiment (IGEX–98), further details of which are given in Section 3.5.

An example of one such experiment, which adopted this technique of using ground coordinated points to calculate transformation parameters, is that described by Bazlov et. al.[1999]. Here a transformation between PZ-90 and WGS 84 was determined by directly comparing the coordinates of eight co-located sites, the locations of which are shown in Figure 3.3.

Figure 3.3 Location of Sites Used to Determine Transformation Parameters [Bazlov et. al., 1999]

Each of these eight locations had previously been precisely coordinated in the PZ-90 reference frame using Geodetic-Intercosmos (Geo-IK) satellites that were instrumental in establishing the PZ-90 reference system [Bazlov et. al., 1999]. Theses satellites are equipped with Doppler transmitters, laser ranging reflectors, a radio ranging system, light beacons and radio altimeters. All that was then needed was to coordinate these same points in WGS 84, and this was achieved by collecting data from geodetic quality dual-frequency GPS receivers. Data was logged at a thirty second sample rate over a period of approximately one month, with each site contributing data spans from one to seven days.

The quoted accuracy of the relative WGS 84 coordinates is at the decimeter level, and these have been linked to the PZ-90 system with an accuracy of 0.1 metres [Bazlov et. al., 1999]. Using the computed coordinate differences, in accordance with a least-squares estimation technique, the following transformation parameters were consequently derived.

$$\begin{bmatrix} X \\ Y \\ Z \end{bmatrix} = \begin{bmatrix} -1.1 \\ -0.3 \\ -0.9 \end{bmatrix} + \left(1 - 0.12 \times 10^{-6}\right) \begin{bmatrix} 1 & -0.82 \times 10^{-6} & 0 \\ 0.82 \times 10^{-6} & 1 & 0 \\ 0 & 0 & 1 \end{bmatrix} \begin{bmatrix} U \\ V \\ W \end{bmatrix} \quad (3.3)$$

where:

X, Y, Z = coordinates in WGS 84

U, V, W = coordinates in PZ-90

From Equation 3.3, it can be seen that there is some discrepancy from the parameter values quoted in Equation 3.2, although both sets suggest that the major factor in the transformation is a small clockwise rotation about the z-axis. [Bazlov et. al., 1999] states that, because the network of points used was regional, these parameters can only be considered to be valid for Russia and its surrounding areas. This perhaps is a major contributing factor in the differences between the two sets of results.

3.3 Time Scales

Accurate timing is fundamental to both the GPS and GLONASS systems. This is considered in some detail in Chapter 4. However, to briefly summarise, in each system a minimum of four pseudoranges must be observed to define an instantaneous 3-Dimensional position, i.e. three position unknowns plus a clock parameter needed to determine the clock offset between the highly accurate system time and the non-precise time within the receiver. However, as has been stated in Chapter 2, GPS and GLONASS each use a different time scale. As it is the time measurements that are multiplied by the speed of light to derive range, a proper account of this difference, regardless of how small it may be, must be made when combining observations from both systems.

3.3.1 THE GPS and GLONASS Time Scales

GPS uses its own continuous system time called 'GPS time', which was created on 6th January 1980. At this time it was synchronised with Universal Coordinated Time (UTC) which ties atomic time to earth rotation [Leick, 1995]. GPS time is still linked to UTC with the stipulation that, apart from leap seconds (which are applied periodically to the more stable atomic time to keep it coincident with earth rotation), the difference between the two should not exceed 1 microsecond. However there are various such atomic scales and GPS time is referenced to UTC as maintained by the U.S. Naval Observatory – UTC (USNO). This is not the recognised time standard, which is called UTC as maintained by the Bureau International des Poids et Mesures – UTC (BIPM) or just UTC. As the atomic clocks of the USNO make up approximately 20 % of the input for the calculation of UTC (BIPM) though, UTC (USNO) has always shown agreement with the international standard to the order of 20 nanoseconds. At the time of writing (March 1999), GPS time is 13 seconds ahead of UTC, as there have been 13 integer second adjustments to the atomic time standard since 1980.

Unlike GPS, 'GLONASS time' takes account of these integer adjustments, which occur when necessary at midnight on either 31st December or 30th June, and thus is a discontinuous time scale. Again, it is now linked to within 1 microsecond of UTC, but that as defined by the former Soviet Union's estimation – UTC (SU). Until recently however that was not the case and as can be seen from Figure 3.4, both UTC (SU) and GLONASS time varied widely from UTC. Following recommendations made in September 1996 by the 85th meeting of the Comité International des Poids et Mesures, to synchronise all global satellite systems, the following changes were made. On 27th November 1996, a time step of 9,000 nanoseconds was applied to UTC (SU), thus making it approach UTC. On 10th January 1997, GLONASS time received a frequency step to adjust its frequency closer to that of UTC (SU), which was followed by a 35,300 nanosecond time step [Lewandowski and Azoubib, 1998]. As a result of this the Russian time scales now differ from UTC by a few hundred nanoseconds only.

Figure 3.4 Representation of the Relationship between the Different Time Scales [Lewandowski and Azoubib, 1998]

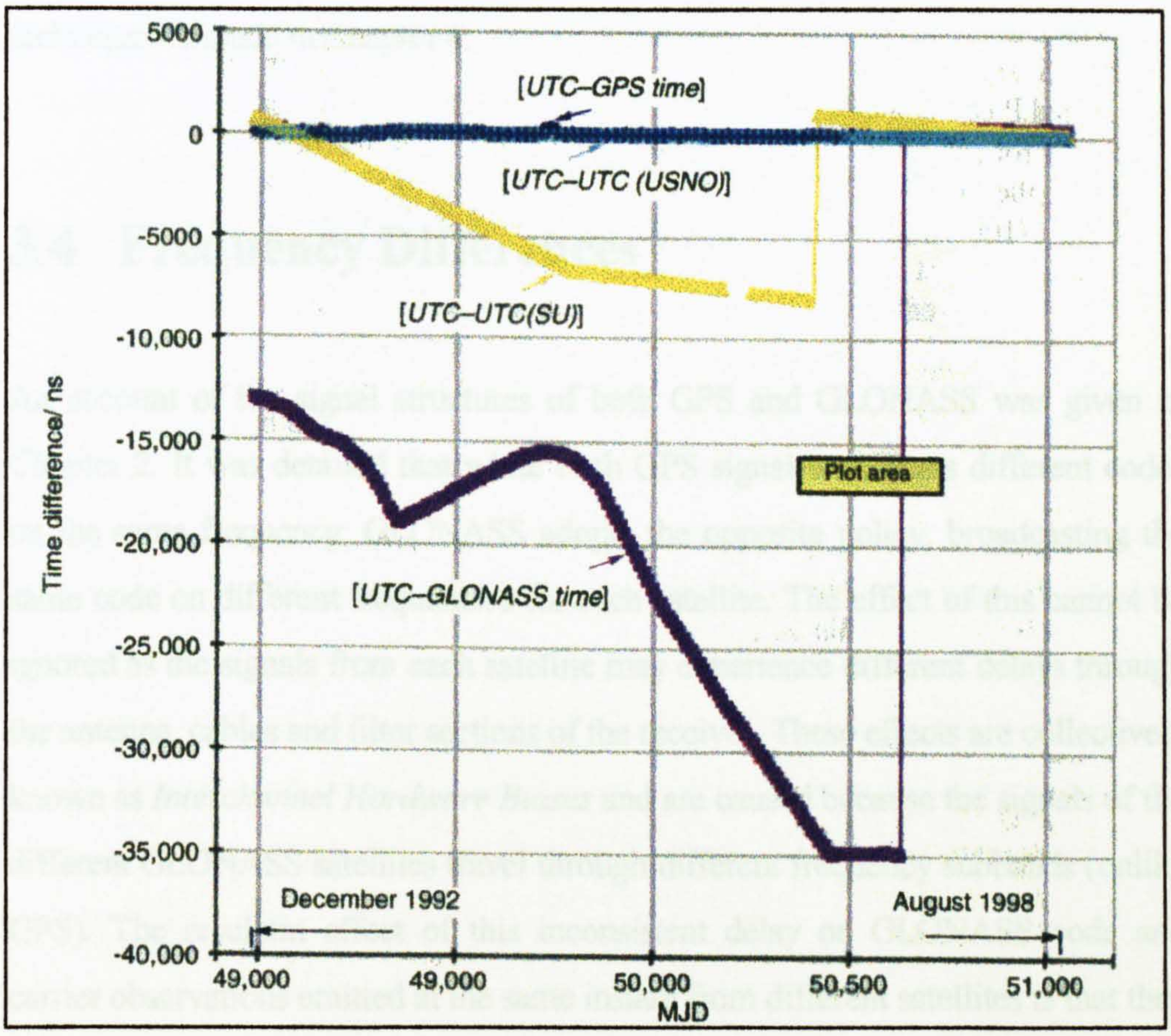

3.3.2 Accounting For the Time Difference

When using a combined GPS/GLONASS solution for positioning, the problem of the two system's using different time scales can simply be overcome by using an extra observation to solve for this extra receiver clock unknown. Thus to determine an instantaneous single point 3-Dimensional position, a minimum of five satellites are required, since there are five unknowns: latitude, longitude, altitude, GPS time, GLONASS time [Blighton, 1999]. By sacrificing an extra observation however, the levels of redundancy and integrity, which are two of the major advantages of the combined system, are reduced. Since the offset of the time-scales is consistent it is however possible, once this offset has been determined, to hold it fixed or model it with the apparent drift between them, and

revert to using four observations if need be. Plans have also been put forward to include the offset of GLONASS time from GPS time in the GLONASS navigation message. Further reference to this problem in application to different positioning techniques is made in Chapter 4.

3.4 Frequency Differences

An account of the signal structures of both GPS and GLONASS was given in Chapter 2. It was detailed that while each GPS signal broadcasts different codes on the same frequency, GLONASS adopts the opposite policy, broadcasting the same code on different frequencies for each satellite. The effect of this cannot be ignored as the signals from each satellite may experience different delays through the antenna, cables and filter sections of the receiver. These effects are collectively known as *Interchannel Hardware Biases* and are caused because the signals of the different GLONASS satellites travel through different frequency subbands (unlike GPS). The resultant effect of this inconsistent delay on GLONASS code and carrier observations emitted at the same instant from different satellites is that they are in fact measured by the receiver at slightly different times with respect to each other.

Receiver calibration and consistent manufacturing of receiver components can substantially reduce the effects of this hardware delay. [Hall et. al., 1997] indicate the extent of this delay on Ashtech GG24 receivers, to be at the metre level for GLONASS pseudorange observables, and to be sub decimetre on GLONASS carrier phase observables. There is however the potential that these effects may change with time, and that any change may not be consistent across the frequency range; for example, phase delays are known to change with temperature [Walsh & Daly, 1998]. [Dodson et. al., 1999] has quantified the extent of thermal effects on an Ashtech GG24 carrier phase solution to be in the region of 10 millimetres with a temperature differential of 25 degrees centigrade.

When dealing with carrier phase data, the fact that GLONASS broadcast on different frequencies, presents an additional problem. In a double difference solution (Chapter 4), each receiver clock correction is scaled by the frequency to change the units to cycles, but as each satellite's frequency is different, the resulting wavelength of each cycle will be different, and thus the observations cannot be cancelled. This is not the case for GPS observations and hence, by using this technique, receiver clock errors can be removed.

3.5 IGEX-98

It was partly with the aim of addressing the differences outlined above that IGEX-98 was initiated. It was an international campaign sponsored by the International Association of Geodesy (IAG) Commission VIII, International Coordination of Space Techniques for Geodesy and Geodynamics, the International GPS Service (IGS), the Institute of Navigation (ION), and the International Earth Rotation Service (IERS) [ION-1, 1998].

In many ways IGEX-98 can be compared to the IGS GPS test campaign of 1992. At that time only the broadcast GPS orbits were available and these were referenced to WGS 84 but not to the International Terrestrial Reference Frame (ITRF). The situation with GLONASS before IGEX was also that broadcast orbits only were available and these were referenced only to PZ-90.

The main purpose of IGEX-98 was to conduct the first Global GLONASS Observation Campaign for geodetic and geodynamics applications, some of the quoted objectives for which were:

- set up a global GLONASS observation network,
- determine GLONASS orbits of metre-quality or better in a well-defined Earth-fixed reference frame (namely, ITRF),
- determine transformation parameters between PZ-90 and ITRF and WGS 84,

- connect the GPS and GLONASS time systems [ION-1, 1999].

Initially observations were due to commence on 20th September 1998, and last until 20th December of the same year. However logistical difficulties delayed the start of the observing campaign until 19th October 1998. A three month observing period would have brought the campaign to an end in January 1999, but the launch of three new GLONASS satellites on 30th December prompted the experiment to be extended until 19th April 1999. Some products of IGEX, such as precise ephemerides are currently available, but information regarding other aspects, such as transformation parameters, are not due for publication until the meeting of the IGEX-98 workshop on 13th – 14th September 1999.

Figure 3.5 shows the global distribution of participating IGEX stations on 10th September 1998, and shows some sixty-three stations distributed over twenty-three countries. With each station continuously recording both GPS and GLONASS data simultaneously at a 30 second interval, there is no doubt that the results derived from this experiment will present a significant improvement on earlier findings. This can therefore only go to improve the potential of combined GPS/GLONASS systems.

Figure 3.5 The IGEX-98 Tracking Station Network [ION-2, 1998].

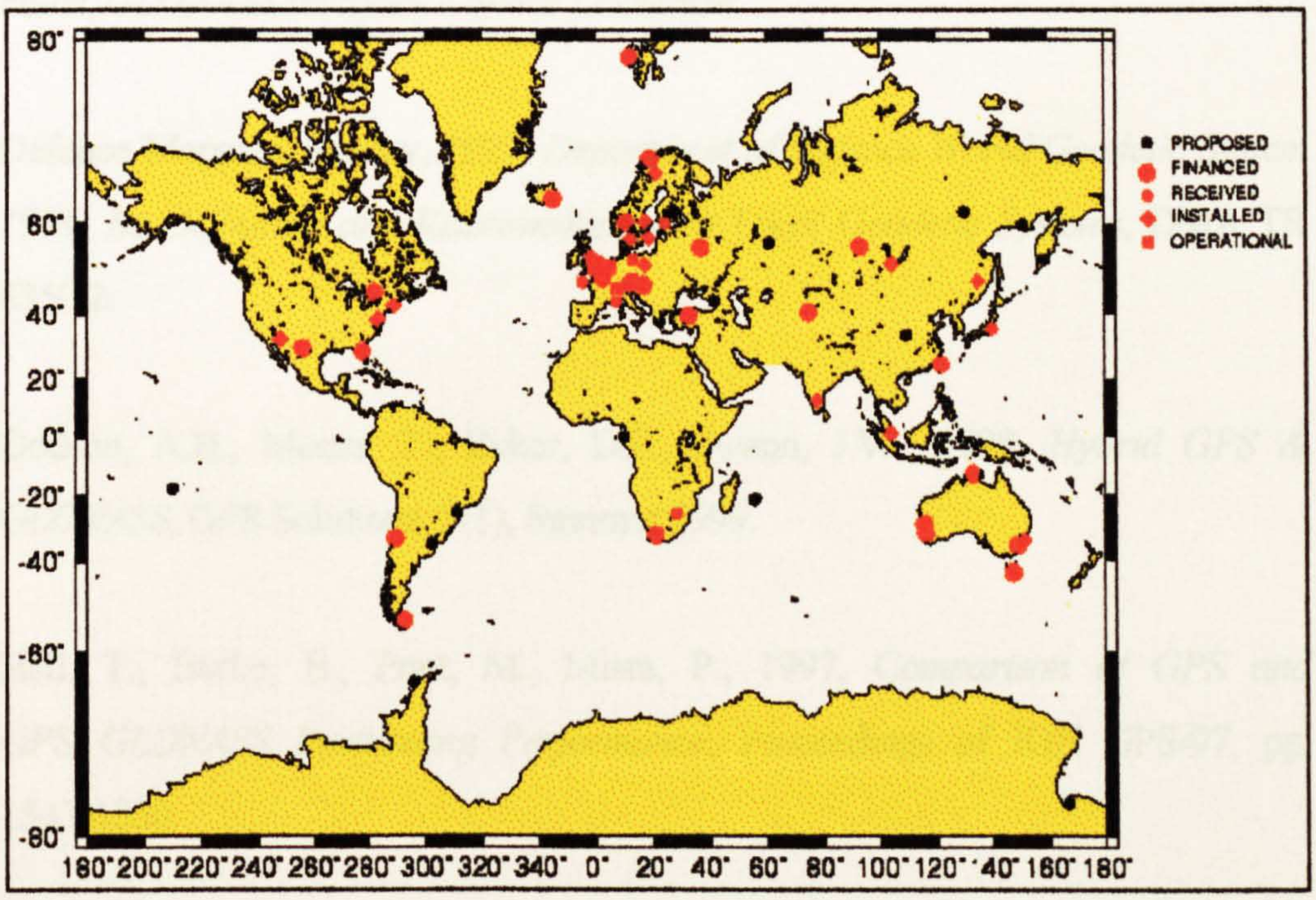

3.6 References

Ashtech, 1997, GG24 GPS+GLONASS Reference Manual, Document Number 630098, Revision B, March 1997. Ashtech Inc, 1170 Keifer Road, Sunnyvale, CA USA 94086

Bazlov, Y.A., Galazin, V.F., Kaplan, B.L., Maksimov, V.G., Rogozin, V.P., 1999, *GLONASS to GPS. A New Coordinate Transformation*, GPS World, January 1999, pp.54.

Blighton, R., 1999, *GPS+GLONASS = better solutions*, Surveying World, January/February 1999, pp.35.

Bomford, G., 1980, *Geodesy*, Fourth Edition, Clarendon Press.

Cross, P.A., 1990, *Position: Just What Does it Mean*, The Journal of Navigation, VOL.43 NO.2, May 1990.

CSIC, 1997, Coordinational Scientific Information Centre of the Russian Space Force, *GLONASS Interface Control Document*.

Defence Mapping Agency, 1997, *Department of Defence World Geodetic System 1984: Its Definition and Relationships with Local Geodetic Systems*, DMA TR 8350.2.

Dodson, A.H., Moore, T., Baker, D.F., Swann, J.W., 1999, *Hybrid GPS & GLONASS*, GPS Solutions, 3(1), Summer 1999.

Hall, T., Burke, B., Pratt, M., Misra, P., 1997, *Comparison of GPS and GPS+GLONASS Positioning Performance*, Proceedings of ION GPS-97, pp. 1543-1550.

ION-1, 1998, Institute of Navigation, URL **http://164.214.2.59/GandG/ion/descript.htm** accessed on 9th July 1998.

ION-2, 1998, Institute of Navigation, URL **http://164.214.2.59/GandG/ion/ION98PPR.htm** accessed on 30th March 1999.

Leick, A., 1995, *GPS Satellite Surveying*, Second Edition, John Wiley & Sons, Inc.

Lewandowski, W., Azoubib, J., 1998, *GPS+GLONASS: Toward Subnanosecond Time Transfer*, GPS World, November 1998, pp30.

Methley, B.D.F., 1991, *Geometrical Geodesy*, Lecture Notes, Department of Topographic Science, University of Glasgow, Glasgow, United Kingdom.

Misra, P.N., Abbot, R.I., Gasposchkin, E.M., 1996, *Integrated use of GPS and GLONASS: Transformation between WGS 84 and PZ-90*, Proceedings of ION GPS-96, pp. 307-314.

Walsh, D., Daly, P., 1998, *Precise Positioning Using GLONASS*, Geomatics Info Magazine, November 1998, pp.82.

Chapter 4

Satellite Observables, Positioning Principles and Techniques

4.1 Introduction

Satellite positioning can conveniently be considered to divide into two fundamental techniques. In the first of these an absolute point position is calculated using a single receiver, and is generally called *Stand Alone Positioning*. The second determines relative positions between two or more receivers and is typically referred to as *Differential Positioning*.

These stand alone and differential positioning concepts can be further divided by examining the receiver's motion. If the receiver is continually located over the same point, then this type of positioning is known as *Static Positioning*. If however, the receiver experiences some motion, then it is referred to as

Kinematic Positioning. The technique of positioning adopted is dependant on the category into which it falls, but is also a function of the accuracy level required and the observables available.

The principles and computational methods required for GPS, GLONASS and GPS/GLONASS stand alone and differential positioning are described in this chapter. Before doing this however, it is necessary to describe the error sources to which satellite navigation systems are susceptible, as some of these error terms appear in the descriptions of the various positioning techniques.

4.2 Factors Affecting Accuracy

Regardless of the positioning technique adopted, the achievable accuracy of satellite based positioning systems is governed by two main factors. These are the number of satellites in view and their distribution relative to the user, and secondly, the quality of the measurements.

4.2.1 Satellite Constellation Geometry

This first factor is referred to as *Satellite Constellation Geometry* and can be quantified by a series of parameters called *Dilution of Precision* (DOP). DOP can be thought of as being inversely proportional to the volume of a polyhedron with the user/receiver position at the apex, and the satellite positions defining the base. Basically, the more widely distributed the satellites, the lower the DOP, and the better the position estimate [Misra, 1995]. This DOP factor can be tailored, to describe the constellation in different terms, which are relevant for the required parameters of the position solution. Positional (PDOP) expresses the influence of the geometry on a Cartesian (X,Y,Z) position, and similarly Horizontal (HDOP) for horizontal

position, Geometrical (GDOP) solves Cartesian position and time, and Vertical (VDOP) for height.

4.2.2 Measurement Accuracy

The accuracy of the measurement is a function of the effect of a number of error sources. These can be grouped into three main areas, namely satellite related, atmosphere related and receiver related error sources.

4.2.2.1 Satellite Related Errors

Satellite related errors are due to either errors in the satellite clocks, or errors in their broadcast positions. The clock error is due to the fact that each satellite's clock is not precisely synchronised with the system time. However, as both GPS and GLONASS satellites each carry onboard four highly accurate and stable atomic clocks, it is possible to determine and model the clock offset for each satellite. In the case of GPS, these values are calculated at the MCS and uploaded to the satellites as part of the navigation message. They are then broadcast in the form of three polynomial terms within the navigation message representing it's offset, drift and ageing behaviour [Teunissen & Kleusberg, 1998]. The GLONASS corrections are calculated at the SCC and uploaded to the satellites where they are again relayed to the receiver as part of the navigation message, but this time take the form of two polynomial terms, representing offset and drift [CSIC, 1997].

The position of the satellite at a particular instant may be computed from information given in the broadcast ephemeris. Due to perturbations in each satellite's orbit, the accuracy of these calculated positions is limited to approximately 20 metres along track and 10 metres across track [CSIC, 1997]. This error translates directly into an error in position. This is one of the major

error sources in stand-alone positioning. More precise orbits with an accuracy of about 0.5 metres have been available for some time for GPS, from post-processed ephemerides determined by the International GPS Service (IGS). A similar service is now available for GLONASS as a product of the IGEX-98 campaign (Chapter 3).

In order to intentionally degrade the accuracy achievable through using GPS, the USDoD has implemented S/A, which further degrades both the quality of the orbits and satellite clock predictions. Further details of this are given in Chapter 2.

4.2.2.2 Atmosphere Related Errors

The effect of the atmosphere on satellite signals can be conveniently split into two components, the ionosphere and troposphere. The ionosphere lies between 50 and 1000 kilometres above the Earth's surface, and has the effect of delaying the pseudorange, but advancing the carrier phase. The cause of this error is due to the signal passing through the non-vacuous material of the ionosphere that consists of molecules and free electrons ionised by the ultra-violet and X-ray radiation of the Sun. It is the number of these free electrons that determine the level of this effect, the magnitude of which may reach as much as 10 metres in the day, falling to 1 to 2 metres at night [Dodson et. al., 1993]. With GPS observations, its navigation message contains a set of parameters which are used in the Klobuchar model to calculate the extent of this correction, further details of which can be found in ICD-GPS [1993]. The situation for GLONASS is somewhat different, as no such information is included and thus fixed model parameters must be assumed [Lewandowski et. al., 1997]. However, if observations from both systems are being combined, there is no reason why the GPS broadcast model parameters cannot be used for GLONASS also. Alternatively, if dual frequency observations are available, it is possible to directly remove the first order effects of the ionospheric delay, as

it is inversely proportional to the frequency of the signal squared. Further details on this effect can be found in Leick, [1995].

For satellite positioning work, the troposphere is considered to lie between the surface of the Earth and the ionosphere. It has the effect of delaying both pseudorange and carrier phase observations but, unlike ionospheric delay, it is not dependent on frequency, as it is a non-dispersive medium, and so cannot be accounted for by using dual frequency observations. The tropospheric delay can be thought of in two parts, the Wet and Dry delay, the combined effects of which can range from 2 - 2.5 metres at the zenith, to 20 - 28 metres at a 5 degree angle [Leick, 1995]. Approximately 90% of the total effect is caused by the dry delay, which is a function of pressure. It can be accurately accounted for using one of a number of models. The wet component is much more difficult to quantify, as water vapour cannot be accurately predicted and modelled, but fortunately only makes up 10% of the tropospheric delay. This equates to a delay of between 5 – 30 centimetres in continental midlatitudes and can be modelled to about 2 - 5 centimetres. For the most accurate modelling of the wet delay, direct measurements of the atmosphere's water vapour content must be made using a water vapour radiometer. Further information about the troposphere can be found in Dodson et. al. [1993].

A third source of error is introduced when, during transit from the satellite to the receiver, the signal experiences interference from local reflectors. This is known as *Multipath*, and means that the reflected signal received at the antenna will have a different path length to that of the direct signal. This difference in path length causes interference in the signal and can result in bias measurements. The extent of this bias depends on the location and type of antenna used, and the satellite elevation i.e. antennas without some kind of ground plane surrounded with reflectors (typically buildings or flat surfaces), and signals received from low elevation satellites will be particularly susceptible to multipath effects. The extent of this error depends on the frequency of the signal, as multipath can be detected over a certain fraction of a wavelength. Not only does this mean that code multipath is much larger than

carrier, but also that GLONASS code measurements are more susceptible to its effects than GPS. This is because the chipping rate for GLONASS is half that of GPS and thus, code wavelengths are double the size. Further information can be found on general multipath in Teunissen & Kleusberg [1998], and more specifically for GPS/GLONASS in Brodin [1997].

4.2.2.3 Receiver Related Errors

As is the case with satellite clocks, receiver clocks do not correspond exactly to system time. However, unlike satellites, most receivers do not have atomic clocks due to the expense involved (each Caesium clock onboard a GPS satellite costs approximately $1 million US dollars), and instead use cheap, but lower accuracy, quartz crystal oscillators. This means that the offset is, in most cases, large and variable, and for this reason cannot be accounted for in the same way as satellite clock error. Any receiver clock error manifests it effects in two ways. Firstly, there is an error in the measured time of flight of the signal, and secondly there is a time-tag error, which results from an incorrectly calculated satellite position at the time of the signal emission. Of the two, the first is by far the most serious as this error is scaled by the speed of light, instead of the speed of the satellite. To determine a position this receiver clock error must be removed or calculated.

Measurement noise within the receiver is another source of error. This kind of error is random with a magnitude which is determined by the precision by which the receiver can make measurements on the incoming signals. Better receivers make more precise measurements as they cross-correlate the PRN codes more effectively and this results in less noisy observables. As both the code and carrier loops are able to align with the incoming signals to a fraction of a percent of their chip lengths and wavelengths respectively, the level of noise experienced is much less for carrier than code. Also, as the GLONASS code wavelength is twice that of GPS, it is reasonable to expect GLONASS

code observations to experience twice the noise of the corresponding GPS observations [Brodin, 1997]. Since the nature of the error is random, its effect on position determination can be removed by averaging the measurements over time.

With GLONASS there is a further receiver associated error due to the different frequencies of the satellite signals taking different times to travel through the receiver components. This is discussed in more detail in Section 3.4 of Chapter 3.

4.2.3 Position Error

The collective effect of the errors described in Section 4.2.2 is referred to as the *User Range Error* (URE); its rms. value is denoted by σ_{ure}. The position error can be calculated in terms of this and DOP using equation 4.1.

$$\text{rms. position error} = \text{DOP} \times \sigma_{ure} \qquad (4.1)$$

Hall et. al. [1997] have quantified the pseudorange rms. URE for GLONASS to be in the range of 7 to 10 metres. This compares to values of 25 metres for GPS with S/A enabled and 6 metres with it switched off.

4.3 Pseudorange Measurements

This is the fundamental measurement of both the GPS and GLONASS and is conceptionally very simple, which was one of the initial design criteria for both systems.

On switching on the receiver, it locks onto the signals of all in-view satellites by generating its own equivalent of the ranging code transmitted by the satellite. These two codes are then compared and the receiver's replica code shifted until the two are coincident. This process is called *cross correlation* and is achieved by delaying the receiver-generated code in a *delay lock loop.* This delay equates to the time between the emission of the signal from the satellite and its detection at the receiver. This positioning measurement principle is illustrated in Figure 4.1.

Figure 4.1 Pseudorange Measurement Process

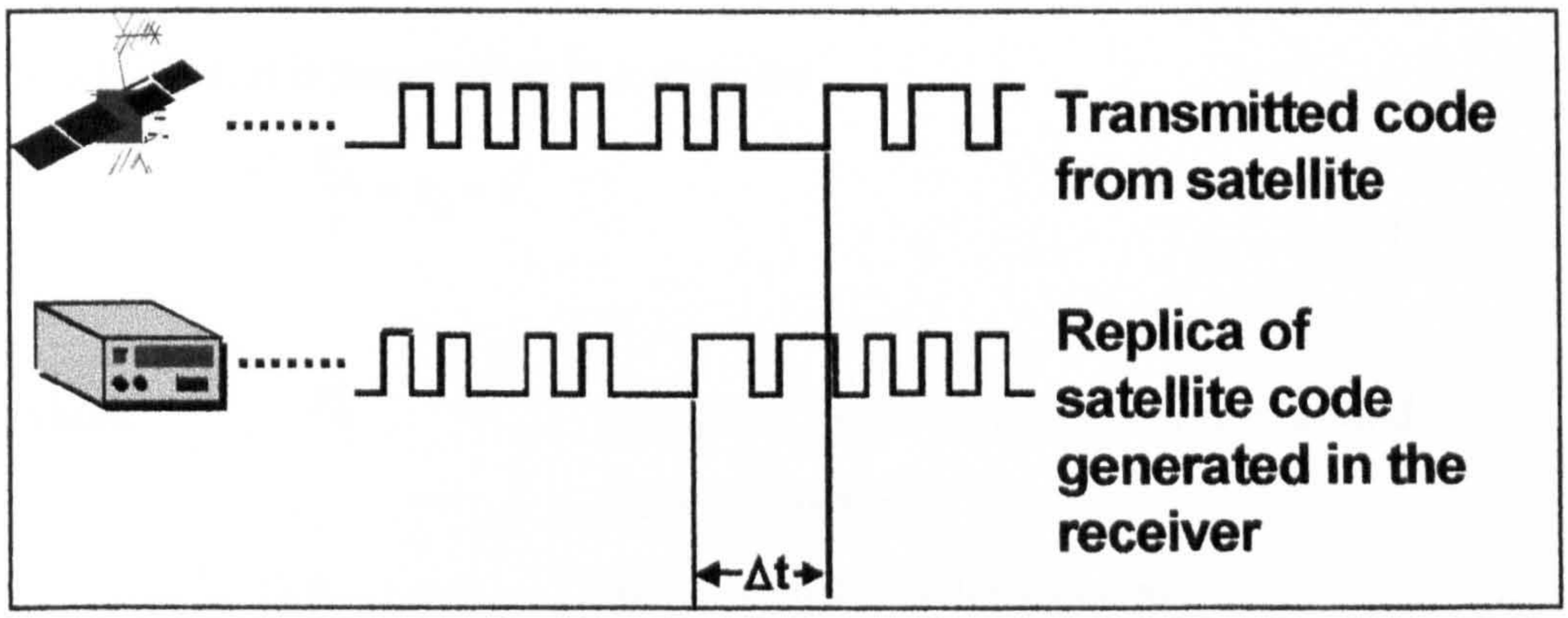

This time delay consists, in part, of the signal travel time and thus the range. However, this signal travel time measurement is contaminated by a series of errors, as outlined in Section 4.2. Thus, the measured value is known as a pseudorange, and can be expressed in the following way:

$$\rho_A^i = T_A - t^i \qquad (4.2)$$

where: ρ_A^i = pseudorange from satellite i to receiver A (seconds)

T_A = time of signal reception at receiver A, in the receiver time frame (seconds)

t^i = time of transmission from satellite i, in the satellite time frame (seconds)

Introducing the clock errors gives:

$$\rho_A^j = (\tau_A + \delta T_A) - (\tau^j + \delta t^j) \qquad (4.3)$$

where: τ_A = time of reception in the system time frame (seconds)

τ^j = time of transmission in the system time frame (seconds)

δT_A = receiver clock offset to system time (seconds)

δt^j = satellite clock offset to system time (seconds)

In addition, it is known that in a vacuum:

$$\frac{R_A^j}{c} = \tau_A - \tau^j \qquad (4.4)$$

where: R_A^j = geometric range between the receiver and satellite (metres)

c = speed of light (metres/second)

Therefore, after adding the remaining error sources:

$$\rho_A^j = \frac{R_A^j}{c} + \delta T_A - \delta t^j + \delta_{ion} + \delta_{trop} + e_A^j + \varepsilon_A^j \qquad (4.5)$$

where: δ_{ion} = ionospheric delay (seconds)

δ_{trop} = tropospheric delay (seconds)

e_A^j = receiver delay (seconds)

ε_A^j = noise term containing measurement noise and multipath (seconds)

Equation 4.5 is the basic ranging equation and is equally valid for both GPS and GLONASS.

4.4 Absolute Positioning by Pseudorange

The primary aim of both GPS and GLONASS is to provide instantaneous and unambiguous stand alone positioning anywhere on the Earth at any time. This is achieved by absolute positioning using pseudorange observations.

To determine position, three coordinate components (X,Y and Z) must be solved for. Theoretically, all that is needed to achieve this are three range measurements, but as has been outlined in Section 4.2, the measurements available are subject to various errors. However, Section 4.2 also details methods of overcoming atmospheric and satellite clock errors, and thus, it follows, that when operating with satellites from a single system, an unambiguous position can be calculated from making simultaneous observations to a minimum of four satellites. The fourth observation is used to determine the receiver clock's offset from system time. When observations from both systems are included it is necessary to determine the receiver clock offset from both system times, and therefore a minimum of five simultaneous range measurements are needed. This principle is outlined in Figure 4.2.

Figure 4.2 Principle of Absolute GPS/GLONASS Positioning

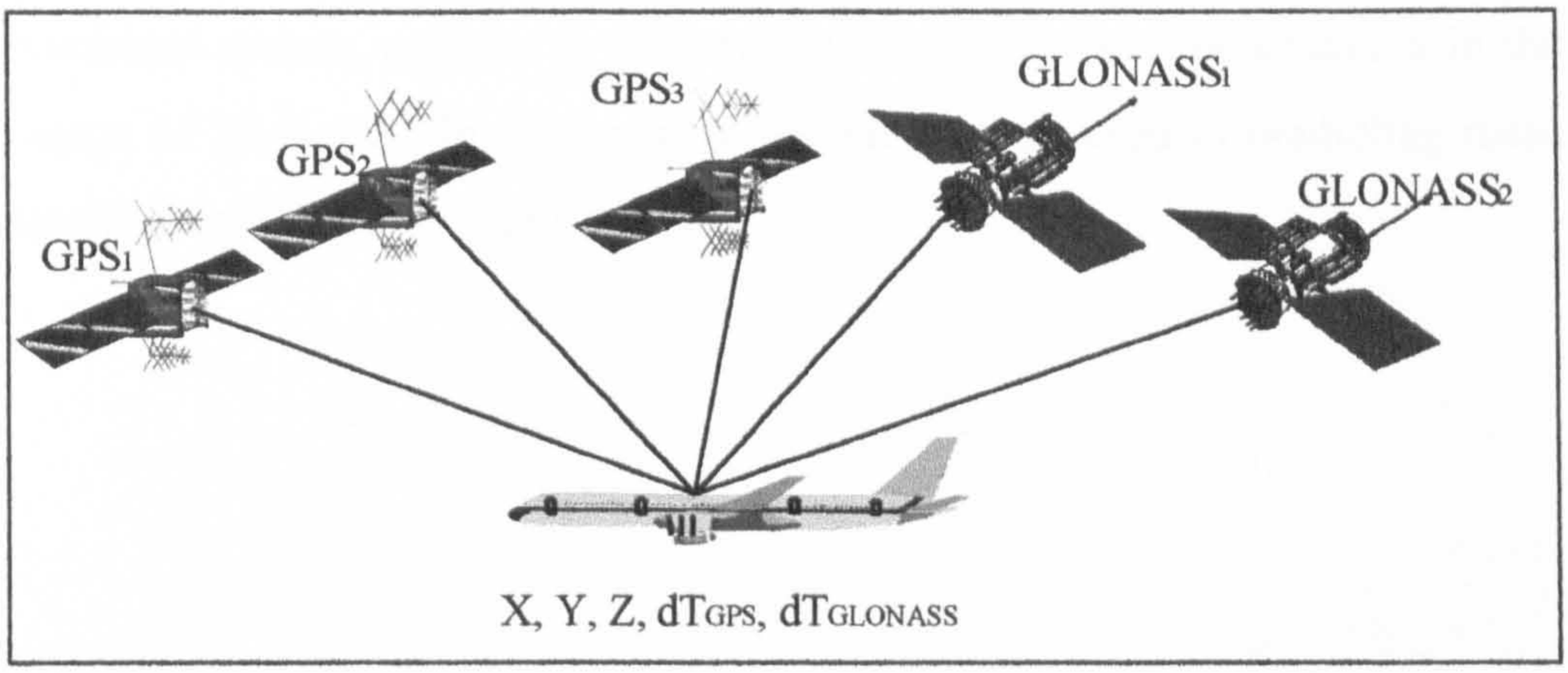

4.4.1 Solution Accuracy

The horizontal position accuracy that may be expected using this positioning technique is, for the GPS system, specified as better than 100 metres (95% of the time) with C/A code measurements, and between 30 to 40 metres for GLONASS. The reason for the comparatively poor performance of the GPS C/A measurements is due to the intentional degradation of the satellite signal using S/A (Chapter 2). However, the achievable accuracy in the field is very much a function of the DOP. This is especially true when dealing with GLONASS, as the current incomplete nature of the constellation results in a highly variable geometry, and thus highly variable achievable position accuracy. Indeed, there are periods during the day when a position solution, using the GLONASS system only, is not possible, due to there not being the minimum of four visible satellites. This is illustrated in Figure 4.3(A), which shows the PDOP values over a 24 hour period at the University of Nottingham on 7th April 1999 for the current GLONASS constellation of fifteen satellites. Figure 4.3(B) depicts the situation for the present GPS constellation of twenty-seven satellites, and finally Figure 4.3(C) gives the same information for the combined constellation of fourty-two useable satellites. It can be seen from this that the lowest (and most consistent) DOP values are achieved when using the combined system, and this is reflected in achievable position accuracy in the region of 20 metres. In all cases the elevation mask used in predicting these satellite visibilities was zero degrees.

Figure 4.3 Satellite Visibility and PDOP Values at the University of Nottingham

A

GLONASS ONLY

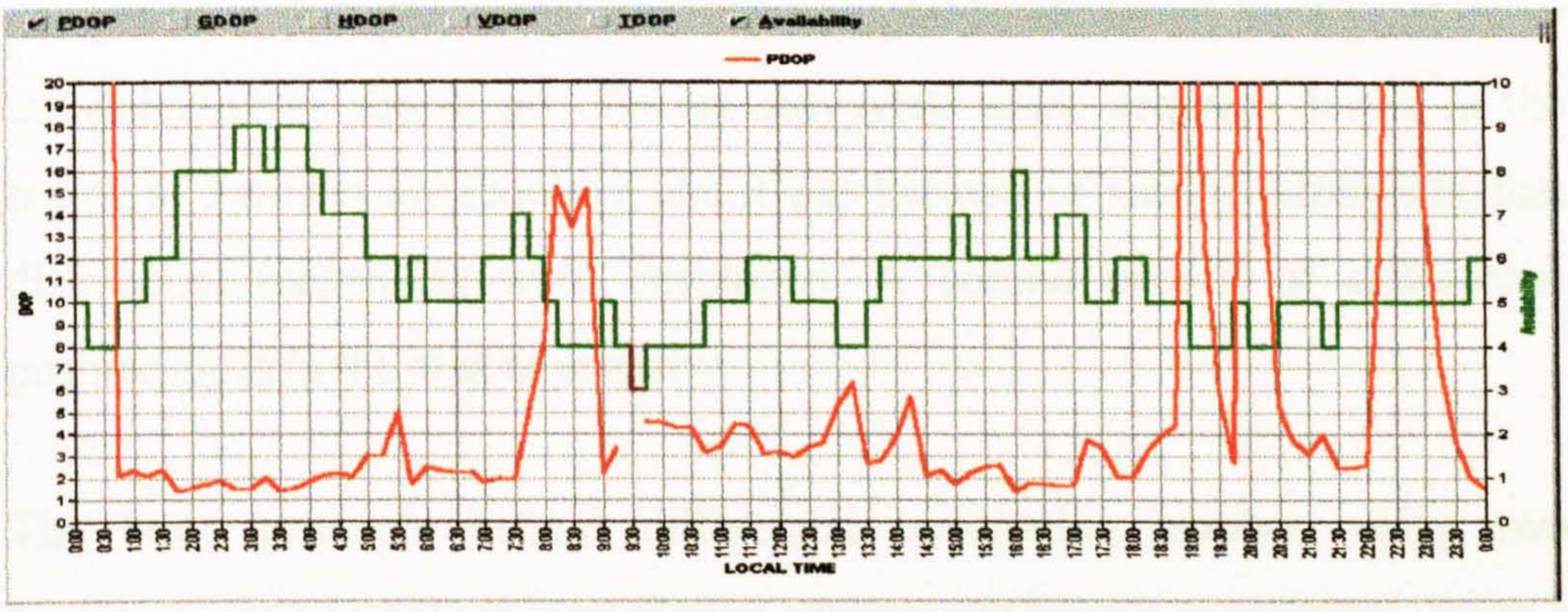

B

GPS ONLY

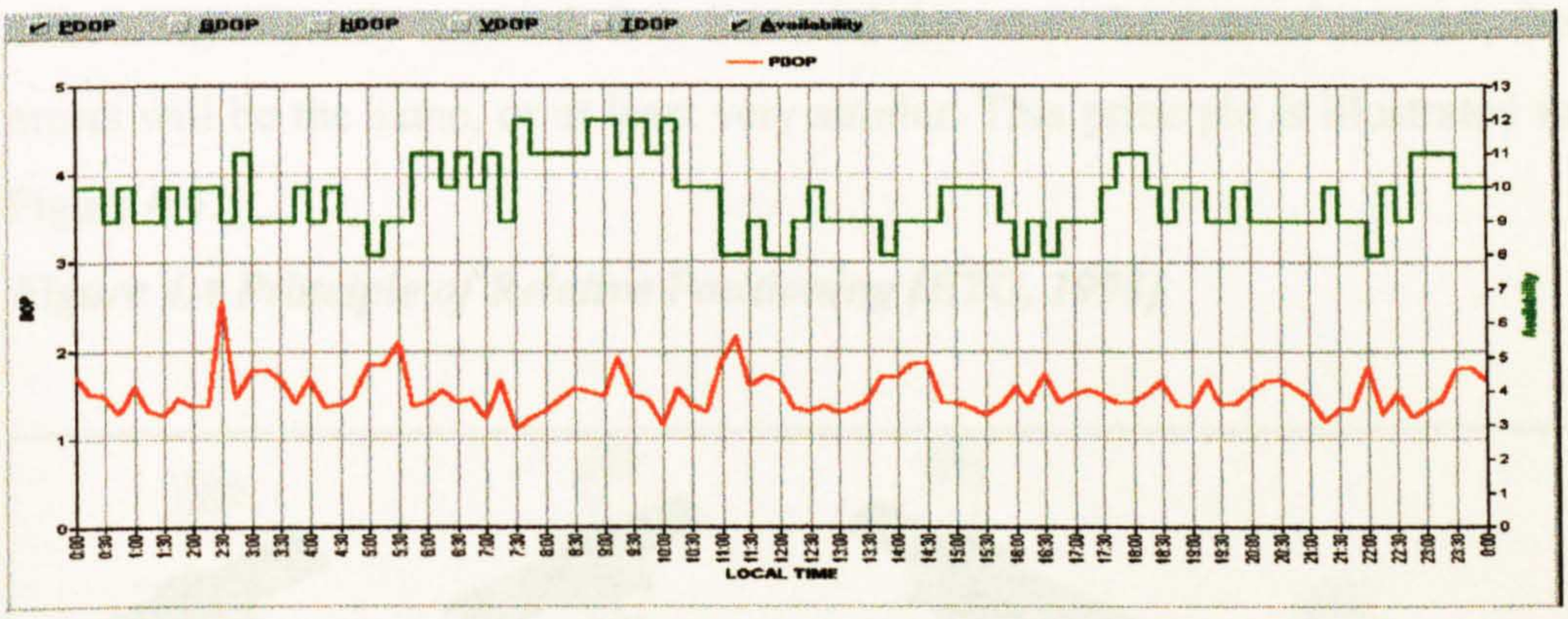

C

GPS/GLONASS

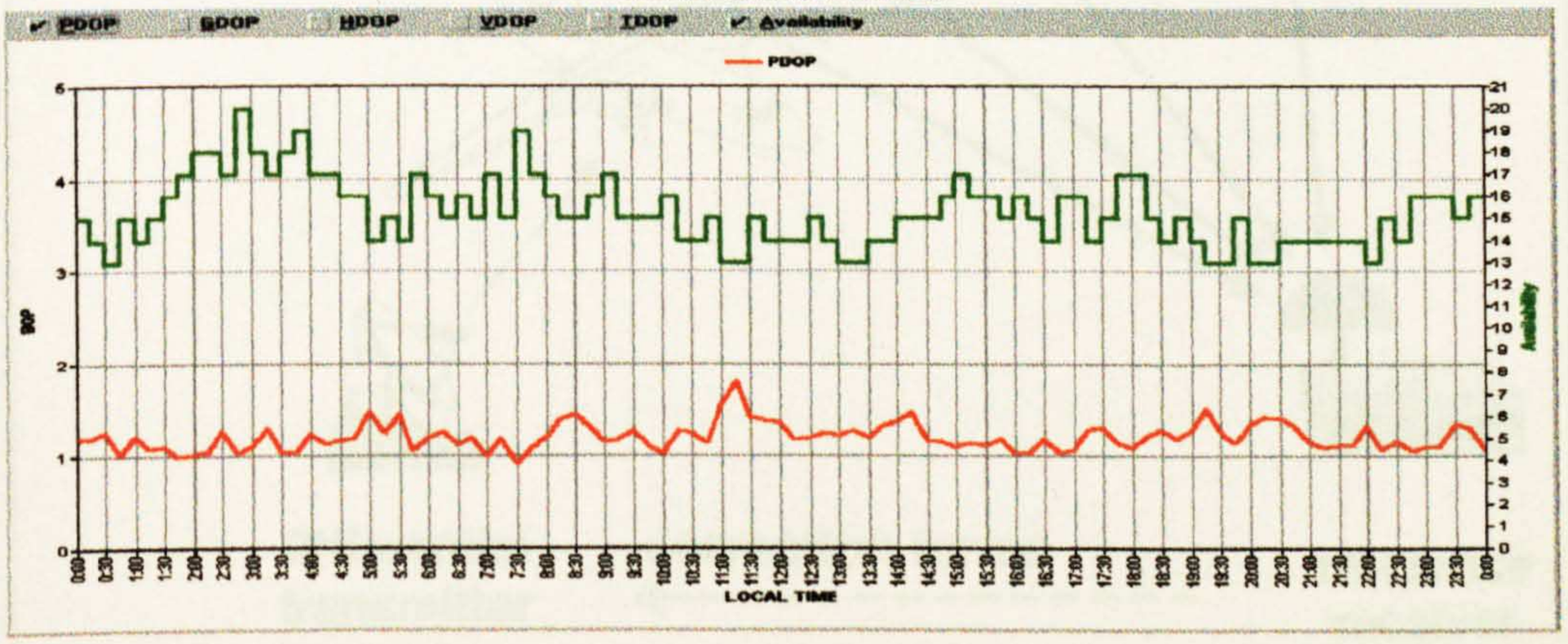

4.5 Pseudorange Relative Positioning

The accuracies quoted in Section 4.4.1 are, for applications such as vessel navigation in the open ocean, perfectly acceptable. However, for a great many tasks, including almost all offshore surveying tasks, accuracy levels in the region of 5 metres are required, and it was because of such requirements, that differential techniques were developed. A second benefit of differential positioning is in the area of integrity.

The basic principle behind differential positioning involves using two receivers, one of which is located over a point with known coordinates. Since a great many of the error sources of satellite navigation are spatially correlated, by combining measurements from both receivers, they should cancel or their effects significantly reduced. It is assumed that over the area of interest, the errors will be the same, or at least very similar. This principle is illustrated in Figure 4.4.

Figure 4.4 Principle of Relative Positioning [ETG, 1998]

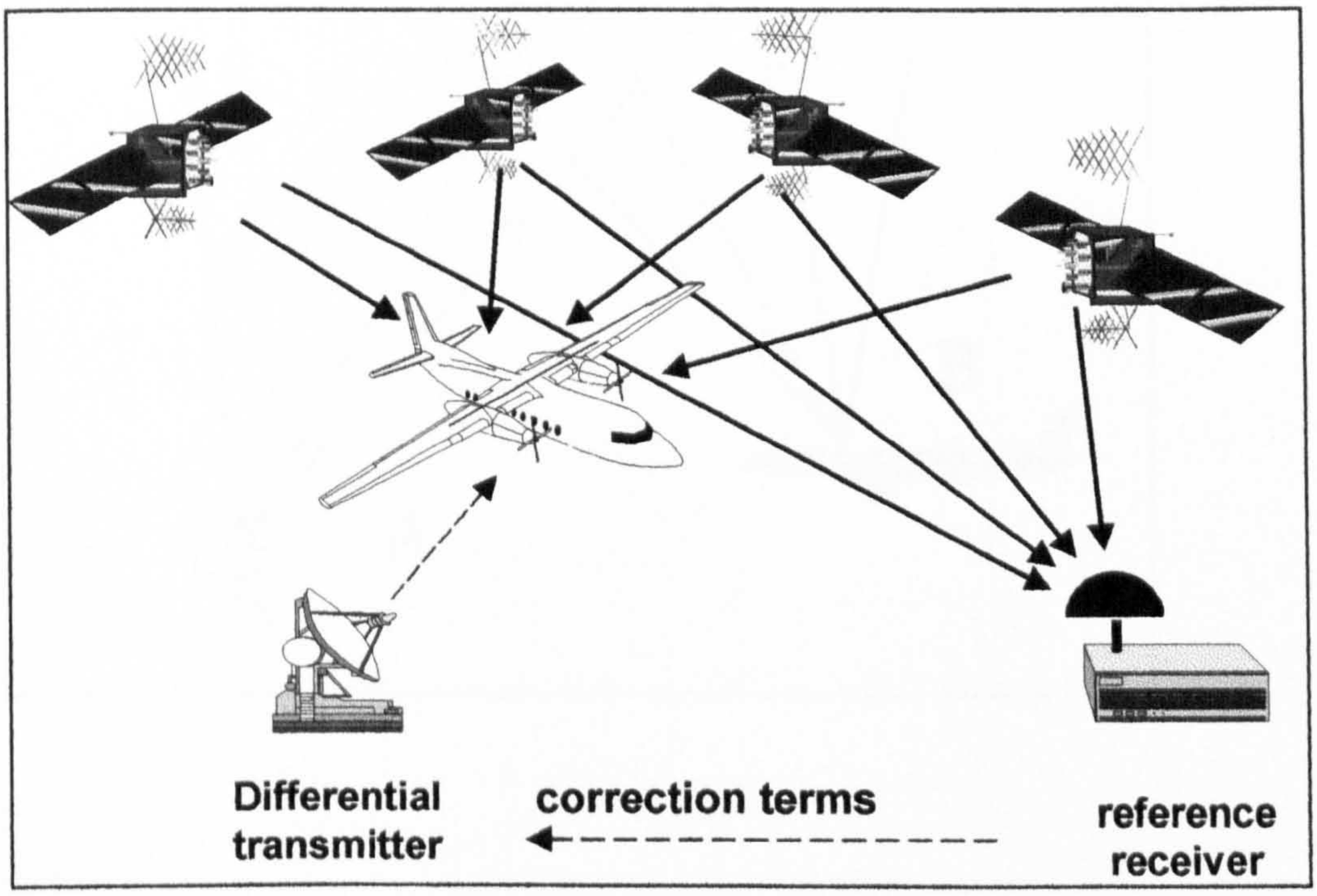

4.5.1 Pseudorange Differencing Techniques

Figure 4.5 gives a representation of a mixed satellite constellation of four satellites [two GPS (i and j), and two GLONASS (k and l)], broadcasting signals to two receivers (A and B). These observations can be differenced (subtracted) in two ways. *Single differencing by receiver* uses the signal emitted from the same satellite, and received at different receivers, whilst *double differencing* uses signals from two satellites received at two receivers. Each technique has a different effect on the error sources outlined in Section 4.2

Figure 4.5 Observations Available for Differencing

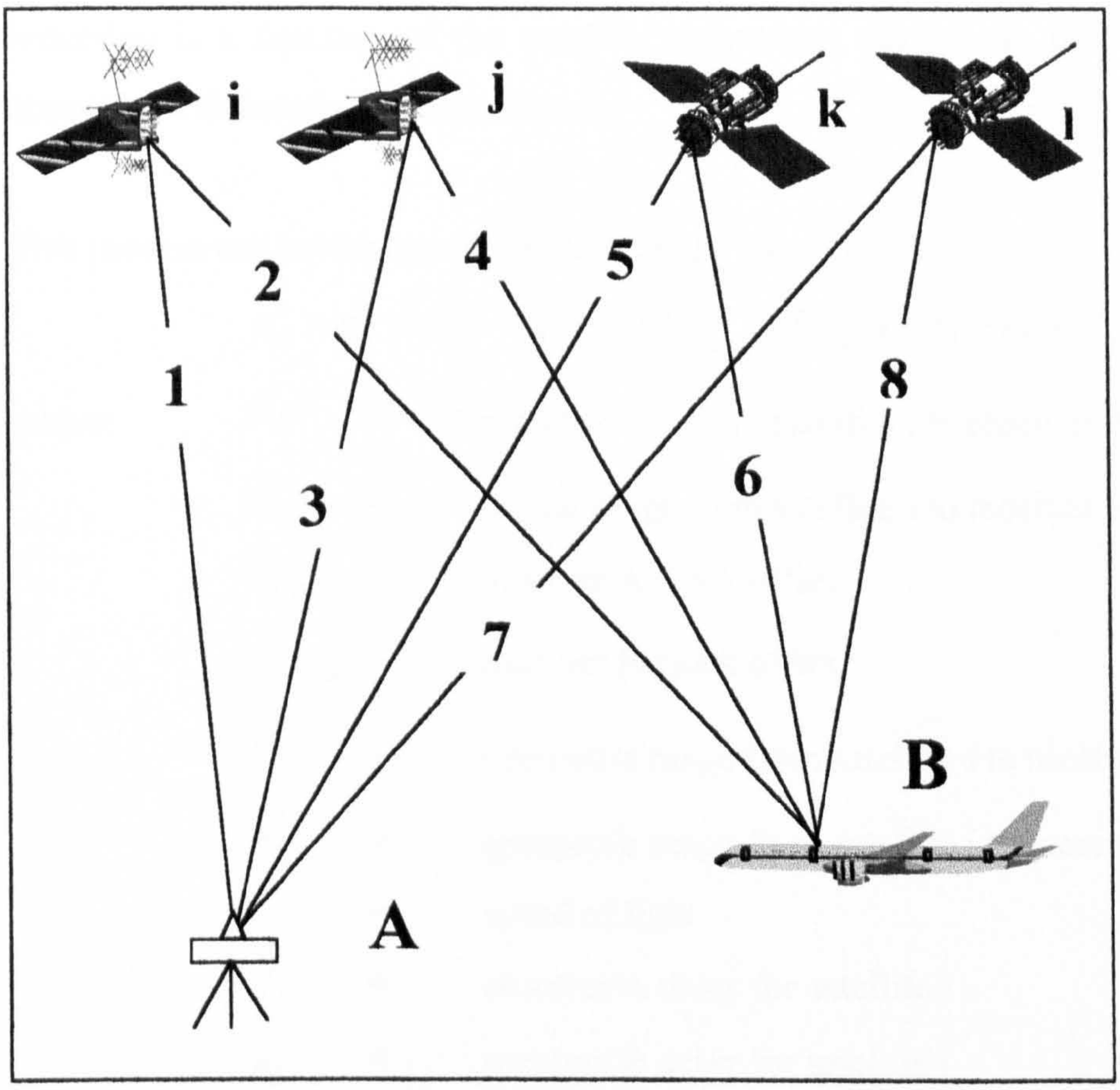

4.5.1.1 Single Differencing by Receiver

If the observations 1 and 2 from Figure 4.5 are differenced, the satellite related errors will be removed, or their effects reduced. However, the satellite clock error, and for GPS satellites, the effects of S/A, will only be completely removed if the signals received at each receiver were transmitted at the same time. If a large distance separates the receivers, then this results in a time mismatch, and some residuals will remain. The majority of this residual will be as a result of the rapid time varying nature of S/A. Any error in the broadcast satellite position should be almost completely removed as any time mismatch results in only a small change in position. Single differencing between receivers will also reduce the atmospheric errors, although the extent of this reduction is a function of the receiver separation, due to the fact that the atmosphere decorrelates with distance.

This process can be expressed mathematically as:

$$\rho_A^i - \rho_B^i = R_A^i - R_B^i + c \times (\delta T_{A_{GPS}} - \delta T_{B_{GPS}}) + e_A^i - e_B^i + \varepsilon_{AB}^i \quad (4.6)$$

where:

ρ_A^i	=	pseudorange from satellite i to receiver A
ρ_B^i	=	pseudorange from satellite i to receiver B
δT_{AGPS}	=	receiver A clock offset
δT_{BGPS}	=	receiver B clock offset
R_A^i	=	geometric range from satellite i to receiver A
R_B^i	=	geometric range from satellite i to receiver B
c	=	speed of light
e_A^i	=	receiver A delay for satellite i
e_B^i	=	receiver B delay for satellite i
ε_{AB}^i	=	single difference noise term

This equation is valid for both GPS and GLONASS satellites (for GLONASS the receiver clock is referenced to GLONASS time), and it shows how the

satellite clock error has been removed. If satellites from one system only are used, then, assuming that the coordinates of A are known, a minimum of four equations are needed to solve for the position of B and the difference between the receiver clocks in the time scale of that system. Indeed, in theory, a receiver clock correction calculated in one system, should be valid at the same epoch for the other. This is because both receiver clock values within each receiver come from the same oscillator, and thus the difference between the GPS time scales of receivers A and B should be identical to the corresponding offset between GLONASS time scales.

4.5.1.2 Double Differencing

If the single difference observable between satellite i and receivers A and B is differenced with the single difference observable between satellite j and receivers A and B (observations 3 and 4), then a double difference observable is formed. The equation for this is written as:

$$\rho^{ij}_{AB} = \rho^{i}_{AB} - \rho^{j}_{AB}$$

$$\rho^{ij}_{AB} = (\rho^{i}_{A} - \rho^{i}_{B}) - (\rho^{j}_{A} - \rho^{j}_{B})$$

$$\rho^{ij}_{AB} = [R^{i}_{A} - R^{i}_{B} + c \times (\delta T_{A_{GPS}} - \delta T_{B_{GPS}}) + e^{i}_{A} - e^{i}_{B} + \varepsilon^{i}_{AB}] -$$

$$[R^{j}_{A} - R^{j}_{B} + c \times (\delta T_{A_{GPS}} - \delta T_{B_{GPS}}) + e^{j}_{A} - e^{j}_{B} + \varepsilon^{j}_{AB}]$$

$$\therefore \quad \rho^{ij}_{AB} = R^{i}_{A} - R^{i}_{B} - R^{j}_{A} + R^{j}_{B} + \varepsilon^{ij}_{AB} \qquad (4.7)$$

where:

ε^{ij}_{AB} = double difference noise term

Equation 4.7 shows that, in the case of GPS, this processing technique removes both the satellite and receiver clock unknowns, leaving only the three coordinate unknowns. Because all GPS satellites broadcast on the same frequency the receiver hardware delay, which is a function of frequency, will cancel fully and so no residual error will be present. Thus, to solve for the three

coordinate unknowns, a minimum of three double difference observations need to be used, which are calculated from observations to four satellites.

When observations from both systems are mixed together the following situation arises:

$$\rho_{AB}^{jk} = \rho_{AB}^{j} - \rho_{AB}^{k}$$

$$\rho_{AB}^{jk} = (\rho_{A}^{j} - \rho_{B}^{j}) - (\rho_{A}^{k} - \rho_{B}^{k})$$

$$\rho_{AB}^{jk} = [R_A^j - R_B^j + c \times (\delta T_{A_{GPS}} - \delta T_{B_{GPS}}) + e_A^j - e_B^j + \varepsilon_{AB}^j] -$$
$$[R_A^k - R_B^k + c \times (\delta T_{A_{GLO}} - \delta T_{B_{GLO}}) + e_A^k - e_B^k + \varepsilon_{AB}^k]$$

$$\rho_{AB}^{jk} = R_A^j - R_B^j - R_A^k + R_B^k + e_{AB}^{jk} + \varepsilon_{AB}^{jk} \qquad (4.8)$$

where:

e_{AB}^{jk} = double difference receiver delay

Unlike in Equation 4.7, one cannot say with the same degree of certainty that the receiver delays in Equation 4.8 will automatically cancel, as one is referenced to GPS time and the other to GLONASS time. However, despite this fact, it is reasonable to assume that both are the same due to the reasons as detailed in Section 4.5.1.1.

4.5.2 Differential GPS/GLONASS

Differential GPS (DGPS) and Differential GLONASS (DGLONASS) are the names given to real time relative pseudorange positioning tasks. It is conceptually a very simple process whereby a receiver is located at a point with known coordinates, from whose observations range and range rate corrections to each satellite are calculated. Computing a range value between the known receiver and satellite locations and, then subtracting the observed value from this, derives these corrections. Each correction contains aspects of ephemeris, satellite and receiver clock, atmospheric and, in the case of GPS,

S/A errors. They are then time-tagged with the time the satellite signal was received, and transmitted to the user via a terrestrial radio link or communications satellite.

Depending on the range between the reference and remote receiver and the method of transmission used, there will be some offset from when the corrections were calculated and when they are used. This is called *Age of Correction,* and it is a very important factor in determining the achievable accuracy of the system. As this value increases, the size of any errors which decorrelate with time also increases. S/A is a rapidly varying error source, and so DGPS accuracy is affected to a much greater extent than DGLONASS by Age of Corection. Ashtech have quantified the effect of Age of Correction on both DGPS and DGLONASS, and these results are duplicated in Figure 4.6.

Figure 4.6 DGPS and DGLONASS Position Accuracy[Ashtech, 1997]

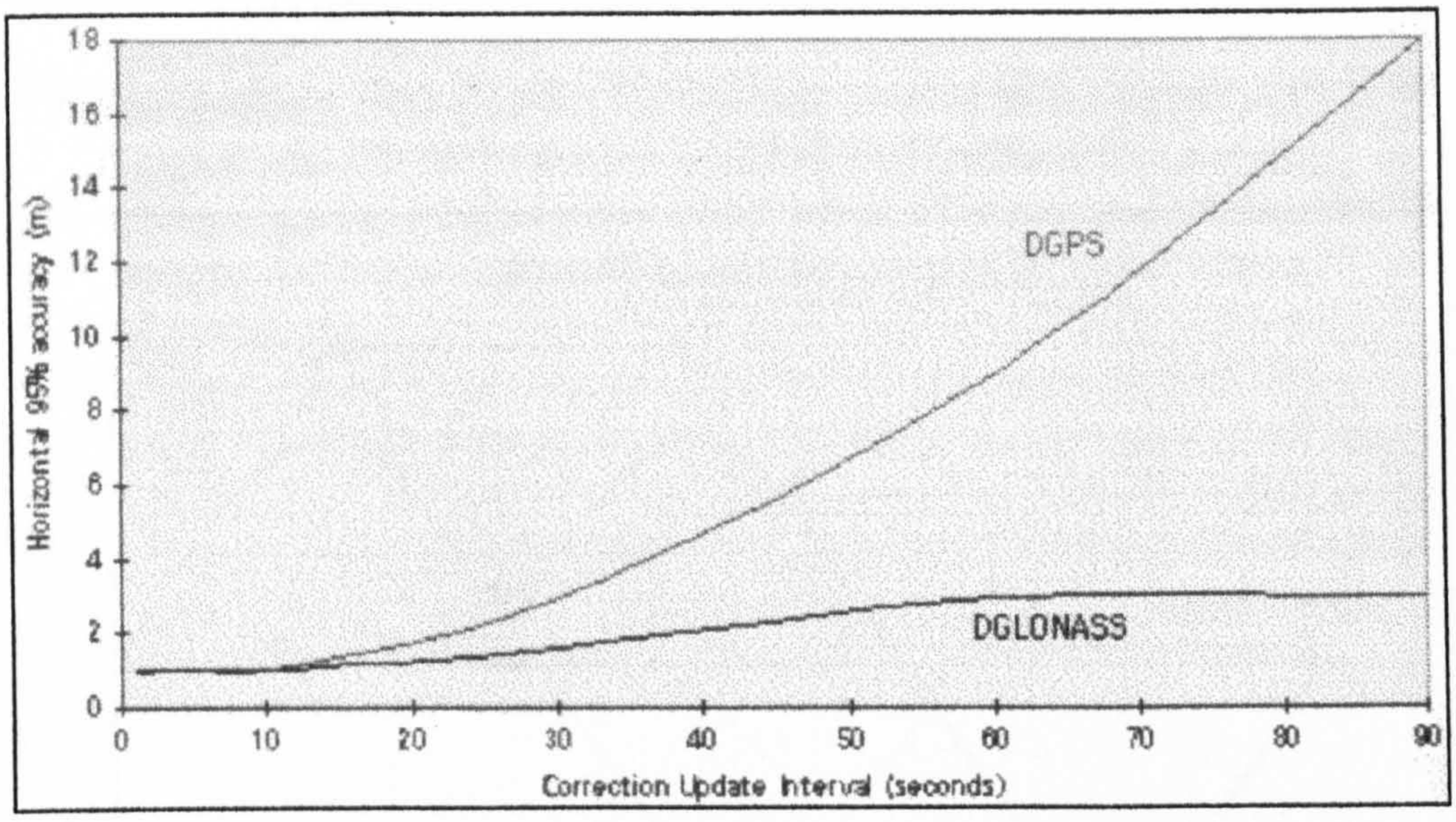

Figure 4.6 clearly shows how S/A dramatically degrades the accuracy of DGPS in comparison to DGLONASS once the Age of Correction exceeds 20 seconds. In a combined differential solution, increasing the weighting of the GLONASS observations as the Age of Correction increases can control the effect of S/A on GPS. This property has led to interest being shown from major differential service providers e.g. Racal and Fugro in offering GLONASS corrections.

Details of offshore field trials carried out by Fugro using DGLONASS in comparison to DGPS can be found in Orpen and Hinsch [1997].

4.6 Carrier Phase Measurement

If both the ranging and navigation codes are removed from the incoming satellite signals, what is left is the raw carrier. The wavelength of the carrier is, for L1 GPS, 19 cm and, for L1 GLONASS between 18.63 - 18.75 cm. As this value is much smaller than the corresponding pseudorange wavelengths it can be measured much more precisely; to the order of a few millimetres. As with pseudorange measurements, these carrier phase measurements are obtained by comparing the signal generated by the satellite with one replicated in the receiver. The resultant observable is the phase difference between the two and is illustrated in Figure 4.7.

Figure 4.7 The Carrier Phase Observable

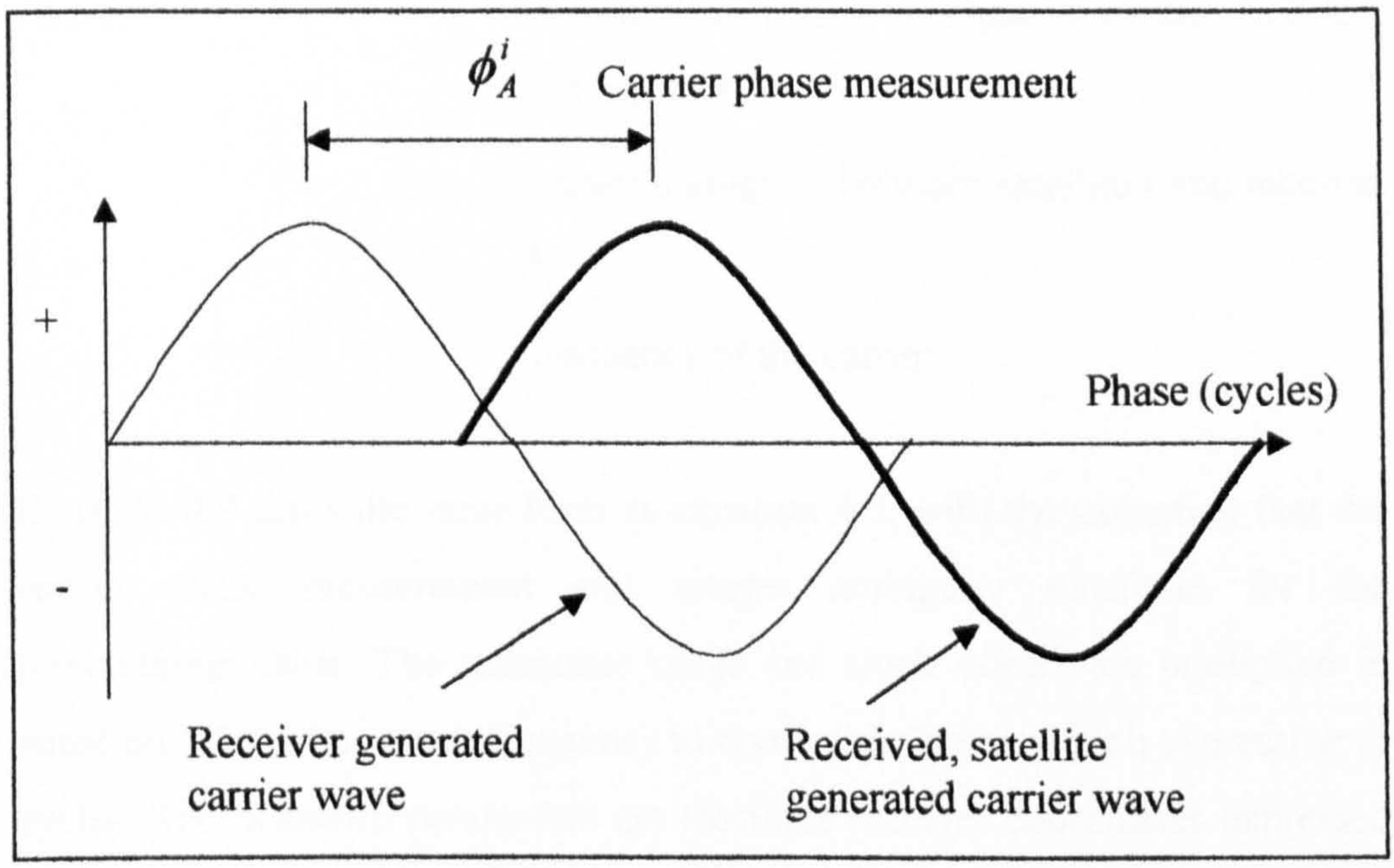

The problem with the measurement depicted in Figure 4.7 is that it is ambiguous, as only the fractional part of the wavelength is measured. It

therefore cannot be used directly to determine a satellite to receiver range, as there is an addition unknown with each observation. These unknowns are integer numbers of whole wavelengths and are referred to as the *initial integer ambiguities*. From the instant the initial fractional wavelength is measured, the receiver starts to count the number of full cycles it receives from each satellite. This enables the change in range to be determined and, more importantly, when the initial integer ambiguity is solved for, it can be used with this value to determine an unambiguous range. This remains the case until there is a break in the carrier count when, at which point, the count starts again and a new ambiguity value has to be determined. Such an occurrence is referred to as a *cycle slip* and is normally caused by the satellite signal being temporarily obstructed from the antenna by objects such as trees and buildings.

The basic carrier phase observable can be expressed in the same way as the pseudorange e.g. as in equation 4.5:

$$\phi_A^i = \frac{f^i}{c} R_A^i + f^i(\delta T_A - \delta t^i) - N_A^i - d_{ion} + d_{trop} + e_A^i + \varepsilon_A^i \quad (4.9)$$

where:
- ϕ_A^i = measured difference in phase between satellite i and receiver A
- N_A^i = integer ambiguity between satellite i and receiver A
- f^i = frequency of the carrier

Equation 4.9 takes the same form as equation 4.5, with the exception that the carrier phase measurement and integer ambiguity substitute for the pseudorange value. The geometric range and clock offsets are multiplied in equation 4.5 by the carrier frequency to convert the units of each expression to cycles. The unknown parameters are the three receiver coordinates expressed through the geometric range, the receiver clock offset and the initial integer ambiguity.

If dual frequency observations are available, they can be combined linearly to form different observables. An example of one such technique is the *widelane* combination, whereby the L2 measurement is subtracted from the L1 measurement. In the case of GPS, the resultant observable has an equivalent frequency of 347.82 MHz and a wavelength of 86.2 cm. This increased wavelength has potential benefits in ambiguity search and cycle slip detection procedures. However, as the only combined system receivers available throughout the project were L1 only units, these processes were not examined. Further information on them can be found in Ffoulkes-Jones [1990], and a full derivation of the carrier phase equation, in Leick [1995].

4.7 Carrier Phase Relative Positioning

From equation 4.9 it can be seen that the basic carrier phase observable suffers from the same sources of error as the pseudorange observation. Thus, as with pseudoranges, carrier phase observations can be differenced in various ways to remove some of these errors. There is however an additional unknown that needs to be accounted for when dealing with carrier phase observations: the integer ambiguity of each observation needs to be resolved if centimetre level positioning accuracy is to be achieved.

4.7.1 Single Differencing by Receiver

Referring to Figure 4.5, if observations 1 and 2 are differenced, then the following equations can be derived:

$$\phi^{j}_{AB} = \phi^{j}_{A} - \phi^{j}_{B}$$

$$\phi^{j}_{AB} = [\frac{f^{j}}{c} R^{j}_{A} + f^{j}(\delta T_{A_{GPS}} - \delta t^{j}) - N^{j}_{A} - \delta_{ion} + \delta_{trop} + e^{j}_{A} + \varepsilon^{j}_{A}]$$

$$-[\frac{f^{j}}{c} R^{j}_{B} + f^{j}(\delta T_{B_{GPS}} - \delta t^{j}) - N^{j}_{B} - \delta_{ion} + \delta_{tro} + e^{j}_{B} + \varepsilon^{j}_{B}]$$

$$\phi^i_{AB} = \frac{f^i}{c}(R^i_A - R^i_B) + f^i(\delta T_A - \delta T_B)$$

$$- N^i_A + N^i_B + e^i_A - e^i_B + \varepsilon^i_{AB}$$

$$\phi^i_{AB} = \frac{f^i}{c} R^i_{AB} + N^i_{AB} + f^i \delta T_{AB_{GPS}} + e^i_{AB} + \varepsilon^i_{AB} \qquad (4.10)$$

where:

ϕ^i_{AB} = single difference carrier phase, between satellite i and receivers A and B

N^i_{AB} = single difference integer ambiguity between satellite i and receivers A and B

R^i_{AB} = single difference range between satellite i and receivers A and B

$\delta T_{AB\,GPS}$ = single difference receiver clock offset

Equation 4.10 is valid for both GPS and GLONASS observations (for GLONASS the receiver clock is referenced to GLONASS time), and it has the same effect on the error sources as outlined in Section 4.5.1.2 for single difference pseudorange observations. A minimum of four satellites giving four, single difference observations are needed to resolve the integer ambiguities. Again this is the case for GPS, GLONASS or GPS/GLONASS for the reasons detailed in Section 4.5.1.1.

4.7.2 Double Differencing

As with pseudoranges, it is possible to further difference equation 4.10 with a second single difference between the same receivers and another satellite, to form a double difference. If, as shown in Figure 4.5, satellite j (observations 3 and 4) is used, then equation 4.11 can be derived:

$$\phi^{ij}_{AB} = \phi^i_{AB} - \phi^j_{AB}$$

$$\phi_{AB}^{ij} = [\frac{f^i}{c} R_{AB}^i + N_{AB}^i + f^i \delta T_{AB_{GPS}} + e_{AB}^i + \varepsilon_{AB}^i]$$

$$-[\frac{f^j}{c} R_{AB}^j + N_{AB}^j + f^j \delta T_{AB_{GPS}} + e_{AB}^j + \varepsilon_{AB}^j]$$

$$\phi_{AB}^{ij} = \frac{f}{c} R_{AB}^{ij} + N_{AB}^{ij} + \varepsilon_{AB}^{ij} \qquad (4.11)$$

where:

ϕ_{AB}^{ij} = double difference carrier phase observable

N_{AB}^{ij} = double difference integer ambiguity

R_{AB}^{ij} = double difference range between satellites i and j and receivers A and B

Equation 4.11 is valid for any pair of GPS satellites used in the double difference process. As all GPS satellites transmit on the same frequency, then $f^i = f^j$, and the receiver clock terms, which are scaled by frequency, cancel [Ashkenazi et. al., 1998]. The same is true for the receiver hardware delays. The unknowns remaining after double differencing are the receiver coordinates and the double difference integer ambiguity. As with GPS single differencing, a minimum of four satellites is required for a double difference solution. However, only three double difference ambiguities are solved for, instead of four, as the double difference algorithm contains a difference between satellites.

When dealing with double difference observables formed from a GPS and GLONASS satellite, or indeed two GLONASS satellites, the situation becomes much more complicated because each satellite broadcasts on a different frequency. This means that in addition to the possibility of a residual receiver delay, the receiver clock correction terms no longer cancel, as each is scaled by a different frequency. Referring again to Figure 4.5, if satellites i and k are used (observations 1, 2, 5 and 6), the equation for this scenario can be written as:

$$\phi_{AB}^{ik} = \phi_{AB}^{i} - \phi_{AB}^{k}$$

$$\phi_{AB}^{ik} = [\frac{f^i}{c} R_{AB}^i + N_{AB}^i + f^i \delta T_{AB\,GPS} + e_{AB}^i + \varepsilon_{AB}^i] -$$

$$[\frac{f^k}{c} R_{AB}^k + N_{AB}^k + f^k \delta T_{AB\,GLO} + e_{AB}^k + \varepsilon_{AB}^k]$$

$$\phi_{AB}^{ik} = \frac{f^i}{c} R_{AB}^i - \frac{f^k}{c} R_{AB}^k + N_{AB}^{ik} + f^i \delta T_{AB_{GPS}}$$

$$- f^k \delta T_{AB_{GLO}} + e_{AB}^{ik} + \varepsilon_{AB}^{ik} \qquad (4.12)$$

A further observable, which removes the ambiguity term if no cycle slips occur, can be created if the double difference equation is differenced with respect to time. This is called a triple difference, but after successive differencing the Signal to Noise Ratio (SNR) degrades considerably, and thus is particularly susceptible to cycle slips (Section 4.7.3). Triple differencing has not been implemented in any software routines described in this thesis, and thus will not be described further. A full description can however be found in Leick [1995].

4.7.3 Cycle Slips

As mentioned in Section 4.6, the computed integer ambiguity value for a satellite only remains valid whilst lock is maintained on that satellite signal. When this lock is lost and then reacquired, the receiver will assign a new integer ambiguity value to the satellite, and thus a new integer ambiguity value will have to be determined before unambiguous ranges to that satellite can again be determined. These cycle slips can be as a result of incorrect signal processing within the receiver, high receiver accelerations, interference from other radio sources, high ionospheric activity and most commonly from the obstruction of the satellite signal by objects such as trees and buildings. As the carrier phase characteristics of GPS and GLONASS are very similar, both are affected to a similar degree by this process.

In order to use carrier phase measurements for precise and reliable positioning some means of detecting and repairing cycle slips must be implemented, and thus has been the subject of a great deal of research, resulting in a variety of techniques being developed. If the receiver is static, then the rate of change of the carrier phase should be smooth, and coincide with the change in the satellite orbit. The triple difference carrier phase observable can be used to detect a cycle slip in these circumstances, as the result will be an obvious spike in the solution residual. If however the receiver is moving it will be impossible to distinguish between the effect of receiver motion and the presence of a cycle slip.

When dealing with Kinematic data, some other means of detecting cycle slips must therefore be utilised. This topic has been the subject of recent research at the University of Nottingham [Roberts, 1997], with a summary of the techniques investigated presented below:

1. As both the pseudorange and carrier phase data is measured simultaneously, it is therefore possible to directly compare the epoch by epoch change in pseudorange with the change in carrier phase. If the difference between these exceeds a pre-set tolerance it is then reasonable to assume that a cycle slip has occurred.

2. If L1/L2 data is available it is possible to use the *4 Observable Equation* (4.13), which was originally formulated by Melborne [1985].

$$N_{LW} = (\phi_{L1} - \phi_{L2}) - \frac{(f_{L1} - f_{L2})}{(f_{L1} + f_{L2})} \times \left(\frac{\rho_{L1}}{\lambda_{L1}} + \frac{\rho_{L2}}{\lambda_{L2}} \right) \qquad (4.13)$$

where:

N_{LW} = Wide Lane Ambiguity (cycles)

ρ = L1 or L2 Pseudorange (metres)

λ = L1 or L2 Carrier Phase Wavelength

(metres)

f = L1 or L2 Frequency (Hz)

ϕ = L1 or L2 Carrier Phase (cycles)

Generally N_{LW} varies smoothly from epoch to epoch, and thus any large jump in its value can be attributed to a wide lane cycle slip.

3. In addition to the carrier phase and pseudorange data, most receivers also output Doppler readings at each epoch. These values can be used to forward predict the carrier phase value to the next epoch. Again, if the difference between the computed and observed values exceed a pre-set tolerance, then a cycle slip can be flagged.

4. Ionospheric residual is a measure of the difference between the L1 and L2 carrier phase measurements caused by the different effect of the ionosphere on the observations. It changes slowly with time unless a cycle slip occurs which will cause a sudden jump in its value, indicating the presence of the cycle slip. As with the 4 Observable Equation, L1/L2 data must be available if this technique is to be used.

4.7.4 Phase Smoothing of Pseudoranges

It has already been stated that it is only possible to measure a satellite to receiver range directly using a pseudorange. It is however possible to measure the changes in these ranges over time using both carrier phase and pseudorange observations. As these changes should be identical between the two observations, the only difference being the opposite effect of the ionosphere on the measurements (Section 4.2.2.2), it is therefore possible to use the better

precision of the carrier phase observations to improve or smooth the pseudorange measurement. However, the use of carrier phase data carries with it the associated risks of cycle slips which, if undetected, will contaminate the accuracy of the phase smoothed pseudorange. The results of all pseudorange tests presented in this thesis are derived from GPS and GLONASS phase smoothed pseudoranges, as recommended by Ashtech. Within both the Ashtech and Bernese RINEX converters (Chapter 5), this process of phase smoothing is identical, as both apply the smoothing corrections found in the Raw Binary files. There is no mention of how this smoothing function is generated in any Ashtech manuals read by the author, but after personal correspondences with Ashtech California, the following information was obtained.

The smoothing function is calculated in the receiver by averaging the (slowly varying) difference between carrier phase and raw range, both first being converted to metres. This correction is calculated as:

Correction = (average range-phase) – (instantaneous range-phase)

The time constant used in deriving the average value was also quoted as being somewhere in the region of 30 seconds, but no specific value was given.

4.7.5 Adapted Double Difference Carrier Phase Processing Strategies

The difficulty, as outlined in Section 4.7.2, of receiver clock corrections not cancelling in the double difference GPS/GLONASS or GLONASS phase observable, making it impossible to successfully resolve integer ambiguities, has led to the development of a variety of approaches to processing GLONASS and GPS/GLONASS carrier phase data. The principles of some of these processing strategies and the techniques adopted within the GAS software are described below.

Work at the University of Leeds [Walsh and Daly, 1996] has looked at the possibility of initially using GPS only observations in a conventional ambiguity search procedure. Once these GPS ambiguities are correctly resolved, a position, accurate to centimetre level, is then available and this is then used to determine the errors in the GLONASS carrier phase measurements (including receiver clock error) outlined in Section 4.7.2. Whilst lock is kept on at least four GPS measurements, it is possible to monitor and update the GLONASS related errors and the GLONASS measurements may also be included in the final position solution, especially if the GPS PDOP is high i.e. to improve the poor GPS position. If however, the number of visible GPS satellites falls below the minimum number (four) for a continued position solution, the GLONASS measurements can be included in the positioning computation using the last calculated calibration values. This is where the major benefit of such a technique lies, and it was developed with the aim of being used on engineering sites for static positioning where, after successful initialisation, the antenna would be moved into areas with a great many obstructions, and thus not enough visible GPS satellites.

Rossbach and Hein [1996] have adopted a somewhat different policy to processing double difference GPS/GLONASS and GLONASS/GLONASS carrier phase observables. They adopt a technique whereby the frequencies of the two satellites making up the double difference, are scaled to a common frequency, of which both are integer multiples. By doing this, the modified double difference ambiguities remain as integers, although their values will be very high, due to the small auxiliary wavelength which occurs as a result of the common frequency. For GLONASS/GLONASS double differencing on L1, the resultant wavelength is approximately 65 micro metres and for GPS/GLONASS it is even smaller, being in the range 880 to 890 nano metres, which corresponds to the wavelength of infra-red light. It is clearly impossible to fix such small values to the nearest integer due to receiver noise and other error sources. However, as they are so small, it is perfectly acceptable to fix to the nearest thousands for GLONASS/GLONASS or even hundreds of

thousands for GPS/GLONASS, and so effectively form a float solution. Results of tests using this technique have proven its feasibility, returning results accurate at the centimetre level for static solutions and at the decimetre level for kinematic solutions.

Another approach when dealing with combined double difference observables, is to simply to make no attempt to fix the GLONASS ambiguities, but instead to leave them as real numbers. These extra observations achieved through using GLONASS can still be used in the GPS ambiguity search process and is the technique which has been documented by Landau and Vollath [1996]. They found that over a 10 metre baseline, such a procedure resulted in improved ambiguity resolution time and accuracy.

After examination of the existing double difference software (PANIC), it was decided that, to avoid major changes at all levels of the processing strategy, for reasons detailed in Chapter 5, it would be necessary to scale the value of each GLONASS frequency to GPS. By doing this however, the integer nature of the GLONASS carrier would be destroyed and thus it would be impossible to fix the integer ambiguities. However, as with Landau and Vollath, these observations are still successfully included in the search process of the GPS ambiguities, and results obtained from this technique are presented in Chapter 5.

A fourth processing technique is that proposed by [Pratt et. al., 1997] where, by using code-based estimations of the receiver clock terms, the integer nature of the double difference ambiguity term is maintained. In their tests, double difference observables were formed between GPS-GPS and GLONASS-GLONASS combinations only. This is because any residual clock error is scaled by the frequency difference between the satellites making up the observable. Choosing a GLONASS reference satellite from the middle of the GLONASS frequency range gives a clock term coefficient of approximately 7 MHz. If a GPS-GLONASS double difference is formed, however, the clock term coefficient grows to approximately 30 MHz. Because this coefficient is

multiplied by any residual clock error, all processing has been limited to GPS-GPS or GLONASS-GLONASS double differencing. The success of this technique is directly related to the accuracy with which the clock unknown can be calculated, and this is in turn is a function of the accuracy with which the pseudoranges can be measured. Clearly error sources within the receiver and the effect of multipath will therefore have a marked effect on the potential of such a technique.

Finally, Leick et. al. [1995] have developed a processing strategy to deal with the double difference observable, when dual frequency data is available. Initially, the GLONASS carrier phase observations are scaled to a mean frequency, in order to eliminate receiver clock error. However the coefficients of the single difference ambiguities still depend on the satellite frequencies. In order to obtain an explicit double difference formulation, a single difference ambiguity approximation is introduced by solving for a wide-lane single difference ambiguity using dual-frequency carrier phase and pseudoranges. If this estimation is sufficiently close to the correct value of the ambiguity, it then becomes theoretically possible to estimate the double difference ambiguity and constrain it to an integer. A full derivation of the equations involved in this process can be found in Leick et. al. [1995] or Leick [1998].

4.8 References

Ashtech, 1997, *GG24 GPS+GLONASS Receiver Reference Manual*, Reference 630098 Revision B, Ashtech Inc., 1170 Kifer Road, Sunnyvale, CA USA 94086.

Ashkenazi, V., Moore, T., Swann, J., 1998, *Advantages and Problems Encountered In Combining GPS and GLONASS Carrier Phase Observables*, Proceedings of GNSS-98, Toulouse, France, Volume 2 IX-0-03.

Brodin, G., 1997, *GNSS Code and Carrier Tracking in the Presence of Multipath*, Proceedings of ION GPS-97, pp.1389-1398.

CSIC, 1997, Coordinated Scientific Information Centre of the Russian Space Force, *GLONASS Interface Control Document*.

Dodson, A.H., Hill, C.J., Shardlow, P.J., 1993, *The Effects of Propagation Errors on GPS Measurements*, Lecture Notes, 6th International Seminar on the Global Positioning System, The University of Nottingham, Nottingham, United Kingdom.

European Tripartite Group [ETG], 1998, Multi-Modal Education Workshop.

Ffoulkes-Jones, G.H., 1990, *High Precision GPS Surveying by Fiducial Techniques*, PhD Thesis, The University of Nottingham, Nottingham, United Kingdom.

Hall, T., Burke, B., Pratt, M., Misra, P., 1997, *Comparison of GPS and GPS+GLONASS Position Performance*, Proceedings of ION GPS-97, pp.1543-1550.

ICD-GPS-200, 1993, *NAVSTAR GPS Interface Control Document*.

Landau, H., Vollath, U., 1996, *Carrier Phase Ambiguity Resolution using GPS and GLONASS signals*, Proceedings of ION GPS-96, pp. 917-923.

Leick, A., 1995, *GPS Satellite Surveying*, Second Edition, John Wiley&Sons, Inc.

Leick, A., Li, J., Beser, J., Mader, G., 1995, Processing GLONASS carrier phase observations: Theory and first experience, Proceedings of ION GPS-95, pp. 1041-1047.

Leick, A., 1998, GLONASS Satellite Surveying, Journal of Surveying Engineering, May 1998, pp. 91-99.

Lewandowski, W., Danaher, J., Klepczynski, W.J., 1997, *Experiment Using GPS/GLONASS Common-View Time Transfer Between Europe And North America*, Proceedings of ION GPS-97, pp.271-277.

Melbourne, W.G., 1985, *The Case for Ranging in GPS-Based Geodetic Systems*, Proceedings of First International Symposium on Precise Positioning with the Global Positioning System, 'Positioning with GPS-1985', Vol. 1, pp. 373-386, Rockville, Maryland.

Misra, P., 1995, *Integrated use of GPS and GLONASS in Civil Aviation,* MIT Lincoln Laboratory, Lexington, MA 02173.

Orpen, O., Hinsch, P., 1997, *GLONASS for Offshore Applications*, Proceedings of ION GPS-97, pp.989.

Pratt, M., Burke, B., Misra, P., 1997, *Single-Epoch Integer Ambiguity Resolution with GPS-GLONASS L1 Data*, Proceedings of ION-GPS 97, pp.1737-1746.

Roberts, G.W., 1997, *Real Time On-The-Fly Kinematic GPS*, PhD Thesis, The University of Nottingham, Nottingham.

Rossbach,U., Hein, G.W., 1996, *Treatment of Integer Ambiguities in DGPS/DGLONASS Double Differencing Carrier Phase Soultions*, Proceedings of ION GPS-96, pp. 909-916.

Teunissen, P.J.G., Kleusberg,A., 1998, GPS for Geodesy, Second Edition, Springer.

Walsh, D., Daly, P., 1996, *GPS and GLONASS Carrier Phase Ambiguity Resolution*, Proceedings of ION GPS-96, pp. 899-907.

Chapter 5

Software Development and Validation

5.1 Introduction

As mentioned in Chapter 1, it was decided that a great deal of the available project time should be spent modifying the existing GPS Analysis Software (GAS) to process combined GPS/GLONASS observations, as this could then act as a tool to quantify the potential benefits or problems of combined use. The software, its development, and the tests used to validate any modifications are detailed in this Chapter. In addition to this, some of these tests provide the first indication of the relative performances of the systems for static positioning.

The GAS software package has been developed over the past decade within the IESSG and has been exclusively coded in Fortran 77. It was written and initially run on the University's ICL VME mainframe, which provided very good diagnostic capabilities, but suffered from a limited storage capacity and became slow when many users attempted to access it at the same time. With a new Silicon Graphics UNIX workstation becoming available for use within the IESSG, the solution to these problems was to run GAS on this platform. All software development and data processing has been produced on this Silicon Graphics workstation. An additional advantage of using this method is the excellent debugging software which is on offer. This proved invaluable in both the development of new, and the alteration of existing, code.

5.1.1 GAS

GAS has a modular design, consisting of several independent programs, each designed to perform a separate part of the total processing procedure. This is illustrated in Figure 5.1. It takes, as its initial input, data in the Receiver Independent Exchange (RINEX) format, which was developed at the Astronomical Institute, University of Bern, of which Gurtner [1995] gives more detail. This RINEX data is then converted into specific formats for processing in subsequent routines. These formats are, for the observational data, Nottingham specific .NOT files, and for the ephemeris files, the .SP3 standard which was conceived by the US National Geodetic Survey for the distribution of precise GPS ephemeris. Further information on the .SP3 standard can be found in Remondi [1989]. Examples of all of these formats are presented in Appendix A. The routines which perform these tasks are Filter and Con2SP3 (CONvert to SP3) respectively. In addition to re-formatting, Filter can also be used to perform a number of additional tasks, one of which is to derive autonomous position using pseudorange data. Further reference is made to Con2SP3 in Section 5.2 and to Filter in Section 5.3.

Figure 5.1 Schematic of the Relationship between the GAS Modules

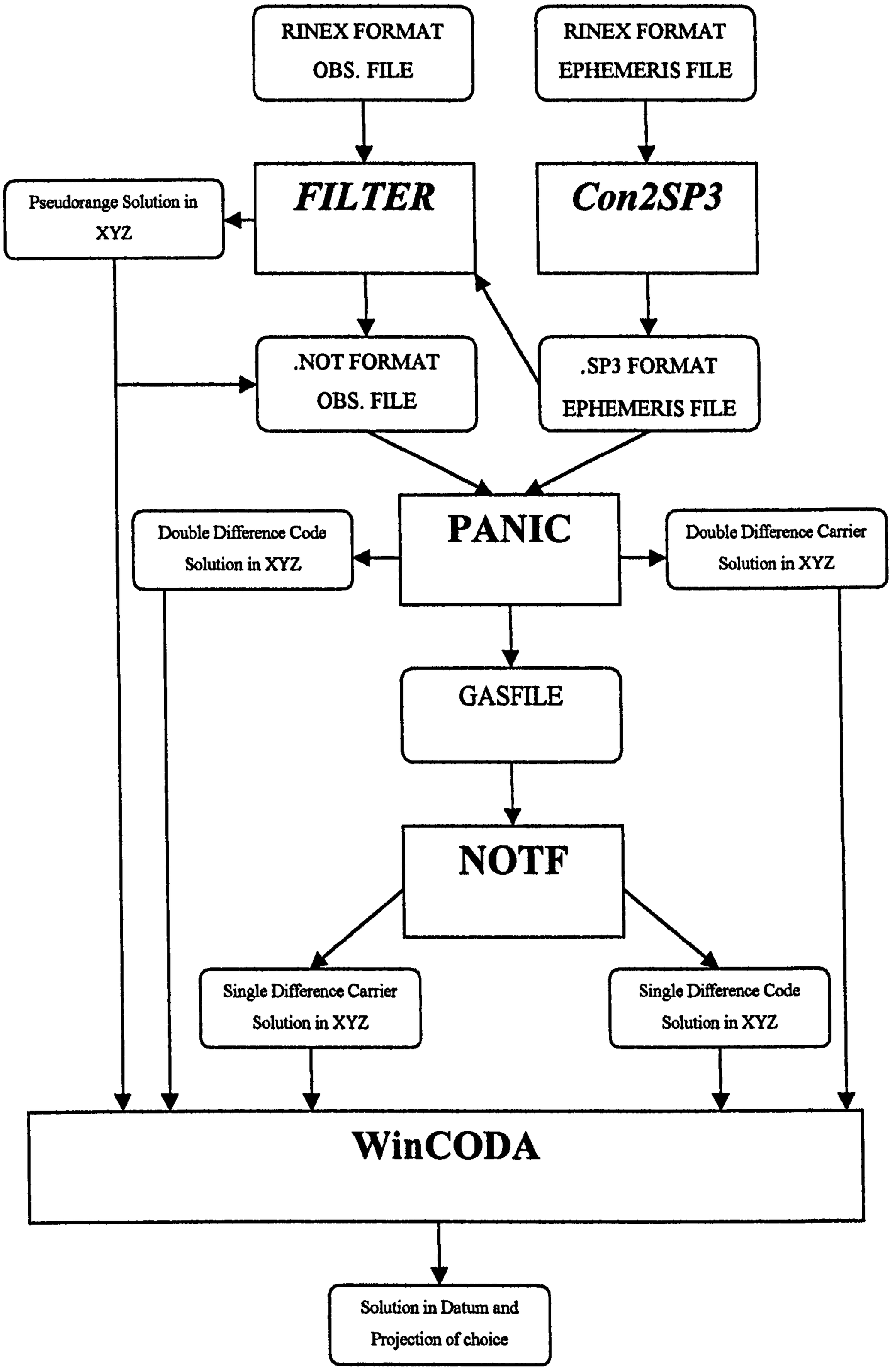

With the data in a suitable format, the main processing routine PANIC (Program for the Analysis of Networks using Interferometric Carrier phase or Code) can be operated. PANIC has been used with great success to process GPS data from a number of projects within the IESSG e.g. monitoring of land movement within the U.K. [Penna, 1997]. It can process either code or carrier observations, from anything between two and thirty stations, using double differencing techniques. Another function of PANIC is to further re-format the observational and ephemeris data into a combined data file called a *GASFILE*, which serves as the input to the NOTF (New On-The-Fly) program [Hansen, 1996].

NOTF is the latest processing utility and, although it too can handle both static and kinematic pseudorange and carrier phase data, it was designed specifically to resolve carrier phase ambiguities in a kinematic environment. Unlike PANIC it uses single differencing to form its observables.

The output coordinates from Filter, PANIC and NOTF are in the form of Cartesian coordinates (Chapter 3), which while useful for defining satellite orbits, are not particularly conducive to visualising position. They can therefore be converted to latitude, longitude and height, and if required, be projected onto one of a number of datums using the WinCODA package. WinCODA is a Windows version of the DATUM package, which was written within the IESSG for the task of transforming points throughout the European Union from local datum's to WGS 84 [Eurocontrol, 1993]. All positioning results described in this thesis have been transformed from WGS 84 to the Ordnance Survey of Great Britain 1936 (OSGB 36) datum, and projected onto Ordnance Survey of Great Britain National Grid (OSGB NG) using this piece of software. This additional step has been taken to make the representation and analysis of the resultant positions somewhat easier.

5.2 Con2SP3

Con2SP3 is the name given to the routine which converts GPS broadcast ephemeris to a .SP3 format for use in all other routines. The obvious start point for software alteration was, therefore, with this routine. There are however fundamental differences between the approaches to ephemeris calculations adopted by the GPS and GLONASS systems. These differences are detailed in Sections 2.3.5.1 and 2.4.5.1 respectively, and resulted in the need for the creation of an almost entirely new processing package.

Initially, it appeared that, due to the fact that a satellite position in Cartesian coordinates was given directly in the GLONASS RINEX file, the coding of a new routine would consist of little more than re-formatting the data to the .SP3 format. However, as the update rate for these point positions is every 30 minutes, a typical .SP3 file might have as few as one or two data points for a particular satellite. This presented a problem in the positioning routines of Filter and PANIC, which use an 8^{th} order interpolation routine to produce an interpolated orbit at any epoch of interest. Further information on the Everett interpolator used in these routines can be found in Moore [1986].

Because of this requirement for eight satellite positions (four each side of the epoch of interest), there were, in most cases, insufficient satellite coordinates in the ephemeris to allow the GLONASS satellites to be included in the position solution. It therefore became necessary to increase the number of data points in each satellite's ephemeris, and this was achieved by adopting the policy of using a 4^{th} order Runge–Kutta integration of the differential equations presented in Section 2.4.5.1. The period of this integration has been set to 1 second, giving 1800 discrete positions for each ephemeris update, and thus, more than fulfils the requirement of the interpolation routine.

All coordinates within this .SP3 file were at this stage still described in terms of PZ-90 (Chapter 3). While this is not a problem when differencing

GPS/GLONASS observations as the datum differences will appear simply as orbital errors and thus will largely cancel depending on baseline length, the same cannot be said for single point positioning. Some sort of transformation therefore had to be implemented and it was decided to include this process as an option at this stage. The parameters adopted for this transformation were those calculated by Misra [1996]. A description of the estimation technique and the parameters themselves are quoted in Section 3.2.2.2. These parameters were felt to be most appropriate, as they are the ones used within the Ashtech GG-24 receivers, from which all of the test data was gathered.

Another point to consider in the generation of this .SP3 ephemeris, was that of the time scales to which it was referenced. GLONASS RINEX ephemeris is referenced to UTC, but GPS RINEX ephemeris is referenced to GPS time, so some account of this clearly had to be made. As almost all RINEX observational data is referenced to GPS time, it was decided to shift the GLONASS time-tags to those of GPS. GPS time is equal to UTC time + the number of leap seconds added since 1980. This leap second value is thus added to the GLONASS time-tag, to bring it into coincidence with GPS time.

An ASCII *Control File* defines the variables for each program within the GAS processing package. This allows not only various data files to be selected for processing but also specifies the processing options to be used. To maintain this flexibility, it was decided to include both the transformation and time-tag shift processes as options within this file. The alterations to the standard Con2SP3 control file, as described in Stewart et. al. [1995], are detailed below:

OPTIONS

REFERENCE **'GLONASS'** or **'GPS'**

DIFF **'13'**

CONVERSION **'YES'** or **'NO'**

The 'REFERENCE' terms relates to the time frame of the output .SP3 ephemeris, and if GPS is selected then the integer number of seconds specified in 'DIFF' is added to the time-tags before writing to the .SP3 file. 'CONVERSION' relates to the datum of the .SP3 output, and if YES is selected then a transformation between PZ-90 and WGS 84 will be performed.

5.2.1 Validation of the Ephemeris Routine

The result of the changes described previously can be seen in an example GLONASS .SP3 file presented in Appendix A. However, some check of the validity of the approaches adopted had to be undertaken before moving on.

The first test performed involved slightly modifying the code to perform a forward integration using the data given at one data point in the broadcast ephemeris, for a period of 30 minutes, and comparing the results with the next broadcast ephemeris value. This not only proved that the Runge-Kutta integration was working correctly, but also provided a check as to the method for calculating the satellite clock correction. Results using this process, for a single epoch with ephemeris information available for five GLONASS satellites are presented in Figure 5.2.

Figure 5.2(A) shows the difference in position, in terms of X, Y, Z and also as a vector. These values have been derived by subtracting broadcast ephemeris position values for time 10:45:00 (GMT) on 10th July 1997, from those computed for the same epoch by performing a forward integration of the broadcast ephemeris parameters given for 10:15:00 (GMT). Even though this 30 minute time-span is twice the valid period for the broadcast ephemeris used in the integration, it still gives a resultant position which agrees to approximately the 2 metre level with the next set of broadcast ephemeris parameters. This level of agreement proved that the orbital integration routine was working, as it should.

Figure 5.2(B) shows the difference between the computed and broadcast satellite clocks for the same satellites at the same epoch. The difference can be seen to be in the order of 0.5 * 10^{-9} seconds, which again is small enough to indicate that the routine used to calculate the receiver clock correction values was correct.

Figure 5.2 Difference Between Integrated and Broadcast GLONASS Orbits

A

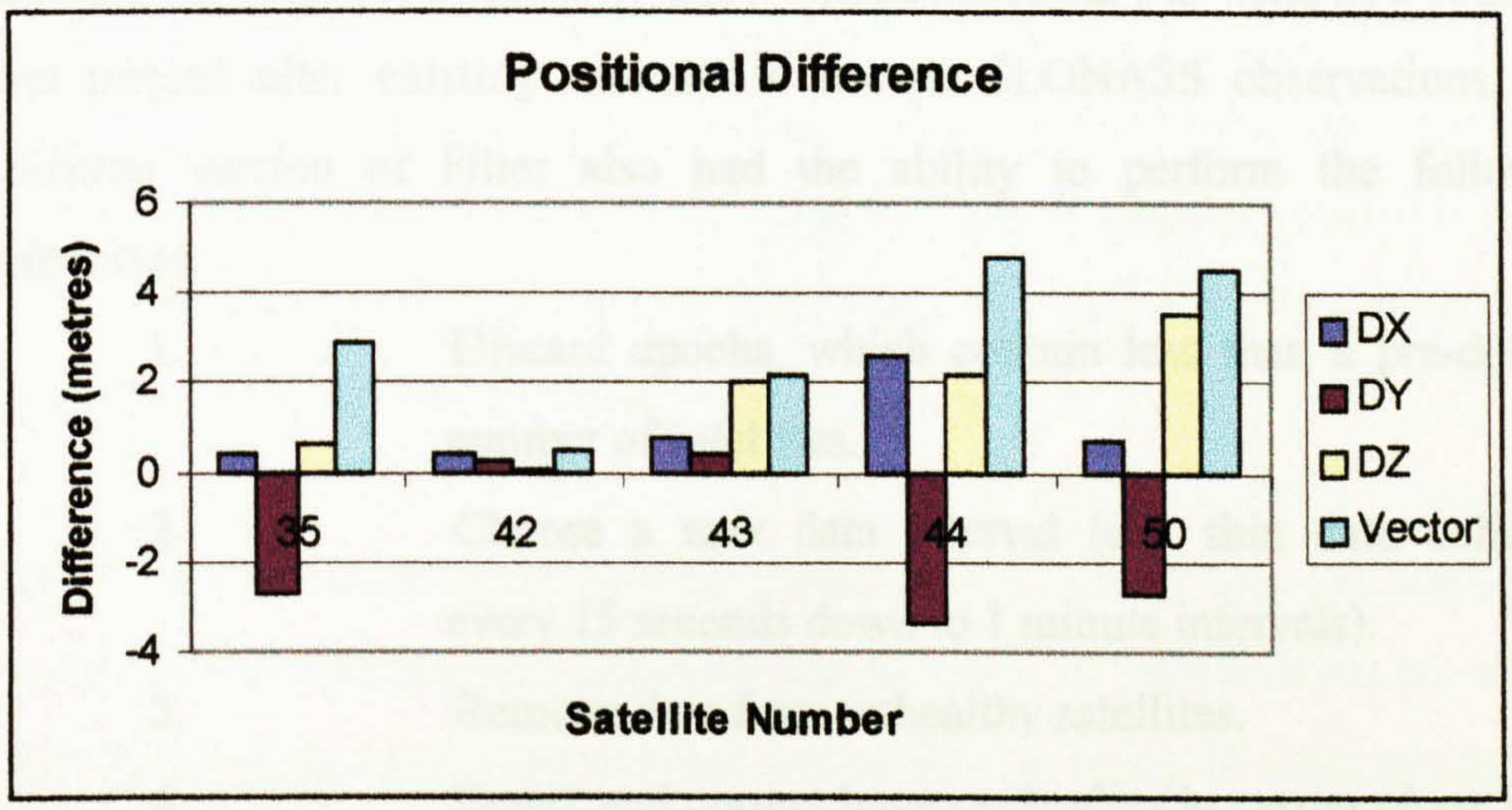

B

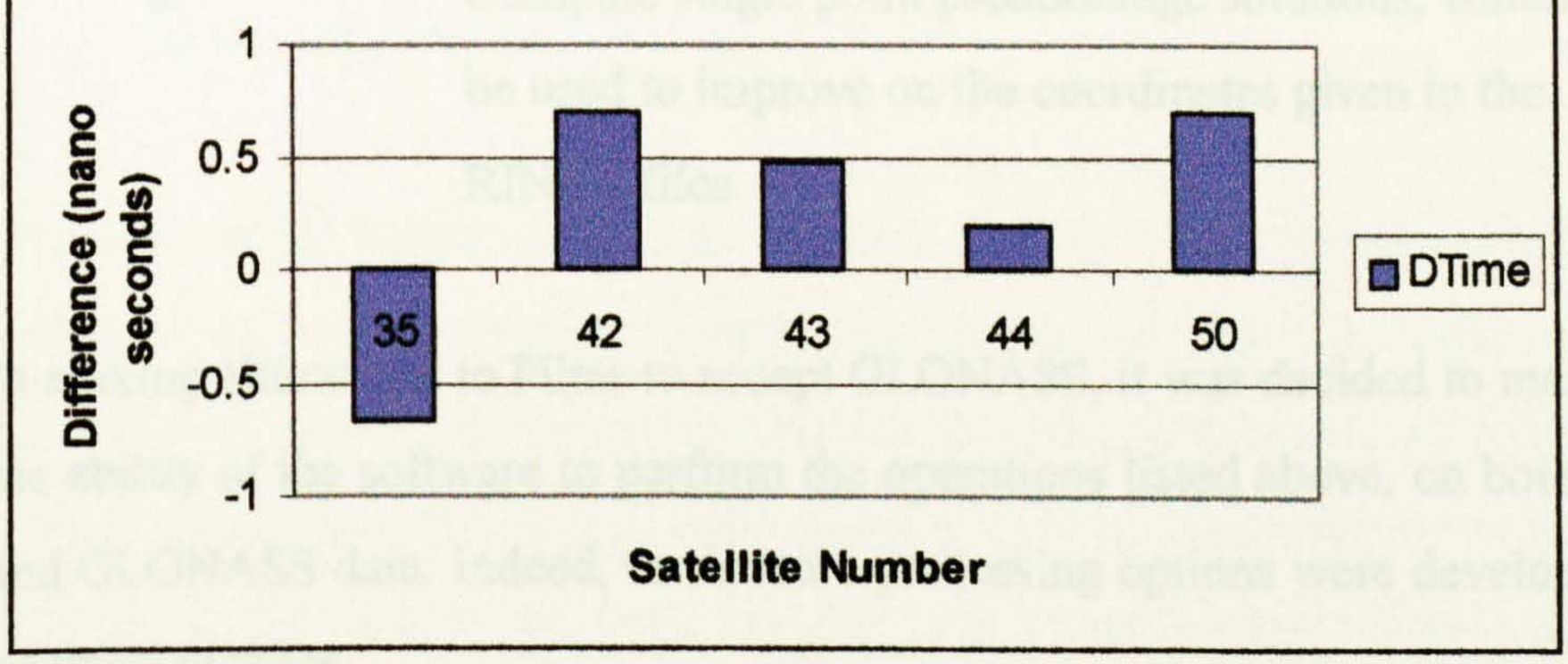

5.3 Filter

Filter is the name given to the GAS module, the main function of which is to convert the standard RINEX format observational files to .NOT format, for processing within PANIC. It therefore became the subject of modification after the successful completion of the GLONASS ephemeris reformatting and interpolation routine. Unlike ephemeris information however, observational data from GPS/GLONASS receivers are very similar, and are thus combined in a single RINEX file. Because of this it was not necessary to write new routines, but instead alter existing routines to accept GLONASS observations. The existing version of Filter also had the ability to perform the following processes:

1. Discard epochs, which contain less than a pre-defined number of satellites.
2. Choose a new data interval (e.g. thin data collected every 15 seconds down to 1 minute intervals).
3. Remove data from unhealthy satellites.
4. Detect and correct large cycle slips in carrier phase data.
5. Specify a time-span for the required .NOT observation files.
6. Compute single point pseudorange solutions, which can be used to improve on the coordinates given in the RINEX files.

In making alterations to Filter to accept GLONASS, it was decided to maintain the ability of the software to perform the operations listed above, on both GPS and GLONASS data. Indeed, three more processing options were developed in addition to these:

7. When dealing with a combined RINEX file the output file and position computed can be specified to be GPS only, GLONASS only, or GPS and GLONASS combined.

8. Scale the GLONASS carrier frequencies to that of GPS.
9. Accept RINEX files produced from either Ashtech or Bernese software.

The first problem which immediately became apparent, was that of maintaining a unique means of identifying satellites, as in a combined RINEX observation file, GPS and GLONASS satellites share the same number, being distinguishable by a **'G'** (GPS) or **'R'** (GLONASS) pre-fix. Maintaining this notation within Filter was not possible, because the satellite identification numbers (SVID) are used in the software to allocate unique positions in a number of arrays. Also a letter/number combination would not follow the existing .NOT format, and could lead to further problems in subsequent operations. Therefore a process by which an individual number is allocated to each satellite had to be devised.

As all GPS satellites are numbered in the range 1 – 32, it was decided to read in the letter pre-fix for each satellite, and if it is a 'G', to leave the ID number as it stands. If however, the satellite is identified as being GLONASS, then the number 32 is added to this slot number, which can range between 1 – 24. This procedure gives the following set of unique SVID numbers:

1-32 GPS
33-56 GLONASS

The next alterations to be made lay with the cycle slip detection software within Filter. This routine works by noting the change in pseudorange between consecutive epochs, and then comparing this distance with the change in carrier phase count multiplied by the signal wavelength, to bring it into units of metres. If the difference between the two values lies outside a pre-set tolerance, it is reasonable to expect a cycle slip to have occurred. As detailed in Chapter 2, the wavelength of a GPS L1 signal is 19.03 cm, but varies from 18.56 centimetres to 18.71 cm for GLONASS. If these specific GLONASS wavelengths were not accounted for, each GLONASS satellite would be

flagged as suffering from a cycle slip at each epoch, and an attempt made to fix the carrier phase count, thus introducing a cycle slip.

The methodology of the routine introduced to determine the wavelength of signals from individual GLONASS satellites is outlined as follows:

1. Detect if the satellite is GLONASS.
2. Find its true SVID number.
3. Relate this number to its frequency number '***n***'.
4. Calculate the actual frequency by substituting ***n*** into equation 2.4.
5. Calculate the wavelength using this frequency value.

In order to keep the values of the integer ambiguities as small as possible in any subsequent search routines, Filter, on detecting a new satellite, calculates the approximate number of integer cycles between satellite and receiver by multiplying the pseudorange by the wavelength of the signal. This value is then subtracted from the arbitrary carrier phase count to give an integer correction that is applied at all subsequent epochs to the carrier phase value for that satellite. Clearly, the same problem of calculating the appropriate wavelength for GLONASS satellites existed but, by duplicating the process adopted within the cycle slip detection software, this was easily overcome.

As discussed in Chapter 4, the processing of GLONASS carrier phase double difference observables presents specific problems due to each satellite's broadcasting on a different frequency. One way to overcome this problem is to scale each of these carrier frequencies to that of GPS, and the option to perform this task has also been included within Filter. Stages 1 to 4, as outlined above, are again used to calculate the specific satellite frequency, before the L1 carrier phase count is scaled by the following expression:

$$car1 = car \times \frac{fL_1}{f} \tag{5.1}$$

where:

*car*1	=	carrier phase count in terms of L1 GPS.
car	=	original GLONASS carrier phase count.
fL_1	=	Frequency of L_1 GPS.
f	=	Frequency of the GLONASS satellite.

The next coding operation performed on Filter was to enable it to process a combined observational file in terms of GPS only, GLONASS only, or GPS/GLONASS. This ability was believed to be advantageous as, by being able to have any one of the three potential combinations from the same data file, conclusions as to the potential advantages to be gained from augmenting GPS with GLONASS could easily be drawn.

These extra functions are specified as additional options to those already detailed within the Filter 'Control File' [Stewart et. al., 1995], and are outlined as follows:

OPTIONS	
COMBO	**'MIXED' or 'GPS' or 'GLONASS'**
SCALE	**'YES' or 'NO'**

Both these options require very little explanation, with the type of system output to the .NOT file being controlled by the *COMBO* option, and the choice of scaling the GLONASS carrier phase count to that of GPS by *SCALE*.

The final alteration made to Filter was to enable it to handle RINEX data produced from either Ashtech's own software, or that developed by Werner Gurtner at The Astronomical Institute of Berne. As RINEX is supposed to be present the data in a uniform format, it was not initially anticipated that there would be differences in the RINEX files produced from each set of software. However, as can be seen from comparing Figure 5.3 (A) and (B), which show

the RINEX outputs obtained using the same data file from WinPrism (Ashtech) and ASRINEXO (Bernese) respectively, there are certain differences in the amount of information in the file header, and the format of the satellite identifications at the epoch header. It is however worth noting that the actual data values are identical, indicating that the same phase smoothing routine (Chapter 4) is used in each program.

To cope with these differences, a final option was included in the control file. This is detailed below and again requires no explanation:

```
FILES
        INPUT
                SOURCE      'ASHTECH' or 'BERN'
```

The initial design of Filter was such that only data from one ephemeris was used to compute position. However, as has been outlined in Section 5.2, it became necessary to produce individual ephemerides for GPS and GLONASS. Therefore it was necessary to duplicate the ephemeris read and computation routines to accept data from both files when necessary.

In solving for a single point position for GPS, there are four unknown terms (X, Y, Z and receiver clock correction). However, in solving for a combined GPS/GLONASS solution, this number rises to five, with the extra unknown being the second receiver clock offset, this time for GLONASS (Chapter 4). Therefore, the positioning routines themselves also had to be altered, with an extra unknown being incorporated in the solution computation, and correspondingly, an extra observation being required as the minimum to solve for this position.

Figure 5.3 RINEX Files Produced from WinPrism and ASRINEXO

A

```
2                   OBSERVATION DATA    M (MIXED)           RINEX VERSION / TYPE
ASHTORIN                                    16 - AUG - 99 09:56 PGM / RUN BY / DATE
                                                                COMMENT
R212                                                            MARKER NAME
                                                                MARKER NUMBER
                                                                OBSERVER / AGENCY
                       G-XXIV              GG00       N/A       REC # / TYPE / VERS
                                                                ANT # / TYPE
  3851190.3379   -80146.6524  5066665.5434                      APPROX POSITION XYZ
        0.0000         0.0000        0.0000                     ANTENNA: DELTA
H/E/N
     1     0                                                    WAVELENGTH FACT
L1/2
     3    L1    C1                                             # / TYPES OF OBSERV
                     1.0000                                     INTERVAL
    12                                                          LEAP SECONDS
  1998     8    10    11     0   20.000000      GPS            TIME OF FIRST OBS
  1998     8    10    12    29   58.993000      GPS            TIME OF LAST OBS
                                                                END OF HEADER
 98  8 10 11  0 20.0000000  0 16G01G31G29G08G14G02G15G07G16R18R17R03 0.0001111
R20R04R11R12
  19893309.752 6  23114637.645
  38913049.249 6  23760175.724
  13928975.834 6  21915634.931
  25365471.320 5  24779211.910
   4062703.659 6  21156988.666
  21768758.118 6  23867776.109
  15450198.640 7  19909974.615
  25100601.018 5  23055609.985
  23474001.430 5  24133602.567
  15433679.275 5  20124316.238
  43546447.393 2  23647339.635
   7817956.977 5  19283389.883
  34150002.197 5  24143935.833
  19373875.720 5  22123681.328
  13129113.278 5  22812523.780
   30486572.726  5  22364822.064
```

B

```
2                   OBSERVATION DATA    M (MIXED)           RINEX VERSION / TYPE
ASRINEXO V2.9.6 LH  IESSG                   16-AUG-99 09:52     PGM / RUN BY / DATE
                                                                COMMENT
BIT 2 OF LLI (+4) FLAGS DATA COLLECTED UNDER "AS" CONDITION     COMMENT
R212                                                            MARKER NAME
                                                                OBSERVER / AGENCY
                    ASHTECH G-XXIV      GG00                    REC # / TYPE / VERS
                    GEODETIC L1                                 ANT # / TYPE
  3851190.3379   -80146.6524  5066665.5434                      APPROX POSITION XYZ
        0.0000         0.0000        0.0000                     ANTENNA: DELTA
H/E/N
     1     0                                                    WAVELENGTH FACT
L1/2
     2    C1    L1                                             # / TYPES OF OBSERV
  1998     8    10    11     0   20.000000      GPS            TIME OF FIRST OBS
                                                                END OF HEADER
 98  8 10 11  0 20.0000000  0 16G01G31G29G08G14G02G15G07G16R18R17R03
                              R20R04R11R12
  23114637.645    19893309.752 2
  23760175.724    38913049.249 2
  21915634.931    13928975.834 3
  24779211.910    25365471.320 2
  21156988.666     4062703.659 3
  23867776.109    21768758.118 2
  19909974.615    15450198.640 3
  23055609.985    25100601.018 2
  24133602.567    23474001.430 2
  20124316.238    15433679.275 2
  23647339.635    43546447.393 1
  19283389.883     7817956.977 2
  24143935.833    34150002.197 1
  22123681.328    19373875.720 2
  22812523.780    13129113.278 1
  22364822.064    30486572.726 1
```

Because S/A does not affect GLONASS pseudorange observations, the quality of these measurements can be assumed to be of a higher standard to those of GPS. To take some account of this, it was decided to weight the observation equations by means of the relative standard errors of the two systems. Equations 5.2 and 5.3 were derived for this procedure.

For GPS $$Ax = 1 \tag{5.2}$$

For GLONASS $$\frac{s^{gps}}{s^{glonass}} Ax = 1\frac{s^{gps}}{s^{glonass}} \tag{5.3}$$

where:

A	=	the design matrix relating the observations to the parameters.
x	=	the vector of the parameters.
s^{gps}	=	standard error of GPS pseudorange observations (25 metres).
$s^{glonass}$	=	standard error of GLONASS pseudorange observations (7 metres).

If a Kalman version of this Least Squares routine had been implemented it would have been possible to add process noise. This way the measurements could have been weighted correctly, rather than factorising one with respect to the other. However, the existing positioning routines within Filter were relatively simple, being used primarily to provide approximate coordinates for poorly defined points.

5.3.1 Validation of Filter

As with Con2SP3, on completion of the coding modifications outlined above, it was necessary to test the validity of the changes. Checks had to be performed

on each of the reformatting, cycle slip and positioning routines. The results of these are detailed below.

5.3.1.1 Reformatting the Data

As this is the primary task of Filter, it is imperative that the data is reformatted correctly. This is particularly true for the carrier phase data, which is set to approximately the same value as the pseudorange when converted to metres, and in the case of GLONASS, may also be scaled to the wavelength of L1 GPS.

In order to test the correctness of these routines, a single epoch's worth of combined observational data was chosen at random. Figure 5.4(A) shows the data in RINEX form, Figure 5.4(B) shows the .NOT format of this, with no scaling of the carrier to GPS, and finally 5.4(C) shows the data in .NOT format again, but this time with scaling of the GLONASS carrier count.

Figure 5.4 Random Epoch of Combined GPS/GLONASS Observational Data in RINEX and .NOT Format

(A)

```
98  8 10  8 57 40.0000000  0  5G15R18R09R10R17
  21512070.923    -6523558.945 3
  21104388.307    -6969805.218 2
  23409388.634    -6492610.93912
  23244416.444    -6733286.33412
  19119943.533    -6466362.778 1
```

(B)

```
970  118660.0000000  0  -0.99999000    5   15 41 42 49 50
   21512070.923   0   113046696.055
   23409388.634   0   125356214.061
   23244416.444   0   124603634.666
   19119943.533   0   103032174.222
   21104388.307   0   113171433.782
```

(C)

```
970  118660.0000000  0  -0.99999000    5   15 41 42 49 50
   21512070.923   0   113046696.055
   23409388.634   0   123017168.934
   23244416.444   0   122150232.725
   19119943.533   0   100475981.461
   21104388.307   0   110904309.498
```

From examining these three files, it is clear that the pseudorange data has been re-written to the .NOT files with no error. The same cannot however be immediately said of the carrier phase data, as it has been significantly altered. However, as the epoch selected for analysis is only 40 seconds after the start of the processing run of Filter, the carrier phase count, when multiplied by the wavelength of the signal, should still almost be in coincidence with the pseudorange, assuming that there have been no cycle slips. If the carrier phase count for satellite 41 in Figure 5.4(B) is multiplied by the wavelength of this satellites signal (18.6742946 cm) then a range of 23,409,388.83 metres is produced. As this is only 20 centimetres different from the L1 pseudorange value, it was concluded that the routine to determine wavelength of the GLONASS satellites, and in turn to shift the initial integer part of the carrier phase count to the pseudorange, was working correctly. Figure 5.4(C) has its GLONASS carrier phase counts further scaled to those of GPS, and again the validity of this can be checked by multiplying the count by the wavelength of an L1 GPS signal (19.0293672 cm). This gives for satellite 41, a range of 23,409,388.89 metres, which is again very close to the broadcast pseudorange, thus proving the validity of the technique. The small difference in the pseudoranges computed from the carrier phase counts in Figure 5.4(B) and (C) is due to the fact that the count is shifted only by an integer amount in (B), but in (C) it is shifted by a real number.

5.3.1.2 Cycle Slip Detection

The cycle slip detection routine within Filter is designed to serve as a means of detecting large cycle slips only. To check the validity of the system for GLONASS a test was performed, whereby an hour of combined GPS/GLONASS data, collected at a 1 second interval, was processed three times through Filter with tolerance levels of 500, 100 and 10 cycles respectively, for the cycle slip detection. The number of satellites visible at each epoch within this data set range between 10 and 7 for GPS, and between 8 and 6 for GLONASS. The result of this test is presented in Table 5.1.

Table 5.1 Cycle Slip Detection within Filter

A

Tolerance In Cycles	SVID	L1 Slip
500	43	22,142,707

B

Tolerance In Cycles	SVID	L1 Slip
100	43	-222
100	43	22,142,707
100	2	-194

C

Tolerance In Cycles	SVID	L1 Slip
10	43	-222
10	43	22,142,707
10	2	-194
10	4	25
10	4	-13

A large Slip was detected on Satellite 43 which, on examining the data file, occurred as a result of the receiver losing lock on that particular satellite for ten consecutive epochs. On examination of the Signal to Noise Ratio (SNR) of the satellites, the value for Satellite 43 was found to be very low, 10 decibels

(dB), and this may explain why this gross cycle slip occurred. However, for all other epochs it appears that the Slip routine was finding no more Slips on the GLONASS satellites than on GPS. Indeed as the Slip tolerance is reduced, it is GPS satellites that are flagged as suffering from small cycle slips. This not only proved that the routine was functioning correctly for GLONASS satellites, but that, in the case of this data set at least, that GLONASS observations are no more likely to suffer from cycle slips than GPS.

5.3.1.3 Position Computation

In order to test the validity of the results obtained from the positioning routines within not only Filter, but PANIC, and NOTF also, it was necessary to process data collected at a point, the coordinates of which were already precisely known. The coordinates derived from each GAS package could then be compared against the known or *Truth* coordinates, and any potential error highlighted. Where possible commercial software has also been used to process the same data and thus provide a further check/comparison of the new positioning routines employed within GAS.

On 10th August 1998, data from both the IESSG's Ashtech GG-24 GPS/GLONASS receivers was recorded on a point with known coordinates, for a period of 90 minutes between 11:00 and 12:30 (BST). It is this data set that has been used to validate the positioning routines within all three software routines, as it provides a consistently high number of good quality GPS and GLONASS observations, which allow for reasonable comparisons of the positioning accuracies achievable using GPS and GLONASS. Also, with a 1 second recording interval, the 90 minute time-span gives some 5400 epochs of data, which should be enough to highlight any potential errors in the coding. This data was logged on a Zero Base-Line (ZBL), the principle of which is illustrated in Figure 5.5. Satellite visibility plots for the GPS, GLONASS, and GPS/GLONASS constellations at this time, are given in Appendix C1.

The *Antenna Splitter* used not only allows two receivers to access the signals received from a single antenna, but also suppresses the power output from one of the receivers which is used to power the antenna. This is necessary, as doubling the power input to the antenna could have introduced interference into the observations.

Although using a ZBL is not necessary for the autonomous single point positioning performed within Filter, it is necessary to simultaneously record data on more than one receiver for both PANIC and NOTF, which are differential processing packages. The main advantage of collecting data on a ZBL when testing differential positioning routines, is that the location of the antenna, the antenna its self, and the cabling connecting the antenna to the receivers are all identical. The resultant positions derived from each receiver at the same epoch should therefore be identical, and thus the difference between them should be zero. Any errors or biases will be easily identifiable, as they will appear as vector difference between the positions. The results obtained through PANIC and NOTF will be discussed in Sections 5.4.1 and 5.5.1 respectively.

There are two positioning routines within Filter, and both have been modified to accept GLONASS data. The first of these assumes that the receiver is moving and thus calculates a new solution each epoch, while the second performs an accumulated solution, as it assumes the receiver to be statically located over the same point.

Figure 5.5 Zero Base-Line Operation

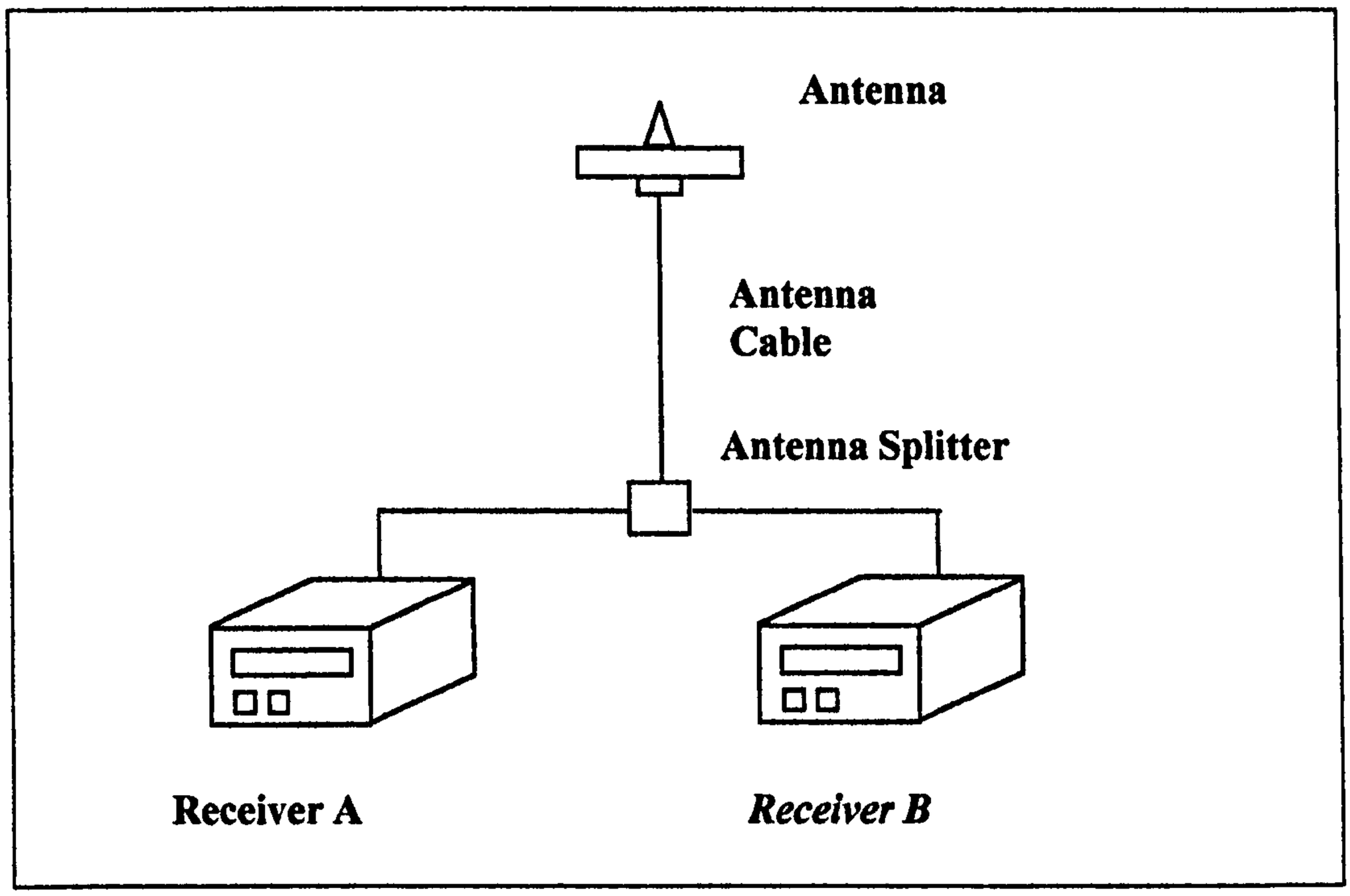

The known WGS 84 coordinates of the antenna are:

52° 56′ 26.47439″	North	3851174.654 X
01° 11′ 32.28300″	West	-80152.879 Y
98.682 m	Height	5066647.153 Z

when transformed to OSGB 36 and projected onto OSGB NG using WinCODA this gives:

454377.039	Easting
338451.379	Northing
51.271	Height

The quality of the coordinates quoted above needs to be quantified, as they have assumed to be the *Truth* values in all, subsequent tests. There are four coordinated points located on the roof of the IESSG. The first of these, *Turret 1*, used as a basis for its coordinate definition, 18 months of Continuously

Operating Geodetic Receiver (COGR) observations. The absolute accuracy of its coordinates can therefore be assumed to be well below the centimetre level. The coordinates of the three remaining points, one of which has been used in the trials subsequently detailed, have all been defined with respect to this on four separate occasions using a Differential Carrier Phase Solution. The repeatability of the results obtained has been sub-millimetre in plan and at the millimetre level in height. Thus, the absolute accuracy of the WGS 84 coordinates quoted above can still be assumed to be at the level of a few millimetres. These coordinates have then been transformed to the OSGB 36 datum and projected onto OSNG to make their analysis and representation clearer, using the WinCODA package. As OSGB 36 is not a homogeneous datum, the accuracy of this transformation is a function of point position and can reach a maximum of +/- 10 metres using WinCODA. However, as both the computed and observed points share the same location, any error introduced during this procedure are identical, and thus comparisons of these relative coordinates should still be accurate to the levels quoted for WGS 84.

The first test performed was on the epoch by epoch routine with GPS only, GLONASS only, and finally combined GPS/GLONASS data, being processed for the full 90 minutes for one of the receivers only (Receiver 12). In an attempt to account for the different reference systems used by GPS and GLONASS, the GLONASS ephemeris used in these computations was first transformed from PZ 90 to WGS 84, as detailed in Section 5.2. The results of these tests, in terms of plan and height components, are presented in Figures 5.6 and 5.7 respectively. In each, the difference between the known and derived coordinates at each epoch is shown. This has been calculated by subtracting the derived value from the *truth*, and this is the convention that has been used in all subsequent difference calculations.

Figure 5.6 (A), and in particular Figure 5.7 (A), show quite clearly the effect that S/A has on a GPS solution, with the position varying by some 60 metres in Easting, 120 metres in Northing, and 150 metres in height. The advantage

Figure 5.6 Difference in Filter Pseudorange Plan Coordinates

A

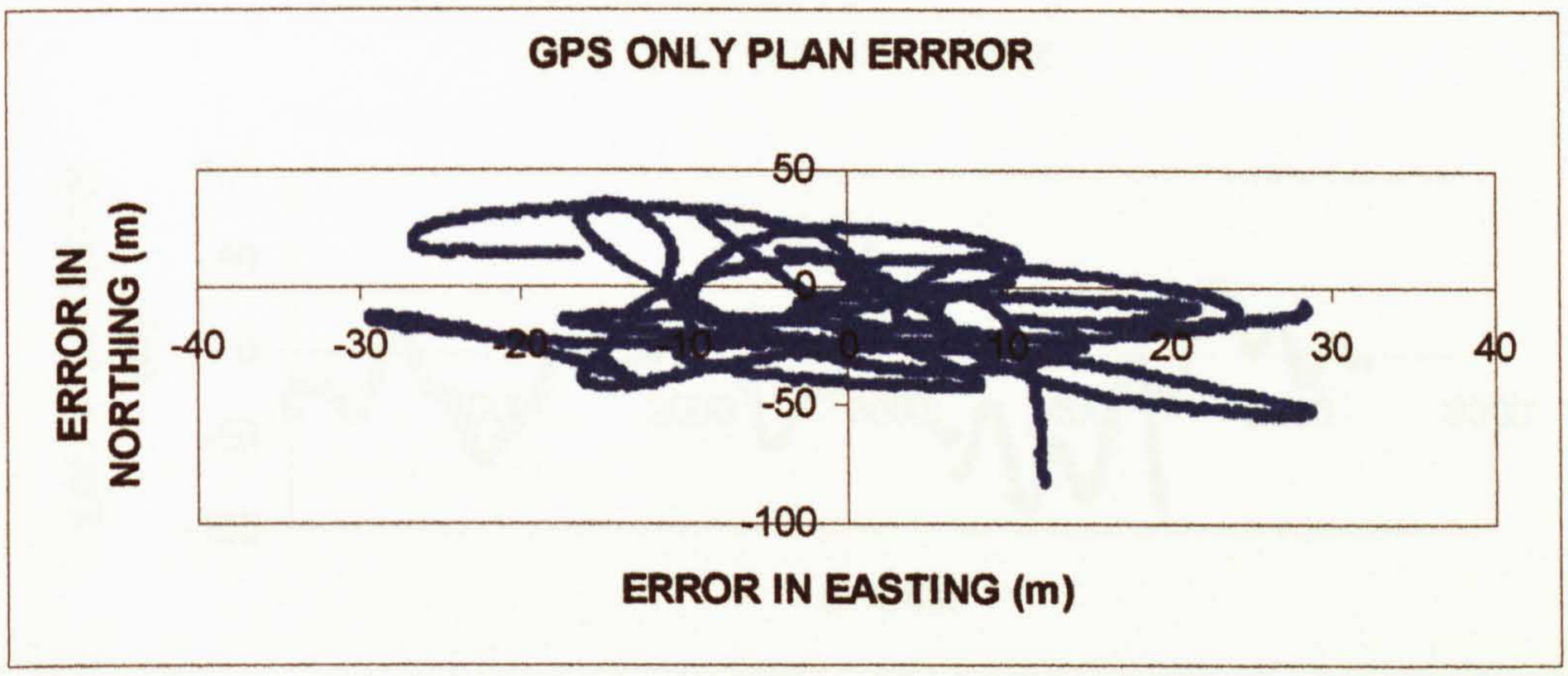

B

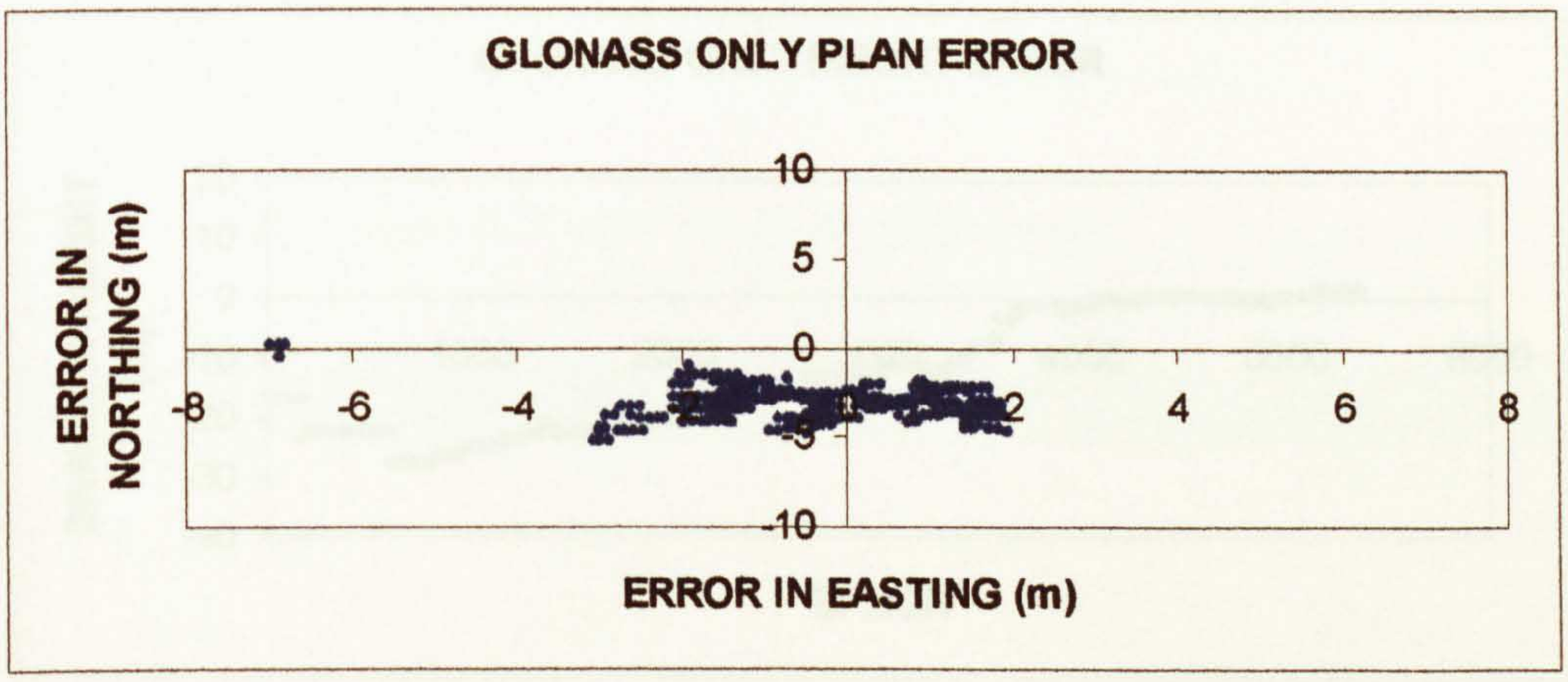

C

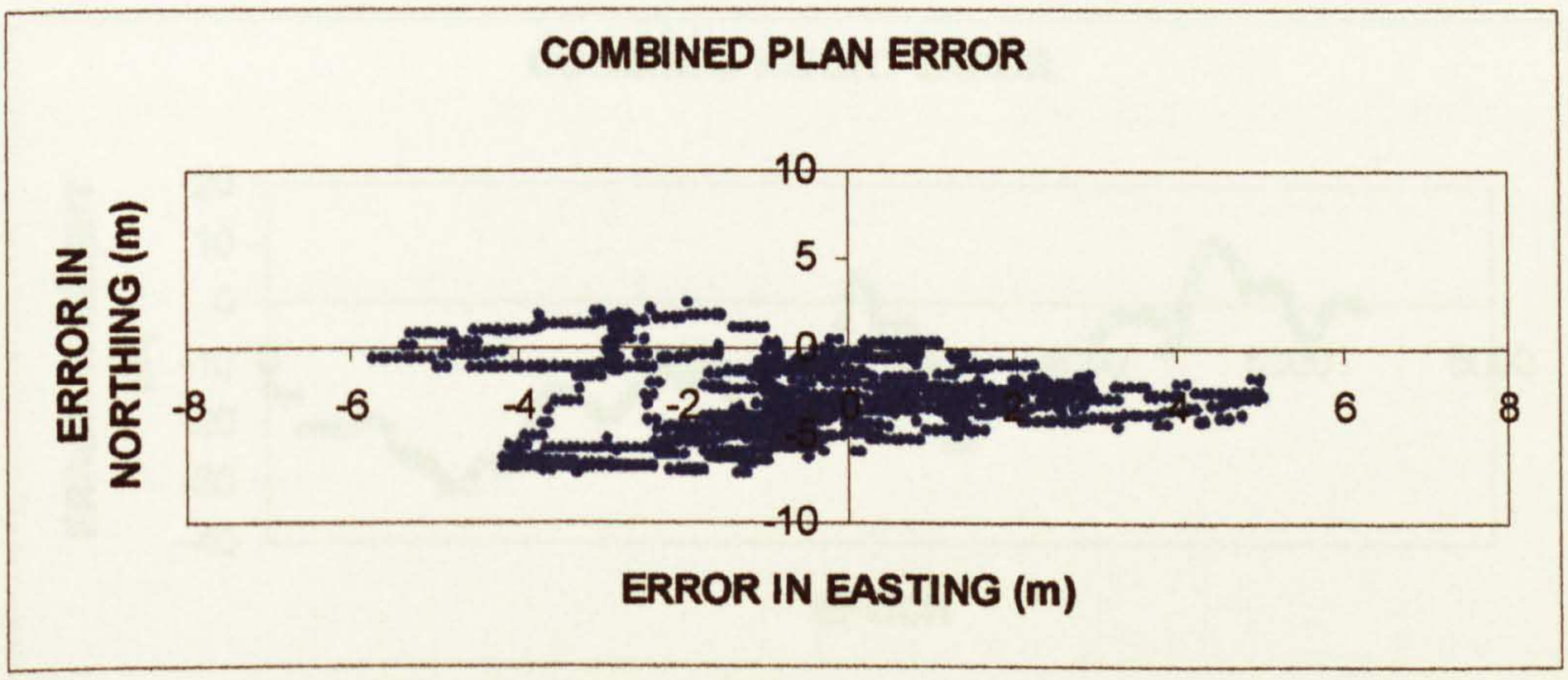

Figure 5.7 Difference in Filter Pseudorange Height Values

A

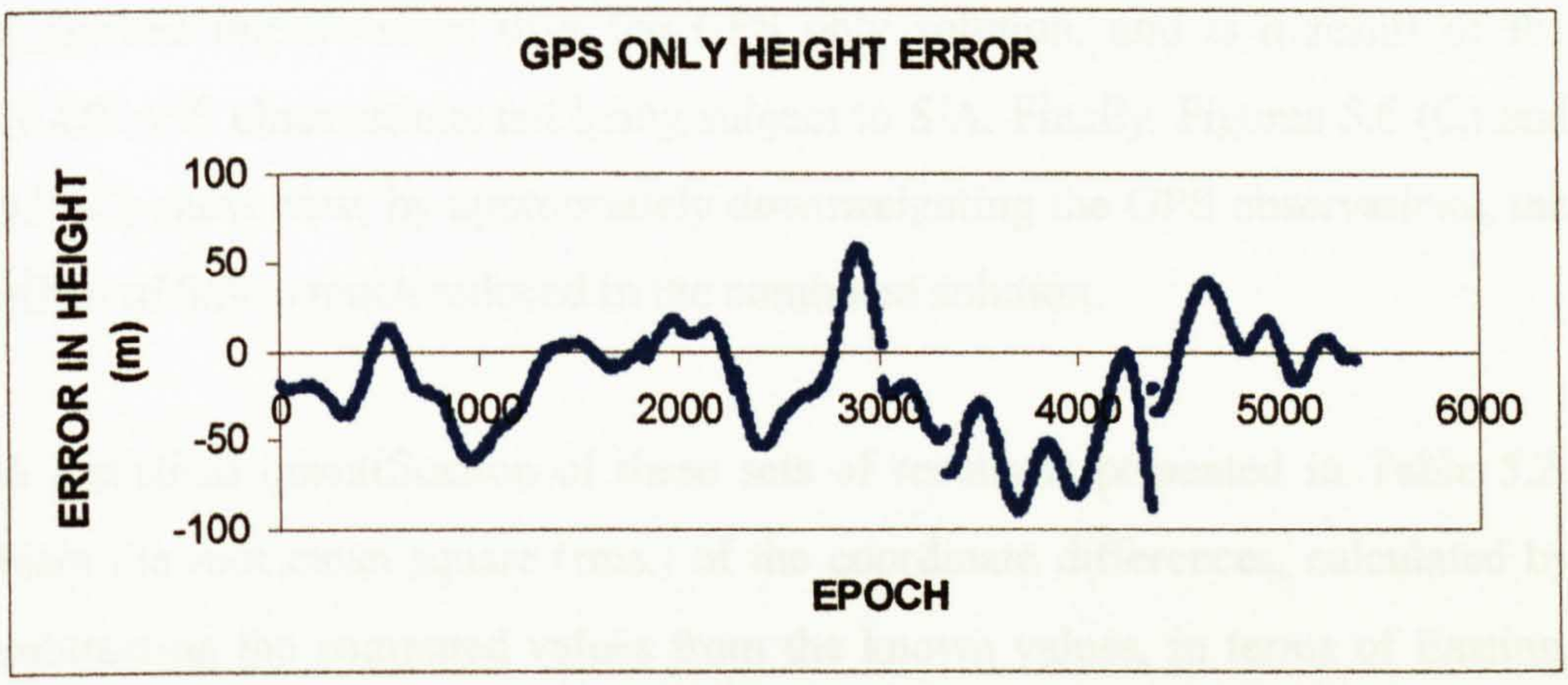

B

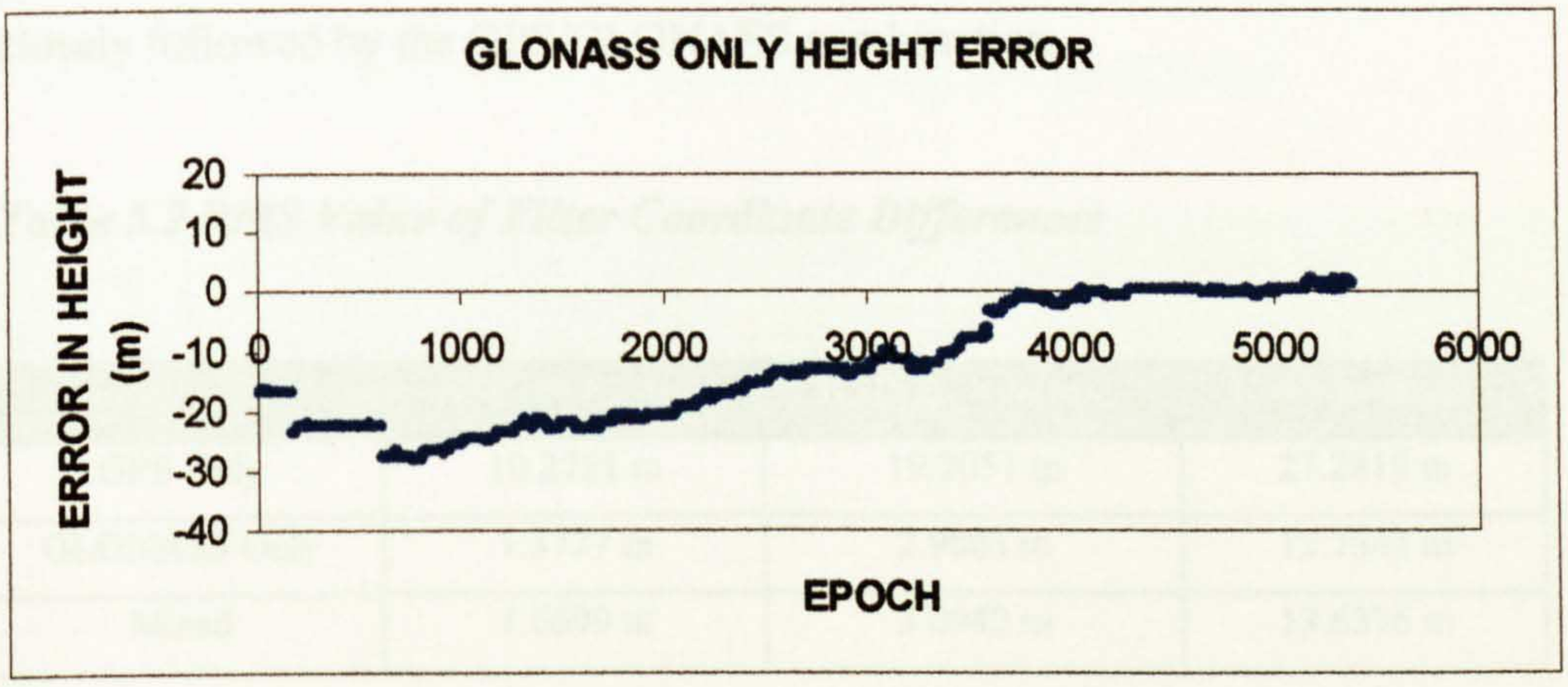

C

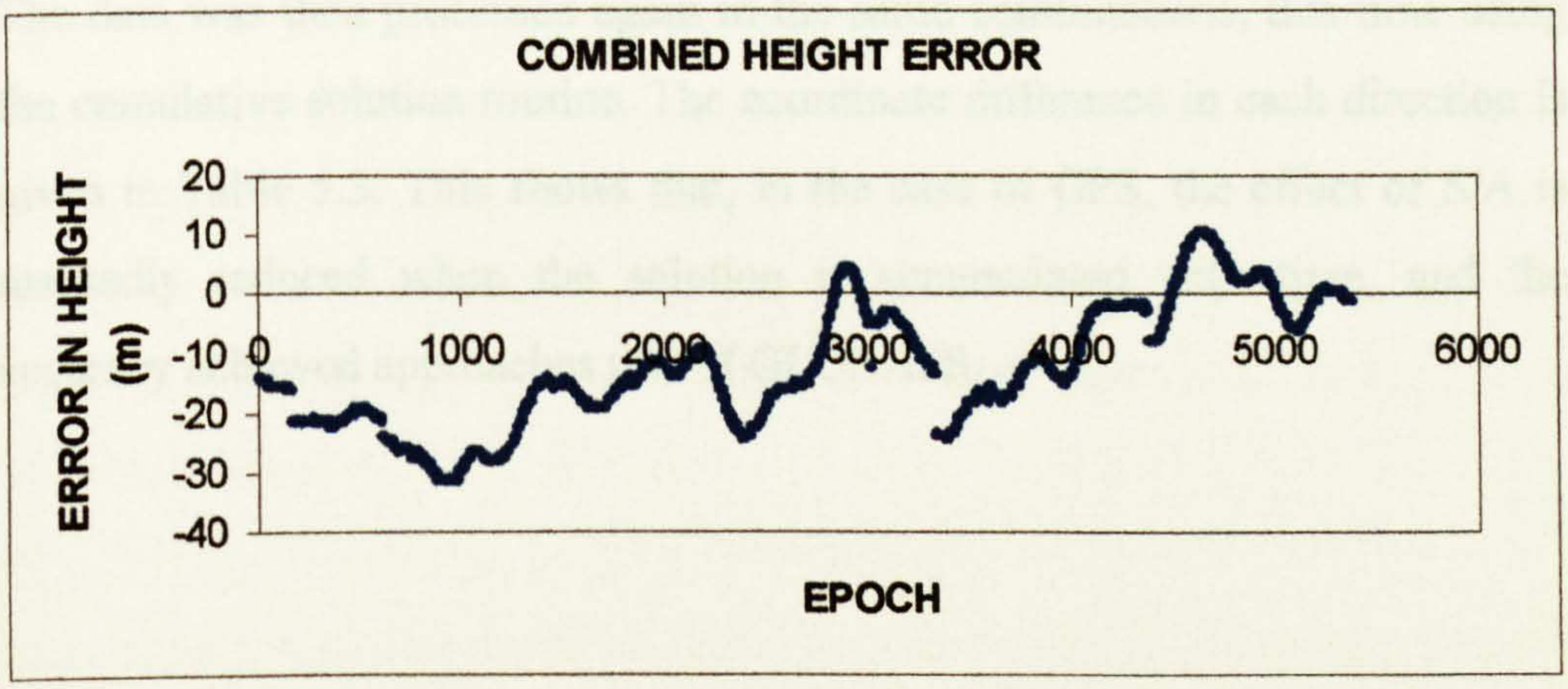

which GLONASS has for single point positioning can be equally easily seen in Figures 5.6 (B) and 5.7 (B), where the position varies by approximately 10 metres in Easting, 5 metres in Northing, and 20 metres in height. This is clearly a marked improvement over the GPS only solution, and is a result of the GLONASS observations not being subject to S/A. Finally, Figures 5.6 (C) and 5.7 (C) show how, by appropriately downweighting the GPS observations, the effect of S/A is much reduced in the combined solution.

A statistical quantification of these sets of results is presented in Table 5.2. Here the root mean square (rms.) of the coordinate differences, calculated by subtracting the computed values from the known values, in terms of Easting, Northing, and Height is given for each of the three system combinations. It can be seen again that the GLONASS only system yields the most accurate results, closely followed by the GPS/GLONASS combination.

Table 5.2 RMS Value of Filter Coordinate Differences

Combination	RMS in Easting	RMS in Northing	RMS in Height
GPS Only	10.2751 m	19.2051 m	27.2819 m
GLONASS Only	1.3777 m	2.9863 m	12.7541 m
Mixed	1.6699 m	3.0942 m	13.6376 m

The data was then processed again in the same combinations, this time using the cumulative solution routine. The coordinate difference in each direction is given in Table 5.3. This shows that, in the case of GPS, the effect of S/A is markedly reduced when the solution is accumulated with time, and the accuracy achieved approaches that of GLONASS.

Table 5.3 Difference in Filter Accumulated Coordinate Solution

Combination	Difference in Easting	Difference in Northing	Difference in Height
GPS Only	0.419m	-4.867m	-11.804m
GLONASS Only	-0.231m	-1.856m	-14.673m
Mixed	0.561m	-4.017m	-16.943m

The same process was then performed on coordinate values obtained from the same data set, which was this time processed through Ashtech Office Suite (AOS), which was the first commercially available GPS/GLONASS processing package released by Ashtech. Further details of AOS can be found in Ashtech [1997]. The results from this test are presented in Table 5.4.

Table 5.4 Difference in AOS Accumulated Coordinate Solution

Combination	Difference in Easting	Difference in Northing	Difference in Height
GPS Only	41.583m	-314.955m	-634.939m
GLONASS Only	17.302m	3.315m	-13.192m
Mixed	17.593m	3.591m	-21.531m

It is obvious from examining the results presented in Table 5.4 that the GPS only solution obtained from AOS is grossly in error. The same data set was processed numerous times through this processing package, with the same results being obtained on each occasion, before Ashtech were contacted. No satisfactory explanation was however received. The results for GLONASS only and mixed GPS/GLONASS are however reasonable, but not of the same level of accuracy as returned from Filter.

In summary, both the epoch by epoch and accumulated positioning routines have been successfully altered to process both GPS and GLONASS observations. In the case of epoch by epoch positioning especially, the

potential benefits of the GLONASS system have been demonstrated. Also, the accuracies of the GLONASS solutions detailed above, act as further proof as to the validity of the ephemeris computation software detailed in Section 5.2.

5.4 PANIC

PANIC is the name given to the main GAS processing module. It takes the .SP3 and .NOT format files produced by Con2SP3 and Filter respectively, and produces either code or carrier double difference position solutions. Another function of PANIC is to further reformat and combine the observational and ephemeris data into single file called a *GASFILE*, which serves as the input to NOTF. With the successful completion of the modifications necessary to both Con2SP3 and Filter, this was the next routine to be modified.

As both the GLONASS ephemeris and observational data had been already altered to the specified format, the number of changes required within PANIC were not as far ranging as those in the earlier routines. After altering, where necessary, the arrays to accept SVIDs up to 56, and specifying an additional read routine to enable both GPS and GLONASS ephemerides to be read in simultaneously, combined GPS/GLONASS pseudorange data was processed for the first time. Initially, it was intended to single difference the GLONASS carrier phase observations, while continuing to double difference the GPS carrier phase observations. However, after extensive attempts at modifying the code to achieve this, it was decided to abandon this approach. This was because, while PANIC was originally written to be flexible for future modifications, the extent of the modifications necessary for GPS/GLONASS integration were never considered by the original authors. For example, issues such as choosing GPS/GLONASS base satellites and changes necessary to the storage arrays, would have necessitated major structural changes in all aspects of the program. Therefore a second approach was devised and adopted where, by simply scaling the GLONASS carrier frequencies to that of GPS (Chapter

4), one base satellite only need be specified, and the standard double difference carrier phase solution remains valid. The one drawback of this technique is that the resultant GLONASS ambiguities are non-integer.

5.4.1 Validation of PANIC

As with Filter, it was necessary to quantify the validity of the changes made to PANIC, and quantify the potential effect of combining GPS and GLONASS in double difference code and carrier phase solutions. The results of the tests performed on the same data set, as detailed in Section 5.3.1.3, are described below.

5.4.1.1 Reformatting the Data

During the development of the kinematic GPS processing software (NOTF), that would use as its basis the single difference observable, it was decided to use the tried and tested routines within PANIC to perform the initial data management. Extensive tests of PANIC had validated its ability to produce accurate and reliable GPS satellite positions, tropospheric delay values, elevation angles, and pre-organised single difference observables. The output from PANIC was therefore combined in a single output file, the *GASFILE*, which served as the initial input to NOTF. The first test performed on the new version of PANIC was to ensure that the contents of this GASFILE remained valid for combined GPS/GLONASS observations.

An example of a GASFILE is included in Appendix A. By comparing the code, carrier and ephemeris information within this file, with the same information in the corresponding .NOT, and .SP3 files, this information was validated, as it remained the same. It is worth noting that, if the only reason for using PANIC is to obtain the GASFILE then, the GLONASS carrier phase information

present in the .NOT input files, should not be scaled to the GPS frequency. This is because NOTF uses single differencing by satellite observables, and therefore the problem of differencing between satellites is not experienced.

A full description of the format of the GASFILE can be found in Hansen [1996]. However in summary, the information included at each epoch contains the observations outlined above and in addition elevation and tropospheric delay values calculated for each satellite at each epoch. However, as neither of the routines used to calculate these values uses as an input the carrier phase value, it was not necessary to alter these in any way, and the results obtained from them are equally valid for both GPS and GLONASS.

5.4.1.2 Position Computation

As already mentioned, PANIC can calculate double difference position solutions, from either code or carrier phase data. The results derived are therefore divided into two further sub-sections. All coordinates have been converted from their original Cartesian format, to Eastings, Northings and Heights by the process detailed in Section 5.1.1.

5.4.1.2.1 Pseudorange ZBL Double Difference Solution

The results obtained by processing the 90 minute data set for GPS only, GLONASS only, and finally GPS/GLONASS are detailed in the following tables. As can be seen from these results, quite a marked difference between the GPS and GLONASS solutions was observed. One possible explanation for this is the greater number of GPS observations used in the position calculations. In an attempt to quantify the effects of this, results of a fourth

test, whereby the number of GPS only observations used in the solution were reduced below the level of GLONASS only, have also been included. This was achieved by flagging random GPS satellites as being unhealthy within Filter, and was performed to make a direct comparison of GPS and GLONASS more valid. Clearly for such a comparison to be fully valid, the constellations of the satellites in both systems would need to be identical, but by reducing the number of observations used in the solution, it was hoped to see if there was any noticeable effect on the results.

As with the single point positioning experiment detailed in Section 5.3.1.3, it would have also proved beneficial to compare the results presented below, with those obtained through commercial packages. However, WinPrism does not have the facility to process pseudorange data, and AOS experienced difficulties in processing the data set successfully.

Table 5.5 PANIC Pseudorange Residuals

Combination	Number of Obs.	RMS DD Residuals
GPS Only	40036	0.0834m
GLONASS Only	27033	0.8509m
Mixed	72449	1.3287m
Reduced GPS	25209	0.0805m

Table 5.5 lists the rms. residuals associated with each of the solutions. The partial nature of the GLONASS constellation is reflected in the fact that there are approximately only two thirds the number of observations used in the GLONASS only solution, as in the GPS only solution. As expected, the mixed solution delivers the most observables, with a total which exceeds the sum of the number of observations for GPS and GLONASS only, as these specified a different base satellite for each solution while the combined solution uses only one such satellite. Looking at the rms. double difference residuals, it is immediately obvious that the most precise results have been achieved through using GPS alone. This is a complete reversal from the results obtained through

using the stand-alone positioning routines within Filter, and demonstrates how the effects of S/A can be removed through differencing the observations. Even when the number of observations used in the GPS solution are reduced to a lower level than those in the GLONASS solution, there is no major change in the precision achieved, which still remains some ten times that of GLONASS. In an attempt to explain the comparatively poor precision of the GLONASS observations, PANIC was run again, this time with the coordinates of both stations fixed to the truth value. The resulting residuals of each satellite pair would highlight any errors in the data, as the expected result on a ZBL should be zero.

The associated residuals between each satellite pair have been reproduced in Figure 5.8 for each of the three satellite combinations. Figure 5.8 (A) shows how the double difference residuals between satellite 15, the base satellite in this case, and all other GPS satellites, appear to be random in nature, with a mean oscillation of +/- 0.2m, and have no bias. The GLONASS double difference residuals, this time with satellite 35 acting as the base satellite, are presented in Figure 5.8 (B). It is immediately obvious from this, that the residuals of all the satellite combinations are biased. The extent of this bias ranges from 0.5 metres for satellite pair 35-50, upto 1.5 metres for satellite pair 35-36, and appears to be quite consistent throughout the entire processing period. This finding agrees with published results from other research projects, for example, Hall et. al., [1997] quote observed pseudorange biases in the region of 1-3 metres on their GG-24 receivers. Indeed, Ashtech themselves experienced pseudorange biases of 1.5 metres in various ZBL tests used in the evaluation and development of their receivers [Gourevitch et. al. 1996].

These *inter-channel biases*, as they are more commonly known, are caused as a result of the same GLONASS signals taking different times to travel through the Radio Frequency (R/F) section of each receiver. This is due to the fact that each GLONASS satellite broadcasts on a different frequency, and so it is not a problem for GPS satellites, which all broadcast on the same frequency. This partly explains why the precision of the GPS observables is much better.

Figure 5.8 Panic Pseudorange Residuals between Satellite Pairs

A

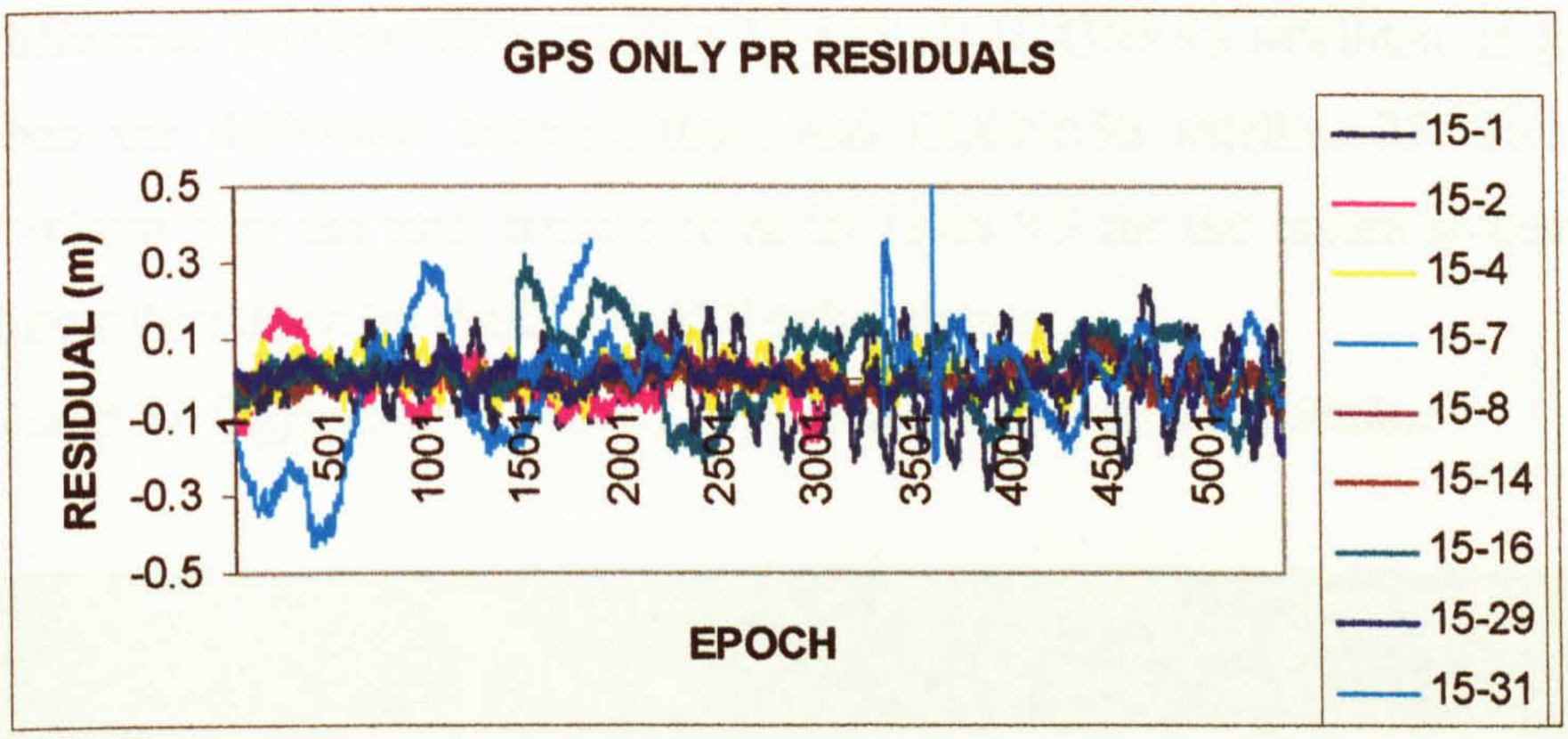

B

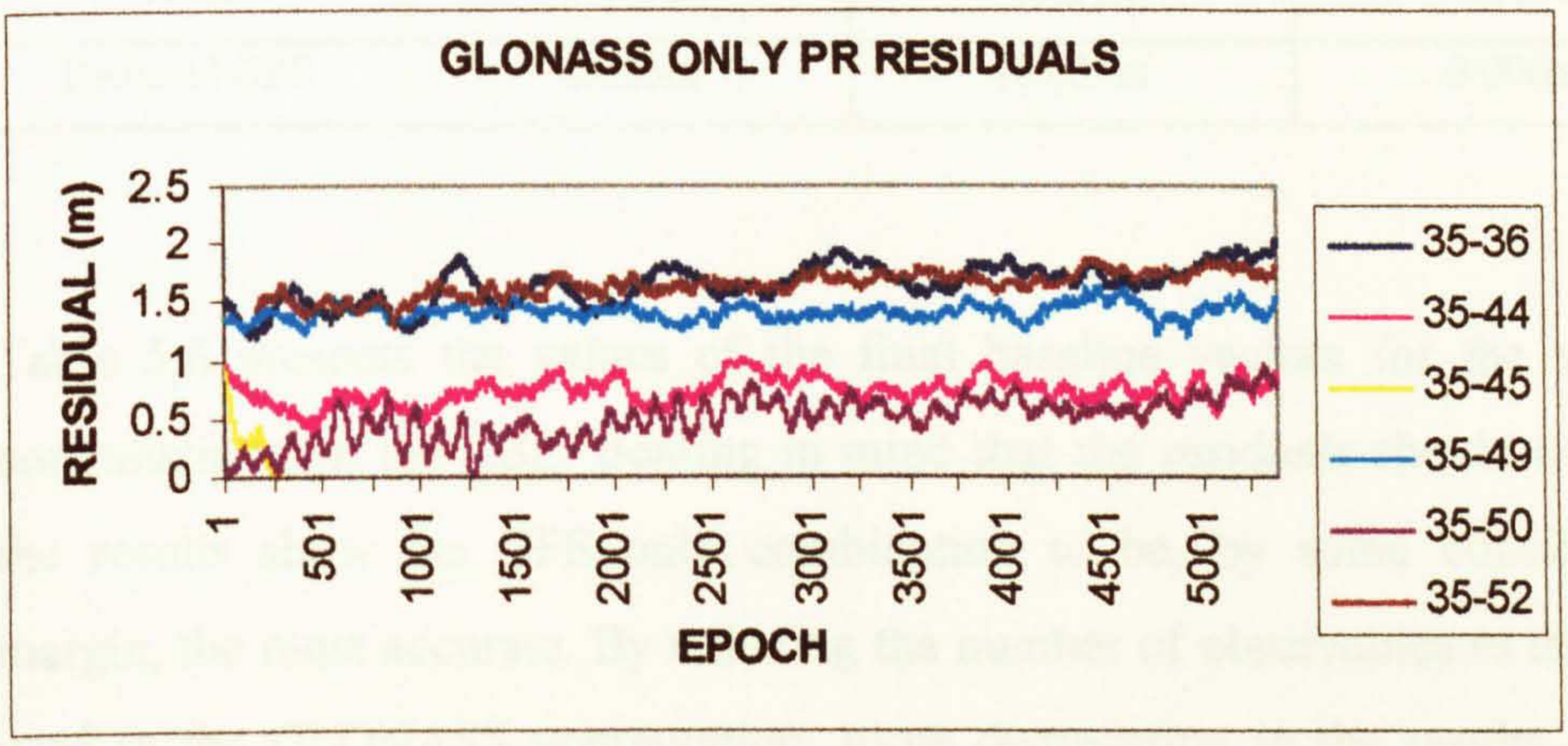

C

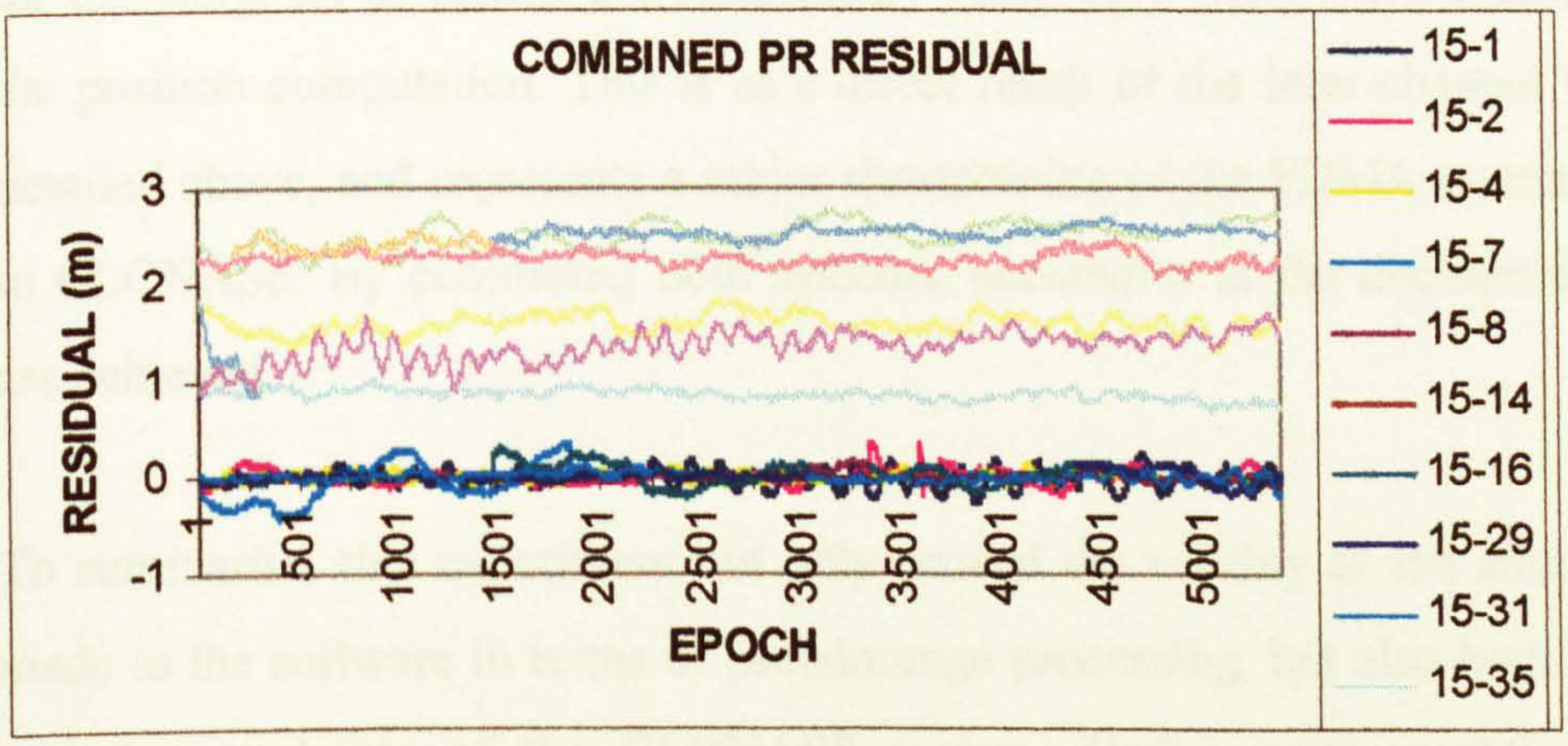

Finally, Figure 5.8 (C) shows the pseudorange delay between satellite 15 and all other satellites. Again all GLONASS satellites exhibit some inter-channel bias, the extent of which is this time marginally greater, as the frequency difference between GPS satellite 15 and all GLONASS satellites, is greater than the difference between them and GLONASS satellite 35. This also explains why the rms. errors quoted in Table 5.5 for the mixed solution are larger than those for the GLONASS only solution.

Table 5.6 Difference in PANIC Pseudorange Coordinate Solution

Combination	Difference in Easting	Difference in Northing	Difference in Height
GPS Only	0.005m	-0.017m	0.002m
GLONASS Only	-0.117m	-0.702m	-0.623m
Mixed	0.003m	-0.126m	-0.168m
Reduced GPS	0.025m	-0.035m	0.006m

Table 5.6 presents the values of the final baseline vectors for the various combinations on the ZBL. Bearing in mind that the residuals should be zero, the results show the GPS only combination to be, by some considerable margin, the most accurate. By reducing the number of observables to the level used in the GLONASS computation, some degradation in the results can be seen to have taken place, but accuracies still remain at the centimetre level. By far the worst set of values, are obtained by using only GLONASS satellites in the position computation. This is as a direct result of the inter-channel biases detailed above, and represents a major shortcoming of the FDMA system used in GLONASS. By combining both systems, accuracies at the decimetre level are achieved.

To summarise, this experiment not only proved the validity of the alterations made to the software in terms of pseudorange processing, but also highlighted a major weakness of the GLONASS system. Under good conditions for

satellite surveying i.e. unobstructed skies, the best position accuracies using differenced pseudorange observations is achieved using GPS alone.

5.4.1.2.1.1 Pseudorange Bias Repeatability

From Figure 5.8 it appeared that there was the possibility that the pseudorange biases experienced could be consistent for each satellite. To investigate this further, two additional sets of ZBL data were each collected from the same location with an 8 day separation between them. This separation was chosen as the GLONASS satellite constellation has a repeat rate of 8 days (Chapter 2).

Figure 5.9 (A) shows the recorded residuals for three GLONASS satellites over a 30 minute period on 20th August 1998, whilst Figure 5.9 (B) shows the residuals for the same satellites over the same period on 28th August 1998. From this it can be seen that the biases appear in the same order between the two sets. However, as neither the magnitudes or their relationships remain the same it cannot be concluded that the bias is an interfrequency bias caused by oscillation errors within the GLONASS satellites themselves. It was therefore decided that the magnitude of the bias could not be directly predicted from the signal frequency. It is worth noting that, while the residuals obtained for all GLONASS satellites on 20th August 1998 were consistent, this was not the case, with the exception of the residuals used in Figure 5.9 (B), for all the GLONASS residuals obtained on 28th August 1998. This was symptomatic of some data sets obtained from the Ashtech GG-24 receivers used throughout the project (Section 5.6).

Figure 5.9 Panic GLONASS Pseudorange Residuals over 8 Day Cycle

A

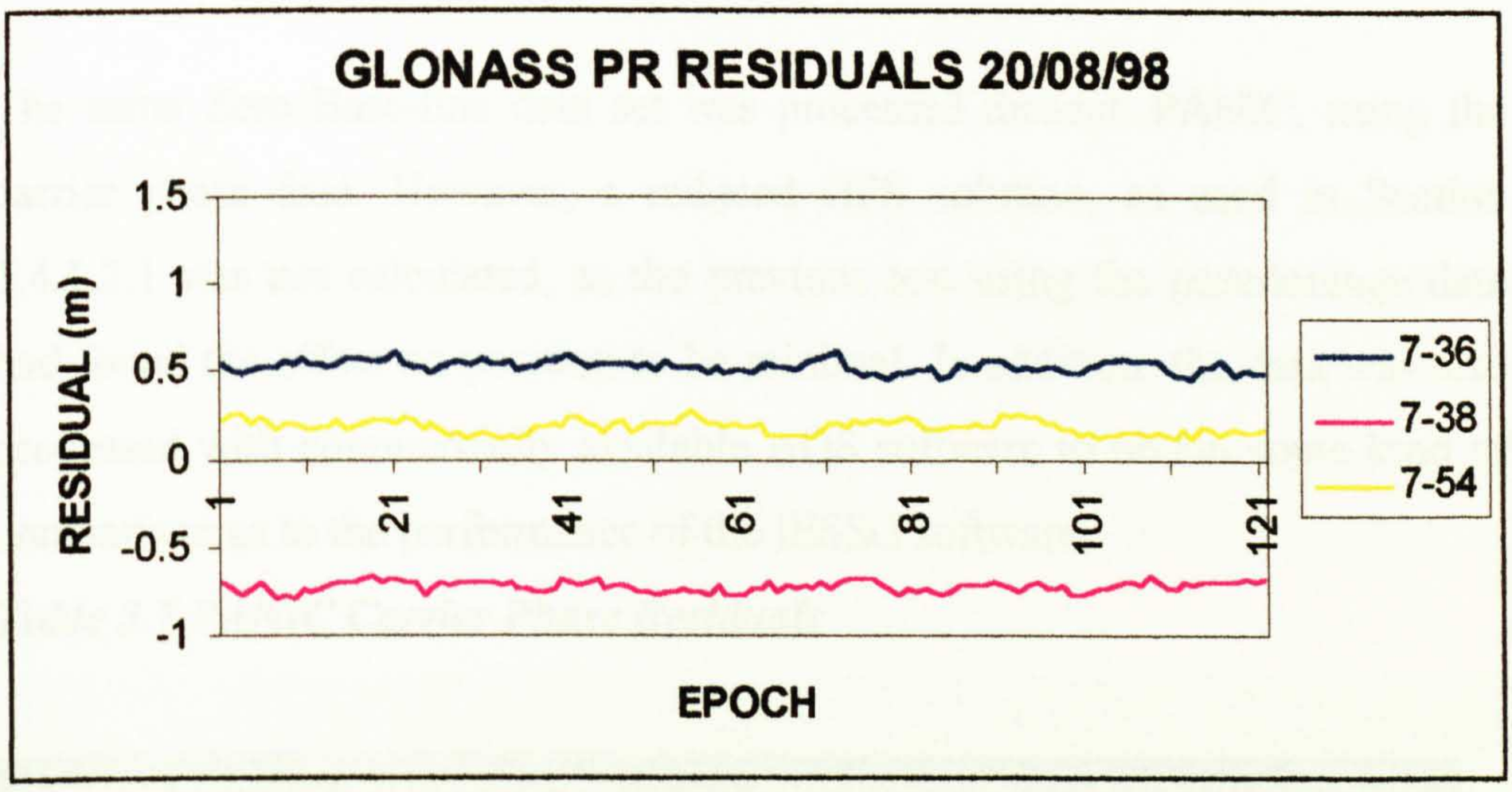

B

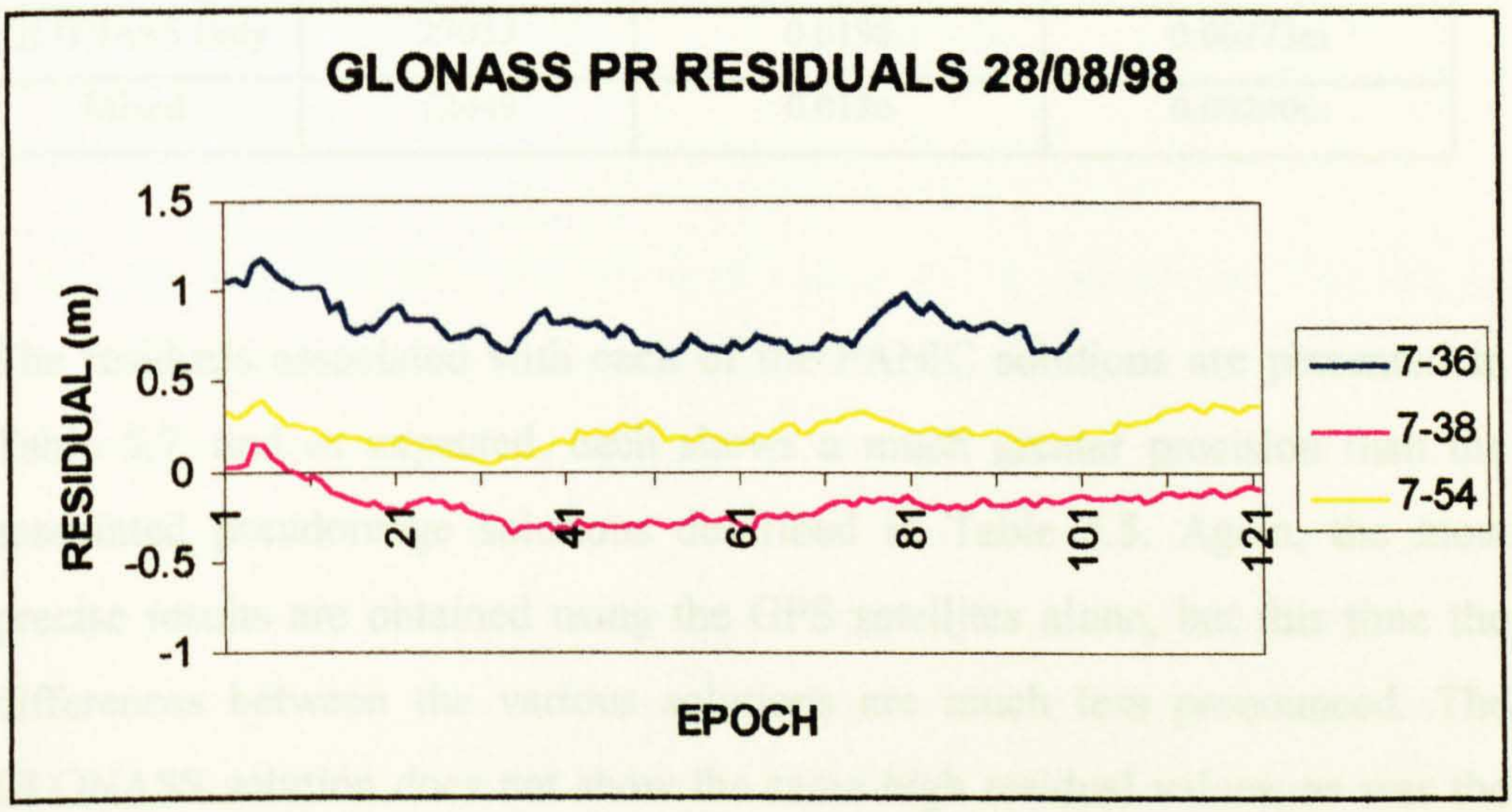

5.4.1.2.2 Carrier Phase ZBL Double Difference Solution

The same Zero Base-line data set was processed through PANIC, using the carrier phase data. However, a reduced GPS solution, as used in Section 5.4.1.2.1 was not calculated, as the previous test using the pseudorange data had found the effect on position to be minimal. In addition, the data was also processed with commercially available AOS software to obtain some kind of comparison as to the performance of the IESSG software.

Table 5.7 PANIC Carrier Phase Residuals

Combination	Number of Obs.	RMS DD Residuals (Cycles)	RMS DD Residuals (Metres)
GPS Only	40036	0.0095	0.00182m
GLONASS Only	27033	0.0196	0.00373m
Mixed	72449	0.0126	0.00240m

The residuals associated with each of the PANIC solutions are presented in Table 5.7, and as expected, each shows a much greater precision than the associated pseudorange solutions described in Table 5.5. Again, the most precise results are obtained using the GPS satellites alone, but this time the differences between the various solutions are much less pronounced. The GLONASS solution does not show the same high residual values, as was the case with the GLONASS pseudorange solution, suggesting that the receiver bias is much less pronounced when dealing with carrier phase data. The reason for this could be the different paths the code and carrier phase data take through the various R/F and signal processing parts of the receiver. This has not been investigated further as it lies outwith the area of expertise within the IESSG and bounds of the research project.

Figure 5.10 illustrates this lack of bias by showing a double difference satellite residual in cycles for each combination. Only one such difference between GPS-GPS and GPS-GLONASS satellites has been shown, to maintain clarity, but all have been examined and found to give similar results. They show the GLONASS residuals to be in the region of 1 centimetre, approximately three times the level of those of GPS, but with a mean value of zero. Again this agrees with Ashtech's own quoted accuracies, as Gourevitch et. al. [1996] found typical double difference RMS residuals of 4 millimetres for GPS and 12 millimetres for GLONASS.

Table 5.8 Difference in PANIC Carrier Phase Float Coordinate Solution

Combination	Difference in Easting	Difference in Northing	Difference in Height
GPS Only	-0.003m	-0.001m	0.028m
GLONASS Only	0.000m	0.000m	0.002m
Mixed	0.004m	-0.002m	0.014m

There are within PANIC two forms of carrier phase positioning. The first of these is a *float solution*, where-by no attempt is made to fix the integer ambiguities. The resultant misclosures on the ZBL for this type of solution are presented in Table 5.8. As can be seen, the values obtained from each of the solutions are accurate to the millimetre level in plan, and centimetre level in height. From this set of results it is clear that the changes implemented within not only the Float positioning routine within PANIC, but also the scaling of the GLONASS carrier frequencies to that of GPS within Filter, were implemented correctly. It is also worth noting that, unlike the double difference pseudorange solution detailed in the previous section, achievable accuracies using double difference carrier phase observations are not reduced by combining GPS with GLONASS.

The second method of carrier phase positioning within PANIC is to attempt to resolve the unknown integer ambiguities. However, as already described, the

Figure 5.10 PANIC Carrier Phase Residuals between Satellite Pairs

A

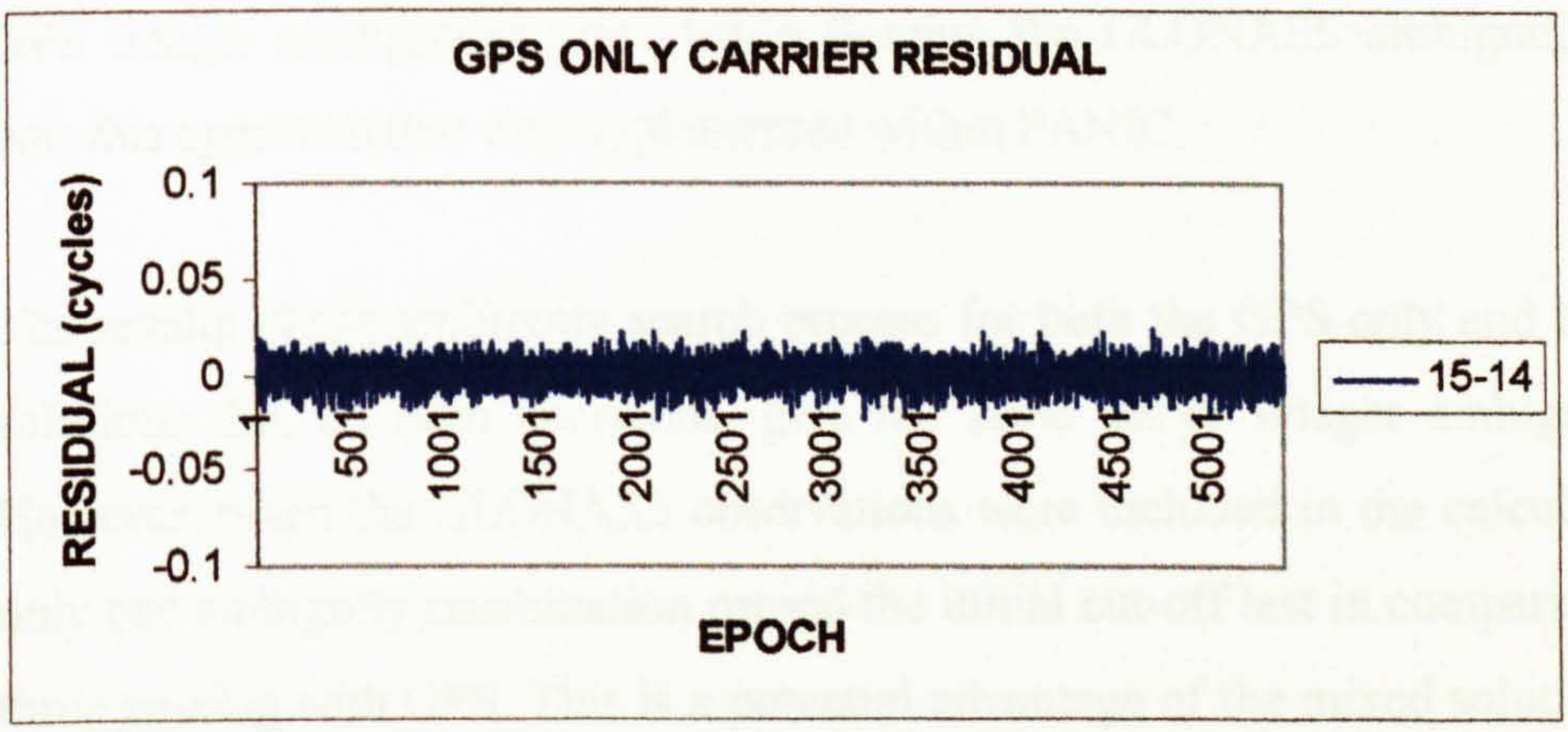

B

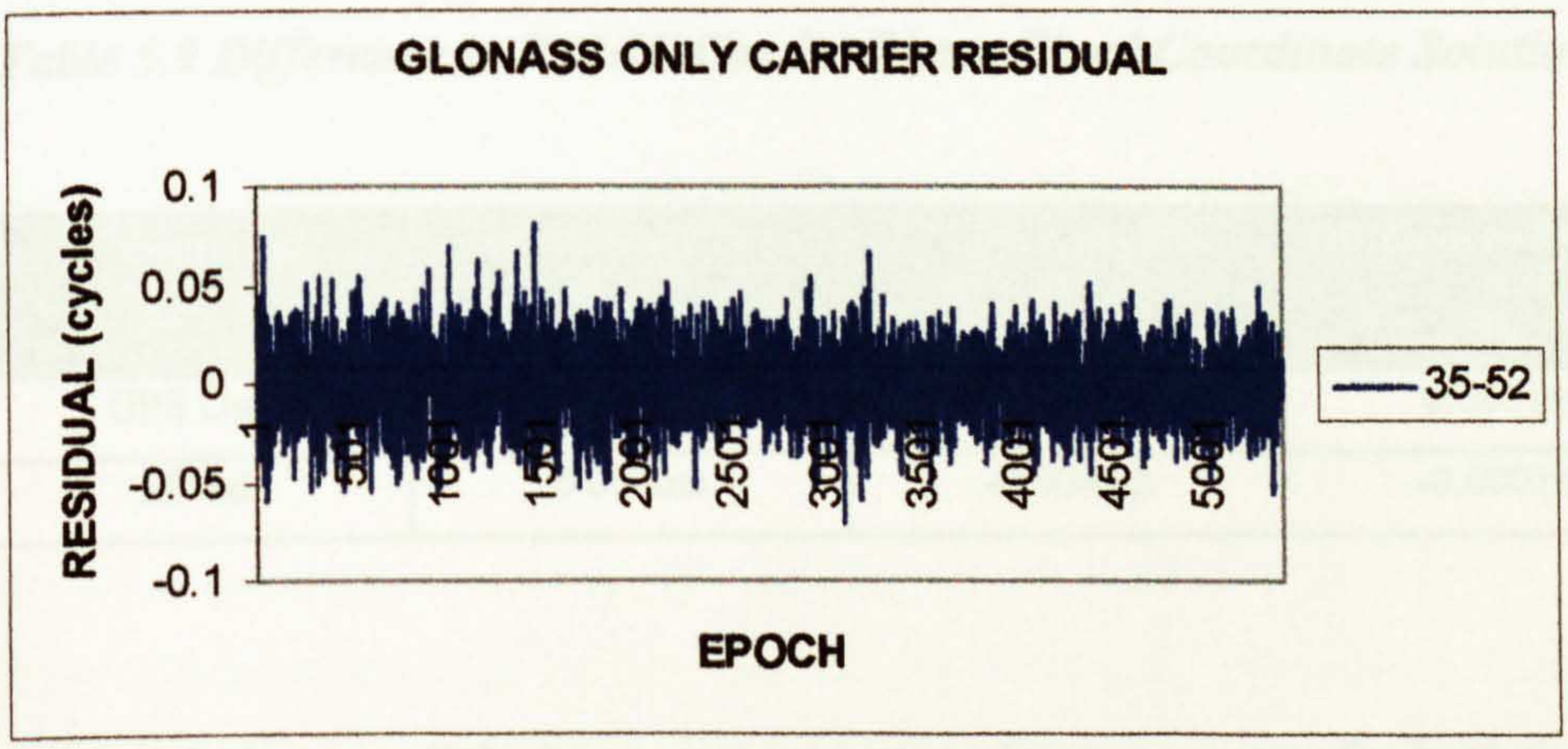

C

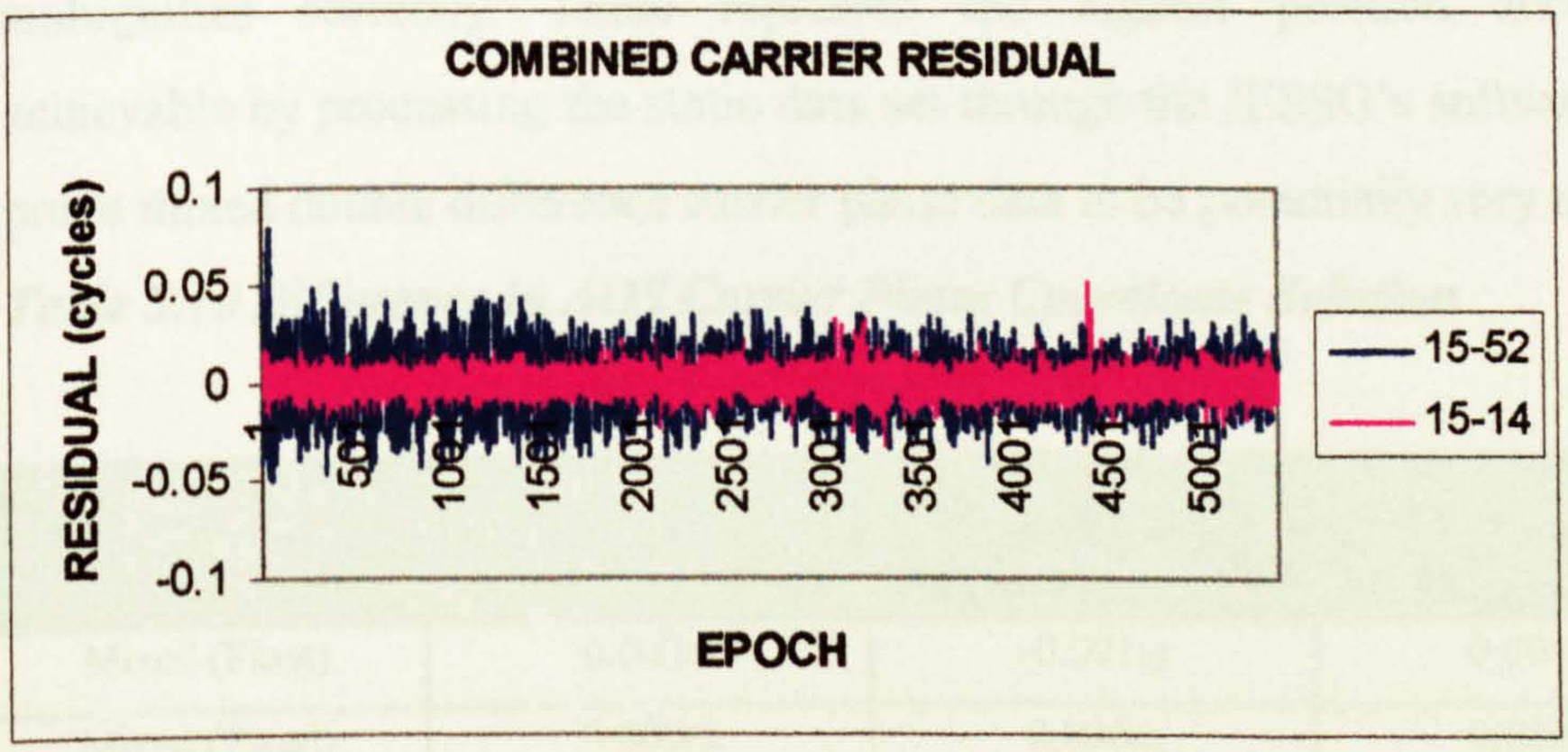

process of scaling the GLONASS frequencies to GPS has the effect of destroying the integer nature of the GLONASS ambiguities. It is however still possible, in a combined solution, to include all observations in the search for GPS integer ambiguities only, while floating the GLONASS ambiguities. It was this approach that was implemented within PANIC.

The results of the ambiguity search process for both the GPS only and mixed solutions did, on both occasions, give the same set of integer ambiguities. However, when the GLONASS observations were included in the calculation, only one ambiguity combination passed the initial cut-off test in comparison to three passing with GPS. This is a potential advantage of the mixed solution, as all incorrect ambiguity solutions were, in this case, immediately dismissed, making it impossible for the search to adopt incorrect values.

Table 5.9 Difference in PANIC Carrier Phase Fixed Coordinate Solution

Combination	Difference in Easting	Difference in Northing	Difference in Height
GPS Only	0.0003m	0.0004m	0.0001m
Mixed	0.0000m	-0.0002m	-0.0001m

Table 5.9 shows a slight improvement in coordinate accuracy for both the GPS only and mixed solution, demonstrating the advantage of fixing integer ambiguities correctly. These represent the highest position accuracies achievable by processing the static data set through the IESSG's software, and prove mixed double difference carrier phase data to be potentially very useful.

Table 5.10 Difference in AOS Carrier Phase Coordinate Solution

Combination	Difference in Easting	Difference in Northing	Difference in Height
Mixed (Float)	0.002m	-0.001m	0.004m
Mixed (Fixed)	0.000m	0.000m	0.000m

Both float and fixed results for the mixed constellation, as calculated by AOS, are listed in Table 5.10. When these results are compared with the corresponding results obtained using PANIC in Tables 5.8 and 5.9, it can be seen that, in both cases, the values obtained are very similar, with errors at the millimetre level for the float solution, and sub-millimetre level for the fixed solution.

5.5 NOTF

The NOTF program is the most recent addition to the suite of IESSG processing software. It was designed as an ambiguity resolution on-the-fly program, to be used with both static and kinematic data, and uses as the basis for its ambiguity search, the method proposed by Euler and Landau [1992]. A full description of NOTF can be found in Hansen [1996], but the basic principles behind it can be outlined as follows. A simple Kalman Filter, formulated in a *UD* factorised manner [Bierman, 1977] with a Random Walk update, is used to add observations to the equation system and also to produce the covariance matrix and initial residual values which are used in the search itself. Observations are added sequentially, and it is possible to process a number of code and carrier combinations. However, as the receiver used to gather the GPS/GLONASS data was single frequency, all results obtained through NOTF are based on only L1 code and carrier observations only. As the observables formed within NOTF are single difference (Chapter 4) the problem created for carrier phase positioning, by different GLONASS satellites broadcasting on different frequencies, is not encountered. This means that the GLONASS carrier phase counts need not be scaled to the frequency of GPS, and thus the integer nature of their ambiguities is maintained. Therefore, integer ambiguity resolution of GLONASS observables is possible using NOTF (Chapter 4). The ambiguities are said to have been successfully resolved when, the lowest sum of the squared residuals for a particular ambiguity combination is significantly better than that of the next best combination. The level of this

difference is dependent on the confidence level and the statistical technique employed. This is discussed in some detail in Hansen [1996], and throughout all tests performed by the author, the recommended combination of a Fischer test (F-test) at the 99 % confidence level, using a search range of +/- five cycles, has been used.

With the successful alteration of PANIC to produce the required input of combined GPS/GLONASS data for NOTF, the changes required within NOTF were not as far reaching as in the modification of the earlier programmes. As with the positioning routines within Filter, two clock unknowns have to be solved for when single differencing combined GPS/GLONASS data, as each is referenced to a different time scale (Chapter 3). In doing this however, an extra observation is needed to solve for this extra unknown and thus, one of the major benefits of combining the systems, that of extra satellite visibility, is somewhat reduced. However, as both these system times are highly stable it is possible, once each clock correction has been determined, to simply continue solving for one clock, and apply the update to the second. This reduces the number of position unknowns back to four, so reducing the minimum number of observations required for a position to be derived to the same level. A position solution can therefore still be derived with, for example, two GPS and two GLONASS satellites. This procedure has been implemented within NOTF.

As illustrated in Figures 5.8 and 5.10, there are considerable differences, not only between the associated errors of the code and carrier measurements, but also between the GPS and GLONASS systems. The existing version of NOTF had already taken this into consideration for GPS observations, with the carrier phase observations receiving much higher weighting than the pseudoranges in the Kalman Filter. Clearly some sort of weighting would also have to be applied to the GLONASS measurements if the best possible results were to be achieved. To determine the levels of this weighting, the single difference residuals for both Code and Carrier Phase data produced, with both station coordinates fixed, were examined. These results are presented in Figure 5.11 and Figure 5.12 respectively.

Figure 5.11 (A) shows the GPS pseudo-range residuals to each satellite, as having a mean of approximately zero, and to oscillate about this value with an amplitude approaching +/- 0.1 metres. The situation for the GLONASS code residuals, depicted in Figure 5.11 (B), shows each satellites residual, with the exception of SV 44, having a consistent bias, which ranges between approximately +0.75 metres and –1.00 metre. When the observations from both systems were combined, the results shown in Figure 5.11 (C) were obtained. From this it was decided that the GLONASS code observations should be down weighted, with respect to those of GPS, by a factor of three in the Kalman Filter.

The GPS Carrier Phase residual is examined in Figure 5.12 (A) and shows a mean of approximately zero in all cases, with an amplitude of +/- 0.015 cycles. Unlike its pseudorange data, the GLONASS carrier phase residuals shown in Figure 5.12 (B) have no obvious bias and oscillate around zero by approximately +/- 0.3 cycles. These results are again combined in Figure 5.12 (C), and from these it was decided to down weight GLONASS carrier phase data by a factor of two in relation to GPS carrier phase observations.

It is acknowledged by the author that accommodating a bias by downweighting the biased observations with respect to the unbiased ones is not correct, as this degrades the GLONASS pseudoranges more than is statistically necessary. A better way to approach the problem would be include these biases as a state in the Kalman filter and to determine it over a period of time. Due to time restrictions on the research, this has not been investigated, but certainly should be examined if further research into this area is undertaken. To minimise the effect of these biases on the resultant position accuracy, it was decided to adopt the weighting policy detailed above.

All subsequent results obtained through NOTF, and presented in this thesis have used these levels of relative weighting between the GPS and GLONASS observations. Further details of the weighting values decided upon for GPS code and carrier observations can be found in Hansen [1996].

Figure 5.11 NOTF Pseudorange Residuals for Each Satellite

A

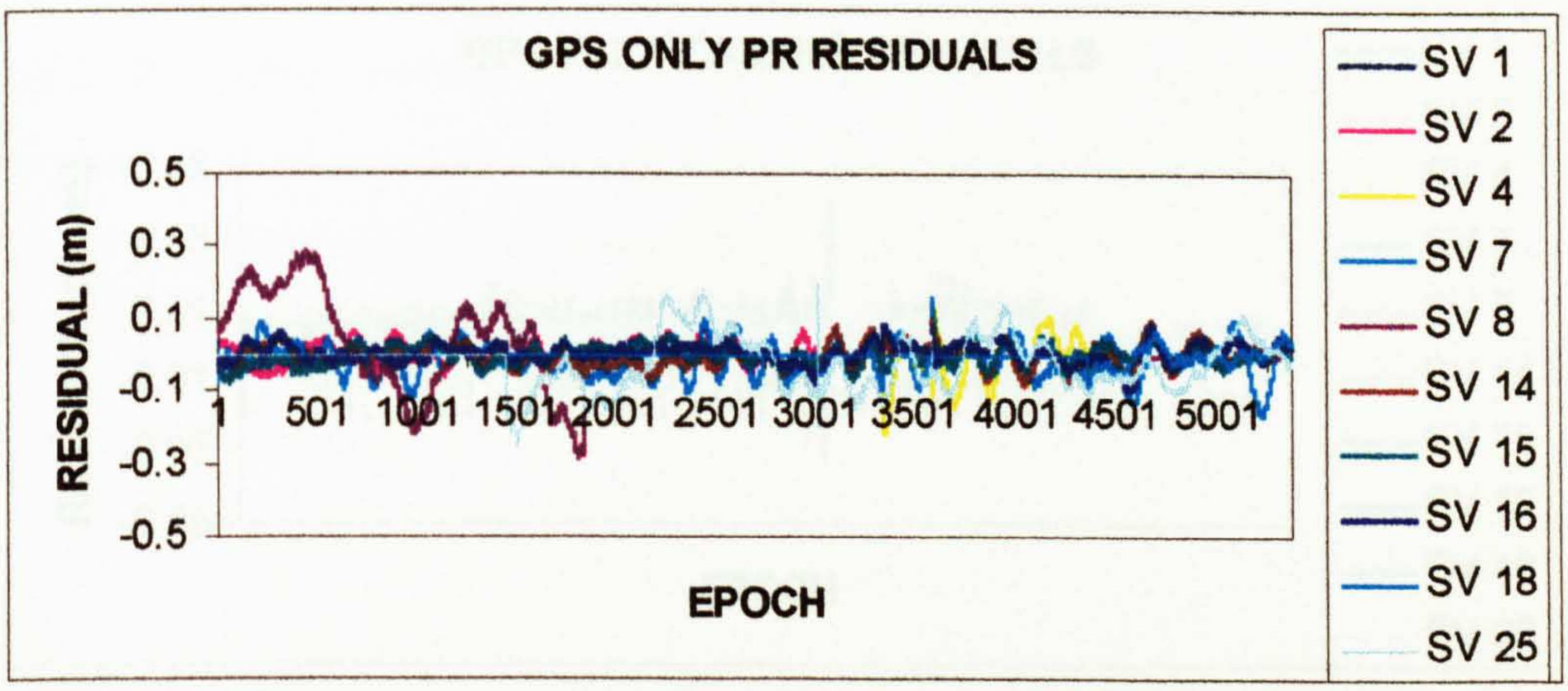

B

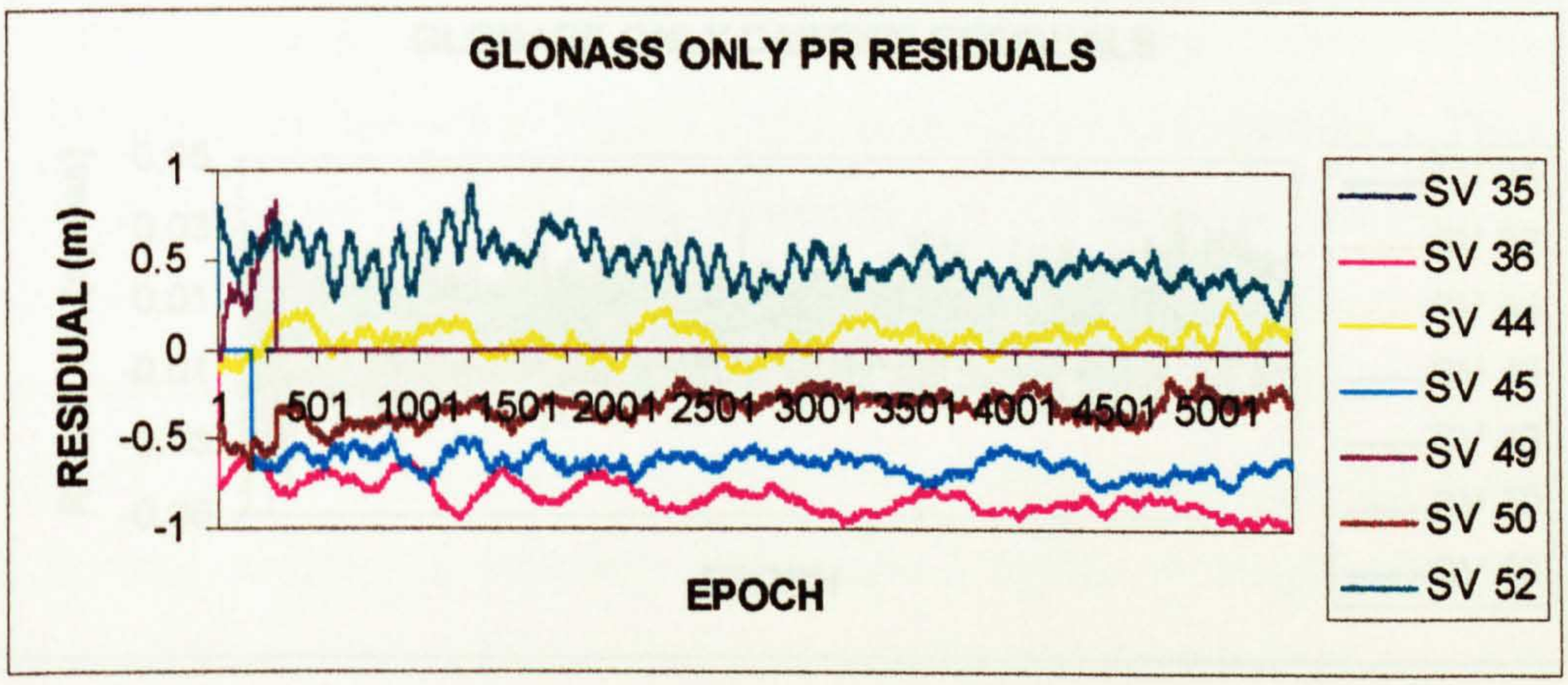

C

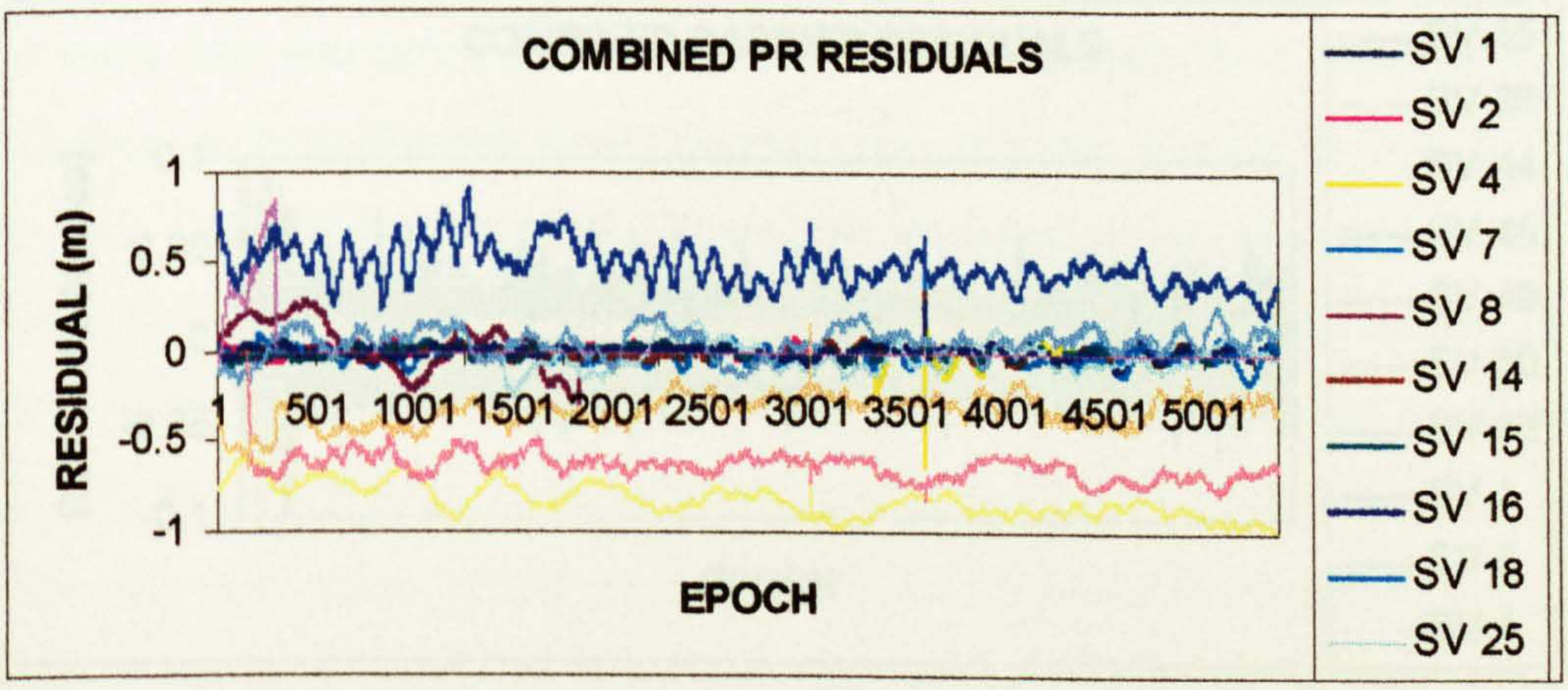

Figure 5.12 NOTF Carrier Phase Residuals for Each Satellite

A

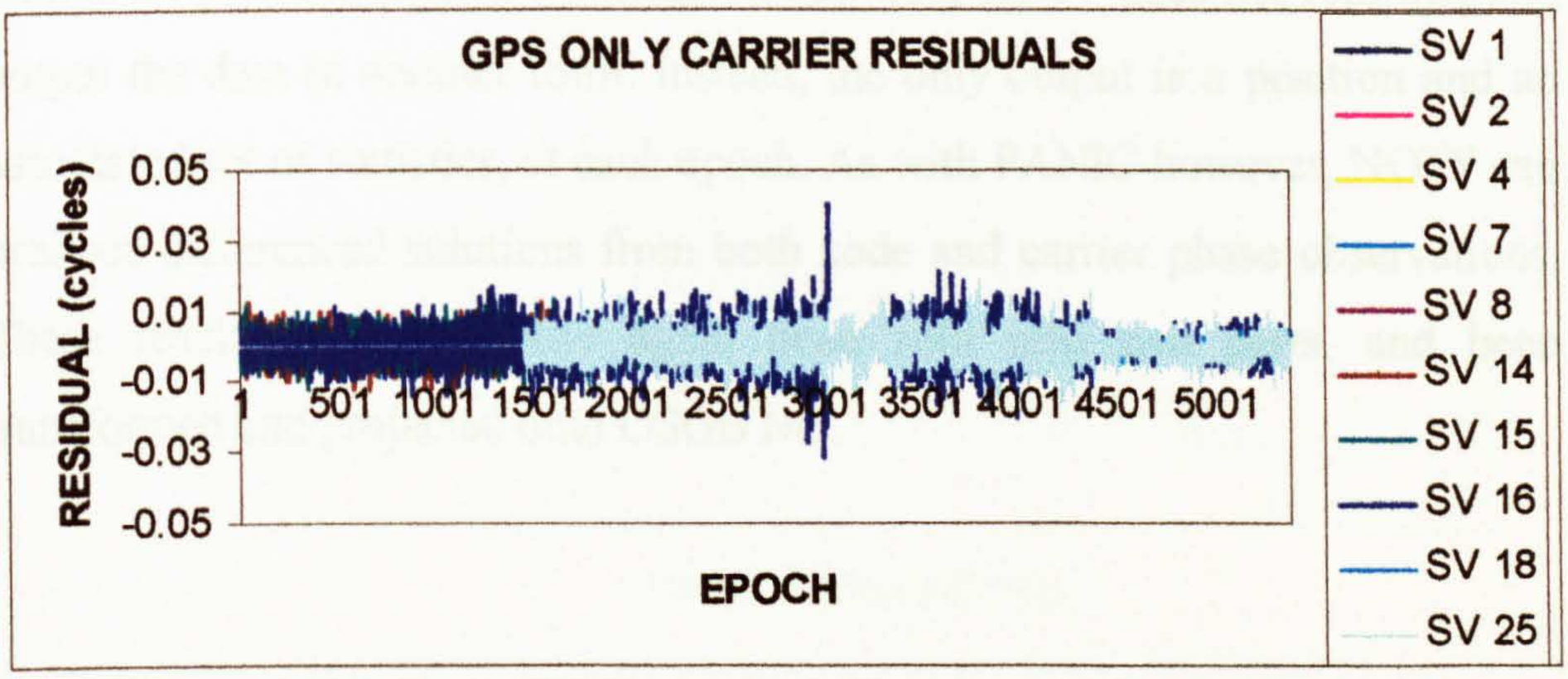

B

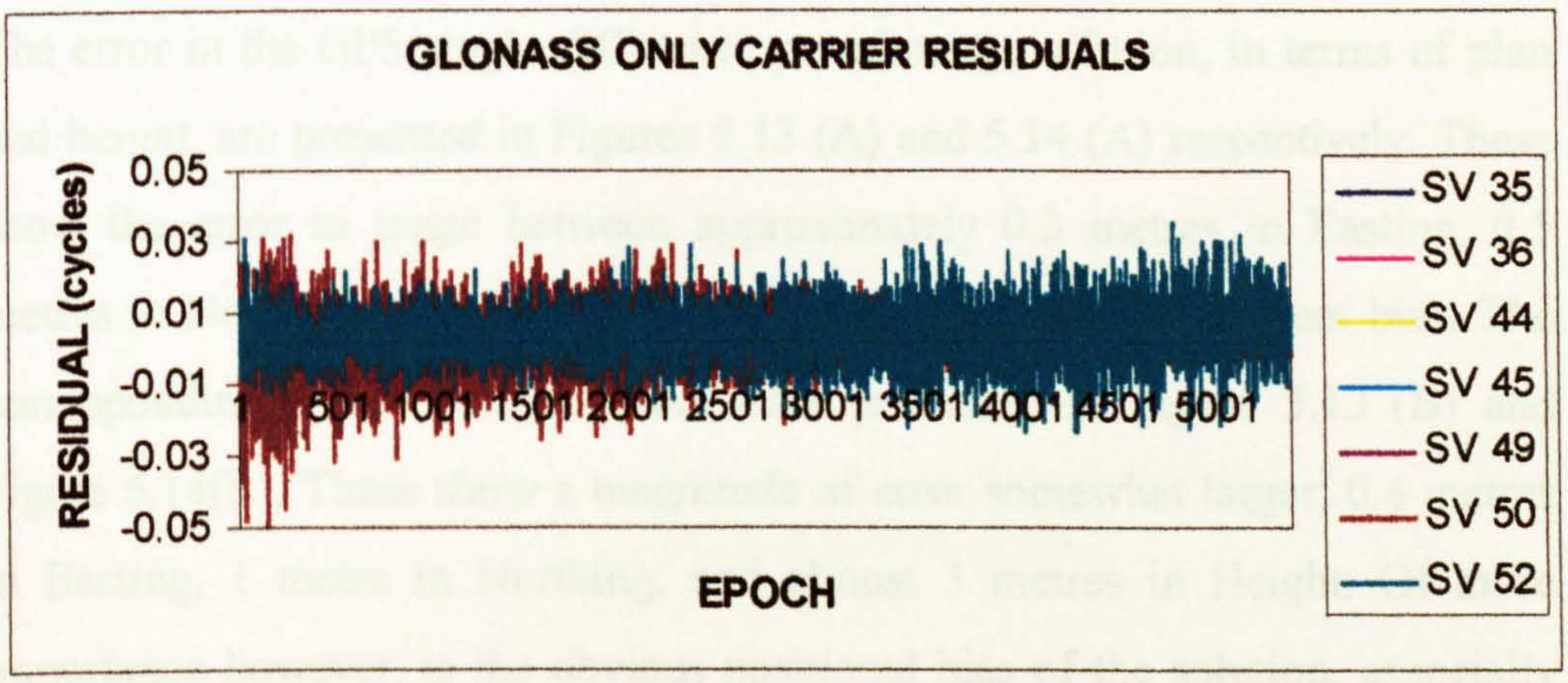

C

5.5.1 Validation of NOTF

Unlike all previous software packages described, NOTF does not reformat and output the data in another form. Instead, the only output is a position and an associated set of statistics, at each epoch. As with PANIC however, NOTF can produce differenced solutions from both code and carrier phase observations. These results have therefore again been split into two parts, and been transformed and projected onto OSGB NG.

5.5.1.1 NOTF ZBL Pseudorange Solution

The error in the GPS single difference pseudorange solution, in terms of plan and height, are presented in Figures 5.13 (A) and 5.14 (A) respectively. These show the error to range between approximately 0.3 metres in Easting, 0.5 metres in Northing, and 0.7 metres in Height, and have no apparent bias. The corresponding values for GLONASS are presented in Figure 5.13 (B) and Figure 5.14(B). These show a magnitude of error somewhat larger; 0.4 metres in Easting, 1 metre in Northing, and almost 3 metres in Height. Of more importance however, is the obvious positional bias of the solution, especially in plan, where the mean of the error values is offset by approximately -1 metre in Easting, and –0.2 metres in Northing. This reflects the results obtained when the same data was processed through PANIC, and is again as a result of the difference in inter-channel biases between the receivers. Finally, Figures 5.13 (C) and 5.14 (C) demonstrate how, by downweighting the GLONASS pseudorange observations in the Kalman Filter, the effect of the mismatch between the receivers can be greatly reduced, and accuracies similar to those using GPS only achieved. These results are quantified in Table 5.11, which shows the rms. values of the errors in each axis, for each combination. From these, it can again be quite clearly seen that there is a bias in the GLONASS solution in all three axis of measurement.

Figure 5.13 Difference in NOTF Pseudorange Plan Coordinates

A

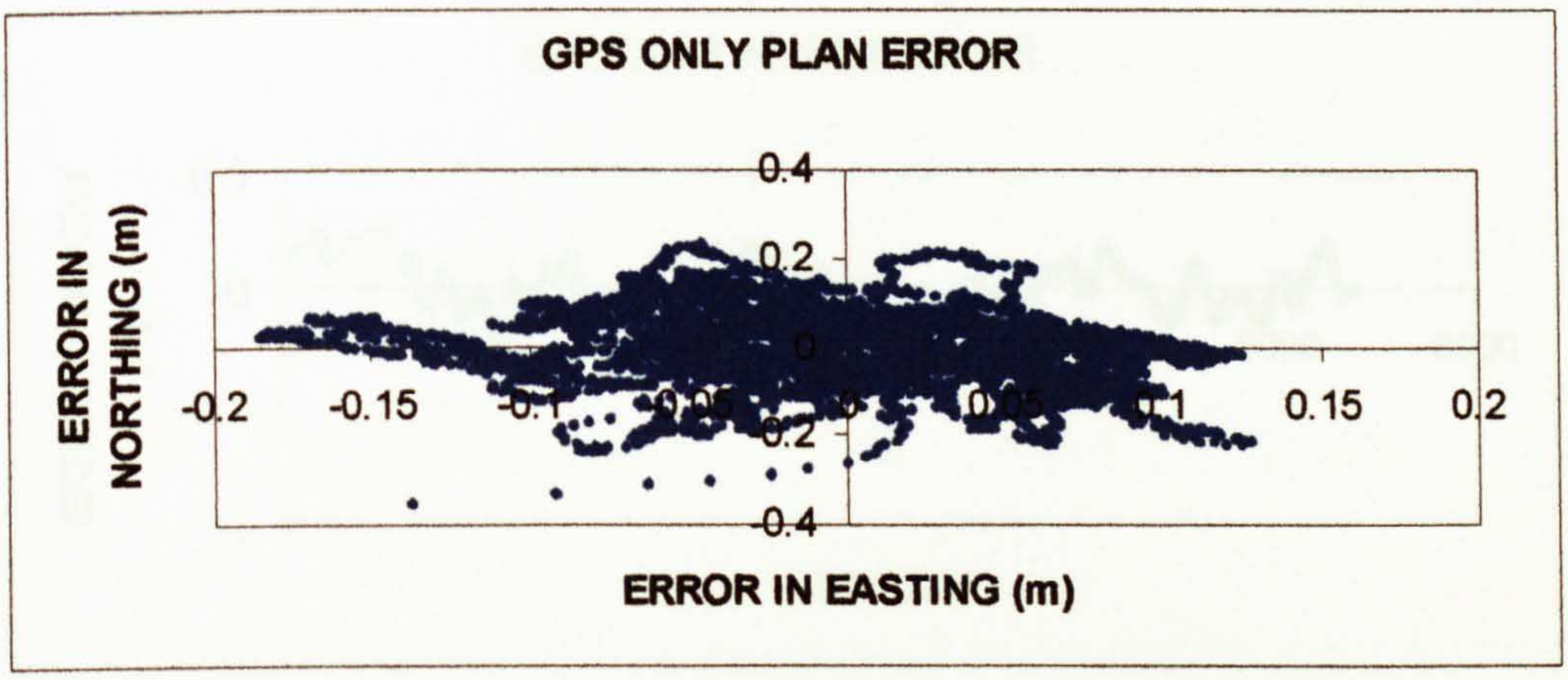

B

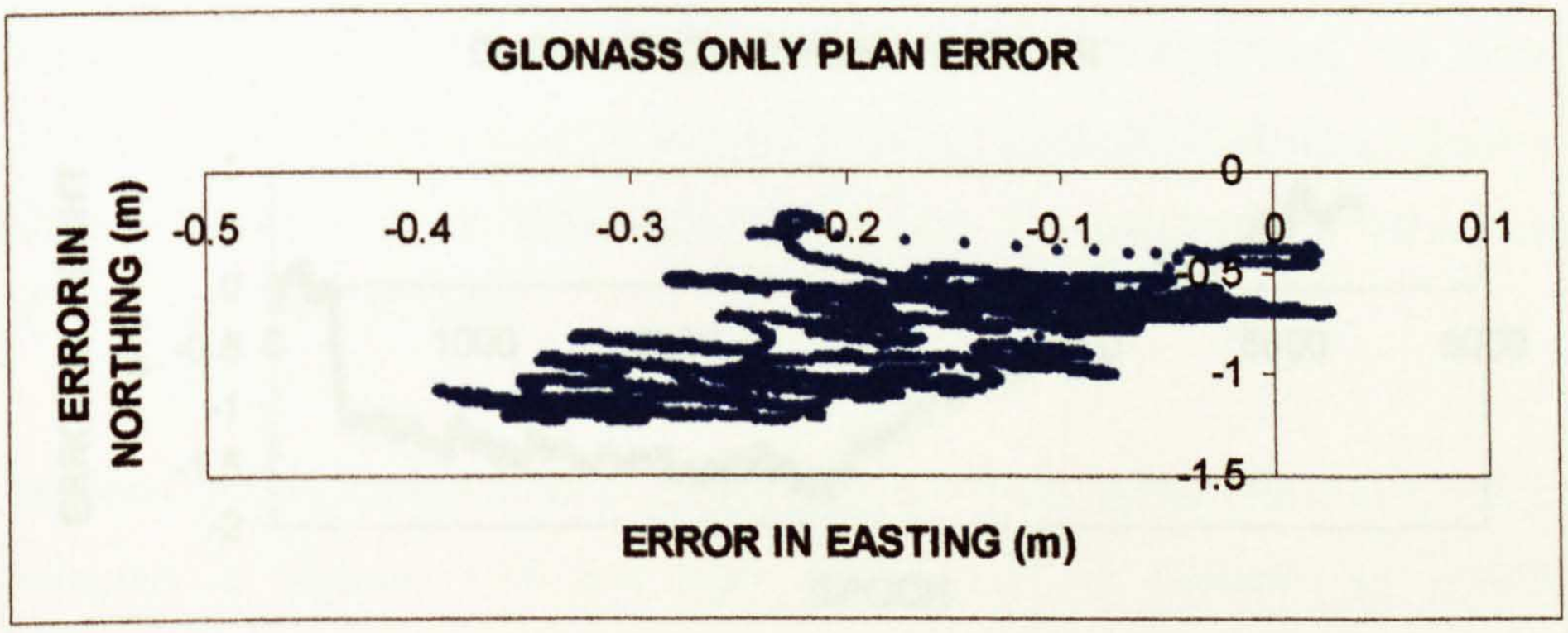

C

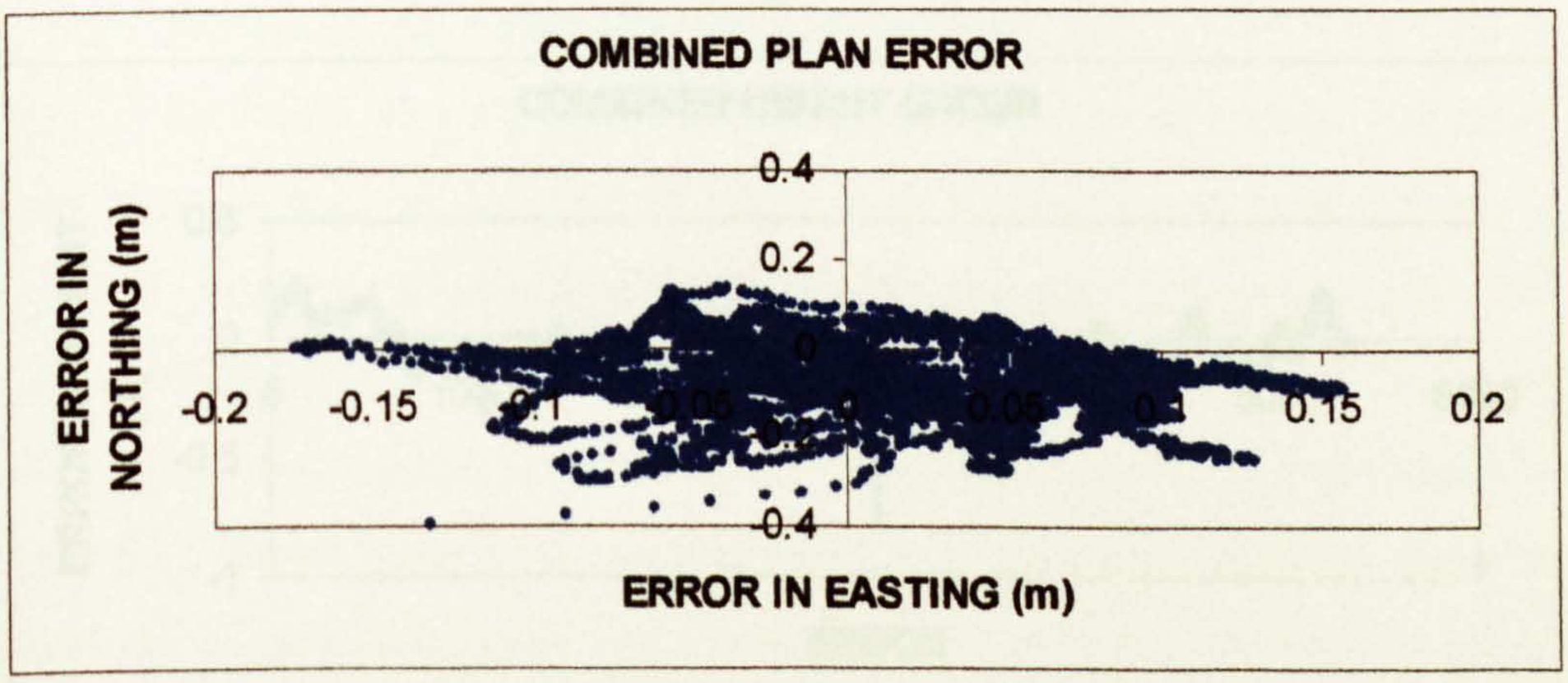

Figure 5.14 Difference in NOTF Pseudorange Height Values

A

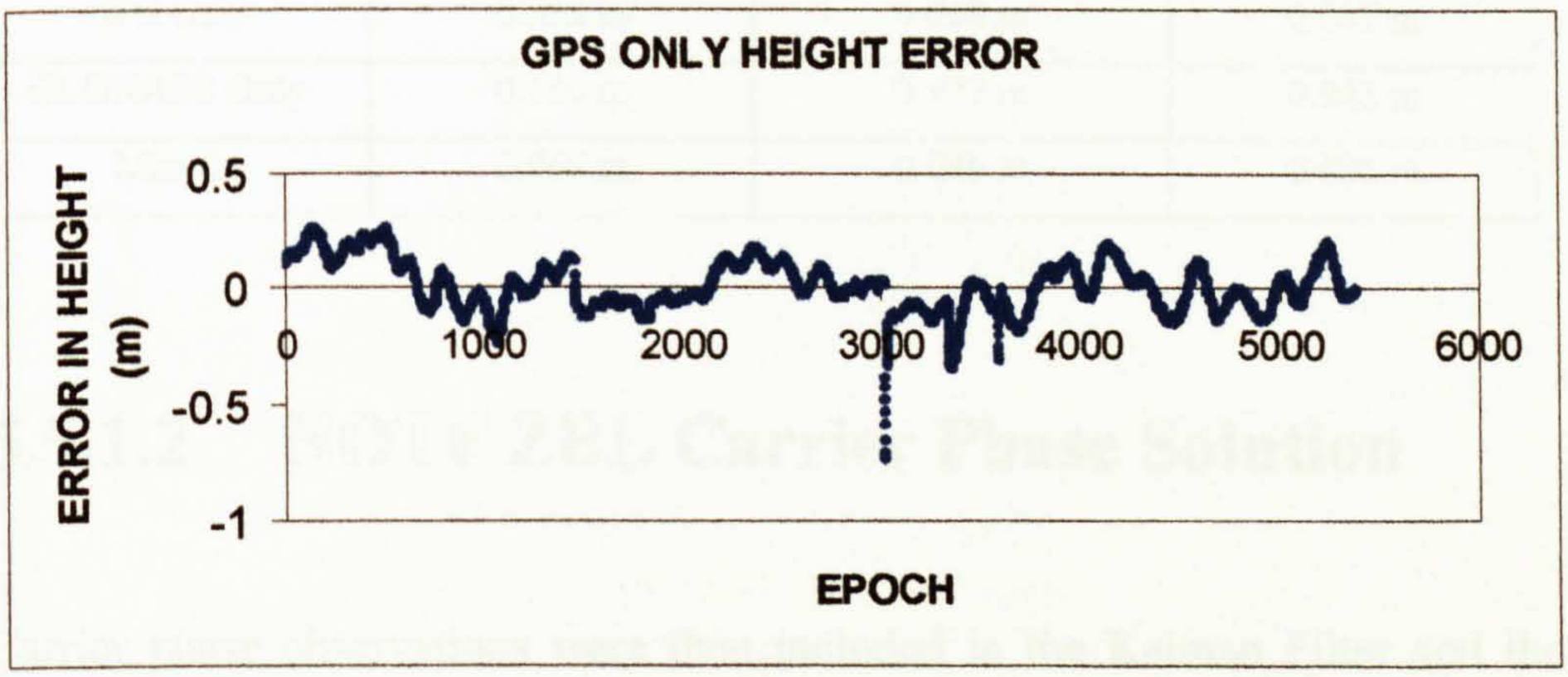

B

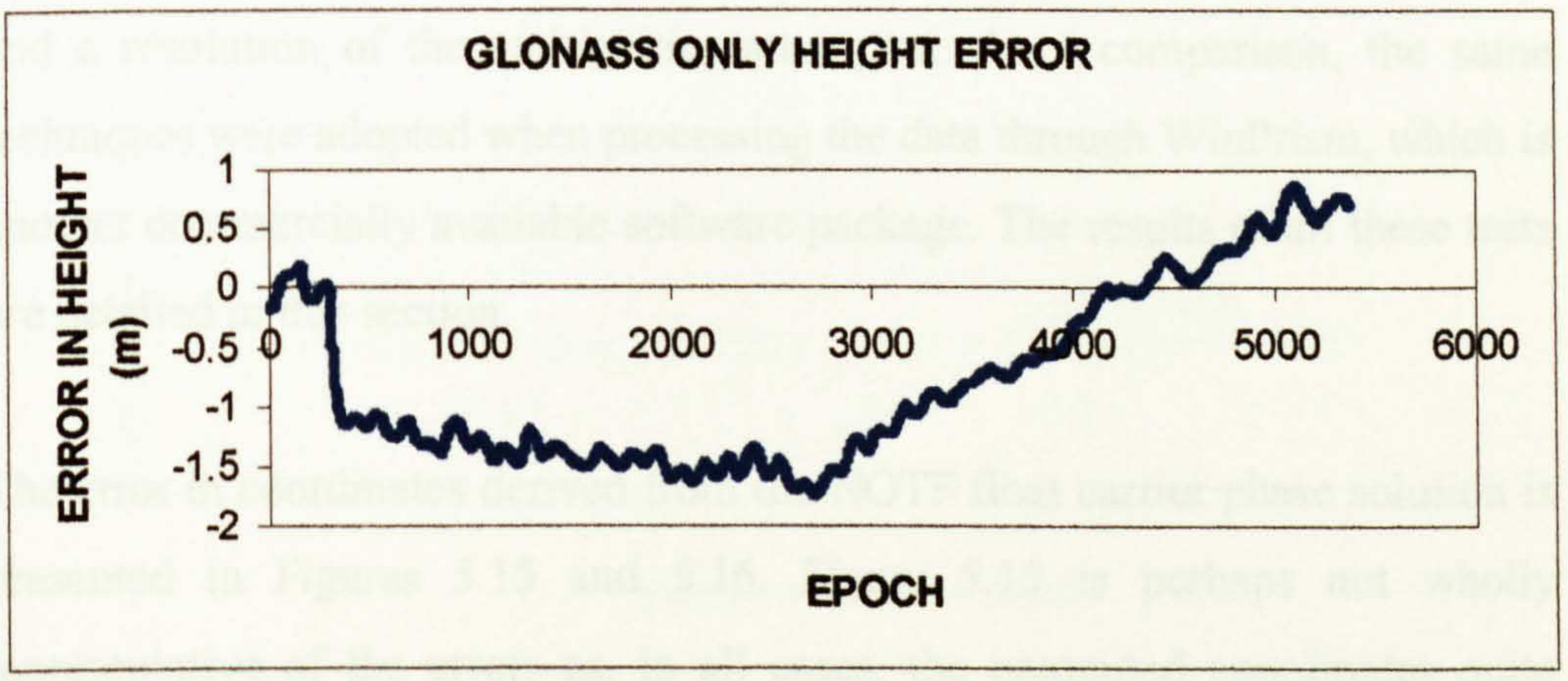

C

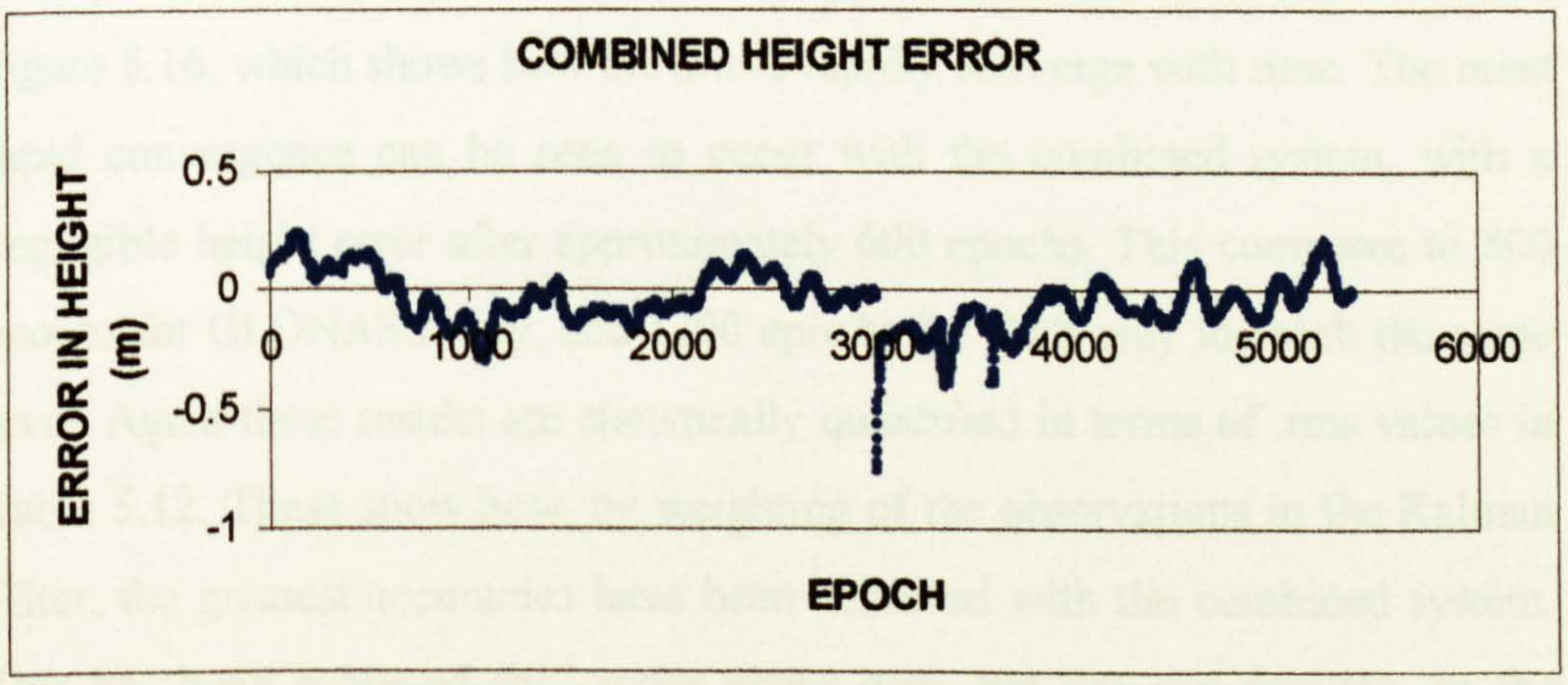

Table 5.11 RMS Values of NOTF Pseudorange Coordinate Differences

Combination	RMS in Easting	RMS in Northing	RMS in Height
GPS Only	0.052 m	0.068 m	0.087 m
GLONASS Only	0.166 m	0.777 m	0.941 m
Mixed	0.049 m	0.086 m	0.096 m

5.5.1.2 NOTF ZBL Carrier Phase Solution

Carrier phase observations were then included in the Kalman Filter and the data set processed twice. In the first run, a float carrier phase solution was produced, while on the second attempt, an ambiguity search was performed and a resolution of the ambiguities attempted. As a comparison, the same techniques were adopted when processing the data through WinPrism, which is another commercially available software package. The results of all these tests are detailed in this section.

The error in coordinates derived from the NOTF float carrier phase solution is presented in Figures 5.15 and 5.16. Figure 5.15 is perhaps not wholly representative of the errors as, in all cases, the computed coordinates quite quickly converge to the truth values and therefore the scatter of errors on the plots predominantly represents this convergence time. This is well illustrated in Figure 5.16, which shows how the errors rapidly converge with time. The most rapid convergence can be seen to occur with the combined system, with a negligible height error after approximately 600 epochs. This compares to 800 epochs for GLONASS only, and 1200 epochs for GPS only to reach the same level. Again these results are statistically quantified in terms of .rms values in Table 5.12. These show how, by weighting of the observations in the Kalman Filter, the greatest accuracies have been achieved with the combined system. This has been achieved for carrier phase data, but not pseudorange, as the GLONASS carrier phase data does not exhibit the same bias as is evident in the GLONASS pseudoranges.

Figure 5.15 Difference in NOTF Float Carrier Phase Plan Coordinates

A

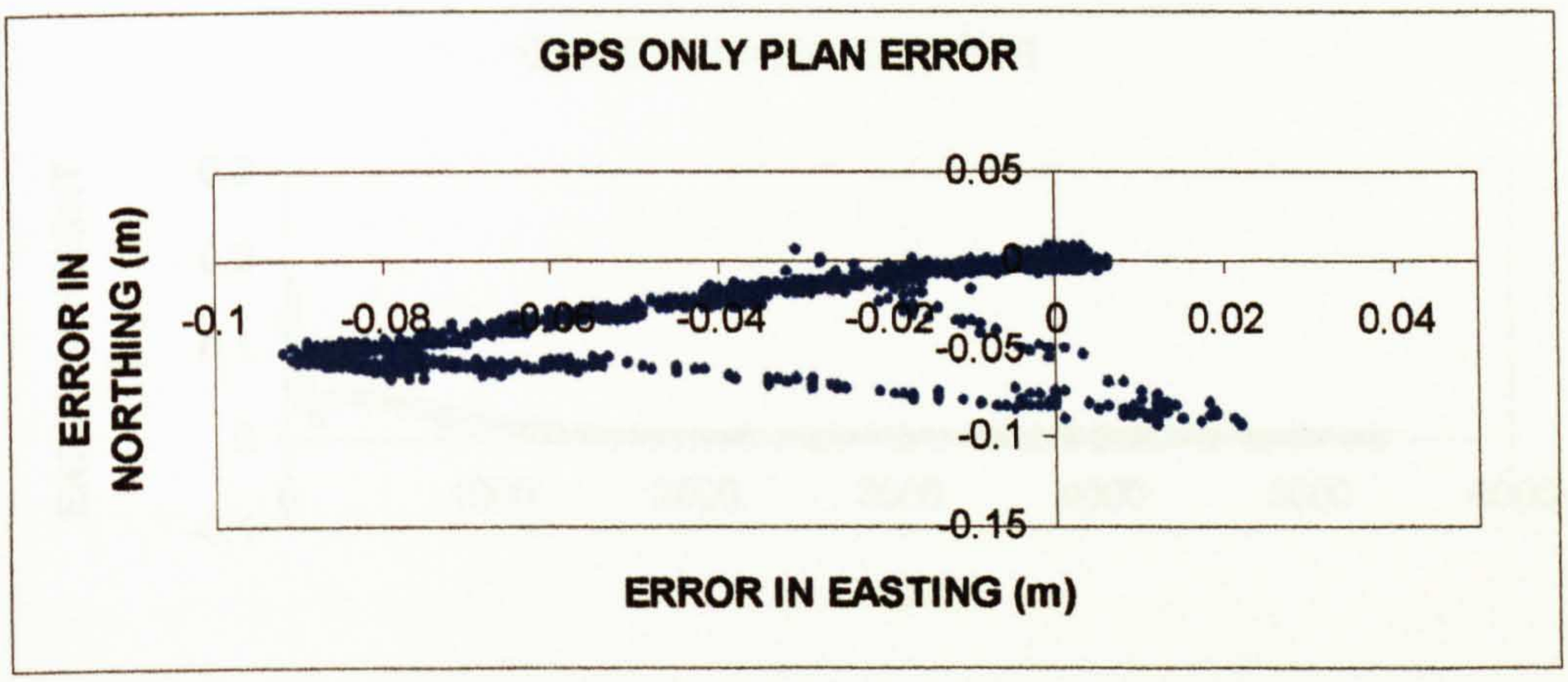

B

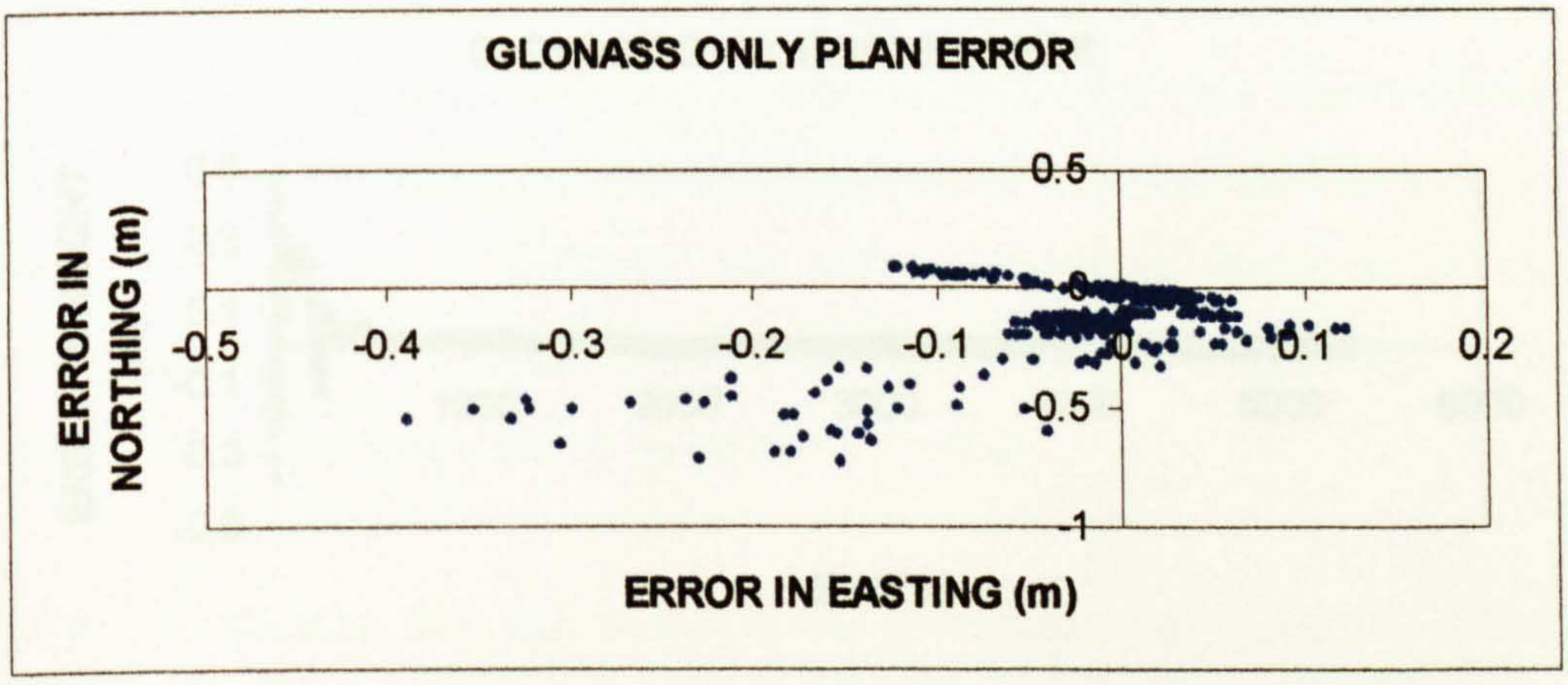

C

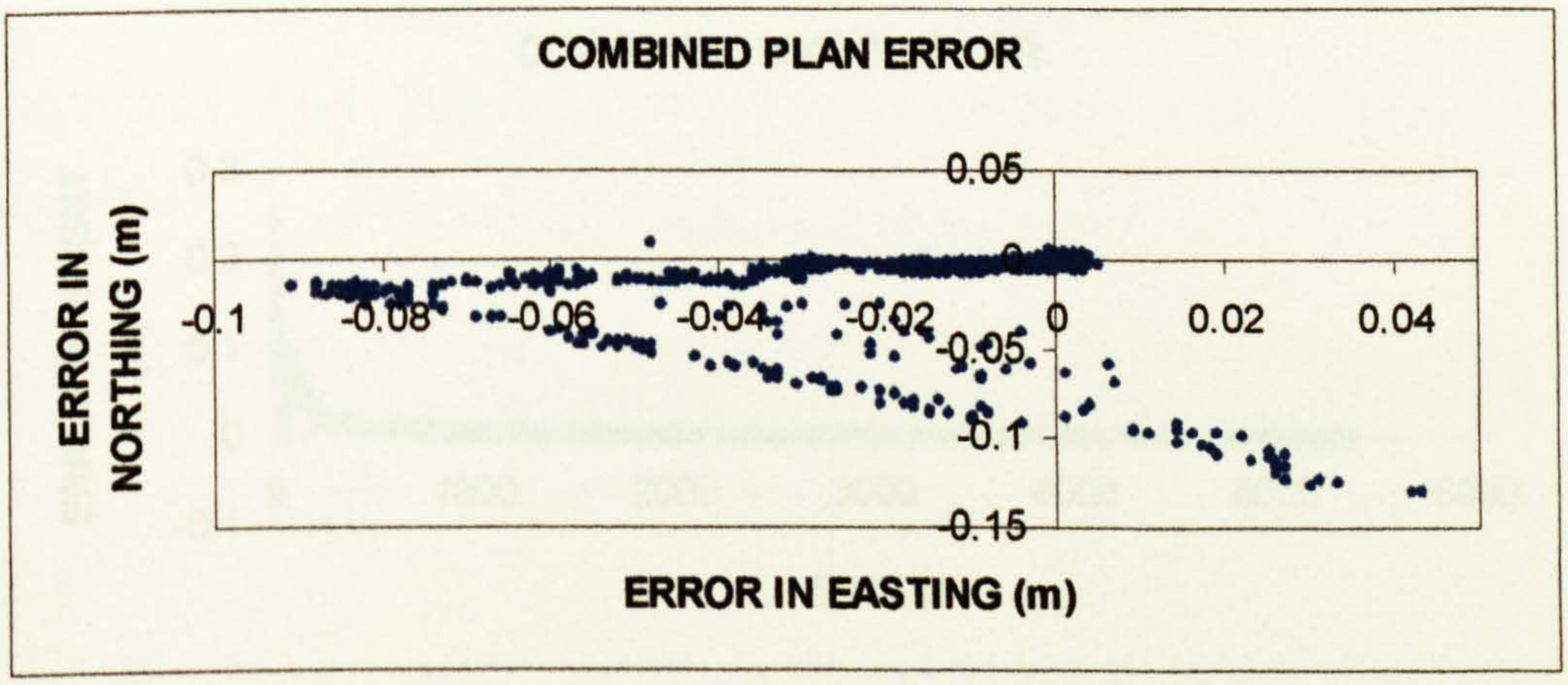

Figure 5.16 Difference in NOTF Float Carrier Phase Height Values

A

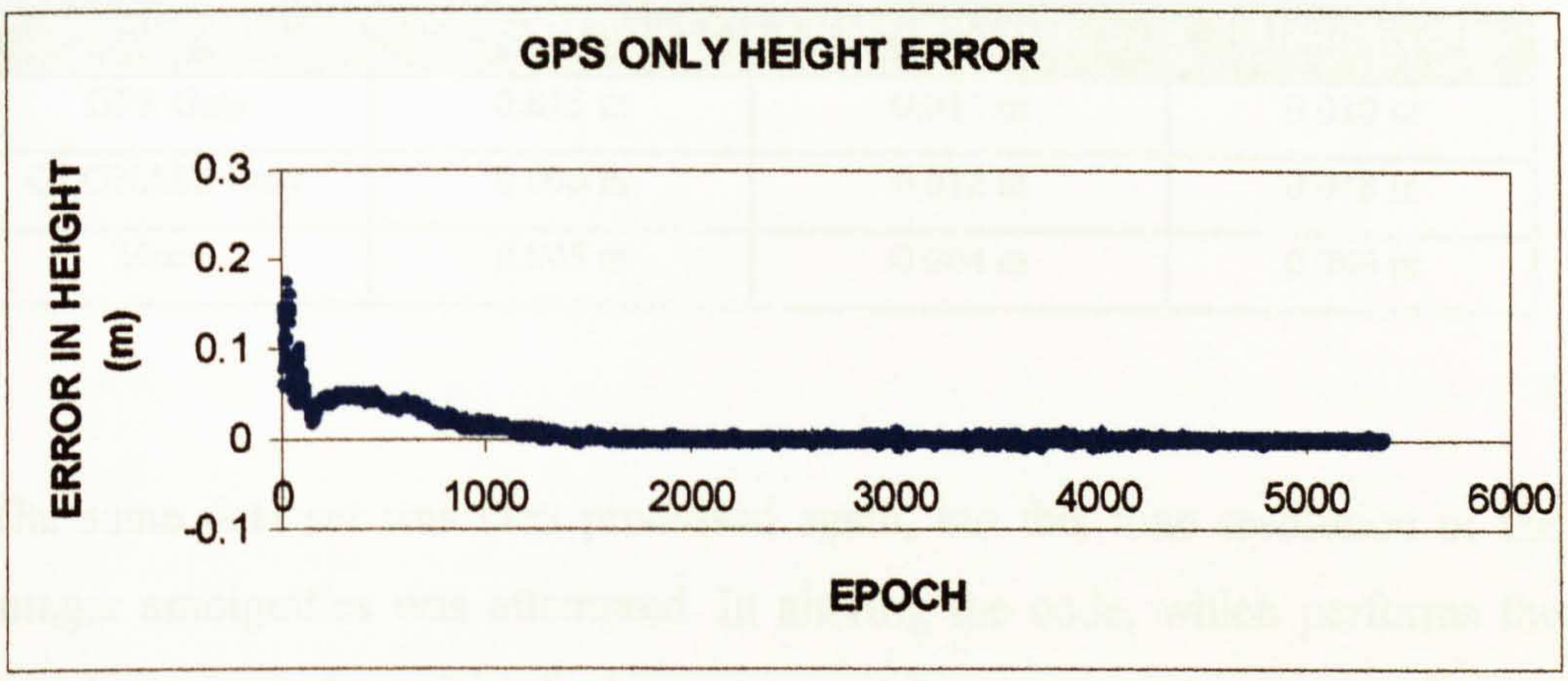

B

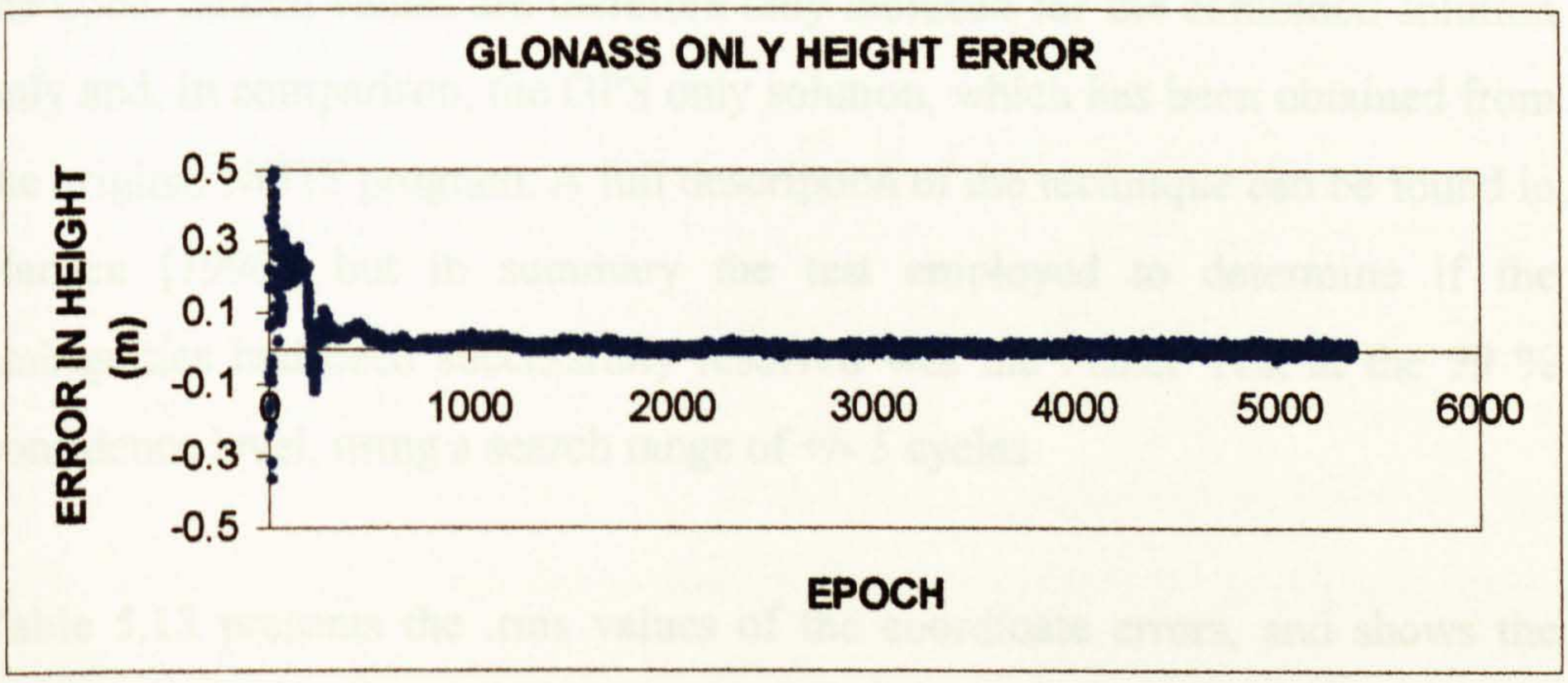

C

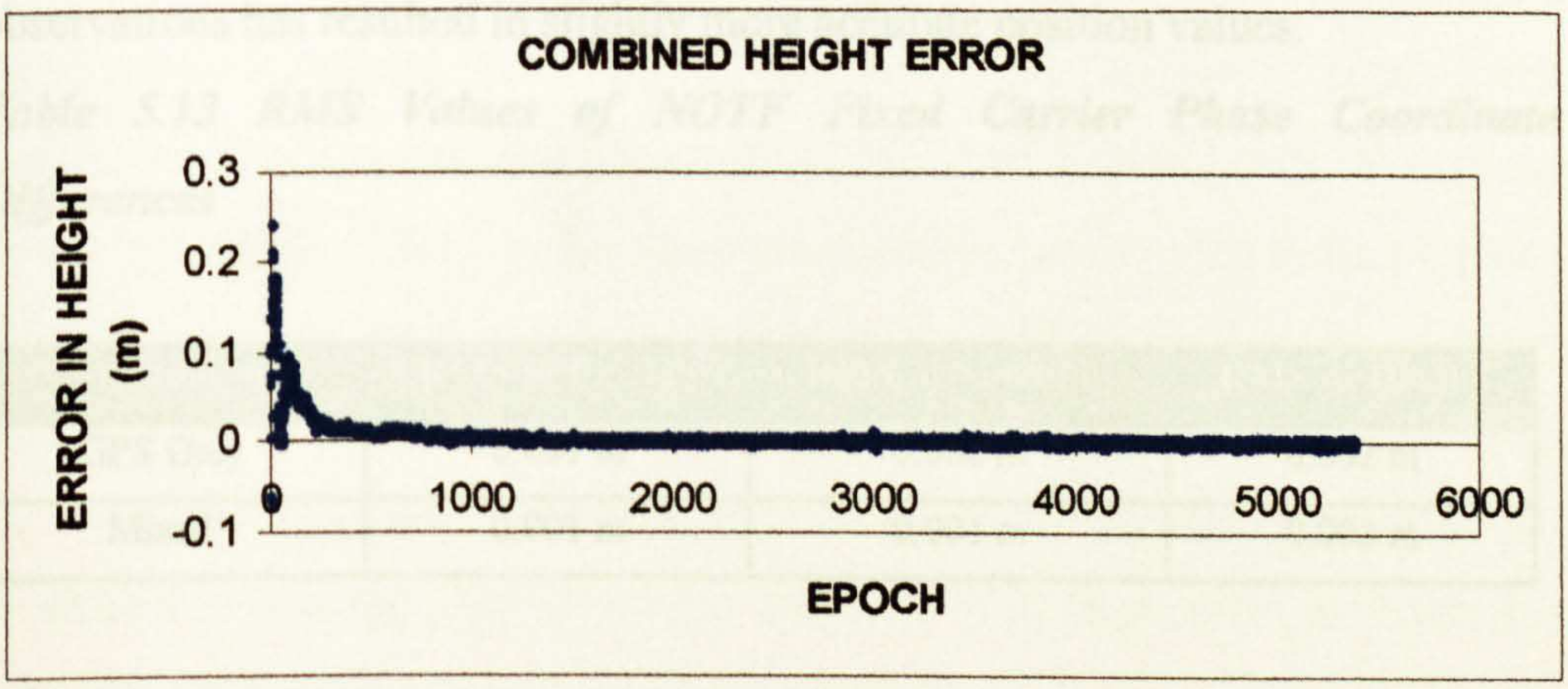

Table 5.12 RMS Values of NOTF Float Carrier Phase Coordinate Differences

Combination	RMS in Easting	RMS in Northing	RMS in Height
GPS Only	0.015 m	0.011 m	0.010 m
GLONASS Only	0.006 m	0.012 m	0.018 m
Mixed	0.005 m	0.004 m	0.006 m

The same data set was then processed again, but this time resolution of the integer ambiguities was attempted. In altering the code, which performs the search, to accept combined observations, it became necessary to make the search routine work only with combined data only, due to the complexity of the code. Search values are therefore only included for the combined solution only and, in comparison, the GPS only solution, which has been obtained from the original NOTF program. A full description of the technique can be found in Hansen [1996], but in summary the test employed to determine if the ambiguities had been successfully resolved was the Fisher Test at the 99 % confidence level, using a search range of +/- 5 cycles

Table 5.13 presents the .rms values of the coordinate errors, and shows the benefits of fixing the integer ambiguities to their correct values in a carrier phase solution. Again, it can be seen that the inclusion of the GLONASS observations has resulted in slightly more accurate position values.

Table 5.13 RMS Values of NOTF Fixed Carrier Phase Coordinate Differences

Combination	RMS in Easting	RMS in Northing	RMS in Height
GPS Only	0.001 m	0.002 m	0.002 m
Mixed	0.001 m	0.001 m	0.002 m

Accuracies at a level of those presented above can only be achieved when the integer ambiguities have been correctly resolved. The output from the ambiguity search process is reproduced in Figure 5.17 (A) for the GPS only solution, and in Figure 5.17 (B) for the combined solution. It can be seen from this that the ambiguity values solved for the GPS satellites is, in both cases, identical, and agrees with the values calculated in PANIC (Chapter 5).

However, the times taken to arrive at these values differ slightly, with the GPS only solution successfully resolving the ambiguities after 3 seconds (epoch 126023), while the combined solution takes 17 seconds (epoch 126037). The relevant ambiguity search details for each of these epochs is reproduced in Appendix B. This shows that this delay is caused by the ratio between the residuals of the best and second best ambiguity combination not being significantly different enough to allow the F-test ratio to be passed. As the receiver clock correction is calculated using the pseudoranges, any error in these will translate to this correction. Now, as the GLONASS pseudoranges experience differing inter-channel biases, this will contaminate the GLONASS clock correction and an accumulation of data will be required before the correct value can be reached. This is the most probable explanation for the delay in the ambiguity resolution and highlights yet again the problems caused by differing inter-channel biases within the GLONASS pseudoranges.

Table 5.14 shows the .rms errors derived from WinPrism for both float and fixed mixed solutions. WinPrism is the latest GPS/GLONASS commercial processing software available within the IESSG, and further details of it can be found in Ashtech [1998]. Again these results agree closely with those obtained through NOTF, with the Fixed solution again giving the highest accuracy results. WinPrism employs a technique of forwards and backwards processing, i.e. once the ambiguities have been successfully resolved earlier epochs are re-processed with these integer values, and thus it is impossible to determine when the ambiguities were successfully resolved.

Figure 5.17 Integer Ambiguity Output From NOTF

(A)

```
3              1              1                7   126023
              14  0.00000000000000000E+00
               2   1.000000000000000
               1  0.00000000000000000E+00
              15  0.00000000000000000E+00
               8   1.000000000000000
               7  0.00000000000000000E+00
              16  0.00000000000000000E+00

127477
              25  -1.000000000000000

129353
               4   1.000000000000000


130387
              18  0.00000000000000000E+00
```

(B)

```
17             1              1               12   126037
              14  0.00000000000000000E+00
               2   1.000000000000000
               1  0.00000000000000000E+00
              15  0.00000000000000000E+00
               7  0.00000000000000000E+00
               8   1.000000000000000
              16  0.00000000000000000E+00
              50  -3.000000000000000
              36  -4.000000000000000
              44  0.00000000000000000E+00
              35   5.000000000000000
              52   5.000000000000000

126038
              49  0.00000000000000000E+00

126186
              45  -2.000000000000000

127477
              25  -1.000000000000000

129353
               4   1.000000000000000

130386
              18  0.00000000000000000E+00
```

Table 5.14 RMS Values of WinPrism Carrier Phase Coordinate Differences

Combination	RMS in Easting	RMS in Northing	RMS in Height
Mixed (Float)	0.011m	0.002m	0.002m
Mixed (Fixed)	0.001m	0.001m	0.001m

To conclude, the results presented in this section, not only prove the validity of the alterations made to NOTF, but also show how, by appropriate weighting of the observations from each system, the quality of both the single difference code and carrier phase position can be improved.

5.6 Abortive Strategies

Whilst the modifications detailed in this chapter suggest a smooth progress of work throughout, this was not always the case. As mentioned in Section 5.4, a great deal of time was spent attempting to modify PANIC to process GLONASS observations in a 'Single Difference' manner, whilst maintaining the existing 'Double Difference' approach with the GPS observations. Increasingly it became obvious that whilst conceptually possible, it was in practical terms impossible due to the existing structure of the code. Thus all research in this area had to be abandoned.

A second problem experienced related to the standard of some of the data sets obtained from the Ashtech GG-24 receivers. The quality of the solutions obtained were for some of the data sets markedly worse than others, causing the author to question the processing rational. However, from comparing a set of results obtained using the modified version of GAS with results obtained from an outside source, Mike Stewart at Curtin University, using the same data set, it was concluded that the data set was in fact in error. Again a great deal of time was spent checking and re-checking the code modifications in an attempt

to account for these apparent errors which resulted from the poor quality input data.

5.7 Summary

It has been proven from the various experiments detailed above that all aspects of the GAS software that were altered for combined GPS/GLONASS processing are performing correctly. Indeed, it was from these results that the potential problems of inter-channel biases on the GLONASS pseudorange measurements were highlighted and quantified. The results clearly demonstrate the benefits of using GLONASS in single point positioning, but in differential code and carrier positioning, the advantages are less obvious. It is however worth noting that the data used in these tests was gathered under ideal conditions, with a clear unobstructed sky, allowing the signals from ample GPS satellites to be received. This is very rarely the case in the *Real World*, and is demonstrated in Chapters 6 and 7, where the various applications under which the GPS/GLONASS receivers have been tested are described and detailed.

5.8 References

Ashtech, 1997, *Ashtech Office Suite for Surveying – User's Manual*, Document Number 630154, Revision A, June 1997. Ashtech Inc., 1170 Keifer Road, Sunnyvale, CA USA 94086.

Ashtech, 1998, *Introduction to WinPrism – User's Guide*, Document Number 630187, Revision A, June 1997. Ashtech Inc., 1170 Keifer Road, Sunnyvale, CA USA 94086.

Bierman, G.J., 1997, *Factorization Methods for Discrete Sequential Estimation*, Academic Press Limited, London.

Euler, H.J., Landau, H., 1992, *Fast GPS Ambiguity Resolution On-The-Fly For Real-Time Appliations*, Sixth International Geodetic Symposium on Satellite Positioning, Ohio, USA.

Eurocontrol, 1993, *Datum: A Report and Software Package for the Transformation and Projection of Coordinates*, Eurocontrol Experimental Centre, EEC Report No. 237, Issued December 1990, revised December 1993.

Gourevitch, S.A., Sila-Novitsky, S., Van Diggelen, F., 1996, *The GG24 Combined GPS+GLONASS Receiver*, Proceedings of ION GPS-96, pp.141-145.

Gurtner, W., 1995, *RINEX: The Receiver Independent Exchange Format Version 2*, http://igscb.jpl.nasa.gov/igscb/data/format/rinex2.txt.

Hall, T., Burke, B., Pratt, M., Misra, P., 1997, *Comparison of GPS and GPS+GLONASS Positioning Performance*, Proceedings of ION GPS-97, pp. 1543-1550.

Hansen, P., 1996, *On-The-Fly Ambiguity Resolution for GPS*, PhD Thesis, The University of Nottingham, Nottingham, United Knigdom.

Misra, P.N., Abbot, R.I., Gasposchkin, E.M., 1996, *Integrated use of GPS and GLONASS: Transformation Between WGS 84 and PZ 90.* Proceedings of ION GPS-96, pp. 307-314.

Moore, T., 1986, *Satellite Laser Ranging and the Determination of Earth Rotation Parameters*, PhD Thesis, University of Nottingham, Nottingham, United Kingdom.

Penna, N.T., 1997, *Monitoring Land Movement At U.K. Tide Gauge Sites Using GPS*, PhD Thesis, University of Nottingham, Nottingham, United Knigdom.

Remondi, B., 1989, *Extending the National Geodetic Survey Standard GPS Orbit Formats*, NOAA Technical Report NOS 133 NGS 46.

Stewart, M.P., Ffoulkes-Jones, G.H., Ochieng, W.Y., Shardlow, P.J., 1995, *GAS: GPS Analysis Software User Manual. Version 2.3*, IESSG Publication, University of Nottingham.

Chapter 6

Applications of GPS/GLONASS Positioning

6.1 Introduction

Whilst the tests carried out in the previous Chapter were useful in determining the validity of the changes made to the software, the conditions under which the data was gathered were quite favourable for satellite positioning i.e. clear unobstructed skies. In order to make some attempt at quantifying the benefit of combined GPS/GLONASS observations over GPS only observations during potential applications, two very different tests were performed. The data gathered was then subsequently processed through both the IESSG software and commercial software packages. Both the tests and their results are detailed and discussed in this Chapter.

6.2 Kinematic Mini-Bus Trials

One of the largest growth areas for satellite positioning over the past few years has been in vehicular positioning. At the base level it can be used as the sole means of positioning individual cars, with the driver navigating from an electronic chart or following voice commands to a pre-specified destination. At the opposite end of the spectrum, it can also be used as a tool in integrated transport networks, which an increasing number of cities are developing. An example of one such system, called the Central Area Transit (CAT) system, can be found in Perth, Australia, where GPS has been successfully used since 1996 as the primary means to position its fleet of buses. This CAT system has an on-bus electronic display and audio announcement upon arrival at each transit stop, giving passengers the location of the current stop and the destination of the next stop. In addition, electronic displays and audio announcements at transit stops inform waiting passengers of future bus arrival times. The whole system is controlled by a central computer, which monitors the location of each CAT city-bus in service (Tsakiri et. al., 1998).

All such systems, regardless of their level of complexity, suffer from the same problems, namely the continuity and accuracy of position determination in areas of restricted visibility (urban canyons). Tall buildings, trees, high sided vehicles and subways all serve to block satellite signals, affecting the DOP values, and in a great many cases, making a position solution impossible to obtain. The most obvious way to reduce this effect is to increase the number of satellites in view, which in most cases should also improve the geometry of the satellite coverage. Clearly, one way of immediately achieving this is to combine the signals from the GPS and GLONASS systems, and thus an interest in the potential benefits presented through combined GPS/GLONASS operation has been particularly noticeable in this field.

In order to attempt to quantify the extent of any potential benefit of GPS/GLONASS operation under such conditions, and to test the performance

of the IESSG software with data from a moving receiver, a trial was conducted around Nottingham.

6.2.1 System Set-Up

One GG-24, and one Z-12 (L1/L2 GPS) antenna were mounted on a University owned Mini-Bus using a roof rack specifically fabricated for an earlier project within the IESSG. The Ashtech Z-12 receiver was included to serve as a comparison as to the performance achievable using the most advanced GPS L1/L2 receiver technology, and to provide a similar L1/L2 dynamic data set, should future work require one. This set-up is depicted in Plate 6.1, which shows the antenna cables running through the window to the receivers, which were secured to the floor of the Mini-Bus. At the IESSG another GG-24 and Z-12 receiver were set-up to record data over previously coordinated points, and these would act as the base stations for post processed differential positioning.

Plate 6.1 Roof Rack, Antenna and Cabling Set-Up

6.2.2 Mini-Bus Route

Commencing at approximately 14:40 (BST) on 18th August 1998, the Mini-Bus was driven along a pre-determined route from the University through increasingly built-up residential areas, and through the centre of Nottingham, to a point approximately 1.5 km from the town centre. At this point the Mini-Bus was stopped for a period of approximately 60 seconds to check the securness of the antennas and roof rack. The mini-bus was then driven back along the same road towards the centre of the city before following a different, but similarly demanding route back to the University Campus. Plate 6.2 shows the situation on leaving the Campus area, and as can be seen, the visibility is reasonably unobstructed. This however is not the case in Plate 6.3, which shows the conditions in the centre of Nottingham. Finally, Plate 6.4 gives an impression of the conditions encountered on the return route to the University of Nottingham, and is typical of more suburban tree lined environments. With the Mini-Bus remaining stationary for 60 seconds prior to driving off and on returning, the total duration of the trial was 35 minutes. With a logging interval of 1 second, this equates to 2100 epochs of data.

Plate 6.2 Conditions on Leaving the University Campus

Plate 6.3 Conditions in the Centre of Nottingham

Plate 6.4 Conditions on the Return Journey to the University Campus

6.2.3 Mini-Bus Trial Results

Figure 6.1 shows the number of GPS and combined GPS/GLONASS satellites visible to the receivers mounted on the mini-bus throughout the trial. The benefits of combining the systems is quite clearly seen, especially around epochs 300 and 1640, when the Mini-Bus was travelling through increasingly built-up areas, resulting in there being less than the minimum requirement of four satellites simultaneously visible to solve for a 3-D position, on a number of occasions. However, with both GPS and GLONASS combined, this was the case much less often. The maximum satellite availability in Nottingham, for the GPS and GPS/GLONASS constellations, at this time is presented in Appendix C2, and these figures show that throughout the trial period, a minimum of five extra satellites were present in the GPS/GLONASS constellation.

Figure 6.1 Satellite Visibility throughout Mini-Bus Trial

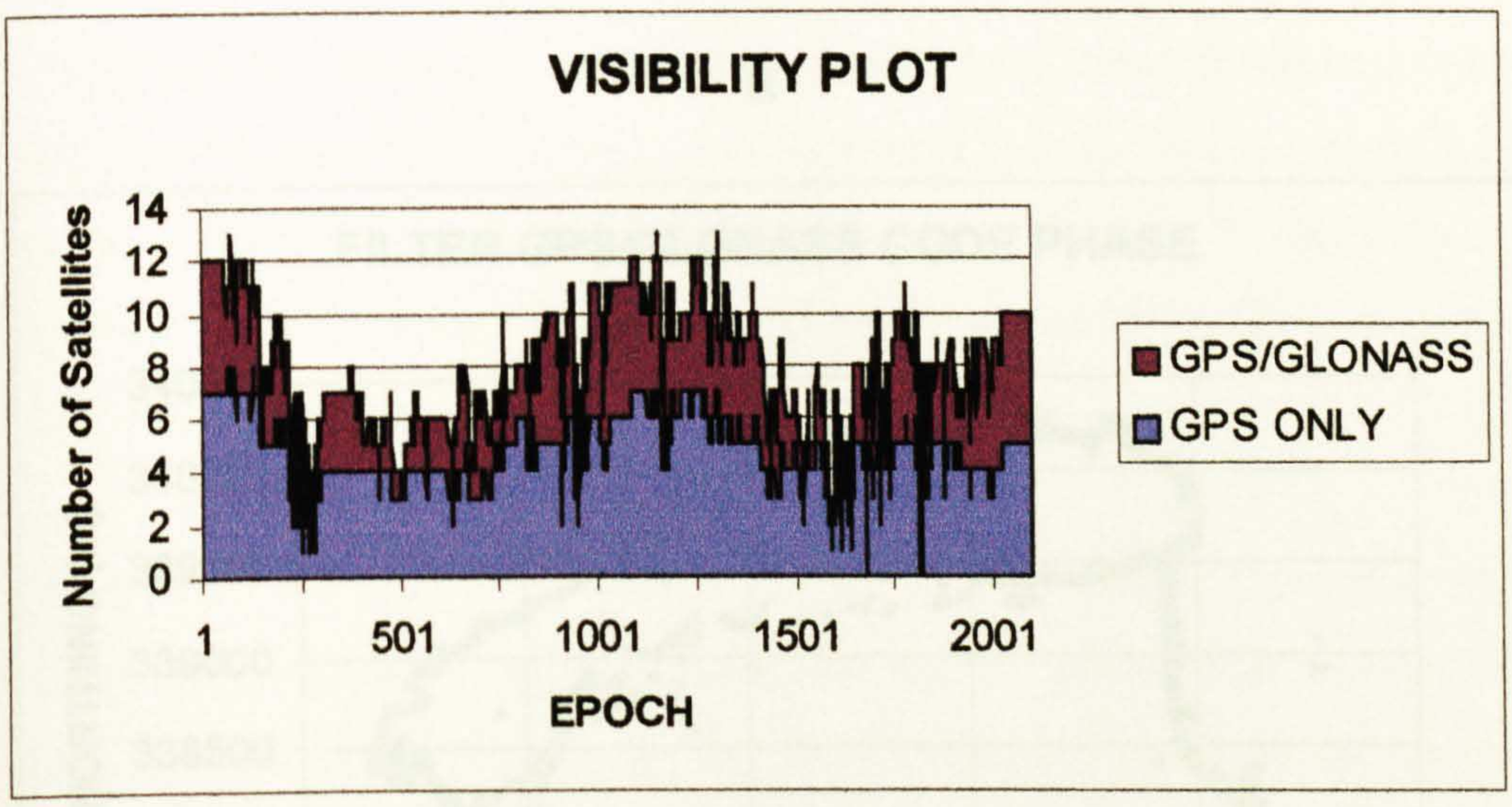

The data collected was first processed through Filter to derive a Stand Alone position at each epoch. Figures 6.2 (A) shows the plan solutions obtained for the GG-24 GPS only solutions. A position solution was derived on 1816 of the 2100 epochs, which equates to 86% of the total. This Figure also shows the location where Plates 6.2 – 6.4 were taken (points 1-3 respectively). Figure 6.2

Figure 6.2 Filter Stand Alone Code Positioning

A

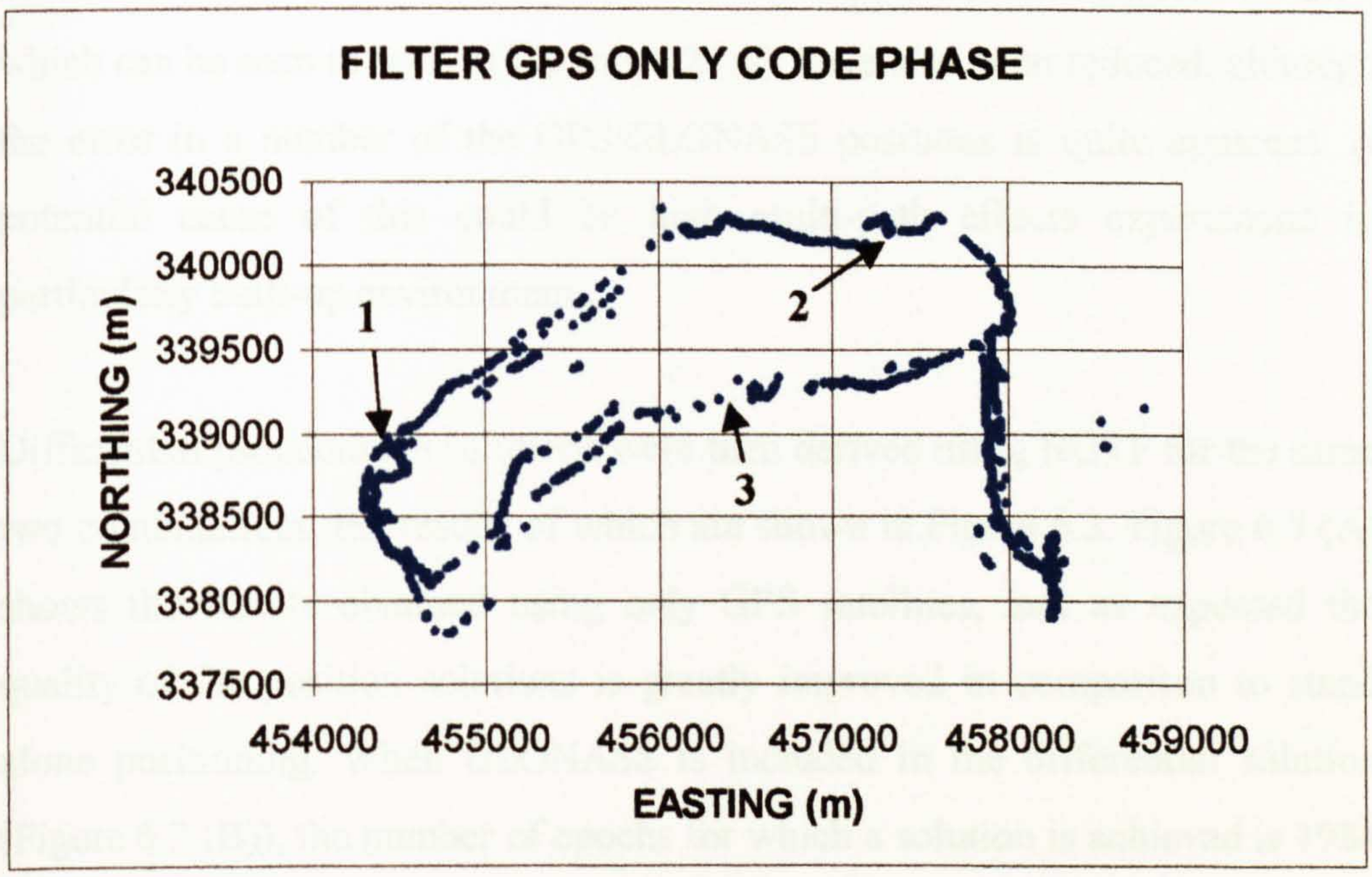

B

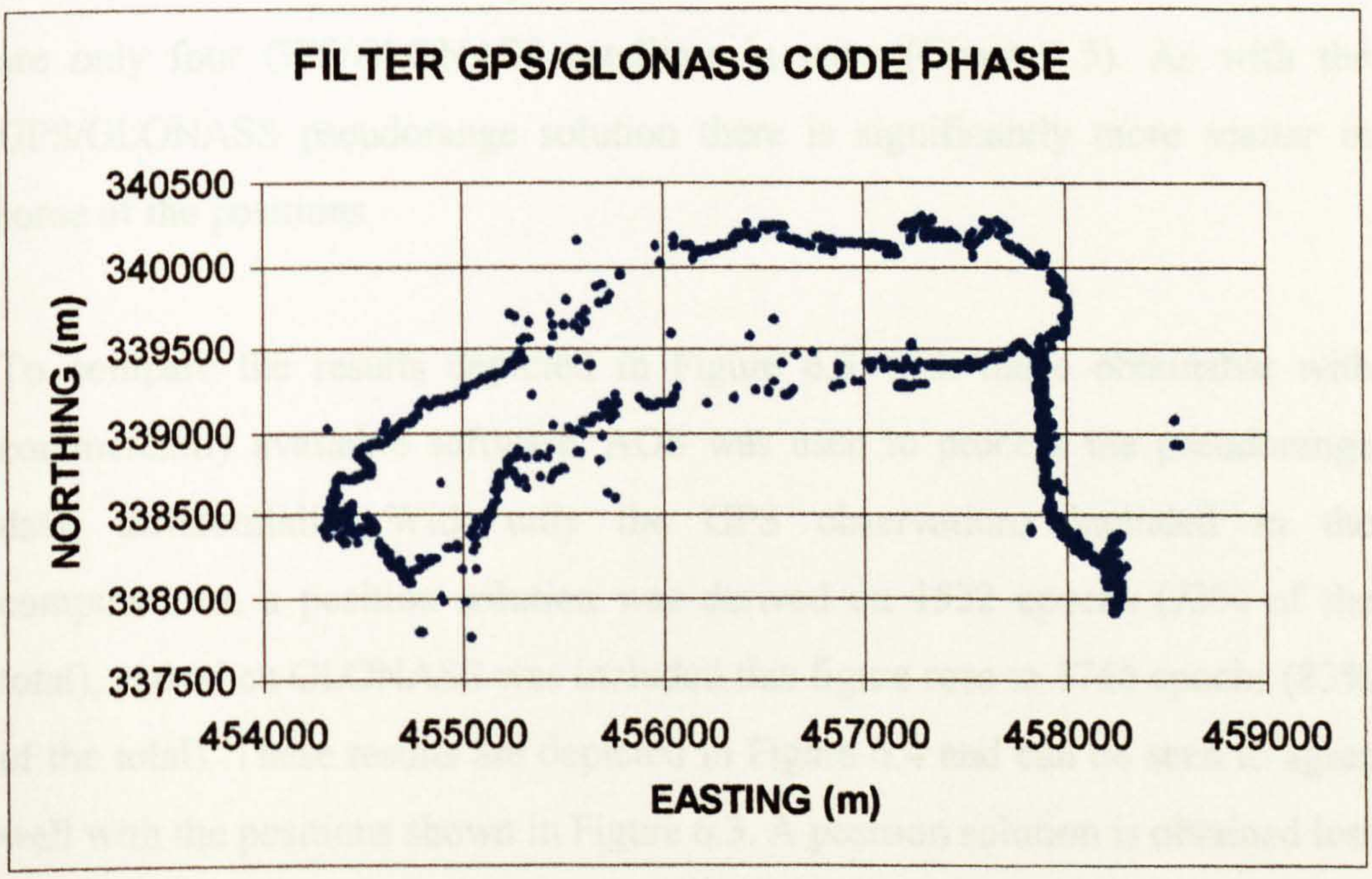

(B) shows the combined GPS/GLONASS solution, and in this case a position was successfully computed on 1935 epochs (92% of the total). It is worth noting that a minimum of five simultaneously visible satellites are needed for an autonomous GPS/GLONASS position (Chapter 3). The effects of S/A, which can be seen in parts of Figures 6.2 (A), have also been reduced, although the error in a number of the GPS/GLONASS positions is quite apparent. A potential cause of this could be high multi-path effects experienced in particularly built-up environments.

Differential pseudorange solutions were then derived using NOTF for the same two combinations, the results of which are shown in Figure 6.3. Figure 6.3 (A) shows the results obtained using only GPS satellites, and as expected the quality of the position solutions is greatly improved in comparison to stand alone positioning. When GLONASS is included in the differential solution (Figure 6.3 (B)), the number of epochs for which a solution is achieved is 1984 epochs (94% of the total). This slight increase in the number of fixes over GPS/GLONASS stand alone positioning results from code alterations within NOTF which allow for a single clock correction to be solved for when there are only four GPS/GLONASS satellites in view (Chapter 5). As with the GPS/GLONASS pseudorange solution there is significantly more scatter in some of the positions.

To compare the results depicted in Figure 6.3 with those obtainable with commercially available software, AOS was used to process the pseudorange data, differentially. With only the GPS observations included in the computations, a position solution was derived on 1532 epochs (73% of the total), and when GLONASS was included this figure rose to 1746 epochs (83% of the total). These results are depicted in Figure 6.4 and can be seen to agree well with the positions shown in Figure 6.3. A position solution is obtained less frequently using AOS than NOTF, with both GPS only and combined GPS/GLONASS solutions. This could be due to AOS rejecting data when either the PDOP or Signal to Noise Ratio (SNR) rise above predefined levels,

Figure 6.3 NOTF Differential Code Positioning

A

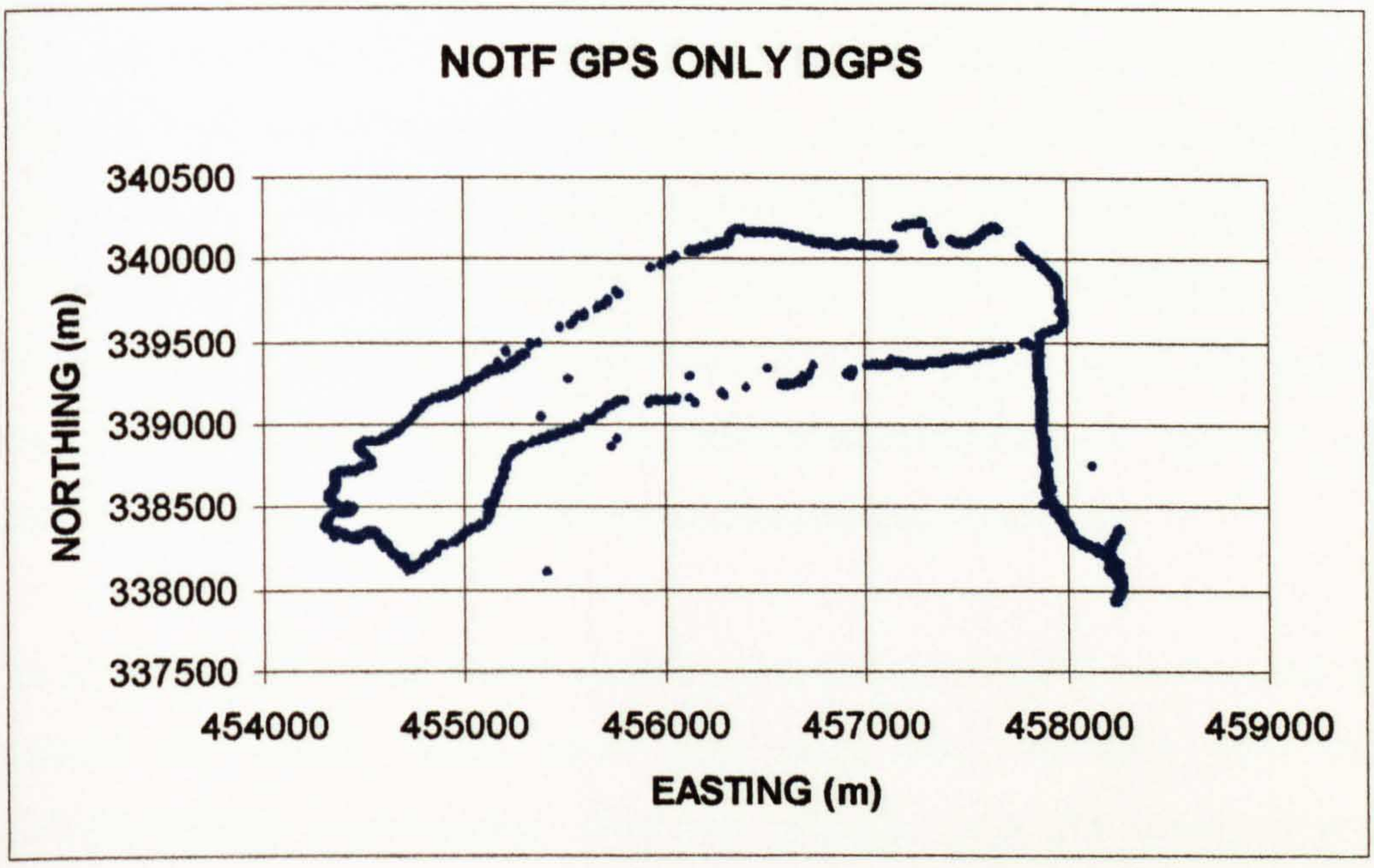

B

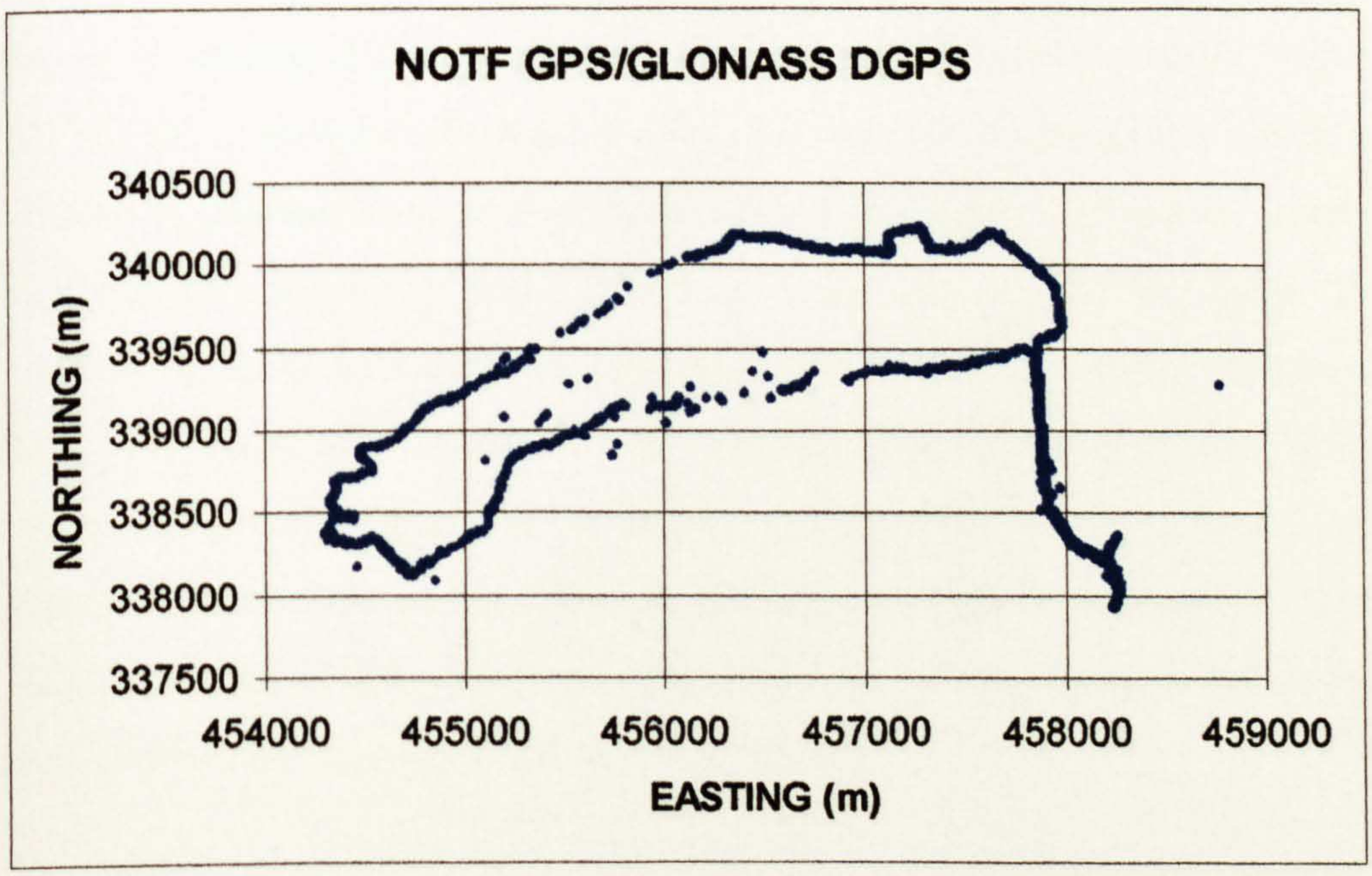

Figure 6.4 AOS Differential Code Positioning

A

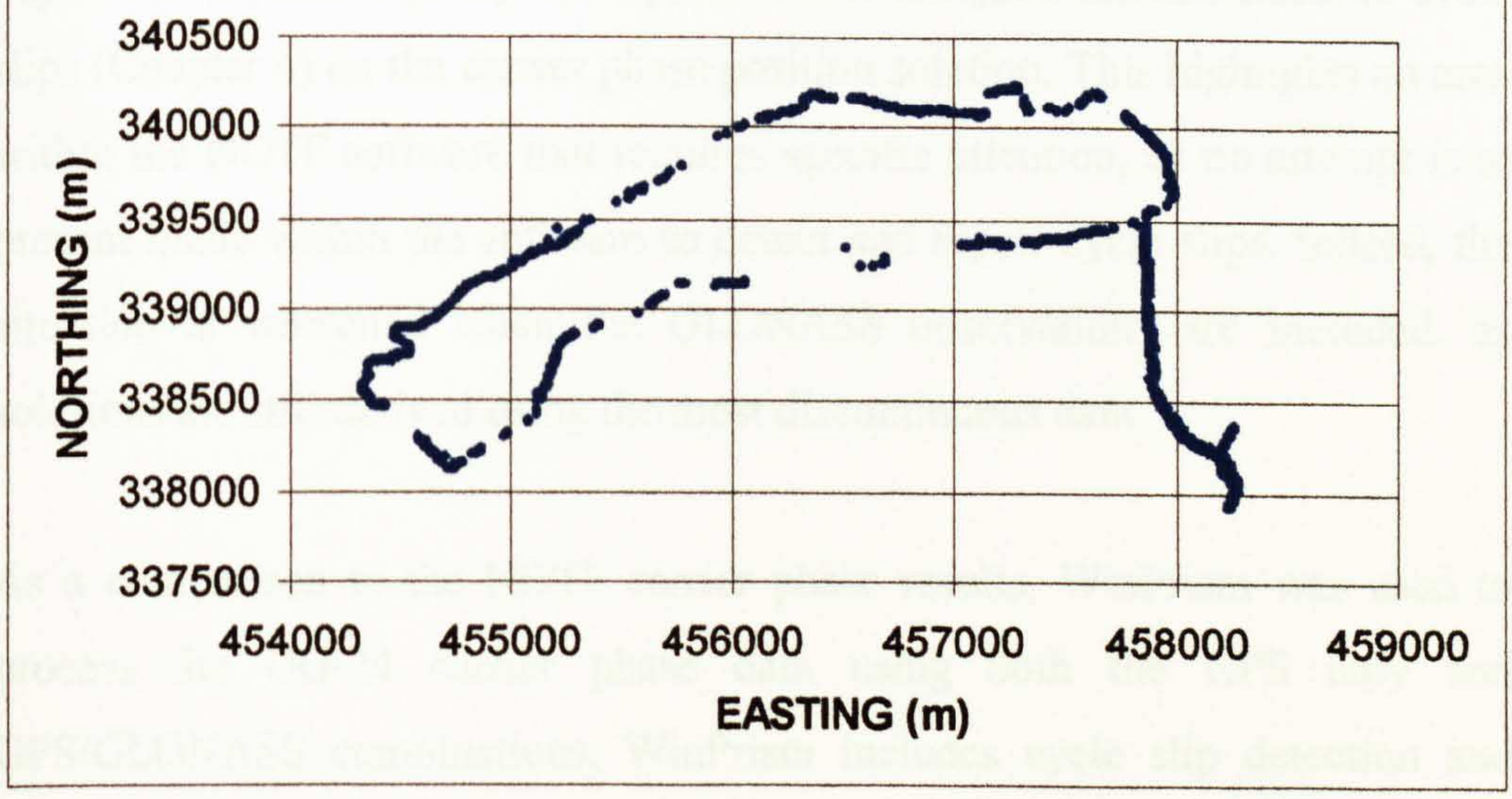

B

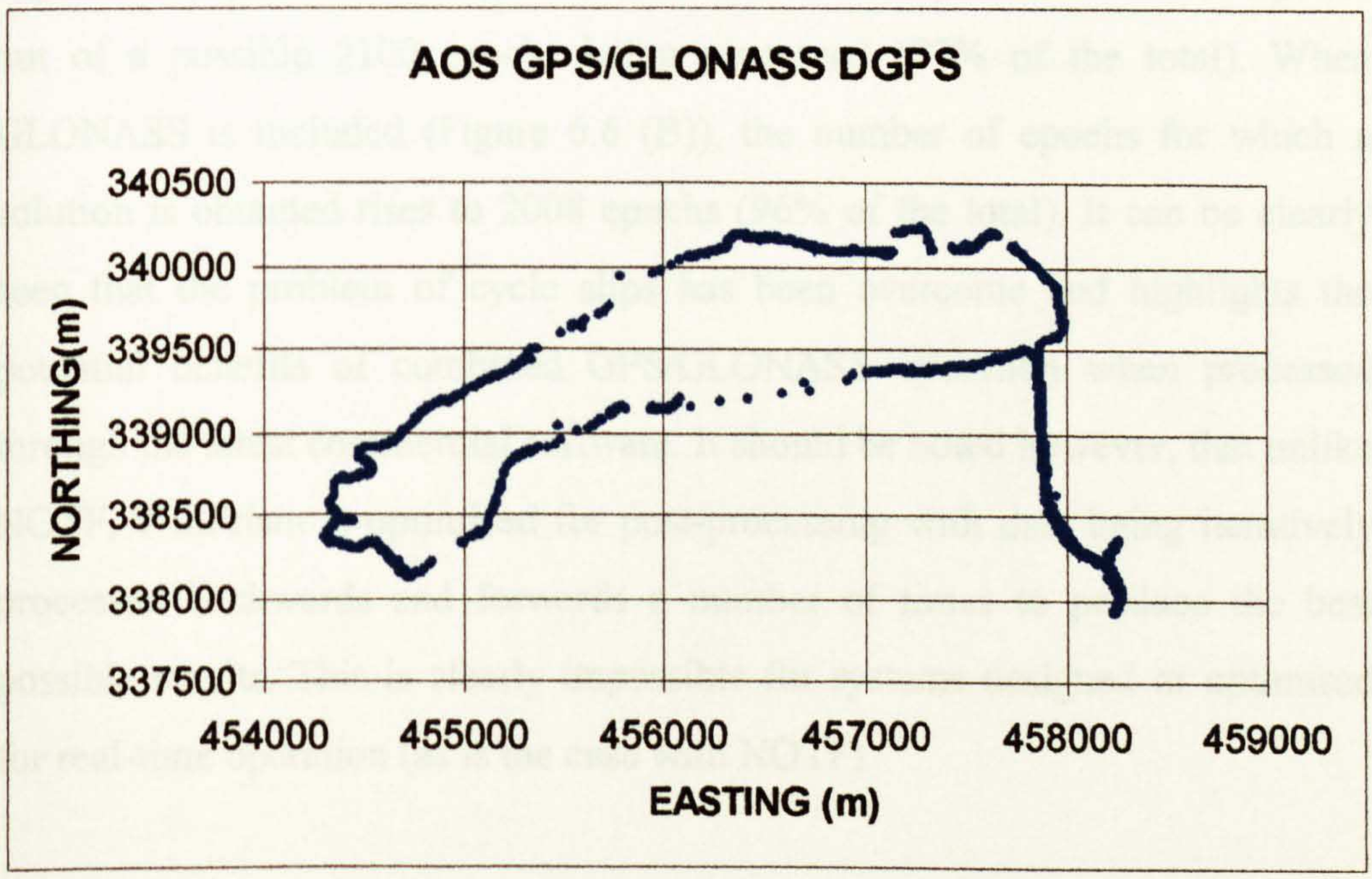

although the author can find no information directly relating to this in the reference manual [Ashtech, 1997].

NOTF was then used to process the carrier phase data for both the GG-24 GPS only and combined GPS/GLONASS data sets. These results are depicted in Figure 6.5 (A) and (B) respectively, and show the quite marked effect of cycle slips (Chapter 4) on the carrier phase position solution. This highlights an area within the NOTF software that requires specific attention, as no attempt is at present made within the software to detect and repair cycle slips. Indeed, the situation is worsened when the GLONASS observations are included, as solutions are still derived using the most discontinuous data.

As a comparison to the NOTF carrier phase results, WinPrism was used to process the GG-24 carrier phase data using both the GPS only and GPS/GLONASS combinations. WinPrism includes cycle slip detection and repair routines, and processes the data iteratively to obtain the highest accuracy position results, further details of which can be found in Ashtech [1998]. Figure 6.6 (A) shows the results obtained for GPS only data, with 1610 epochs out of a possible 2100 epochs being processed (77% of the total). When GLONASS is included (Figure 6.6 (B)), the number of epochs for which a solution is obtained rises to 2008 epochs (96% of the total). It can be clearly seen that the problem of cycle slips has been overcome and highlights the potential benefits of combined GPS/GLONASS operation when processed through the latest commercial software. It should be noted however, that unlike NOTF, WinPrism is optimised for post-processing with data being iteratively processed backwards and forwards a number of times to produce the best possible results. This is clearly impossible for systems designed or optimised for real-time operation (as is the case with NOTF).

Finally, the L1/L2 GPS carrier phase data gathered by the Z-12 was processed through NOTF. Figure 6.7 shows the results obtained through NOTF. These clearly represent a major improvement in position accuracy over the L1 only

Figure 6.5 NOTF Carrier Phase Positioning

A

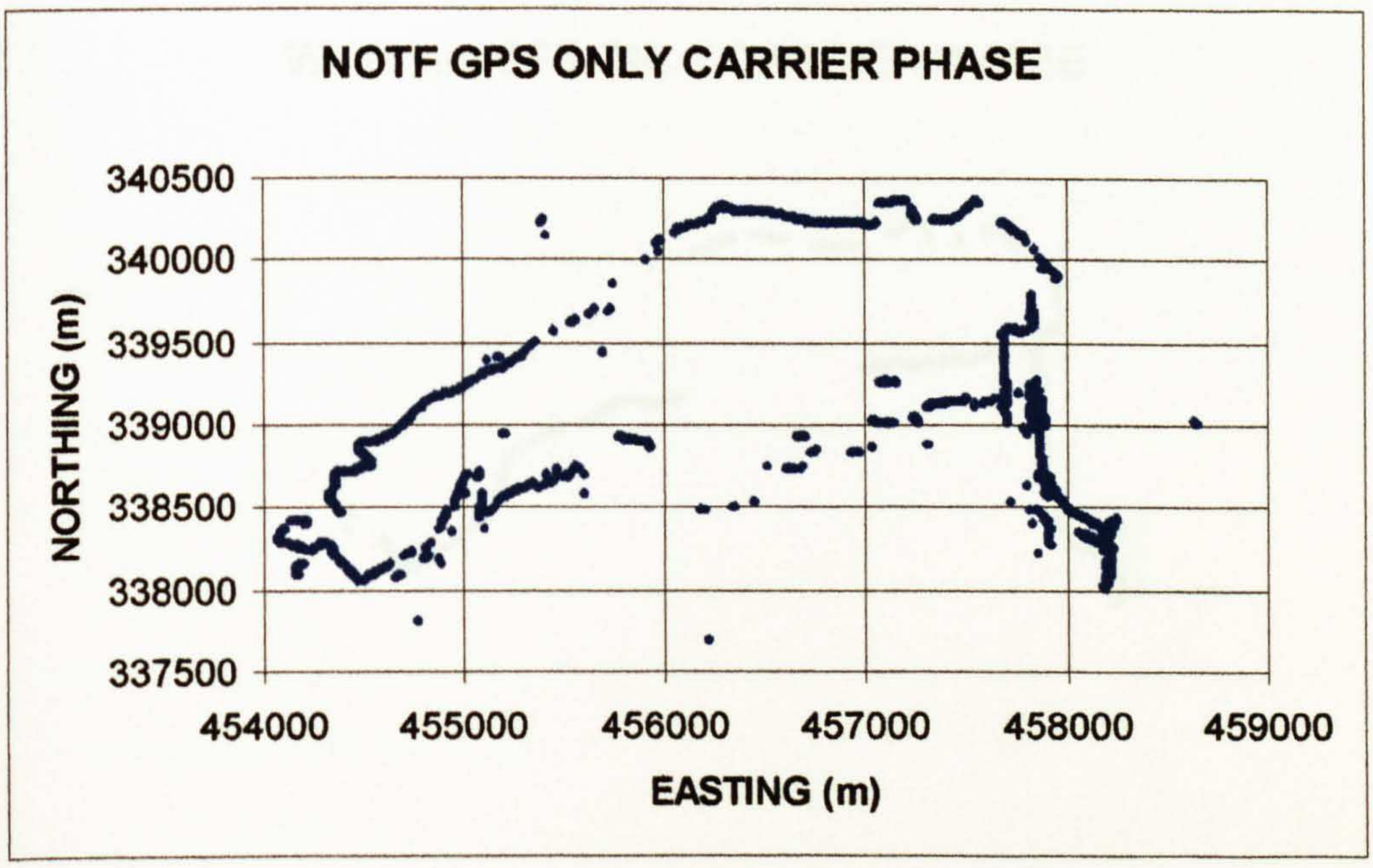

B

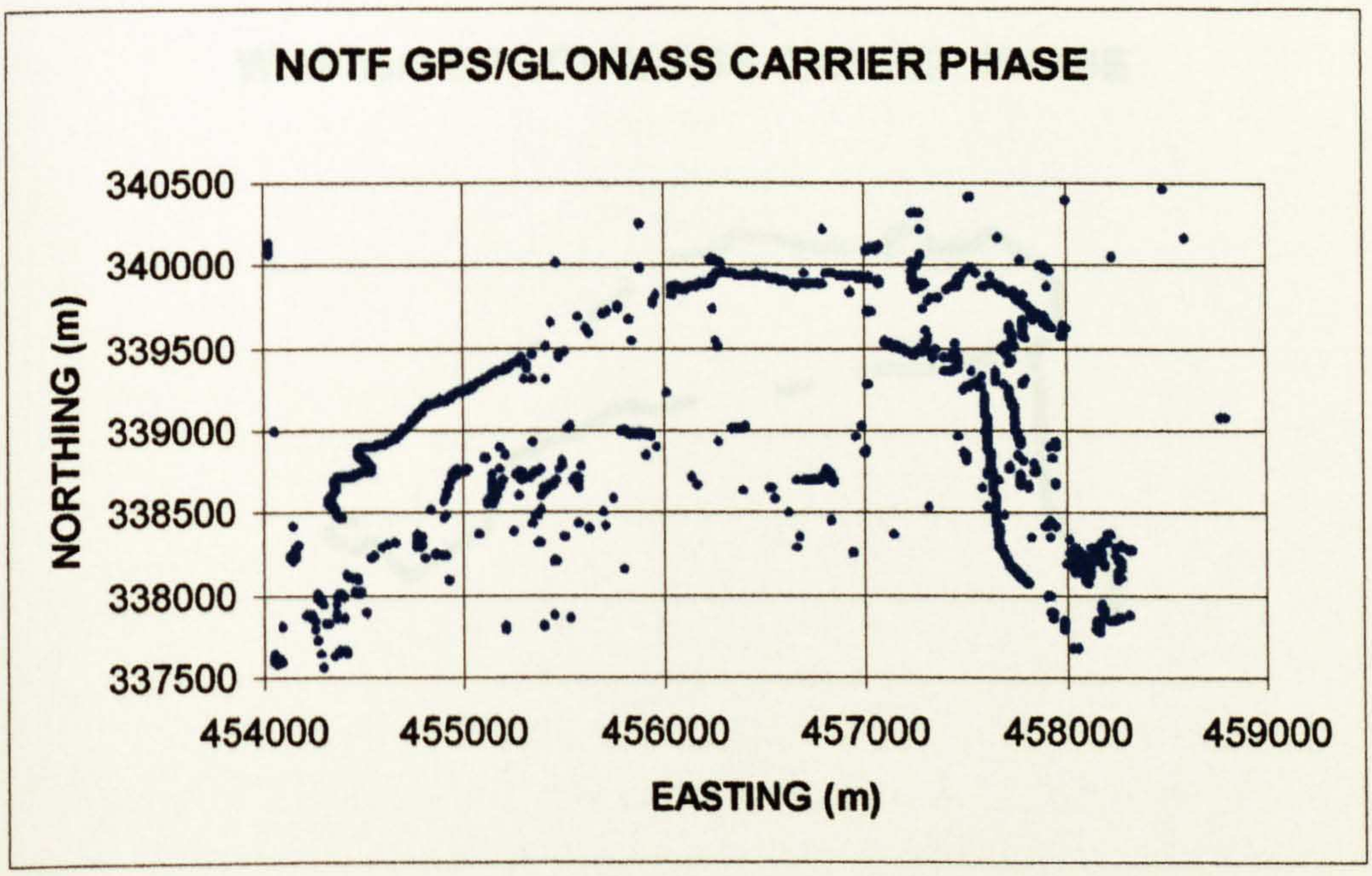

Figure 6.6 WinPrism Carrier Phase Positioning

A

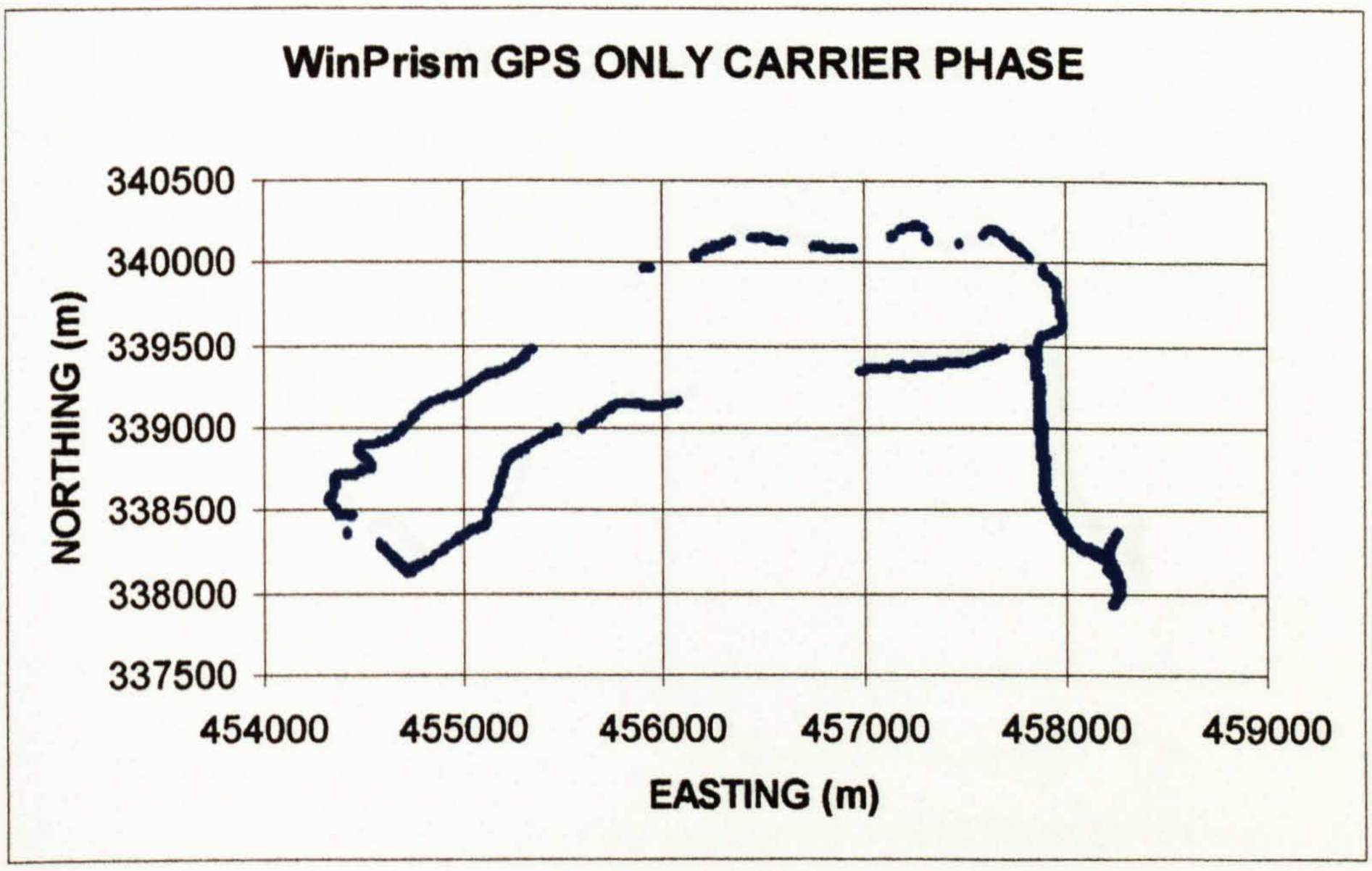

B

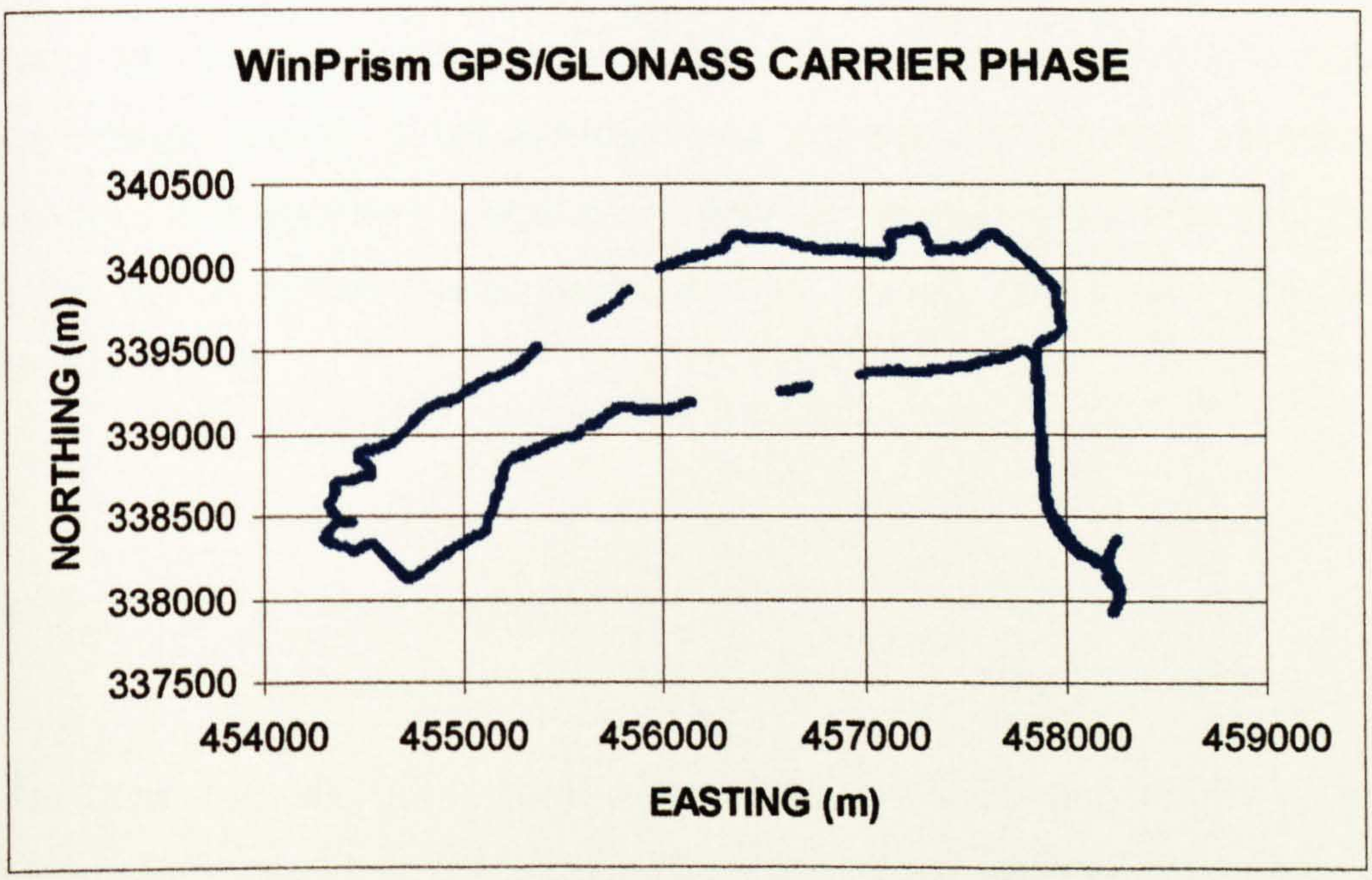

Figure 6.7 NOTF Z-12 Carrier Phase Positioning

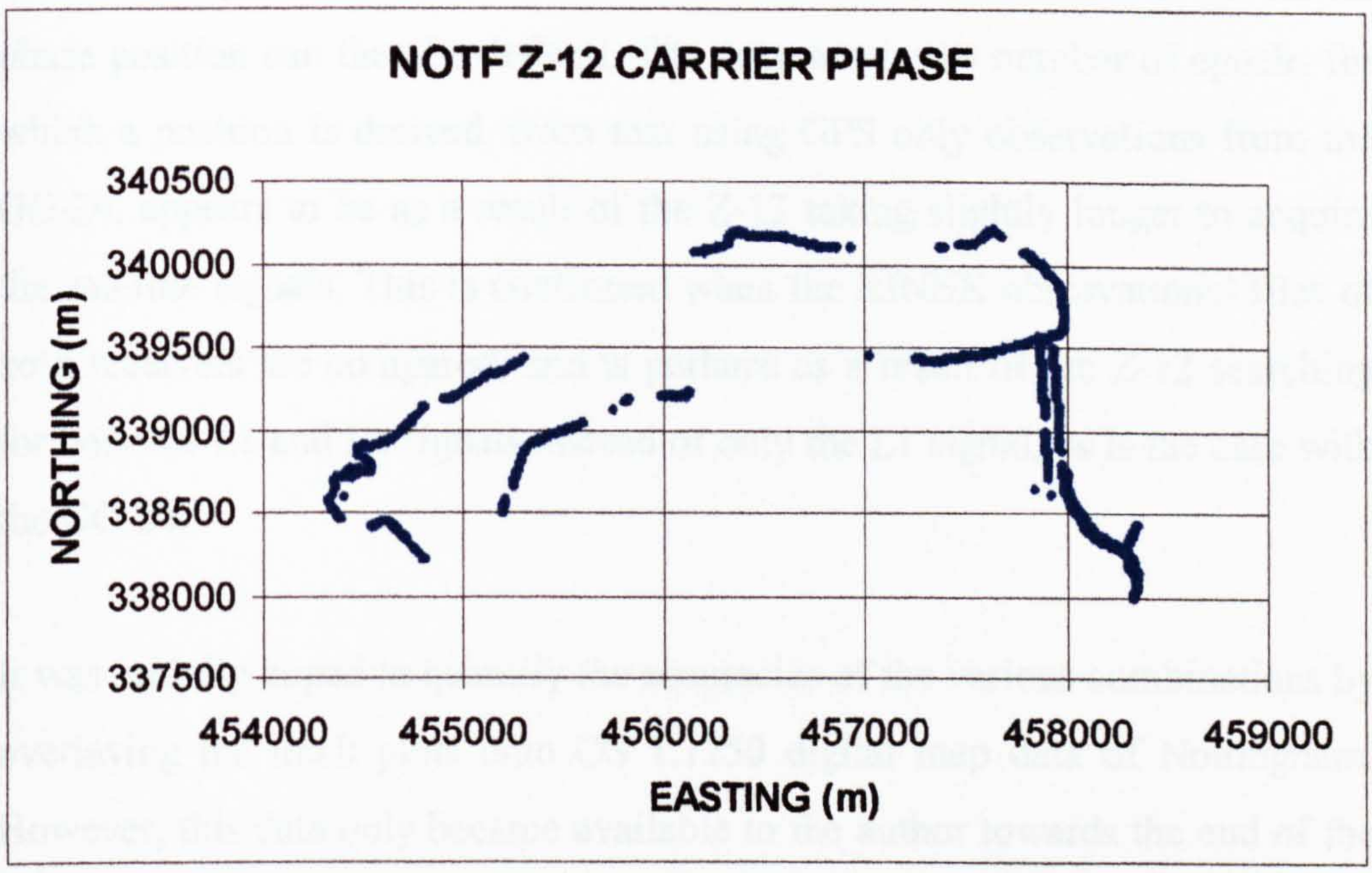

solutions of either GPS or GPS/GLONASS from the same program, with a solution being derived on 1470 epochs (70% of the total). The improvement in accuracy is as a result of the utilisation of the Widelane technique (Chapter 4) to define approximate coordinates, from which a more accurate L1 carrier phase position can then be defined. The decrease in the number of epochs for which a position is derived, from that using GPS only observations from the GG-24, appears to be as a result of the Z-12 taking slightly longer to acquire the satellite signals. This is confirmed when the RINEX observational files of both receivers are compared, and is perhaps as a result of the Z-12 searching for both the L1 and L2 signals instead of only the L1 signal, as is the case with the GG-24.

It was initially hoped to quantify the accuracies of the various combinations by overlaying the track plots onto OS 1:1250 digital map data of Nottingham. However, this data only became available to the author towards the end of the research project and came as NTF (National Transfer Format) files. This format proved to be particularly difficult to manipulate, and while each sheet could be readily viewed using OSView [Ordnance Survey, 1999], the data could not be exported to a more suitable file format i.e. DXF (Drawing Interchange Format). It has therefore been assumed that the track plots are correct if they describe a continuous smooth line, as this was the case with the actual vehicle motion. Sudden deviations from this can thus be assumed to be grossly in error.

6.2.4 Conclusions

The results detailed above confirm that there are undoubted benefits to be gained from combined GPS/GLONASS code phase positioning in vehicle navigation. In the case of autonomous positioning there was a 6% increase in the fix density produced throughout the trial, and when differential pseudoranging was used, this rose to 8%. Processing the carrier phase data has

highlighted the present problem caused by cycle slips within the NOTF software. Hansen [1996] and Roberts [1997] have examined this, but much of this research concentrated on using L1/L2 data, which in the case of GPS/GLONASS has not been available to the author. An investigation into and the implementation of Cycle Slip detection and repair on single frequency GPS/GLONASS data are therefore recommended. The benefits of using dual frequency carrier phase data in areas where cycle slips are likely to occur is also proven. Processing the data through NOTF results in a 16% reduction in the fix density in comparison to the L1 GPS solution, but the accuracy of the position solution is greatly enhanced.

6.3 Bridge Deflection Monitoring

A second very different application to vehicular positioning, for which the possibility of using satellite positioning is receiving interest, is that of monitoring the movement of large structures. This area of research is of particular interest within the IESSG who, in partnership with Brunell University have proposed the use of GPS in producing a health monitoring system for large scale structures. As part of this investigation various trials have been performed on The Humber Bridge since 1995. All these tests primarily used the more advanced L1/L2 GPS receivers, but on more recent occasions both IESSG GG-24 receivers were also used.

The Humber Bridge was opened to traffic in 1981, and at that time it was the longest suspension bridge in the world with a main span of 1,410m. The bridge runs in a virtually North-South direction over the Humber Estuary from Hessle to Barton upon Humber. Including the sidespans, the total length of the Bridge deck is 2,220m, and is supported by two reinforced concrete towers, which stand at a height of 155.5m above the estuary.

As is the case with all suspension bridges, the Humber Bridge is designed to allow for some movement, which is quantified in Ashkenazi and Roberts [1997] at a maximum of +/- 4m. The major controlling factor in this movement is not, as one would expect, loading from traffic, but wind loading. As the predominant wind direction in this area is West-East, perpendicular to the deck, it has been designed to act like an inverted aerofoil, exerting more negative lift as wind strength increases [Brown et. al., 1999].

To investigate the possibility of GPS being used to detect this movement, trials have been carried out with receivers mounted on both the bridge deck and support towers. It is these trials that are described in the following sections.

6.3.1 Deflection of the Bridge Deck

To investigate the deflection of the actual bridge deck under extreme traffic loading, a test was devised whereby five heavily loaded lorries, with a combined weight of approximately 160 tons were manoeuvred over the bridge in tight formation several times. In order to isolate the effect of this loading the bridge was closed to all other traffic. The test took place between 1:30 AM and 2:20 AM (GMT) on 16th February 1998 [to minimise disruption to the general public].

6.3.1.1 System Set-Up

The full distribution of the receivers used on the bridge deck and on the support tower is detailed in Figure 6.8 and an example of how they were attached, depicted in Plate 6.5 A and B respectively. Three receivers were placed at the middle of the midspan (MIDE, 0010 and GG24), a fourth a quarter of the way along the midspan of the bridge (HUM 6) and a fifth at the middle of the southern span (0069). All of these receivers were Ashtech Z-12s,

apart from 'GG24', which was an Ashtech GG-24 single frequency GPS/GLONASS receiver. Not shown on Figure 6.8 and located some 1.5km from the centre of the bridge is the bridge control tower, where a Z-12 and GG-24 receiver were positioned to act as base stations for the trial. As this control tower is not part of the bridge structure, it has been deemed to be stable. The Z-12 antenna was located over a point coordinated previously using GPS, while the GG-24 was positioned at an arbitrary point and coordinated with respect to the Z-12.

Figure 6.8 Location of Receivers on the Bridge

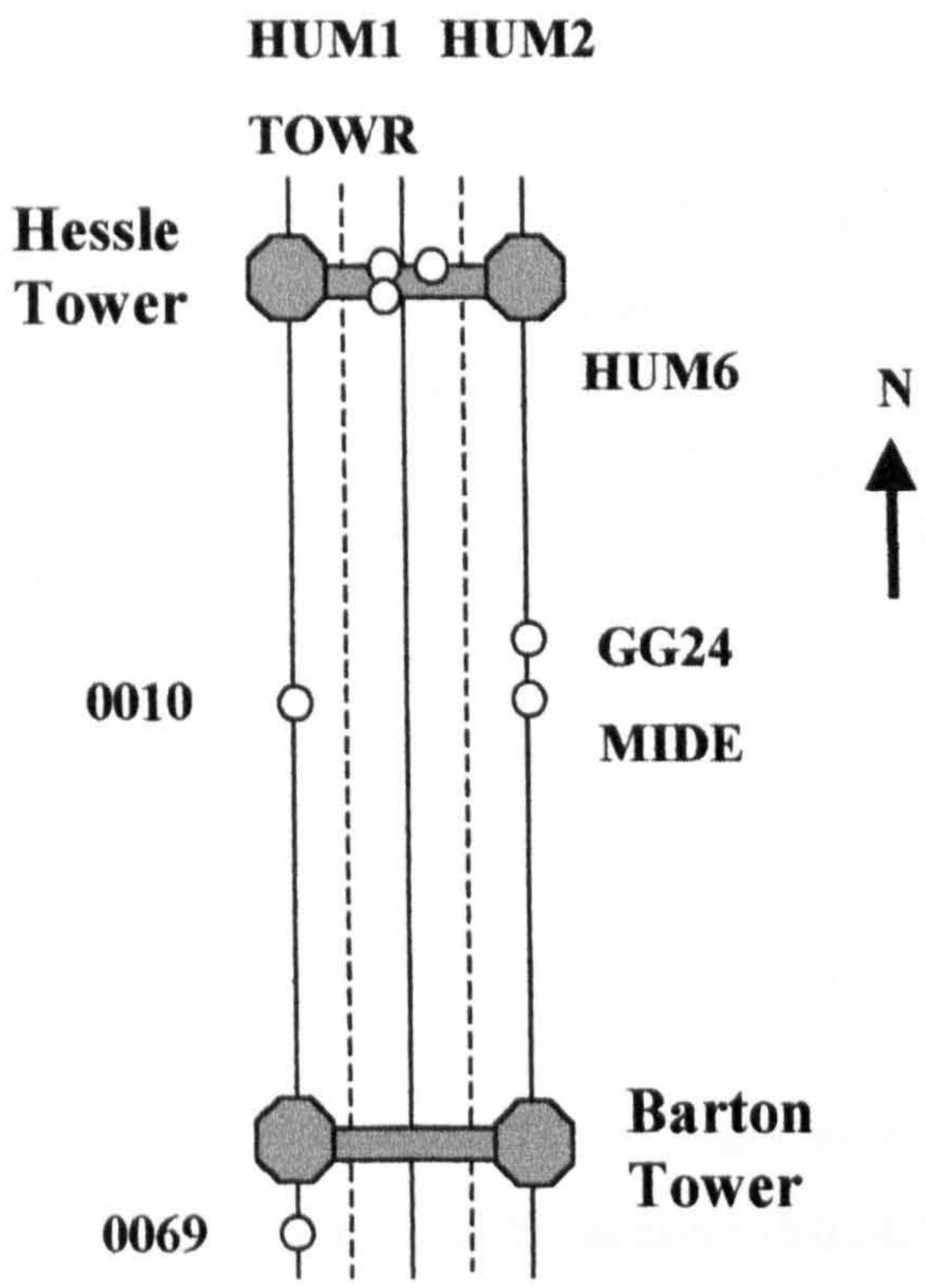

6.3.1.2 Trial Description and Results

The first stage in the trial commenced at approximately 01:33, with all five lorries travelling southbound across the bridge at approximately 45 km/h. Due to a problem with the GG-24 base receiver, data was not successfully logged until 01:36 and thus the effects of this pass were missed. A second pass then occurred at 01:50, with the same five lorries this time travelling south to north across the bridge. After this, two of the lorries transited to the south side of the

bridge, in preparation for the final part of the trial. This consisted of two pairs of lorries driving simultaneously towards the centre of the bridge from opposite ends. When they reached the centre of the bridge at approximately 02:08 they stopped and remained stationary for approximately 5 minutes before driving off.

Plate 6.5 GG-24 Antenna Fastened to Bridge Deck and Support Tower

A

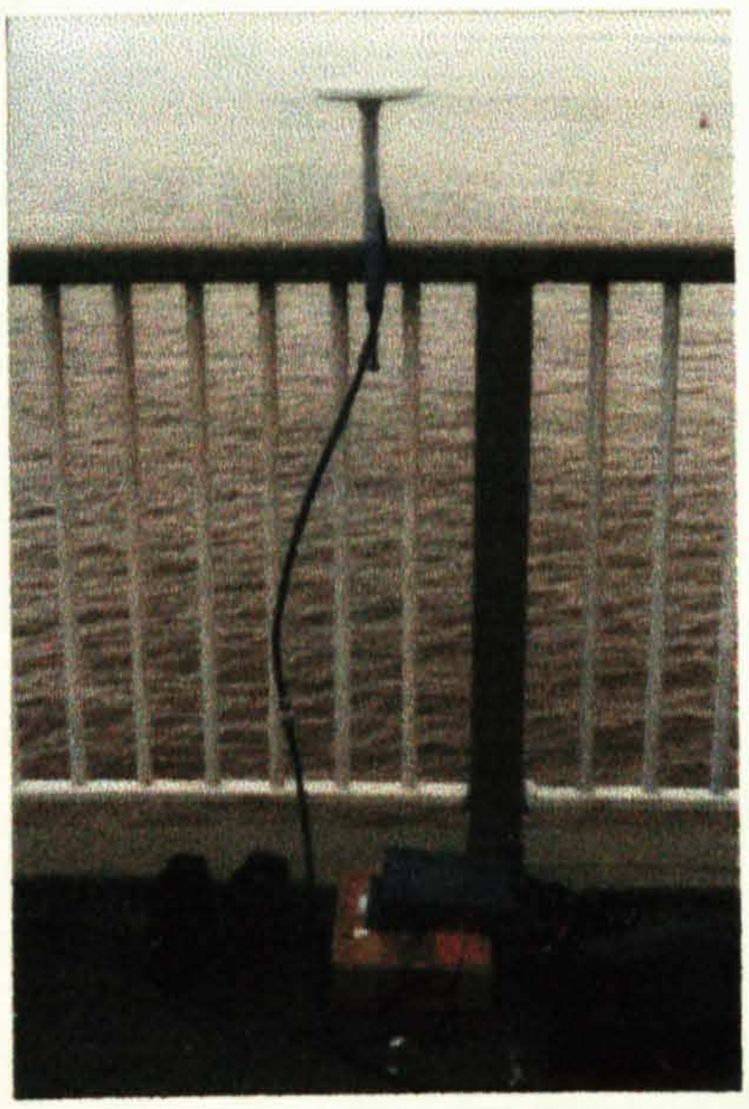

B

For the purpose of this project it was felt necessary to examine the data gathered from only one dual frequency GPS receiver (MIDE), and the single frequency GPS/GLONASS receiver (GG24), as this would enable the evaluation of the relative results obtained through each system. For further information on the results obtained using all the available data, the reader is referred to Ashkenazi et. al., [1998].

Figures 6.9 (A) and (B) show the results obtained from points MIDE and GG24 respectively, when the carrier phase data was processed through WinPrism at an interval of 5Hz and 2Hz respectively [the frequency with which the data was logged]. Both these quite clearly show the effect of the pass at 01:51 as being a downward deflection of 0.5 metres. With the GG-24 data there is however

Figure 6.9 WinPrism Bridge Deck Height Values

A

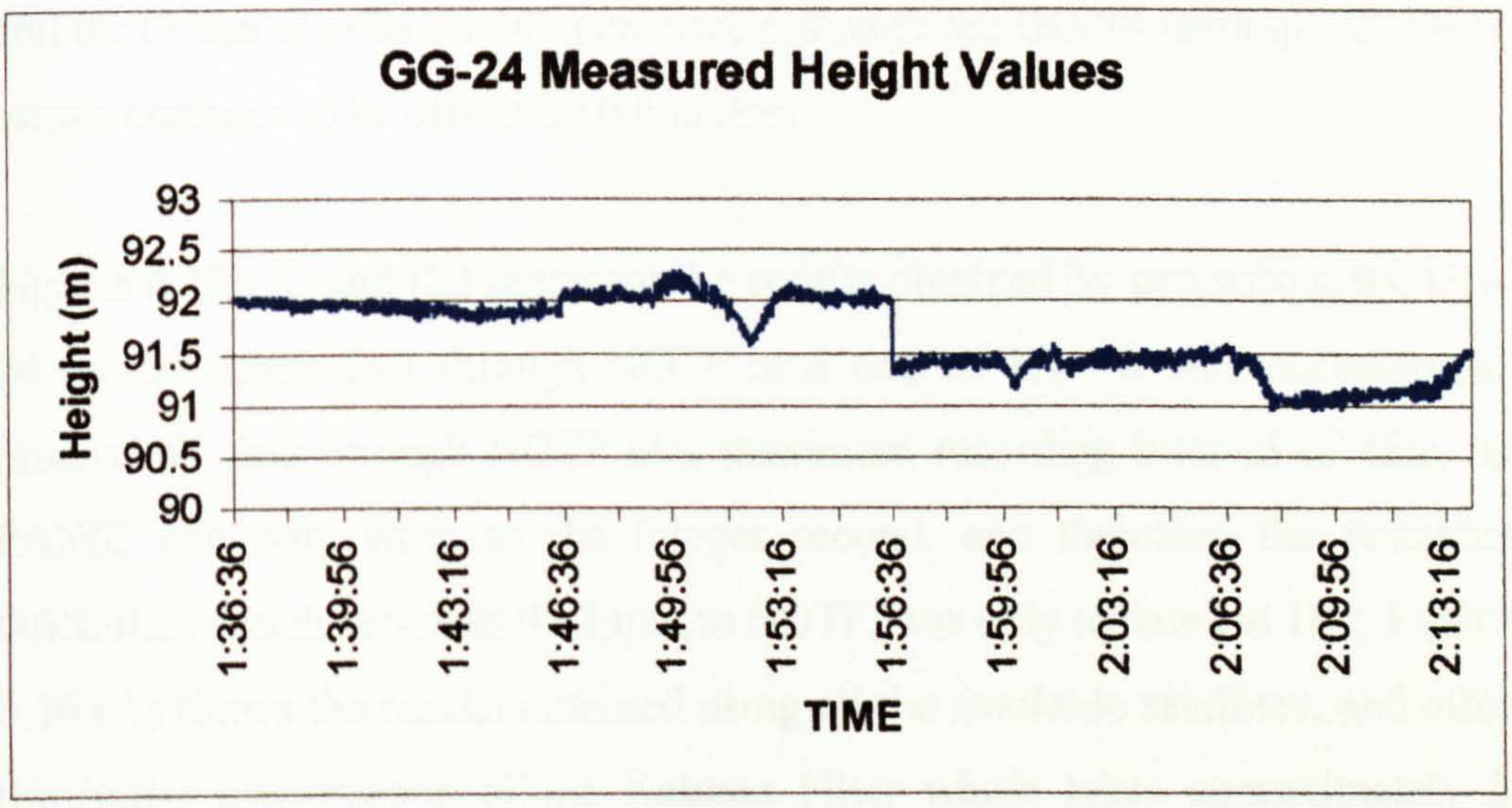

B

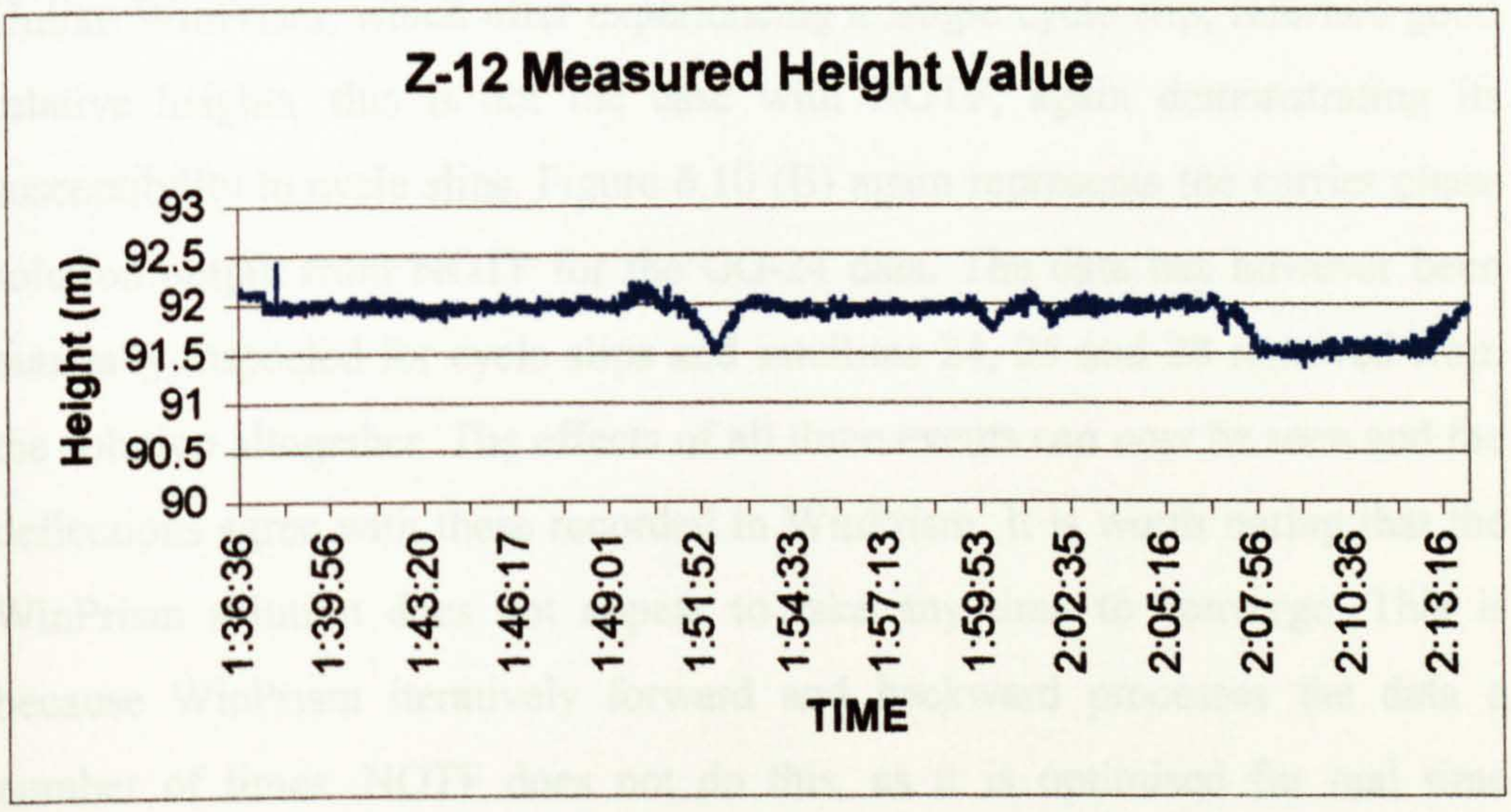

quite an obvious cycle slip at 01:56 resulting in the height of the bridge deck falling by 0.6 metres. The subsequent loading of the two trucks at 02:00, and all five trucks remaining stationary in the middle of the bridge between 02:08 and 02:13 can also be readily detected, although the GG-24 readings for these events continue to be off-set by 0.6 metres.

Figures 6.10 (A) and (B) represent the results obtained by processing the GG-24 carrier phase data through NOTF at a rate of 1Hz. It was necessary to process all data through NOTF at a maximum recording interval of 1Hz, as PANIC can only work to the integer second, and therefore the resultant GASFILE, which serves as the input to NOTF, was only updated at 1Hz. Figure 6.10 (A) shows the results obtained using all the available satellites, and after the initial convergence of the Kalman Filter which takes approximately 3 minutes 20 seconds, the results closely agree with those obtained through WinPrism until 02:02, where a cycle slip deflects the height to 84 metres. Unlike WinPrism, which after experiencing a single cycle slip, returned good relative heights, this is not the case with NOTF, again demonstrating its susceptibility to cycle slips. Figure 6.10 (B) again represents the carrier phase solution output from NOTF for the GG-24 data. The data has however been manually inspected for cycle slips and satellites 24, 25 and 28 removed from the solution altogether. The effects of all three events can now be seen and the deflections agree with those recorded in WinPrism. It is worth noting that the WinPrism solution does not appear to take any time to converge. This is because WinPrism iteratively forward and backward processes the data a number of times. NOTF does not do this, as it is optimised for real time applications where such post-processing would not be possible.

Figure 6.10 NOTF Bridge Deck Height Values

A

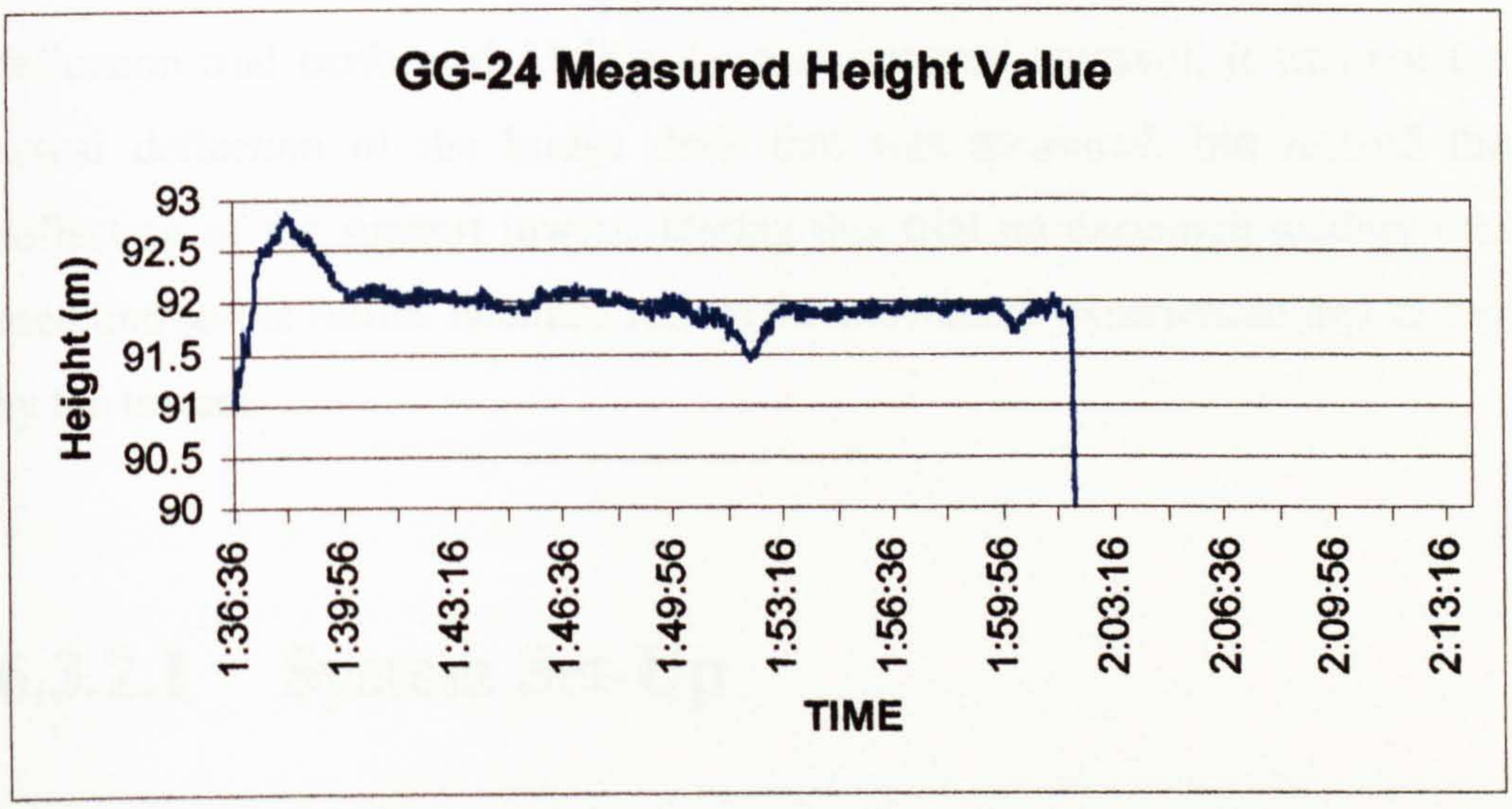

B

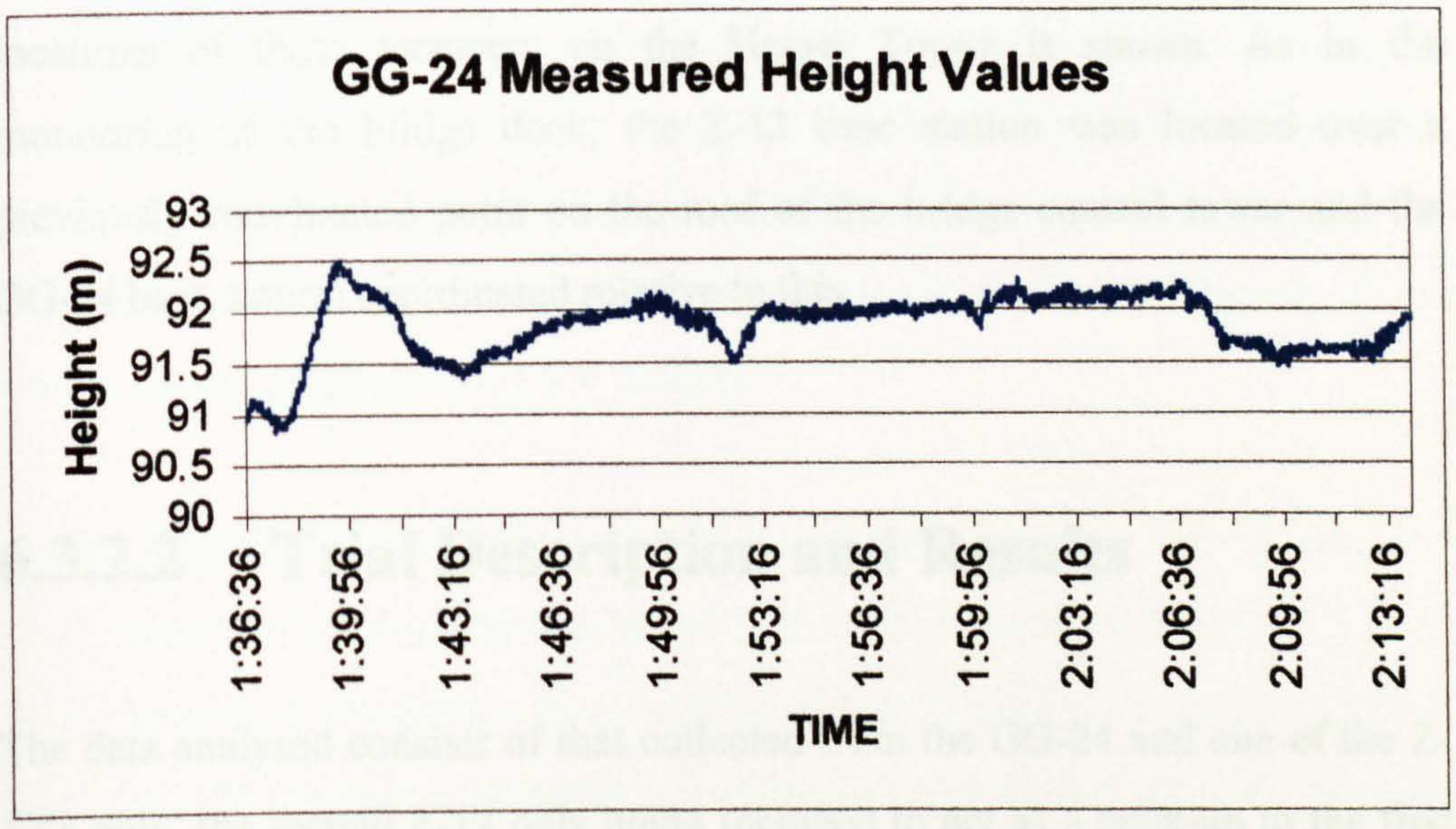

6.3.2 Deflection of the Support Tower

On 12th January 1999, the Humber Bridge was visited again, and another deflection trial performed. Unlike the previous trial however, it was not the actual deflection of the bridge deck that was measured, but instead the deflection of the support towers. During this trial no excessive loading was used and so the results obtained reflect the movement experienced day to day by the towers.

6.3.2.1 System Set-Up

During this trial three receivers were located on the bridge, two Z-12s (HUM1 & HUM2) and one GG-24 (TOWR). Referring back to Figure 6.8, the relative locations of these receivers on the Hessel Tower is shown. As in the monitoring of the bridge deck, the Z-12 base station was located over a previously coordinated point on the roof of the bridge control tower and the GG-24 base station coordinated relative to this.

6.3.2.2 Trial Description and Results

The data analysed consists of that collected from the GG-24 and one of the Z-12's only, the second Z-12 only being included to act as a back-up to the first should it have experienced difficulties. As mentioned above, no specific loading of the bridge occurred during this trial, which instead simply consisted of logging data for a period of approximately 1 hour. It was hoped that in this time any cyclic movement of the tower could be detected, if indeed it existed at all.

Figure 6.11 shows the Easting, Northing and Height values obtained using the Z-12 data recorded at 5Hz, and processed using WinPrism between 12:22:00 and 13:13:00 (GMT) on 12th January 1999. All three coordinate values show a consistency at the cm level, although the effects of a cycle slip at approximately 12:32 can be quite clearly seen. From the coordinate values subsequent to this slip it can however be seen that it was immediately detected and corrected.

Figure 6.12 shows the same values obtained through WinPrism, this time using the GG-24 data, which was also recorded at 5Hz. These results quite clearly demonstrate one of the major limitations of using L1 data, as the effects of numerous cycle slips can quite clearly be seen. In comparison to Figure 6.11, significantly more cycle slips can be seen to have occurred, and they have not been corrected, as subsequent positions experience a sudden jump due to the incorrect integer ambiguity being assigned. The reason for the Support Tower data being particularly prone to cycle slips can perhaps be explained when the location of the receiver antennas is examined (Plate 6.5 B). Unlike the earlier Bridge Deck trial, which offered a relatively unobstructed environment, the antennas on the Support Tower were surrounded by the superstructure of the bridge, and in particular a CCTV camera.

Finally, Figure 6.13 shows the results obtained using the same GG-24 data, this time thinned to a recording interval of 1Hz, and processed through NOTF. As with Figure 6.12 the effects of cycle slips can quite clearly be seen, with their effects on the resultant coordinate values being much greater than was the case with WinPrism. Again this is as a result of a lack of adequate cycle slip detection and correction software being implemented within the IESSG suite of software. However, during periods where no cycle slips occur, the precision of the coordinates is comparable to those obtained through WinPrism.

Figure 6.11 WinPrism Z-12 Support Tower Coordinates

A

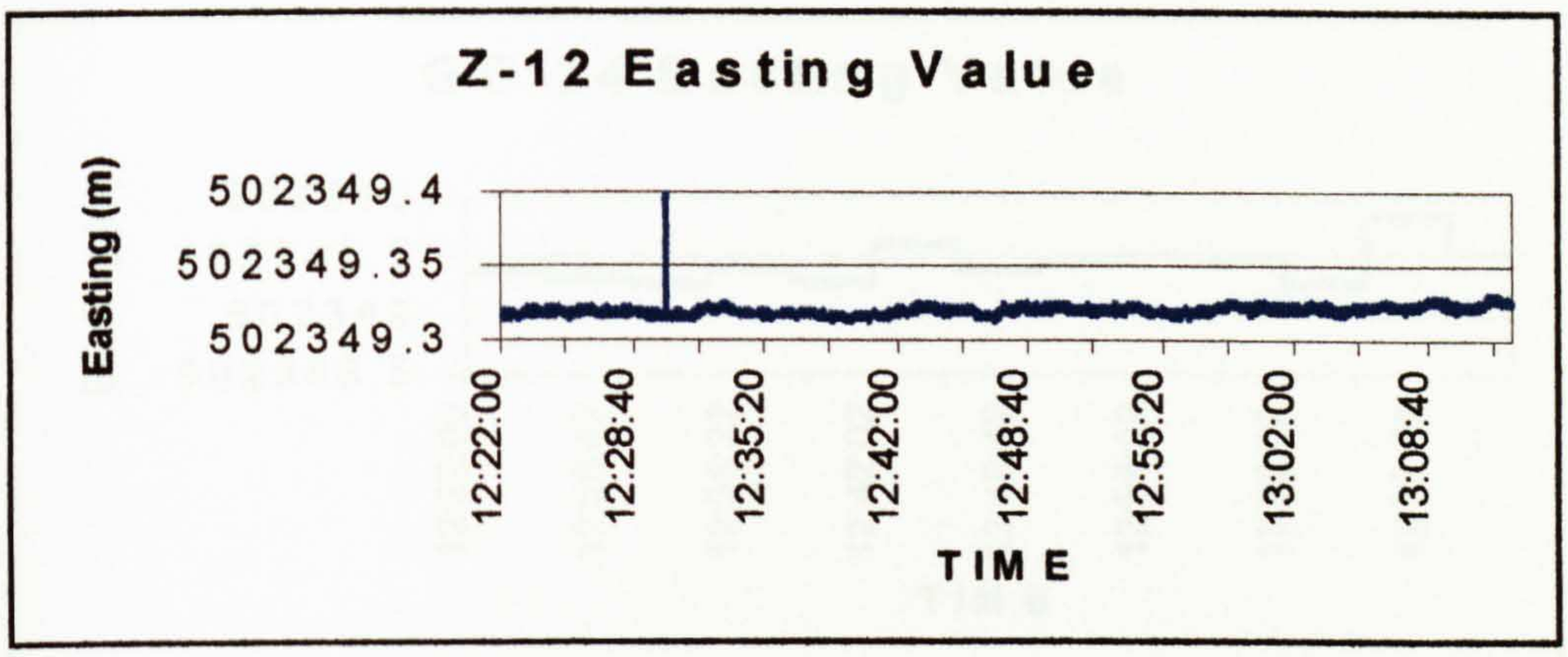

B

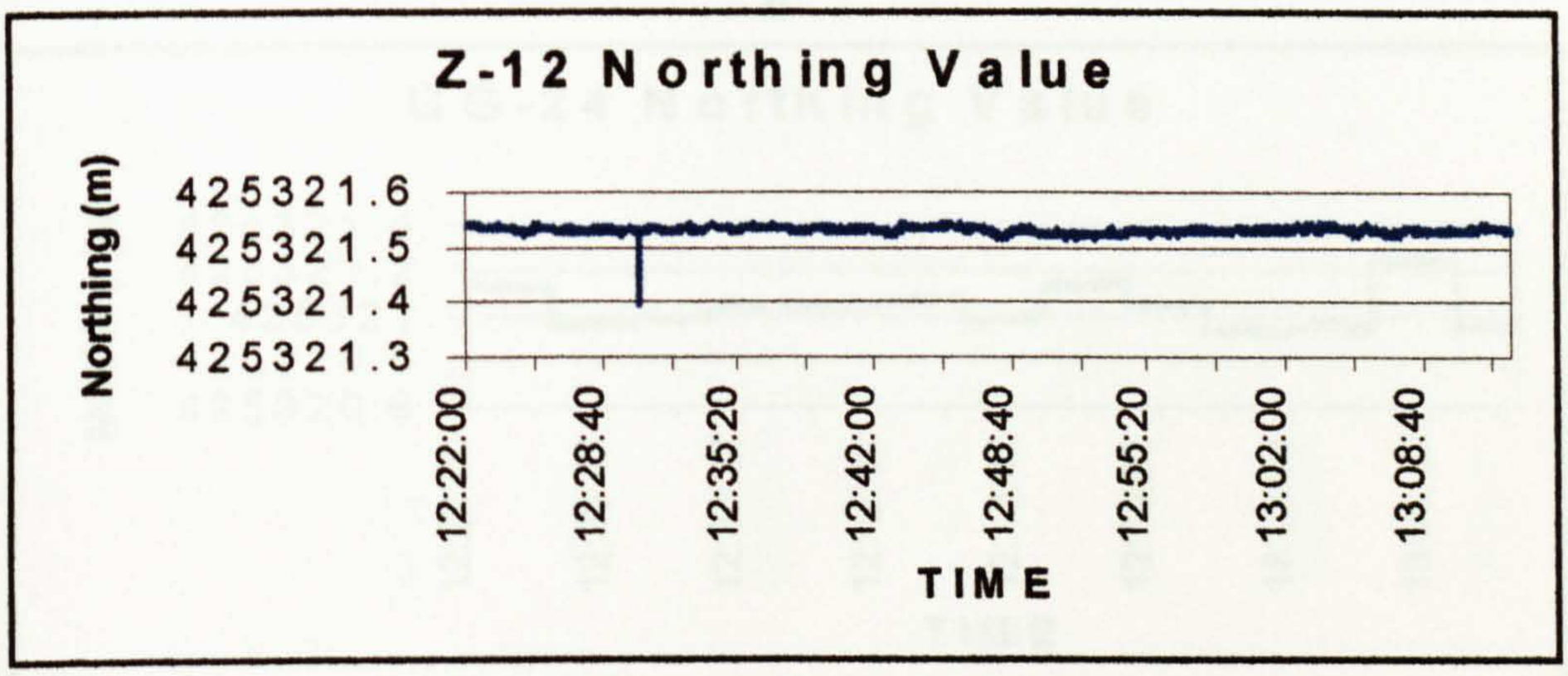

C

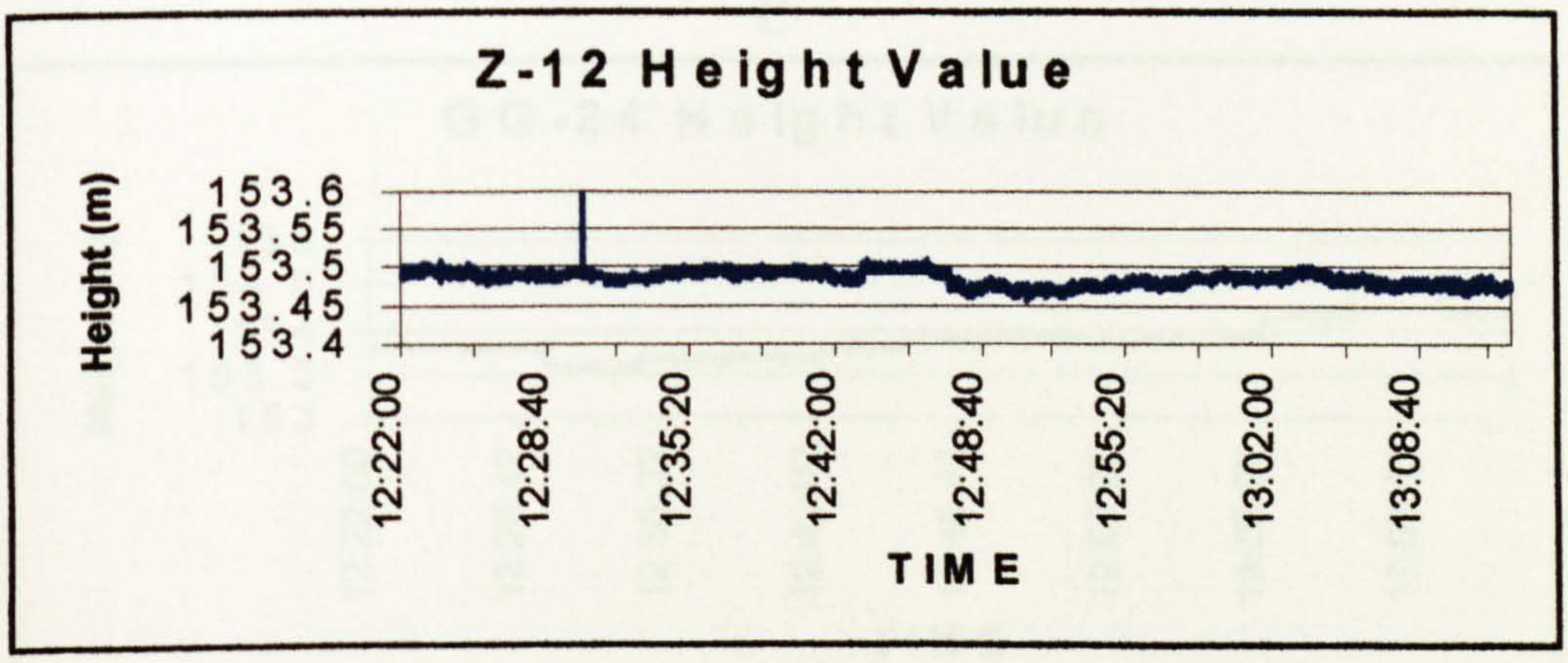

Figure 6.12 WinPrism GG-24 Support Tower Coordinates

A

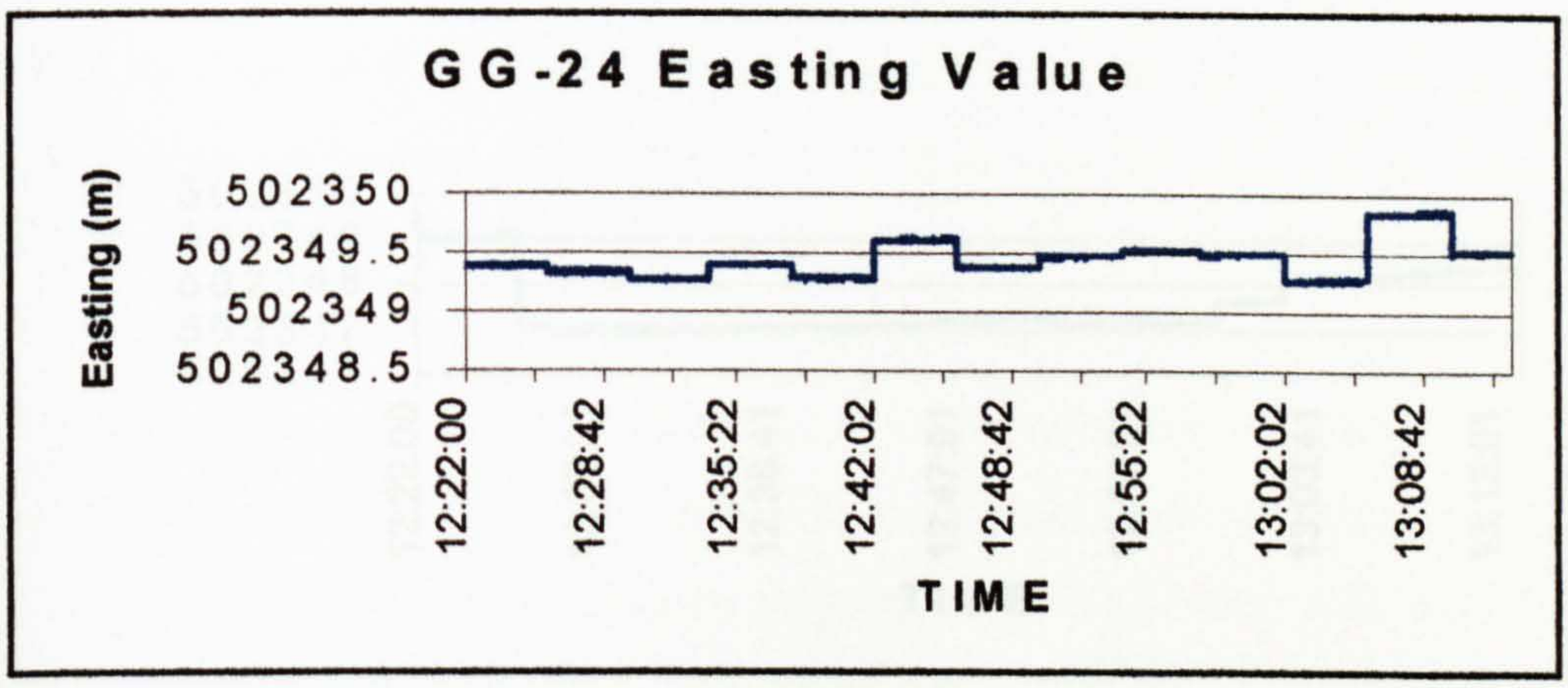

B

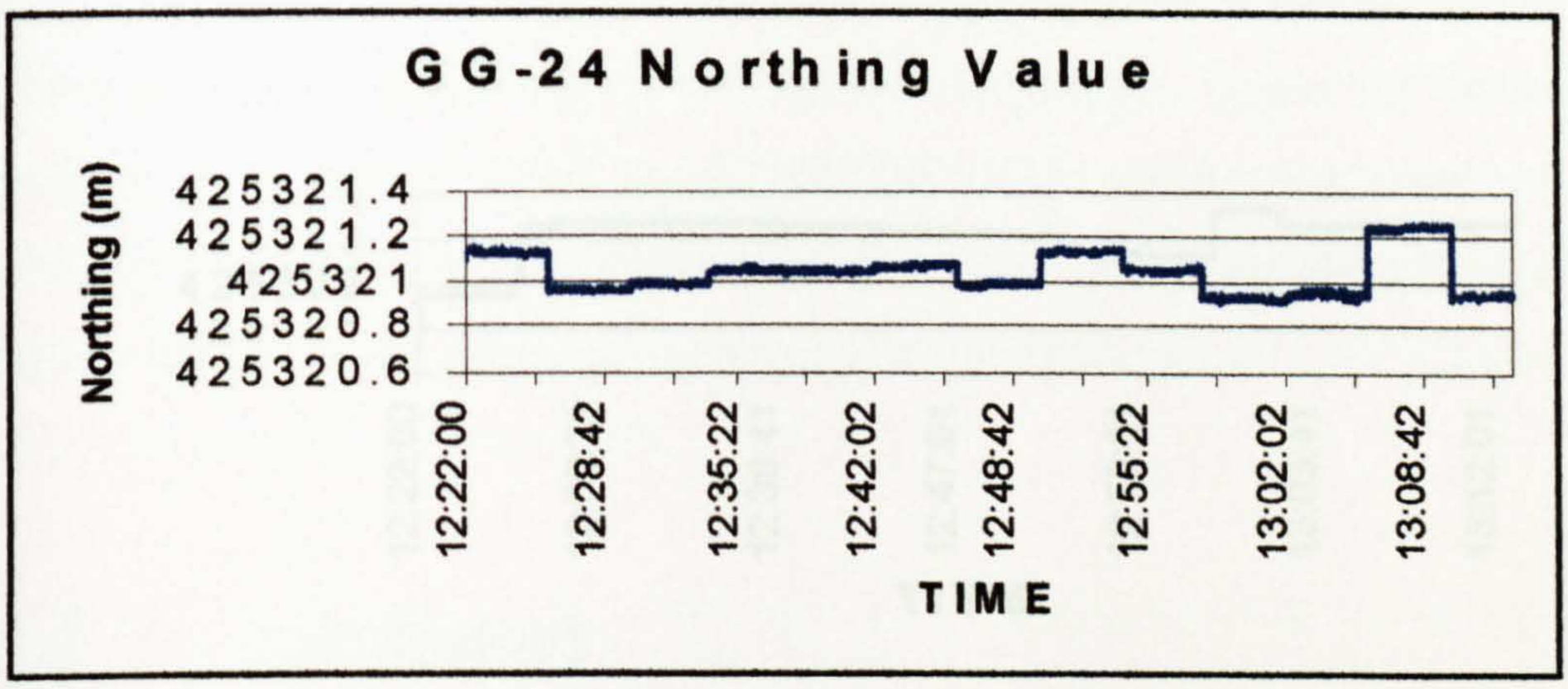

C

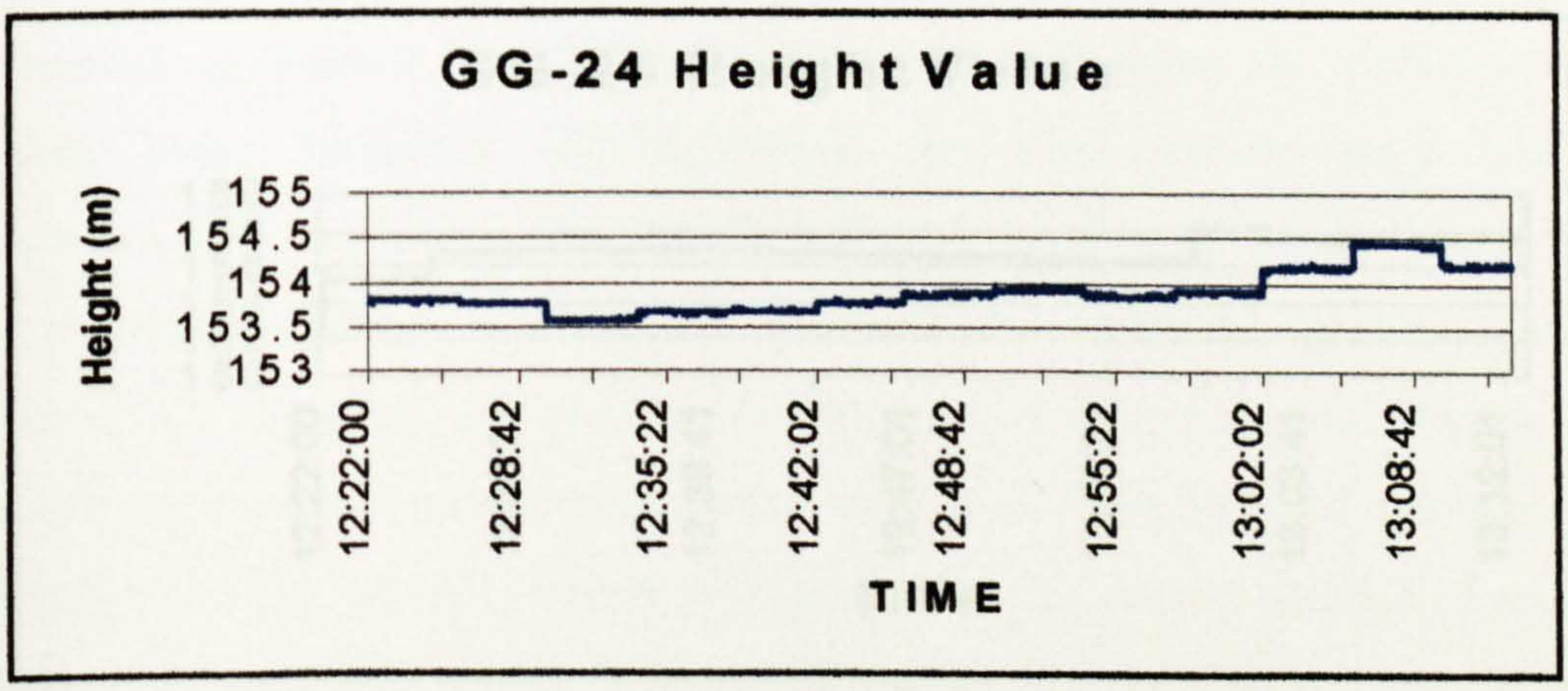

Figure 6.13 NOTF GG-24 Support Tower Coordinates

A

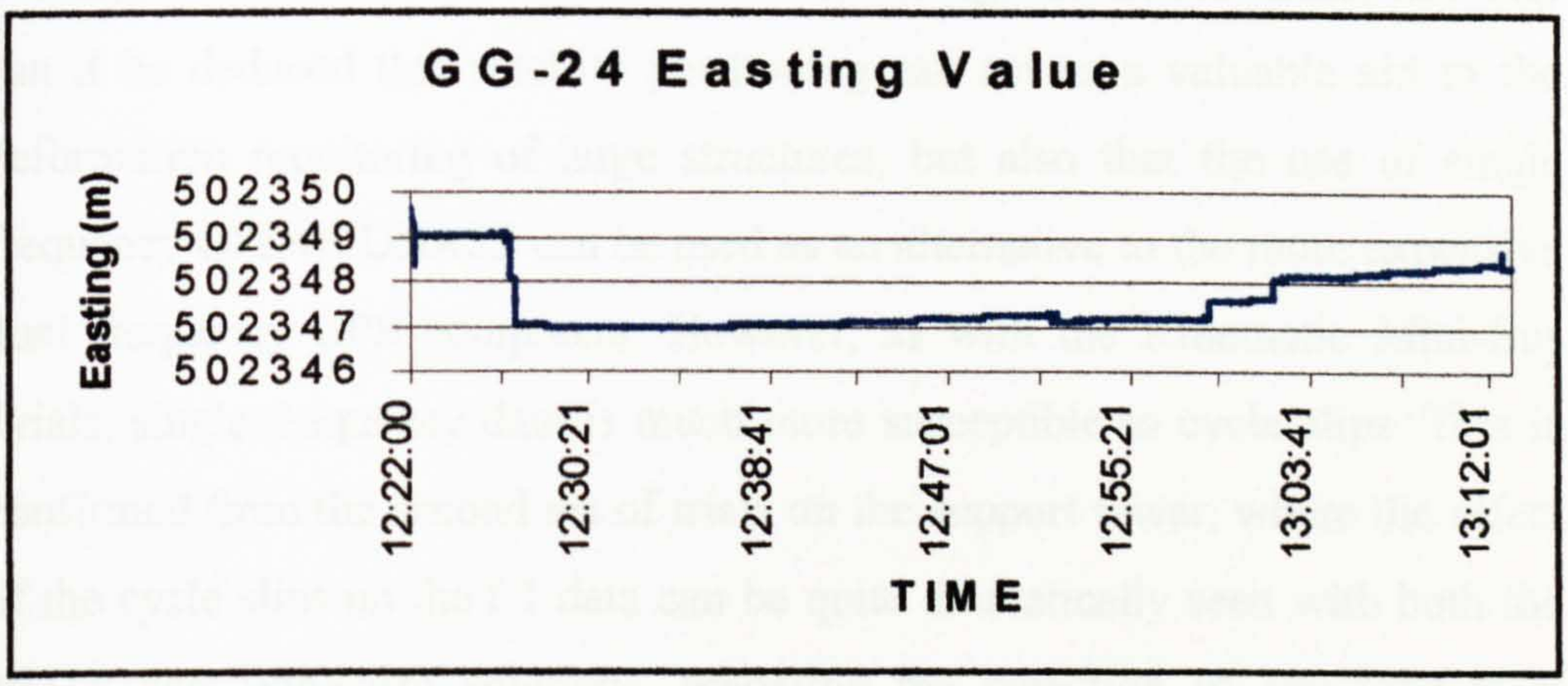

B

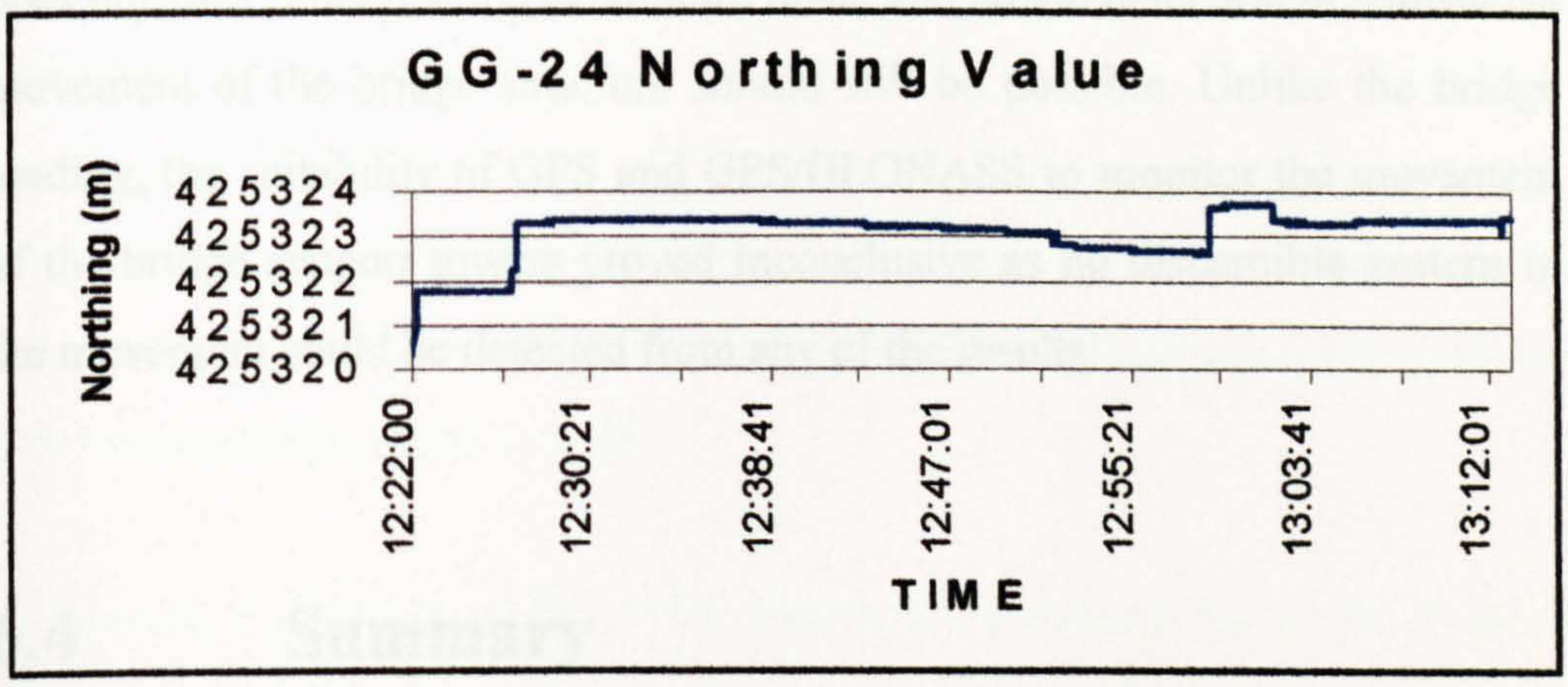

C

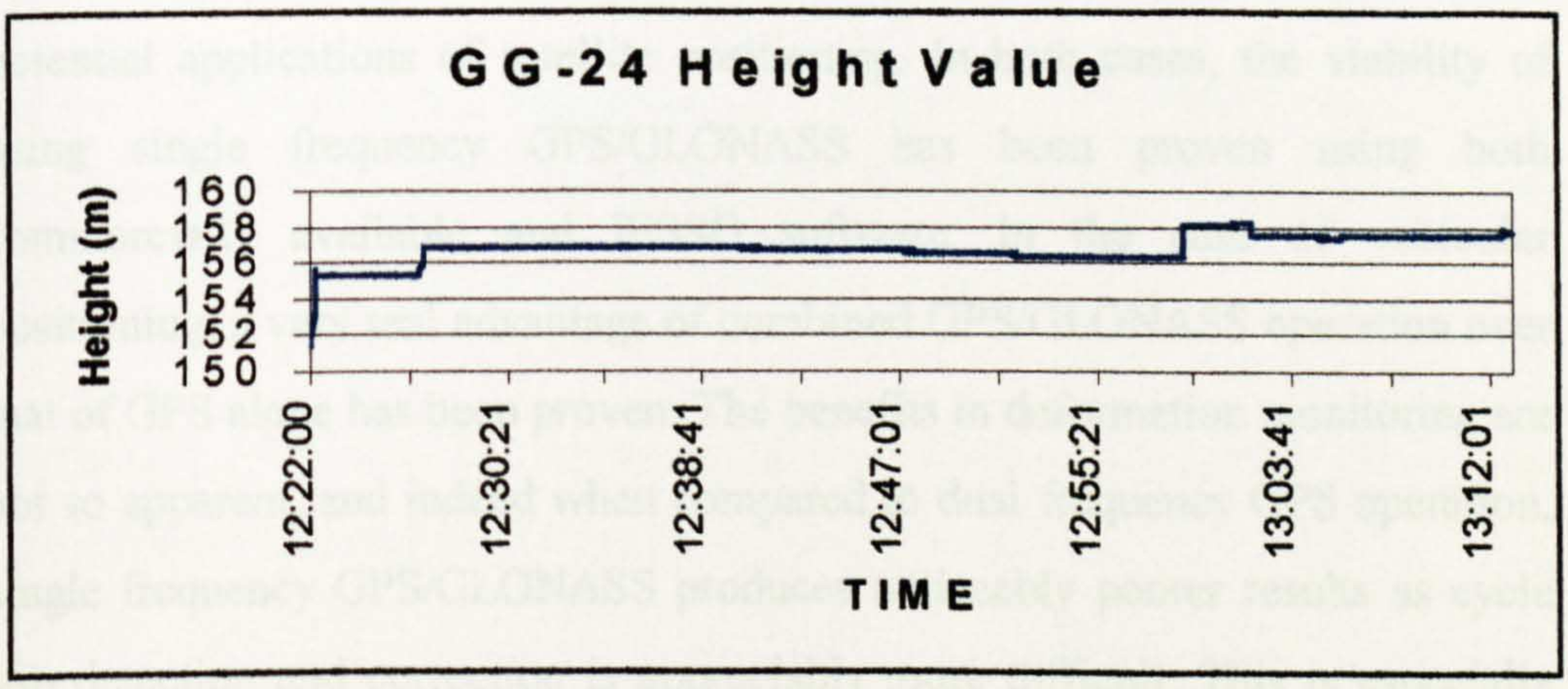

6.3.3 Conclusions

Clearly, from the results obtained from the bridge deflection trials, not only can it be deduced that satellite positioning can act as a valuable aid to the deformation monitoring of large structures, but also that the use of single frequency GPS/GLONASS can be used as an alternative to the more expensive dual frequency GPS equipment. However, as with the Kinematic Mini-Bus Trials, single frequency data is much more susceptible to cycle slips. This is confirmed from the second set of trials on the support tower, where the effect of the cycle slips on the L1 data can be quite dramatically seen with both the NOTF and WinPrism solutions, rendering the detection of any long term movement of the support towers impossible. Relative coordinate precision does however remain at the centimetre level, and so the detection of short-term movement of the bridge structure should still be possible. Unlike the bridge loading, the suitability of GPS and GPS/GLONASS to monitor the movement of the bridge support towers proved inconclusive as no discernible pattern in the movement could be detected from any of the results.

6.4 Summary

The trials detailed in this chapter cover the opposite ends of the spectrum of potential applications of satellite positioning. In both cases, the viability of using single frequency GPS/GLONASS has been proven using both commercially available and IESSG software. In the case of vehicular positioning, a very real advantage of combined GPS/GLONASS operation over that of GPS alone has been proven. The benefits in deformation monitoring are not so apparent, and indeed when compared to dual frequency GPS operation, single frequency GPS/GLONASS produces noticeably poorer results as cycle slip detection and correction is appreciably more difficult. This is especially the case with NOTF, and therefore should be the subject of future investigation. However, with the recent introduction of dual frequency

GPS/GLONASS receivers, it is anticipated that these deficiencies would be dramatically reduced and GPS/GLONASS carrier phase accuracies mirroring those of dual frequency GPS achieved.

6.5 References

Ashtech, 1997, *Ashtech Office Suite for Surveying – User's Manual*, Document Number 630154, Revision A, June 1997. Ashtech Inc., 1170 Keifer Road, Sunnyvale, CA USA 94086.

Ashtech, 1998, *User's Guide – Process*, Document Number 630190, Revision A, November 1997, Ashtech Inc., 1170 Keifer Road, Sunnyvale, CA USA 94086.

Ashkenazi, V., Dodson, A.H., Roberts, G.W., 1998, *Real Time Monitoring of Bridges by GPS*, XXI International Congress FIG, Commission 5 (Positioning and Measurement), Brighton, UK.

Ashkenazi, V., Roberts, G.W., 1997, *Experimental Monitoring of the Humber Bridge using GPS*, Proceedings of the Institution of Civil Engineers: Civil Engineering, 120.

Brown, C., Karuna, R., Ashkenazi, V., Roberts, G.W., Evans, R.A., 1999, *Monitoring of Structures using Global Positioning Systems*, Proceedings of the Institution of Civil Engineers: Structures and Buildings, 122.

Hansen, P., 1996, *On-The-Fly Ambiguity Resolution for GPS*, PhD Thesis, The University of Nottingham, Nottingham, United Kingdom.

Ordnance Survey, 1999, **http://www.ordsvy.gov.uk/home/index.html**

Roberts, G., 1997, *Real Time On-The-Fly Kinematic GPS*, PhD Thesis, The University of Nottingham, Nottingham, United Kingdom.

Tsakiri, M., Stewart, M., Ford, T., Sandison, D., 1998, *Urban Fleet Monitoring with GPS and GLONASS*, Journal of Navigation, Vol. 51 No. 3, September 1998.

Chapter 7

Real Time Kinematic Positioning for Setting Out

7.1 Introduction

Without a doubt, Real Time Kinematic (RTK) positioning offers the greatest flexibility and therefore has the greatest number of potential applications of any of the satellite positioning techniques.

For example, a research project currently under way at the IESSG is focusing on the use of kinematic GPS/GLONASS to monitor river levels. To achieve this it is proposed to mount a satellite receiver on a river buoy together with tilt sensors and pressure transducers for attitude determination of the buoy. Communication satellites will then be used for the data-link between the buoys and reference stations. The ultimate goal is to automatically feed this river

height information into a Geographic Information System (GIS) package, enabling remote, real-time, high precision river level monitoring in a cost-effective manner. Preliminary results indicate that millimetric precision is achievable [Ashkenazi et. al., 1998].

An illustration of an application presently using and benefiting from such technology, is the navigation and docking system employed by Stena Sealink on their HSS 1500 'Super Ferry'. These ships use GPS as their sole means of positioning. To provide the varying levels of accuracy necessary for these applications, two separate systems have been installed. This set-up also provides some form of back-up should one of the systems fail. Figure 7.1 illustrates this navigation set-up and in addition shows 'snap-shots' of the Integrated Bridge Control System (IBCS). The centre bottom picture in particular depicts the confined areas in which the ship sometimes has to operate.

Figure 7.1 Schematic of the Navigation System the HSS Ferries Rely on to Navigate and Dock [Garner, 1998]

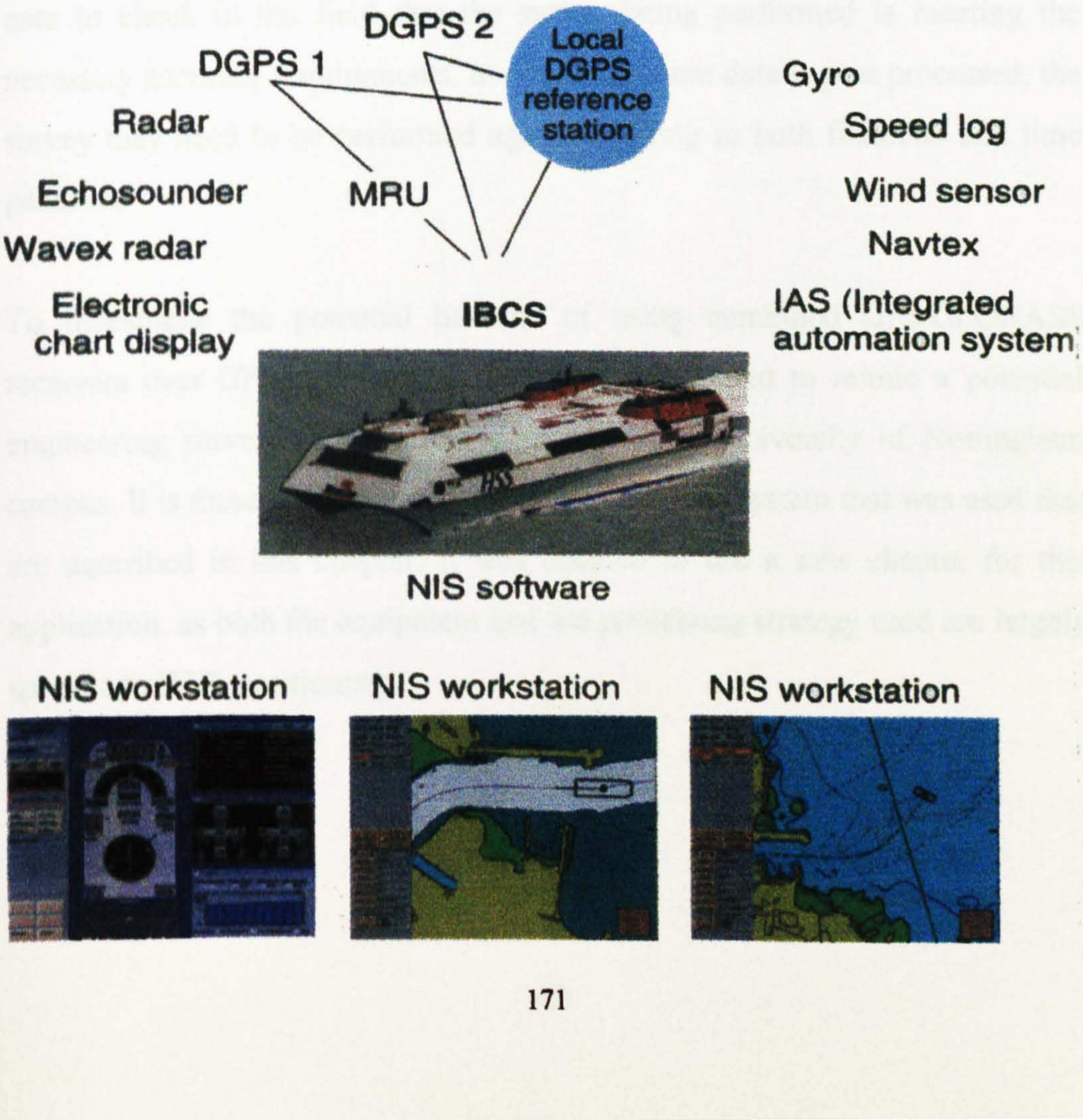

The primary RTK 'GPS1' system uses, where possible, observations received from a reference receiver located in each port and transmitted to the ship via UHF signals, where they are used to produce phase corrections. The achievable range of the system is approximately 8 kilometres and enables positioning to a quoted accuracy of 0.2 metres within narrow channels and confined docking areas. This level of accuracy is an absolute necessity, as unlike conventional ferries, the ship does not dock as such with ropes, but instead couples with a static 'linkspan'. Various techniques such as 'laser ranging' were examined and evaluated before it was decided that RTK GPS provided the most reliable, accurate, quickest and therefore cheapest option. When in open water and out of range of the port beacon, the system then automatically switches to a DGPS system using MF transmitted pseudorange corrections, giving meter level accuracy, until reacquiring an UHF signal from the destination port once more [Garner, 1998].

As RTK systems provide instantaneous positioning and associated quality control values such as HRMS error values (Chapter 4), it is possible for the user to check in the field that the survey being performed is meeting the necessary accuracy requirements. In contrast, where data is post processed, the survey may need to be performed again, resulting in both financial and time penalties.

To investigate the potential benefits of using combined GPS/GLONASS receivers over GPS only units, a set of tests designed to mimic a potential engineering survey, were carried out around the University of Nottingham campus. It is these tests, the results obtained, and the system that was used that are described in this chapter. It was decided to use a new chapter for this application, as both the equipment and the processing strategy used are largely specific to RTK positioning

7.2 RTK System Description

The RTK system used throughout the trials described in this chapter is the Ashtech *FieldMate,* which is a real-time satellite positioning system designed specifically for land survey environments. It was necessary to exclusively use this system for RTK testing because, although optimised for RTK operation, NOTF cannot at present be used in this capacity, as the necessary data encoding/transmission/decoding software has not been written. Fieldmate consists of a base station with known coordinates transmitting its observations to the remote unit. The remote receiver then processes these internally, through a series of algorithms with its own observations, to derive a corrected position for the remote antenna, and if possible to fix ambiguities. Figure 7.2 outlines the system set-up and shows the base station to be made up of satellite receiver/antenna and a radio/modem system, while the remote unit consists of a satellite receiver/antenna, a radio/modem, and a handheld computer.

Figure 7.2 Base and Rover Configuration [Ashtech, 1998]

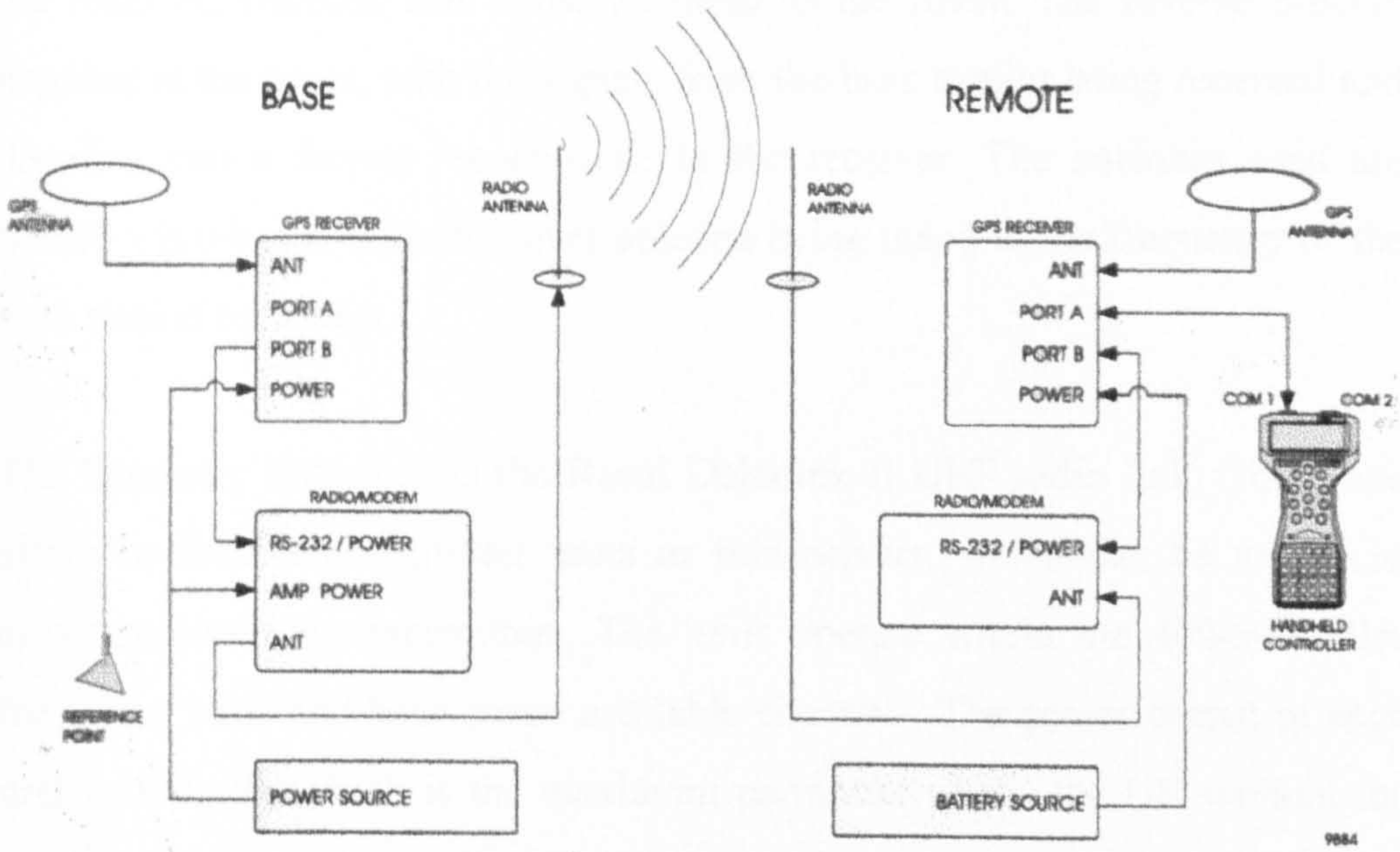

7.2.1 Satellite Receiver/Antenna

RTK systems transmit all available code and carrier phase observables, received at the base station, to one or more remote receivers. Therefore it was thought appropriate to use both GPS L1 only and GPS L1/L2 data to gain maximum comparison with the GPS/GLONASS L1 observations. This meant that two receiver types had to be used. Two Ashtech *GG-24* 24-channel, single frequency receivers were utilised for all L1 only observations, and two Ashtech *Z-12* 24-channel (12 L1 and 12 L2), dual frequency receivers were used for the GPS L1/L2 observations. The appropriate antenna types, with the correct bandwidths (Chapter 2), were used in combination with the receivers.

7.2.2 Radio/Modem

The Radio/Modem component at the base station receives observations from the receiver, encodes and transmits these to the rover. The reverse process happens at the rover, with the signals from the base station being received and decoded into a format recognisable to the receiver. The antennas used are simple whip types, with the rover antenna being tuned to the frequency of the base station broadcast.

The telemetry link used is the Racal Deltalink II UHF radio link. These can either be receiver/transmitter units or transceivers, which can be set up as either receivers or transmitters. The units operate within the 400-500 MHz frequency band and have seven available channels. The power output of each unit is 500mW, which is the maximum permitted within the UK without the need for a broadcasting licence. Although the range specification for these units, operating at the required baud rate (9600) for RTK positioning, is in the region of ~20 km [Racal, 1995], it was found that when line of sight was no longer available this value was substantially reduced. Indeed any off-campus tests, with the base station remaining at the IESSG building, were found to be

impossible because of this, and thus the experiment was restricted to the localised area used. Roberts, [1997] showed that by using a relay station, which is basically a pair of transceiver telemetry links which receive transmitted data from the reference station and re-transmit it to the rover, it is possible to increase the operational range by a factor of two. It was however decided not to pursue this option, as this would not greatly increase the potential of the survey.

Plate 7.1 depicts the roving receiver set-up. Shown, from left to right are a receiving data link, a Z-12 GPS receiver and the Husky handheld computer. The mount into which the receiver and data link are fitted is placed into the rucsack at the bottom of the picture, allowing ease of mobility between points. The receiving antenna is attached to the top right hand corner of this rucsack.

Plate 7.1 The Roving Receiver Set-Up

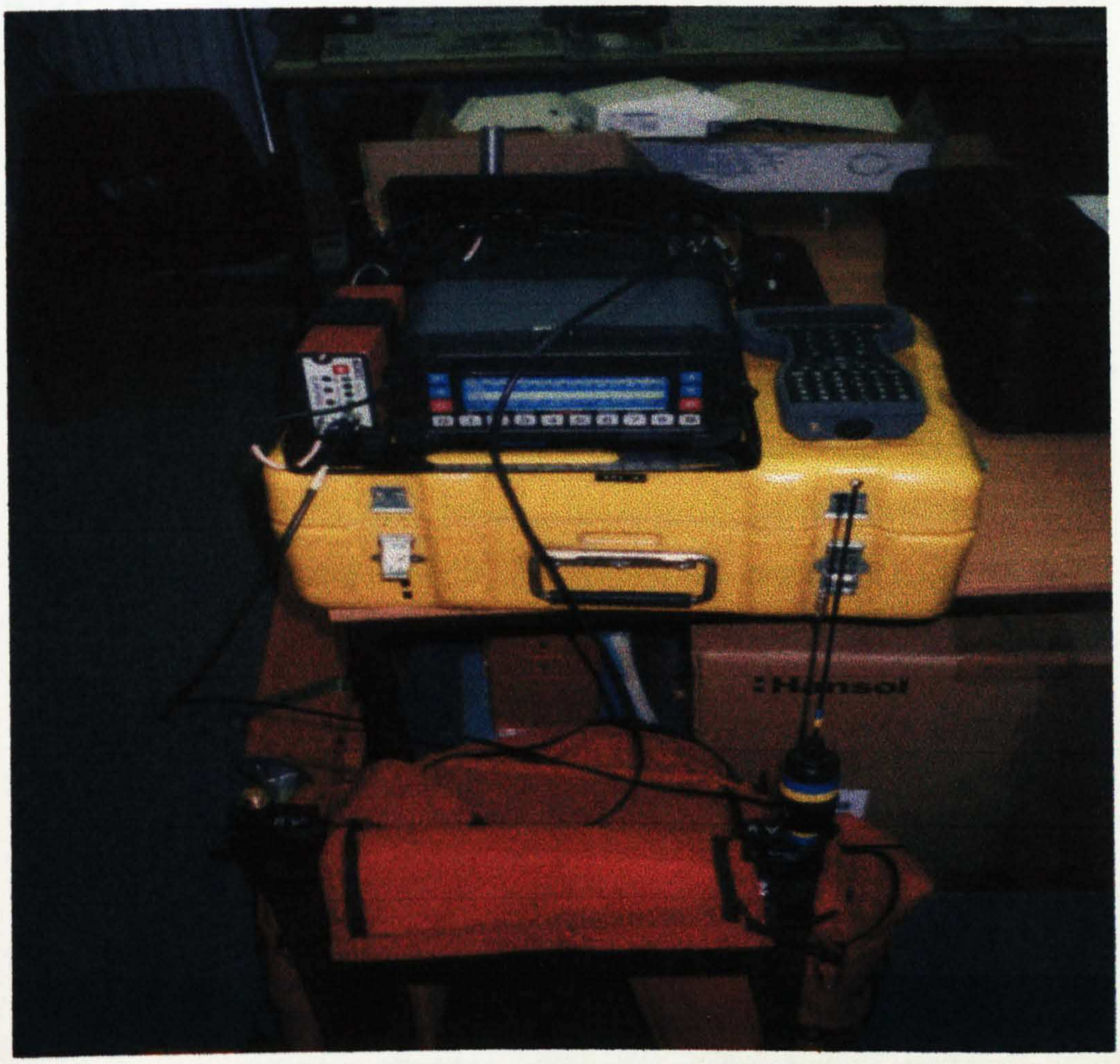

7.2.3 Handheld Computer

The handheld controller used is a Husky Field System 2 (FS/2) computer and is a rugged, all weather unit capable of data storage, data display and communication with the remote receiver.

Running the FieldMate software from this platform, it is possible to initially configure in turn both the base and remote receiver via a serial cable link between controller and receiver. Once the system has been properly configured, operation and performance can be monitored. Position is transferred from the remote receiver to the controller by the same means and is displayed in the input format or, if specified, converted into local coordinates using transformation parameters specified by the user.

Within the unit there are numerous additional functions available. A full description of these can be found in the Ashtech GPS FieldMate Operation and Reference Manual [Ashtech, 1998], but the main ones used in the survey are outlined below.

Audible alarms within the Husky Hunter can be set to warn the operator when the survey is no longer reaching the specified accuracy. This specification of accuracy is achieved by defining the worst acceptable limit for the roving receiver's HRMS and VRMS values. This function proved particularly useful when approaching areas which had particular problems with restricted visibility. The FieldMate software also allows individual points to be simultaneously logged to both the receiver's internal memory and the internal memory of the Husky. Each individual point coordinate can then be simply viewed on the Husky display screen and easily downloaded to a P.C. for further analysis, without the need for any post-processing. This has particular benefits for applications such as setting-out, where a series of pre-defined points can be located and marked in real-time. The quality of these positions can then be checked very quickly, allowing minimum delay before building work

commences. All results presented in Section 7.4 have been gathered using the Husky internal logging function.

It is also worth noting how the display functions that the unit offers are particularly beneficial when using the GG-24 receivers. As seems to be the current trend, the GG-24 comes simply as an OEM Board, mounted in a protective housing. Unlike the Z-12, which includes display screens for analysis and function setting, all programming of the GG-24 occurs through a serial connector and no provision is made for data analysis. Thus, without the handheld device, it would be impossible to have any indication of survey quality in the field.

7.2.4 Processing Within The Roving Receiver

The system described above makes use of the roving receiver's ability to not only track and record its own satellites, but also to receive, decode and process the base station's data, in order to perform ambiguity resolution and position computations in real time. This position and its associated statistics are then output via a serial connector to the Husky Hunter, where it can be seen by the surveyor/operator.

As one would expect from the number of steps outlined above, this process has some latency associated with it. This has been quantified as being up to 2 seconds, depending on baseline length [Ashtech, 1995], and therefore has to be accounted for. Within the FieldMate processing package, an option called *Fast Carrier Phase Differential* (Fast CPD) has been included to deal with this.

With Fast CPD switched off the computation and subsequent display of position is delayed by this latency value. The coordinates displayed on the screen are therefore in the order of 2 seconds old, but the coordinate quality

should be higher as the true data from each receiver is processed from each receiver in a true differenced manner.

When Fast CPD is enabled however, the situation is somewhat different, with a Kalman filter being used to forward predict from the actual data to allow near real time output, with a quoted latency of less than 50 milliseconds. This prediction is usually carried out on the reference receiver's observables, as these should change with a definite trend over time due to the static nature of the receiver. The same cannot be said of the rover's data, which may be subject to sudden and unpredictable changes in velocity. In addition, when dealing with the GPS observables, there will be some additional error since this technique does not correctly account for the effects of S/A [Roberts 1997].

The choice of CPD option to use is very much dependant on both the dynamics of the survey and the accuracy levels required. For instance, if the rover receiver is located on a car travelling at 70 km/h, then a 2 second latency equates to an offset in position of 38.9 metres, and quite clearly the Fast CPD option should be enabled. If however, the dynamics of the rover are slower and it remains static at specific points of interest, as is the case with surveying, then it should be disabled, as this will give the greatest achievable accuracies.

7.3 RTK Field Trials

In order to investigate the potential benefits of a combined RTK GPS/GLONASS solution over GPS alone for a typical engineering *Setting Out* type application, the following trial was devised. A series of nine points were chosen at locations of varying difficulty for satellite observations i.e. close to buildings, under trees etc. Plate 7.2 shows the area in which these points were located, while Plates 7.3 and 7.4 specifically show observations being taken at points 07 and 08. It is worth noting how Plate 7.4 shows the sky-view of point 07 to be extensively disrupted by buildings and vegetation. Indeed, as can be

seen from the results presented in Section 7.4, point 7 proved to be particularly difficult to survey.

Starting and ending at a point with known location (Init.), the coordinates of these nine points were then determined by traditional surveying techniques, further details of which can be found in Section 7.3.1. These coordinates were then assumed to be the *truth* for the rest of the survey. Starting and ending again at point Init. these points were then surveyed in a loop using a Fast Kinematic technique three times, with different receiver/option combinations. The results of these trials are detailed in the Section 7.3.2.

Plate 7.2 The General Survey Area

Plate 7.3 RTK observations being taken at point RTK-7

Plate 7.4 RTK observations being taken at point RTK-8

7.3.1 Traditional Survey

Traditional surveying techniques split position into two parts – height and plan. The height component was introduced by running three levelling loops from the nearest OS bench mark, which is located in the IESSG survey store. A single traverse was then run around the area to introduce plan, and where possible directly occupied the chosen points. However, as points 1,2,3,4,6 and 7 had deliberately been selected to be tight against walls, it was not possible to include them directly as part of the traverse, since a tripod could not be set up over them. Instead, a prism was mounted on a surveyor's detail pole and held manually over the points whilst a distance and bearing were measured from the nearest point on the traverse. At the first point in the traverse, Init., which had known WGS 84 coordinates, observations to a second point, some 200 metres away, with known WGS 84 coordinates were taken. These coordinates were then transformed to OSGB 36 and projected onto OSGB NG using WinCODA (Chapter 5), to allow the bearing between them to be calculated and it was this that was used to orientate each traverse leg in turn. Although derived OSGB

NG plan coordinates obtained through this package are only accurate to approximately +/- 10 metres (Chapter 5), the localised extent of the survey area meant that the offset between the points was consistent. Thus, even though the absolute coordinate values would be in error, an accurate relative comparison could be drawn, which was the aim.

All observations and computations for both the levelling and traverse operations are reproduced in Appendix D. Table 7.1 presents the final adjusted values for each surveyed point in OSGB NG. The height values are with respect to Mean Sea Level (MSL).

Table 7.1 Coordinate Values of Each Point Derived from the Traverse and Levelling Loops

POINT	EASTING	NORTHING	HEIGHT
INIT	454387.360m	338472.651m	38.686m
1	454381.872m	338457.504m	39.175m
2	454353.708m	338431.192m	39.168m
3	454358.728m	338422.190m	39.167m
4	454396.770m	338441.394m	36.140m
5	454220.814m	338505.548m	53.540m
6	454235.045m	338545.744m	52.304m
7	454240.769m	338555.852m	52.271m
8	454223.958m	338698.898m	50.023m
9	454355.837m	338664.575m	43.631m

As was the case with the known coordinate values used in the ZBL tests described in Chapter 5, some quantification of the accuracy of the coordinates quoted above must be made if they are to be considered as truth values.

Examining the plan coordinates first, points Init and Tower, which are used to define the start coordinates and orientation of the traverse, were computed

from 2 hour carrier phase solutions using Ashtech Z-12 GPS data, the RMS values of which were, for both solutions, at the 2mm level. The traverse running from point Init., around all other points, closed back on its self to a vector distance 32mm and this error was distributed around the traverse by means of a Least Squares adjustment. It is therefore reasonable to expect the plan coordinates to be accurate to somewhere in the region of 10mm.

Height was introduced to these traverse points directly, by levelling from the nearest OS benchmark, which is located within the IESSG building. It was installed by precision levelling from a second order benchmark in Nottingham. Now the quoted accuracy of fundamental benchmarks is 0.10m relative to absolute MSL. Primary levelling accuracy is +/- 5mm relative to this, and secondary accuracy +/- 5mm relative to primary. It would therefore be reasonable to assume the height component to be accurate only at the decimetre level. However, a constant height shift between the OS value and WGS 84 was defined by subtracting the WGS 84 height value calculated from another 2 hour carrier phase Ashtech Z-12 data set. The RMS value for the height component of this solution was 4mm. It is reasonable to adopt this value as the initial height accuracy, as this process will have accounted for the potentially larger error in the OS value. Three levelling loops were then run from the benchmark to the various points, and the misclosures of 4, 2 and 11mm evenly distributed around the levelling legs. As with the plan component, the accuracy of the height components of each point can thus be regarded as being at the centimetre level.

7.3.2 Satellite Survey

Unlike the traditional surveying techniques outlined above, when satellite positioning is used, the plan and height components are solved for simultaneously. This is because these systems solve for position in Earth Centred Earth Fixed (ECEF) Cartesian coordinates, of which plan and height

are both components (Chapter 3). Because of the way the constellation appears to receivers on the ground to be predominantly spaced around the horizon, in ideal conditions i.e. open space away from buildings and with an uninterrupted view, the height component is normally found to be the least reliable of the two. It could therefore have been thought to be reasonable to evaluate the worst achievable accuracies by examining the discrepancies in the height values only. However, as already mentioned, a great many of the points observed were close to building, and thus large portions of the sky were blocked from view. Depending on the nature of this obstruction, it could be possible that the plan component may in some of these cases be worse than height, and because of this both have been examined. Also, from examining both components, it has been possible to quantify absolute achievable position accuracies.

In order to draw the best possible comparison of the potential results achievable through the use of satellite positioning, it was decided to occupy the same points on three separate occasions. All three of these trials happened in quick succession on 8th March 1999. The first of these started at 12:24 pm (GMT), and used two Ashtech Z-12 GPS receivers. Because these units offer both L1 and L2 observables they provide theoretically the best accuracies. It was thus hoped that by comparing results obtained using this system with the subsequent L1 only trials, an indication of potential benefits or limitations with respect to dual frequency receivers could be drawn. This trial finished at 13:06, and both Z-12s were then replaced with Ashtech GG-24 L1 receivers with both GPS and GLONASS capabilities enabled. This trial commenced at 15:30 and lasted until 16:01. Immediately after this the GLONASS capability was disabled, so in effect the receivers became an L1 only GPS unit. The survey was then carried out a final time, and all observations were completed by 16:32. A comparison between these last two sets of results would give a direct indication of the benefits, if any, of using both systems.

Ideally, for a true like to like comparison to de drawn, the trials should have been performed on three consecutive days, with the trial commencing 4

minutes earlier each day. By doing this the GPS constellation would have remained the same for each trial. Initially this was the intention, but due to numerous problems with both the base and rover equipment, a full set of data for each trial could only be collected consecutively on 8th March 1999. However, from Appendix C5, which contains satellite availability plots for both GPS only and GPS/GLONASS constellations on that day, it can be seen that during each of the three trial periods, the number of visible GPS satellites remained relatively consistent with each other.

Again the results, which were in the form of WGS 84 Latitude, Longitude and ellipsoidal height, were transformed into OSGB 36 and projected onto OSGB NG Eastings and Northings using the WinCODA package. The height component was directly transformed to the OS Datum by applying a shift of -48.595 metres. As described previously, this value was derived from observations taken at another point on campus with known WGS 84 and OS height components and was a necessary step, as the height control for the points had been introduced directly from an OS Benchmark during the levelling survey. Thus it was not a function of the WinCODA program, and is therefore not subject to the same transformation errors. Not only could these coordinates now be directly compared to the known truth values, but all results could be more easily understood as the units were now in metres instead of degrees, minutes and seconds.

7.4 RTK Results Analysis

In order to achieve some uniformity between these different survey runs, a standard elevation mask of 5 degrees was used throughout. The broadcast correction update rate between the base and remote receiver was always 1 Hz, and the occupation time at each point to be coordinated was 60 seconds. The statistics and coordinates described in this section are thus results of a cumulative solution based on 60 epochs worth of data.

7.4.1 Real Time Statistics

The statistical measures used throughout the actual survey to determine the accuracies being achieved were HRMS and VRMS. Audible alarms were set to go off if and when the values exceeded 0.5 and 1 metres in HRMS and VRMS respectively. This proved invaluable in detecting when the solution had changed from fixed ambiguity to float and thus required time to re-fix before the highest accuracy could again be achieved. In some situations however, it was impossible to re-fix and this could again be determined by examining the rate at which the HRMS and VRMS values were falling.

Table 7.2 shows that, at all points, the combined GPS/GLONASS solution achieved the best RMS residuals. The extent of this improvement proved to be very much a function of the location area, with the greatest improvements being experienced at the sites with the most limited visibilities. Of particular note is extent of the improvement at points 2 and 7, which by using the GPS only system could not be coordinated with a fixed ambiguity solution. However, with the inclusion of the extra GLONASS satellites this was no longer the case, allowing the best possible accuracies to be achieved. This could reasonably be expected, but interestingly there still remained a small improvement at point Init., which occupied an almost ideal location for satellite observations. Various texts have suggested that, in such environments, the use of GLONASS may actually hinder achievable accuracies [Hall et al, 1997], because of problems caused by inter channel biases and its longer chipping rate. Clearly, in this case, this proved not too be the case as the benefits experienced from the improved geometry outweighed any such effects.

Table 7.2 HRMS and VRMS Values of the Roving Receiver at Each Point

POINT	MIXED HRMS	L1 GPS HRMS	L1/L2 GPS HRMS	MIXED VRMS	L1 GPS VRMS	L1/L2 GPS VRMS
Init	0.006m	0.008m	0.011m	0.008m	0.014m	0.013m
1	0.007m	0.027m	0.018m	0.010m	0.030m	0.018m
2	0.015m	0.114m	0.957m	0.024m	0.089m	1.003m
3	0.008m	0.186m	0.015m	0.010m	0.224m	0.015m
4	0.010m	0.125m	0.017m	0.014m	0.226m	0.018m
5	0.005m	0.008m	0.012m	0.009m	0.015m	0.015m
6	0.019m	0.020m	0.027m	0.031m	0.043m	0.038m
7	0.013m	0.036m	0.842m	0.021m	0.074m	1.124m
8	0.019m	0.178m	0.321m	0.031m	0.292m	0.341m
9	0.003m	0.091m	0.013m	0.006m	0.171m	0.023m
Init.	0.005m	0.008m	0.012m	0.008m	0.013m	0.020m

Figure 7.3 perhaps illustrates the potential benefits of combining the two satellite navigation systems in a more obvious fashion. Here the HDOP and VDOP values, which were again available in real-time, are plotted on the same graphs for each of the 3 tests. Tests 1 and 3, which used only the GPS satellite constellation have, as one would expect, very similar values. When the GLONASS constellation is introduced the effect is quite marked, especially at points 2,3,4,6 and 7, where visibility was most impaired. Instead of experiencing sudden jumps, the extra GLONASS satellites have the effect of maintaining reasonable geometry. Throughout the survey it can also be seen that the HDOP value remained lower than the corresponding VDOP value by approximately a factor of 2.

Figure 7.3 HDOP and VDOP Values of the Roving Receiver at Each Point

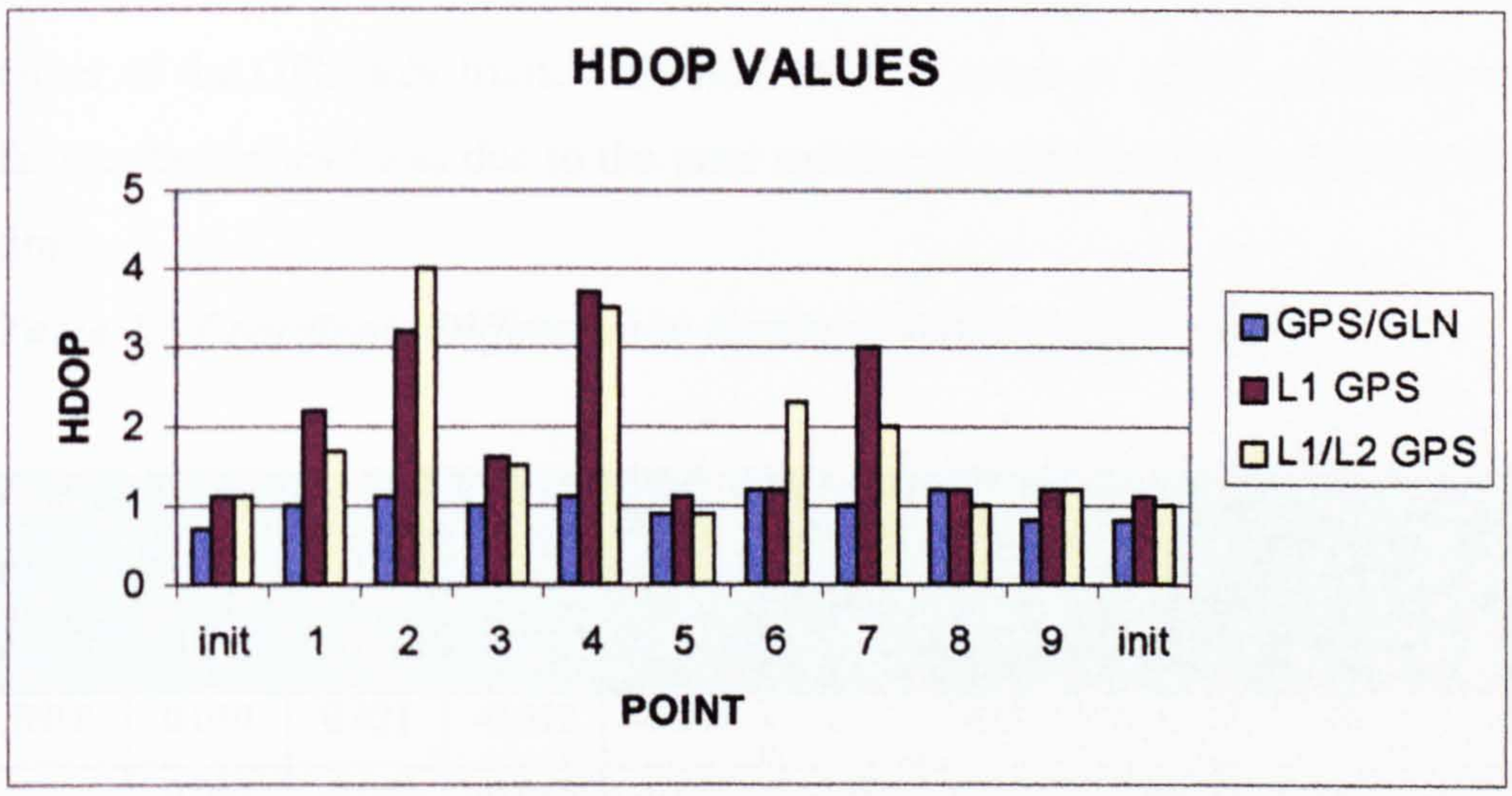

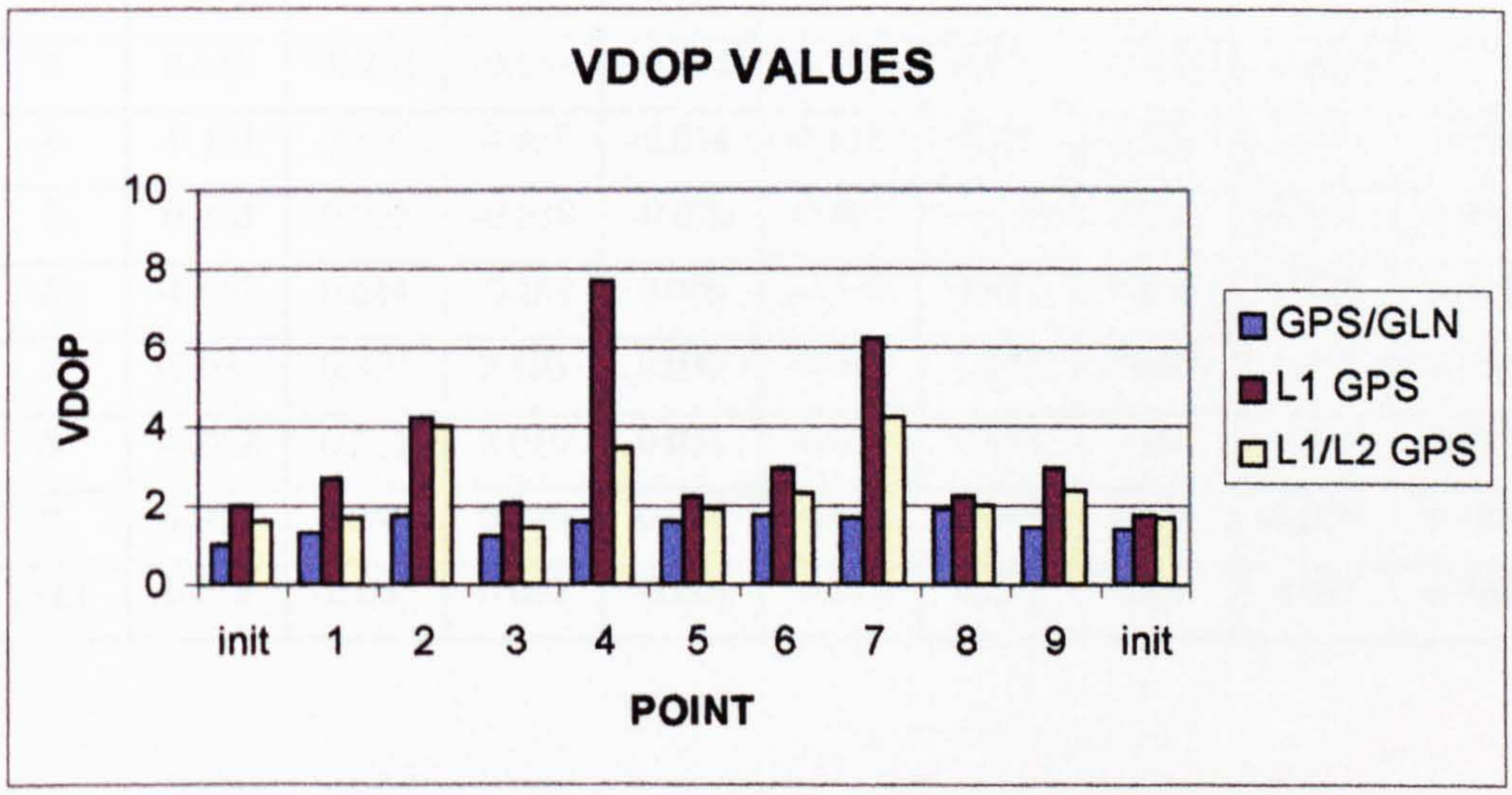

7.4.2 Coordinate Quality

From the real time indicators described above, the suggestion is that the GPS/GLONASS system performed best. However, these are statistical values, and a truer test of success comes from examining the actual achieved coordinate quality.

Table 7.3 presents the error of the coordinates in Easting, Northing and Height in metres, calculated by subtracting the observed satellite positions from those computed in the traverse at each point, for each of the three tests already outlined. It should be noted that no coordinates were recorded at point 2 during either of the GPS only trials. This was not as a result of some sort of system failure, but instead was due to the poor satellite availability at the point at that time.

Table 7.3 Coordinate Difference in Easting, Northing and Height

Point	GPS/ GLN DE	L1 GPS DE	L1/L2 GPS DE	GPS/ GLN DN	L1 GPS DN	L1/L2 GPS DN	GPS/ GLN DH	L1 GPS DH	L1/L2 GPS DH
INIT	0.010	0.021	-0.012	-0.041	0.011	-0.003	0.030	0.038	0.044
1	0.067	-0.086	-0.045	-0.013	-0.09	-0.138	0.024	0.986	0.029
2	0.012	*****	*****	0.032	*****	*****	0.024	*****	*****
3	0.035	-0.242	-0.051	-0.012	0.351	0.076	-0.031	-0.604	0.035
4	-0.131	-0.690	0.007	-0.014	0.622	-0.023	0.081	-1.231	0.088
5	0.000	0.002	-0.018	-0.076	-0.099	-0.118	0.045	0.330	0.036
6	-0.063	0.664	-0.101	0.005	-0.348	0.021	0.015	1.765	0.005
7	-0.044	0.509	3.193	0.050	-0.248	1.285	0.027	1.652	4.056
8	-0.062	0.215	0.010	0.051	-0.011	0.398	0.012	-0.215	0.095
9	0.006	0.249	0.020	0.076	-0.037	0.054	0.025	0.050	0.050
INIT	0.019	-0.055	0.002	-0.001	0.045	0.052	0.031	0.023	0.049

Figure 7.4 represents these figures graphically, and perhaps again gives easier comparison. To enable the smaller values to be seen, the upper and lower limits of the error have been set to +/- 0.5 metres in all three positional directions. Thus, if a value is seen to reach this limit, its true extent can be determined from Table 7.3.

Figure 7.4 Coordinate Error in Easting, Northing and Height

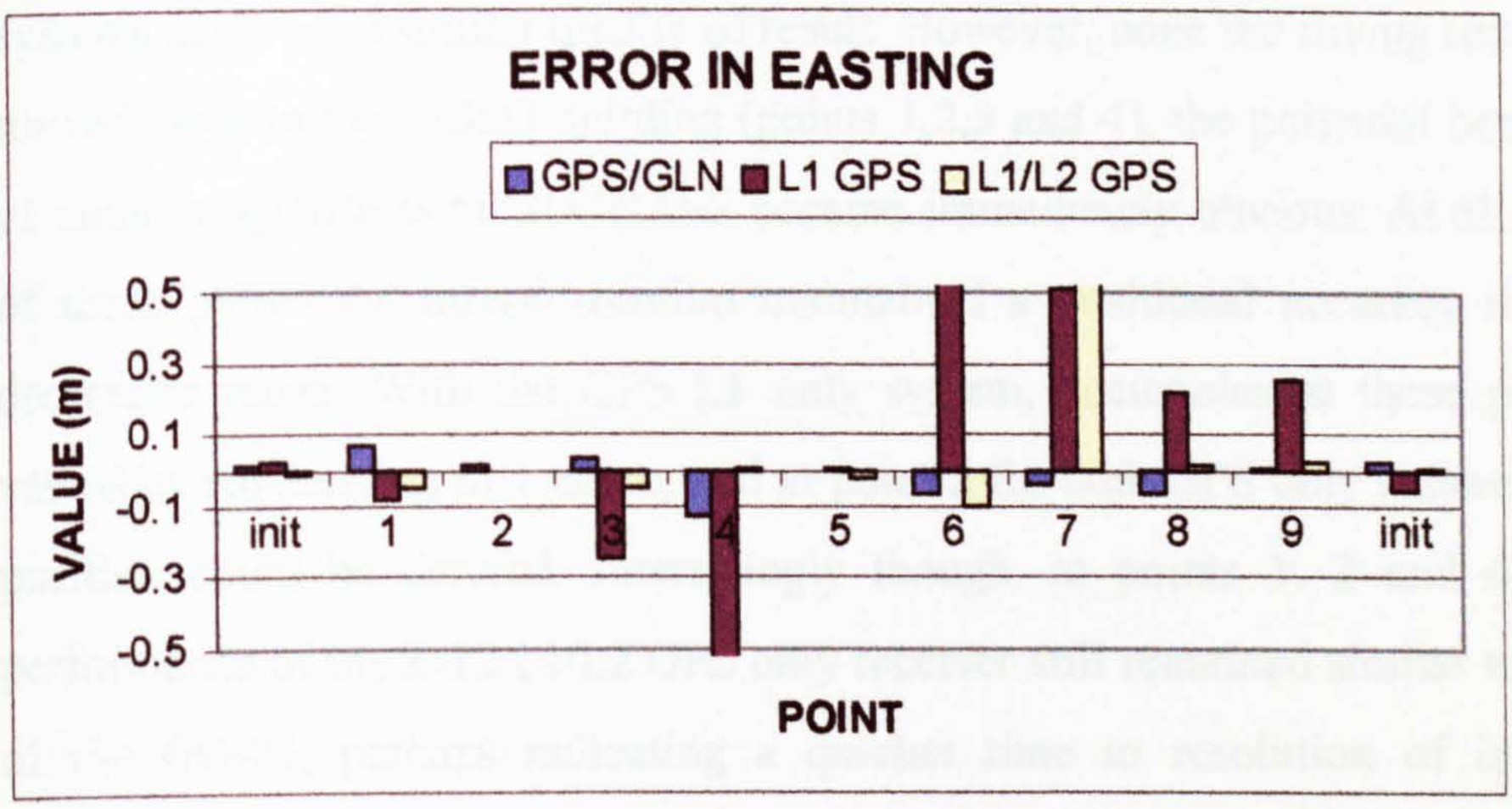

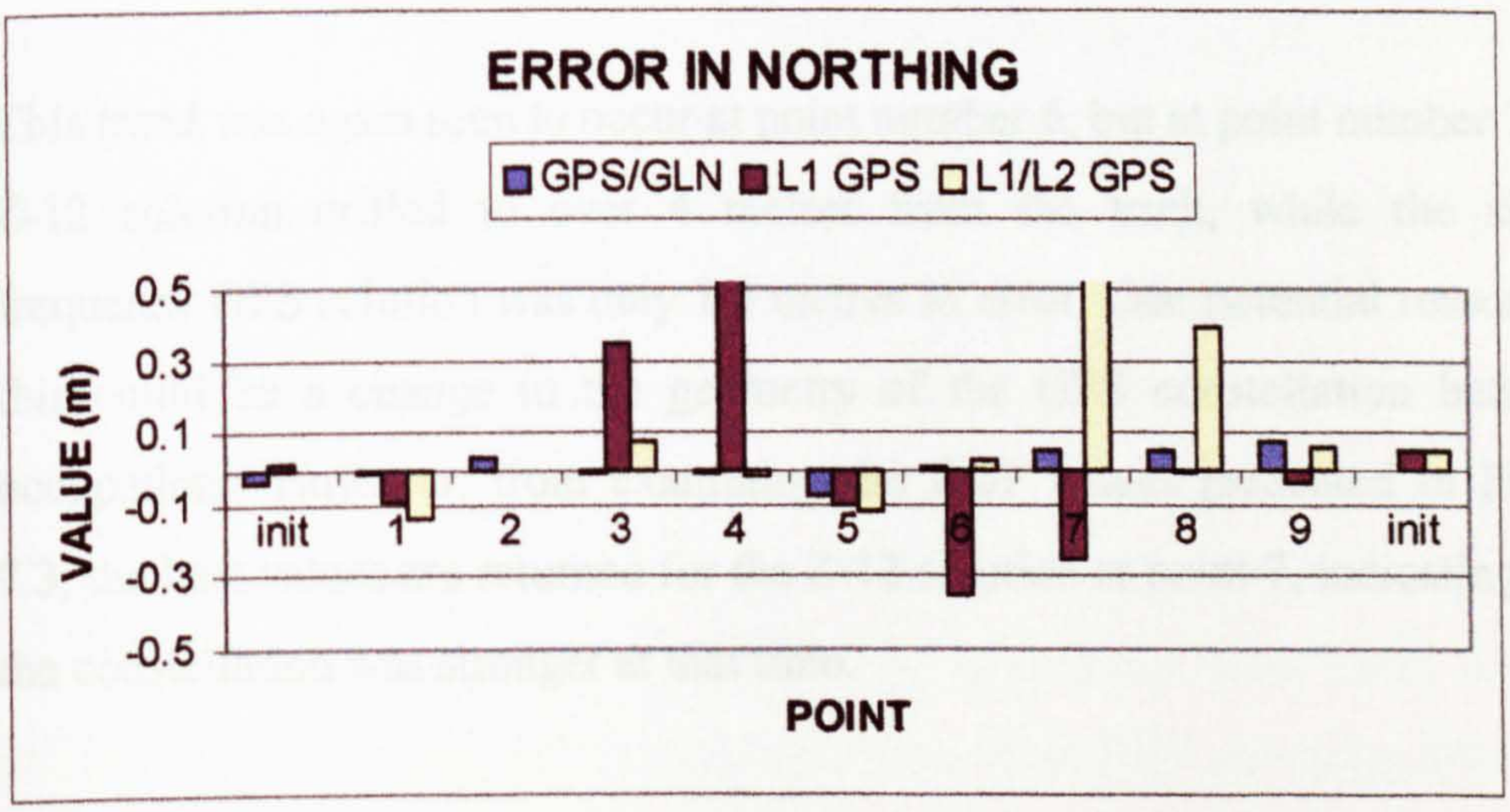

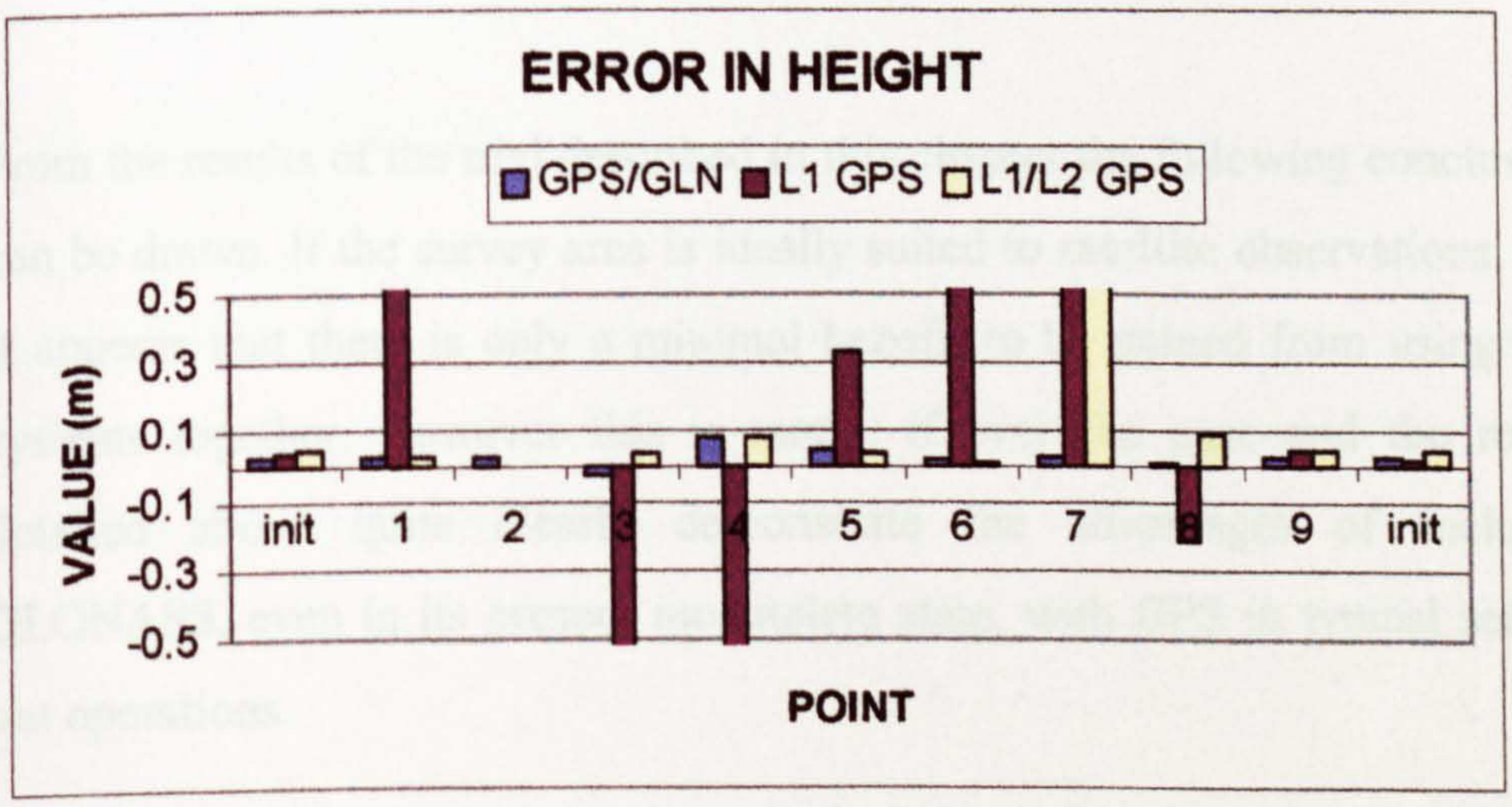

The first conclusion that can be drawn from this set of results is that at the points with a near uninterrupted view of the sky i.e. INIT, 5 and 9, all three systems achieved a similar quality of result. However, once the roving receiver moved close to the IESSG building (points 1,2,3 and 4), the potential benefits of combining GPS with GLONASS became immediately obvious. At all four of these points the mixed solution maintained a positional accuracy in the decimetre range. With the GPS L1 only system, accuracies at these points varied by anything up to 1 metre, and at point 2 for both GPS only systems, no position could be derived. Interestingly though, at points 1, 2 and 4, the performance of the Z-12 L1/L2 GPS only receiver still remained similar to that of the GG-24, perhaps indicating a quicker time to resolution of integer ambiguities after a cycle slip occurred with the dual frequency system.

This trend was again seen to occur at point number 6, but at point number 7 the Z-12 solution drifted to over 4 metres from the truth, while the single frequency GPS solution was only 1.5 metres in error. One potential reason for this could be a change in the geometry of the GPS constellation between occupations. However, from examining the DOP values presented in Figure 7.3, the best values are returned for the Z-12 solution at point 7, indicating that the constellation was stronger at that time.

7.5 Conclusion

From the results of the trial described in this chapter the following conclusions can be drawn. If the survey area is ideally suited to satellite observations, then it appears that there is only a minimal benefit to be gained from using both systems together. However this is rarely, if ever the case and the results detailed above quite clearly demonstrate the advantages of including GLONASS, even in its present incomplete state, with GPS in typical setting-out operations.

Even with centring errors, which are bound to be present from holding a 2 metre pole over a point, the accuracy of the system has been shown to be consistently in the order of a few cm in all environments. For almost all construction setting-out applications this is adequate.

Finally, when examining economic factors, the GPS/GLONASS RTK system again comes out on top, not only against the alternative GPS L1/L2 system, but also traditional surveying techniques. The list price quoted by Rick Blighton of Ashtech is, at present, for a GG-24 Surveyor kit is £9,000, and for a Z-surveyor (the cheaper/newer version of the Z-12), £11,000. As two receivers are required, this represents a saving of £4,000 per system.

The price of the Traverse and Levelling Sets used for the traditional survey come to approximately £10,000. However, the major saving of RTK over this form of surveying is in time. The total time for setting up the RTK system, and performing each survey, was approximately 2 hours. This compares to 3 hours and 5 hours fieldwork respectively for levelling and traversing, followed by a further 4 hours of reductions and computation, resulting in a total survey time of 12 hours to derive the same coordinates. The need for post processing in the office restricts the survey, in that it must be carried out some hours or days prior to the engineering application beginning. With RTK surveying however, work can commence as soon as the points have been located and marked.

7.6 References

Ashkenazi, V., Moore, T., Roberts, G.W., Zhang, K., Moore, R., Close, G., 1998, *Real Time River Level Monitoring By GPS*, Proceedings of GNSS 98, Toulouse, France, Volume 2 VIII-0-02.

Ashtech, 1995, *Ashtech Supplement to Z-12 Receiver Operating Manual Covering RTZ Functions*, Document Number 600292, Revision A, March 1995. Ashtech Inc, 1170 Keifer Road, Sunnyvale, CA USA 94086.

Ashtech, 1998, *GPS Fieldmate Operation and Reference Manual*, Document Number 630253-01, Revision A, July 1998. Ashtech Inc, 1170 Keifer Road, Sunnyvale, CA USA 94086.

Garner, J.P., 1998, *Smooth Sailing*, GPS World, November 1998, pp. 20.

Hall, T., Burke, B., Pratt, M., Misra, P., 1997, *Comparison of GPS and GPS+GLONASS Positioning Performance*, Proceedings of ION GPS-97

Racal, 1995, *Deltalink II Operating Manual*, ref no STM13320, Racal Survey Ltd, Burlington House, 118 Burlington Road, New Malden, Surrey, KT3 4NR.

Roberts, G.W., 1997, *Real Time On-The-Fly Kinematic GPS*, PhD Thesis, University of Nottingham.

Chapter 8

Conclusions and Recommendations for Further Work

8.1 Conclusions

This research has clearly demonstrated the significant benefits of the combined use of GPS and GLONASS for surveying applications in which GPS alone has failed to meet the necessary requirements.

The existing IESSG suite of GPS processing software has been successfully modified to accept combined GPS/GLONASS data. This has been accomplished at all levels ranging from the initial reformatting of RINEX data through to carrier phase processing.

Through using both the modified IESSG software and commercially available packages, various benefits and difficulties in using combined GPS/GLONASS data has been highlighted under various conditions and applications. These can be detailed as follows:

- The achievable accuracy of single epoch autonomous code positioning is greatly improved when GLONASS observations are added to those of GPS. This is because GLONASS signals are not degraded, unlike those of GPS, which are subjected to intentional errors known as S/A. However, when the antenna remains static for an extended period of time and an accumulated pseudorange position is produced, the benefits of adding GLONASS are much less pronounced, as the effects of S/A average out.

- Under ideal conditions the effect of adding GLONASS observations in a differential code solution has been proven to slightly decrease the positioning accuracy. Investigations into the cause of this have highlighted that there exists, between the pair of Ashtech GG-24 receivers owned by the IESSG, a bias in the differenced GLONASS measurements. This is caused by the R/F filters in each receiver being slightly different across the frequency spread of the GLONASS signals, and is therefore not a problem with GPS, as each satellite broadcasts on the same frequency. During kinematic van trials however (Chapter 6), the benefits of a differential GPS/GLONASS system in such an application was proven, as a position was successfully produced much more consistently than with GPS alone. This is due to the extra satellites in the combined constellation fulfilling, more frequently, the requirements to solve for a position. Similar benefits were found when the effect of combined GPS/GLONASS operation during RTK trials was examined (Chapter 7). This confirms that, as expected, in areas where

visibility can be restricted, the benefits of combined GPS/GLONASS positioning are greatest.

- As highlighted in the previous conclusion, GLONASS satellites not only broadcast their signals on a different frequency from GPS, but also on different frequencies from each other. While this was proven to have some effect on code observables, the effect on carrier observables is much more pronounced as the normal method of double differencing no longer remains wholly valid, as the receiver clock correction terms do not cancel. To overcome this problem, a method by which the GLONASS carrier phase counts were scaled to those of GPS was proposed and implemented within the IESSG processing software. This resulted in the successful processing of combined GPS/GLONASS carrier phase data in a double difference form, although it was impossible to fix GLONASS integer ambiguities, as their integer nature is destroyed in the scaling process. As with the differential pseudorange solution, the positional accuracy obtained from the combined solutions were found to be slightly worse than those from GPS alone. Interestingly, when the carrier phase residuals were examined, no apparent bias in GLONASS was found to exist, although the residuals proved to have a higher level of noise.

- Single differencing of carrier phase observations by the receiver will still produce integer ambiguity combinations, even though GLONASS satellites broadcast on different frequencies. Thus, after making the necessary alterations to NOTF, it became possible to fix GLONASS integer ambiguities. The position accuracies obtained from the combined GPS/GLONASS solution are similar to those of GPS alone. It was initially hoped that the time needed to successfully resolve these integer ambiguities would be reduced with the combined solution, as

the extra satellites would increase the search redundancy. In fact the opposite was found to be the case and is thought to be as a result of the pseudorange bias, which serves to contaminate the clock correction estimation.

- During the bridge deflection trials (Chapter 7), it was found that the results obtained from the single frequency GPS/GLONASS receivers were markedly worse than those from dual frequency GPS receivers. This highlighted a shortcoming within the IESSG software, which is particularly susceptible to cycle slips.

The initial aims and objectives of the project were presented in Chapter 1. These have been repeated below and a commentary to each added:

- Modify existing software, and where necessary develop new software and processing strategies to enable combined GPS/GLONASS data to be processed within GAS.

As detailed in Chapter 5, Con2SP3, Filter, PANIC and NOTF were all modified to varying extents to enable GPS/GLONASS data to be successfully processed, and thus this aim was fully met.

- Validate the alterations made to the software through controlled tests, and quantify the relative performance of the system for various means of positioning.

To fulfil this requirement, the modified positioning routines were tested on a sample data set (Chapter 5). From the results obtained from this, not only was the validity of the software proven, but problems with the GLONASS pseudorange measurements identified. Apart from autonomous positioning, the relative performance of combined GPS/GLONASS operation over GPS alone was, under ideal conditions, found to be similar.

- Evaluate the potential benefits of combining GPS with GLONASS in actual applications.

Experiments detailed in Chapters 7 and 8 have proved that there are undoubted benefits in using combined GPS/GLONASS positioning in areas of restricted visibility. However these experiments have highlighted that, when using L1 GPS/GLONASS data, it is particularly difficult to detect/correct cycle slips, using both commercial and particularly IESSG software.

8.2 Recommendations for Further Work

From the research detailed in this thesis, and the conclusions summarised above, the following are recommendations for possible future work in this subject area:

- As mentioned above, the IESSG software proved to be particularly susceptible to cycle slips. This has already been the subject of research, but has concentrated on dual frequency data. It is therefore recommended that an effective single/dual frequency GPS/GLONASS cycle slip detection and correction package be developed and implemented within the IESSG software.

- Although all research undertaken throughout this project has used single frequency GPS/GLONASS data, as that was all that was available, there are now on the market dual frequency GPS/GLONASS receivers, and their performance should be investigated. With this dual frequency data it should be possible to directly solve for ionospheric delay and employ existing dual frequency GPS processing strategies, such as wide-laning to GPS/GLONASS data. Although the program routines within the IESSG software which handle the second frequency would require modification to process dual frequency data, these modifications should be able to be completed quickly, as the

necessary changes will mirror those already implemented within the routines for the single (L1) frequency.

- Although the GPS/GLONASS receivers can record data at intervals up to 5Hz, the existing IESSG software can only process data at a 1Hz processing interval. While this is more than adequate for geodetic type applications, it is possible that high frequency oscillations or movements, which may have occurred in, for instance, the bridge deformation monitoring trial, could be missed. It is therefore recommended that software be updated to process data at whatever rate it was recorded.

- As a product of the IGEX-98 experiment (Chapter 3) which is still ongoing at the time of writing (August 99), precise ephemerides for GLONASS satellites have been produced and are freely available. These are in a .SP3 format, which unfortunately does not exactly agree with the .SP3 format needed by the IESSG software. If the processing software is suitably altered it should not only be possible to investigate the improvements resulting from the use of precise ephemeris, but it should also be possible to process data from the various IGEX sites to investigate performance over varying baseline lengths.

- During the van trial there was an undoubted improvement in the performance of the GPS/GLONASS system over GPS alone in solving for position. There were however still a number of epochs where less than four satellites were simultaneously visible, and therefore it was impossible to derive a position. It would be preferable, in such situations, to at least solve for plan position if possible. If this was also impossible, another option would be to interpolate positions by dead reconing from the previous position solutions.

- In the writing of NOTF it was decided to optimise it for Real Time Operation, but at present it can only be executed in a post processed format. Some attempt should therefore be made to implement it as a real time package. A dual frequency GPS/GLONASS real time OTF package would be at the forefront of satellite positioning and would be sure to have numerous applications.

- One of the major findings in this research was the apparent bias in the GLONASS pseudorange measurements between receivers, caused by varying delays in their R/F components. This has been accounted for within NOTF by downweighting the GLONASS pseudorange measurements with respect to those of GPS. After some thought, it has been decided that this process is incorrect. Therefore, some further investigation into these biases is needed. If they are found to be repeatedly consistent with respect to time then there is no reason why they cannot be included as extra states in the Kalman Filter, and be determined over a period of time.

Finally, as mentioned in Chapter 2, the immediate future of the GLONASS system is of great concern at the moment. The future of GPS appears to be much more certain with firm commitments to further modernisation of the system well into the next millennium. It is therefore reasonable to expect that GPS will act as the backbone to the Global Positioning Industry for the foreseeable future. Indeed plans for regional augmentations to GPS over Europe (EGNOS), Japan (MSAS) and the USA itself (WAAS), all use geostationary satellites broadcasting GPS like L1 signals.

It is also reasonable to expect that at least one other Global Navigation Satellite System, such as *Galileo* [European Commission, 1999a], which is a proposal put forward by the European Commission and the European Space

Agency (ESA) for a second generation satellite system (GNSS-2), will also be realised. As yet it has not been finalised as to whether this system shall be fully independent to GPS or act as a further significant augmentation to it. Interestingly, one of the proposals contained within the EC Galileo Communication is to use the existing GLONASS system as a basis for project development. However, from the most recent documentation available at the time of writing [European Commission, 1999b], it appears that, even should GLONASS be used, it has been decided that Galileo will operate on a basis of CDMA i.e. each satellite will broadcast on the same frequencies. The Reference Frame proposed is the ITRF, and the Time Frame *Galileo Time*, which like GPS time, will be a continuous time scale (no leap seconds applied) close to UTC. The modifications necessary to combine such a system with GPS will therefore not be as far ranging as those required for GLONASS. However, the experiences gained in the combination of separate navigation systems during this research should at least serve as a good basis for any future developments, whatever form they should take.

8.3 References

European Commission, 1999a, *Galileo – Involving Europe in a New Generation of Satellite Navigation Services*, COM (1999) 54 Final, Brussels.

European Commission, 1999b, *GalileoSat – System Specification SP-10-0-1*, NS/0001335, Draft 01, Brussels.

APPENDIX A

Various File Formats

A1 Example of a Mixed RINEX Observation File

```
2                   OBSERVATION DATA    M (MIXED)           RINEX VERSION / TYPE
□
ASRINEXO V2.8.5 LH  IESSG                   25-AUG-98 10:35     PGM / RUN BY / DATE
□
                                                                COMMENT
BIT 2 OF LLI (+4) FLAGS DATA COLLECTED UNDER "AS" CONDITION     COMMENT
R213                                                            MARKER NAME
2                                                               MARKER NUMBER
JWS                 IESSG                                       OBSERVER / AGENCY
13                  ASHTECH GG24        GG00                    REC # / TYPE / VERS
1                   GEODETIC L1                                 ANT # / TYPE
  3851188.6805   -80146.8883  5066767.6553                      APPROX POSITION XYZ
        0.0000       0.0000        0.0000                      ANTENNA: DELTA
H/E/N
     1     0                                                    WAVELENGTH FACT
L1/2
     2    C1    L1                                             # / TYPES OF OBSERV
  1998     8    10     8    57    0.000000      GPS            TIME OF FIRST OBS
                                                                END OF HEADER

 98  8 10  8 57  0.0000000  0  3G15R09R10
  21537363.350    -6390646.50112
  23400925.186    -6537933.51812
  23260714.930    -6645917.11112
 98  8 10  8 57 20.0000000  0  5G15R18R09R10R17
  21524697.075    -6457207.998 3
  21119376.907    -6889429.467 2
  23405120.090    -6515469.50112
  23252528.204    -6689802.55212
  19119521.995    -6468634.704 1
 98  8 10  8 57 40.0000000  0  5G15R18R09R10R17
  21512070.923    -6523558.945 3
  21104388.307    -6969805.218 2
  23409388.634    -6492610.93912
  23244416.444    -6733286.33412
  19119943.533    -6466362.778 1
98  8 10  8 58  0.0000000  0  5G15R18R09R10R17
  21499484.364    -6589701.973 3
  21089447.455    -7049925.056 2
  23413730.358    -6469361.28512
  23236378.863    -6776371.50712
  19120442.178    -6463676.071 1
98  8 10  8 58 20.0000000  0  5G15R18R09R10R17
  21486936.928    -6655638.990 3
  21074554.089    -7129790.456 2
  23418144.549    -6445723.72512
  23228415.259    -6819060.32712
  19121017.388    -6460576.399 1
98  8 10  8 58 40.0000000  0  5G15R18R09R10R17
  21474428.381    -6721371.705 3
  21059707.879    -7209402.501 2
  23422630.522    -6421701.82012
  23220525.929    -6861352.69112
  19121668.721    -6457066.292 1
98  8 10  8 59  0.0000000  0  6G15R18R03R09R10R17
  21461958.598    -6786901.489 3
  21044909.026    -7288761.760 2
  22199334.669    -6670611.58811
  23427187.695    -6397298.02012
  23212710.054    -6903250.38612
  19122396.021    -6453147.202 1
98  8 10  8 59 20.0000000  0  6G15R18R03R09R10R17
  21449526.890    -6852230.511 3
  21030156.728    -7367869.457 2
  22182529.824    -6761073.38011
  23431815.780    -6372515.18212
  23204967.502    -6944755.25612
  19123198.757    -6448821.633 1
98  8 10  8 59 40.0000000  0  6G15R18R03R09R10R17
  21437133.021    -6917360.904 3
  21015451.161    -7446727.545 2
```

A2 Example of a GPS RINEX Ephemeris File

```
2                NAVIGATION DATA                                RINEX VERSION / TYPE
□
ASRINEXN V2.4.1 LH   IESSG                  19-AUG-98 12:28     PGM / RUN BY / DATE
□
MIRAMAR TEST                                                    COMMENT
                                                                END OF HEADER
15 98  8 10 10  0  0.0 0.586954411119E-03 0.409272615798E-11 0.000000000000E+00
    0.133000000000E+03 0.105843750000E+03 0.411409994020E-08-0.320010363042E+00
    0.562518835068E-05 0.728136533871E-02 0.820867717266E-05 0.515365458107E+04
    0.122400000000E+06-0.987201929092E-07 0.109941057548E+01 0.894069671631E-07
    0.982284438650E+00 0.232187500000E+03 0.158261234977E+01-0.807426489697E-08
    0.313227332890E-09 0.000000000000E+00 0.970000000000E+03 0.000000000000E+00
    0.200000000000E+01 0.000000000000E+00-0.931322574615E-09 0.133000000000E+03
    0.000000000000E+00 0.000000000000E+00 0.000000000000E+00 0.000000000000E+00
21 98  8 10 10  0  0.0 0.525224022567E-04 0.159161572810E-11 0.000000000000E+00
    0.430000000000E+02-0.271875000000E+02 0.456733310490E-08-0.156648470052E+01
   -0.146217644215E-05 0.144124421058E-01 0.209361314774E-05 0.515368155861E+04
    0.122400000000E+06 0.558793544769E-07 0.209347859251E+01-0.244006514549E-06
    0.966795181986E+00 0.342218750000E+03-0.278973566847E+01-0.832570394184E-08
    0.253581991279E-10 0.000000000000E+00 0.970000000000E+03 0.000000000000E+00
    0.700000000000E+01 0.000000000000E+00-0.931322574615E-09 0.430000000000E+02
    0.000000000000E+00 0.000000000000E+00 0.000000000000E+00 0.000000000000E+00
23 98  8 10 10  0  0.0 0.263797119260E-05 0.454747350886E-12 0.000000000000E+00
    0.171000000000E+03-0.293125000000E+02 0.452590280773E-08-0.184654773597E+01
   -0.146776437759E-05 0.129379339051E-01 0.185333192348E-05 0.515374645042E+04
    0.122400000000E+06 0.294297933578E-06 0.213229572812E+01-0.651925802231E-07
    0.969919847729E+00 0.348625000000E+03-0.203300431817E+01-0.823605735056E-08
   -0.118219210019E-09 0.000000000000E+00 0.970000000000E+03 0.000000000000E+00
    0.700000000000E+01 0.000000000000E+00-0.465661287308E-09 0.171000000000E+03
    0.000000000000E+00 0.000000000000E+00 0.000000000000E+00 0.000000000000E+00
29 98  8 10 10  0  0.0 0.496462453157E-03-0.126192389871E-10 0.000000000000E+00
    0.119000000000E+03-0.982812500000E+02 0.424160525131E-08 0.249610727456E+01
   -0.502355396748E-05 0.618418154772E-02 0.103358179331E-04 0.515345688629E+04
    0.122400000000E+06 0.540167093277E-07 0.311549798987E+01-0.912696123123E-07
    0.956187606880E+00 0.177531250000E+03-0.198882213239E+01-0.790354350003E-08
   -0.145363197818E-09 0.000000000000E+00 0.970000000000E+03 0.000000000000E+00
    0.700000000000E+01 0.000000000000E+00 0.232830643654E-08 0.119000000000E+03
    0.000000000000E+00 0.000000000000E+00 0.000000000000E+00 0.000000000000E+00
31 98  8 10 10  0  0.0 0.570388510823E-05 0.227373675443E-12 0.000000000000E+00
    0.102000000000E+03-0.260937500000E+02 0.460697761340E-08 0.187995841204E+01
   -0.138953328133E-05 0.810640701093E-02 0.116396695375E-04 0.515362696266E+04
    0.122400000000E+06-0.227242708206E-06-0.176007726400E-01 0.223517417908E-07
    0.958101280741E+00 0.156843750000E+03 0.756753361358E+00-0.799283293357E-08
   -0.504663878419E-09 0.000000000000E+00 0.970000000000E+03 0.000000000000E+00
    0.700000000000E+01 0.000000000000E+00 0.139698386192E-08 0.102000000000E+03
    0.000000000000E+00 0.000000000000E+00 0.000000000000E+00 0.000000000000E+00
 3 98  8 10  9 59 44.0 0.371094793081E-04 0.363797880709E-11 0.000000000000E+00
    0.490000000000E+02-0.252500000000E+02 0.475591238856E-08 0.800923154761E+00
   -0.136718153954E-05 0.176645792089E-02 0.108480453491E-04 0.515369256783E+04
    0.122384000000E+06 0.186264514923E-08-0.236647304624E-01 0.260770320892E-07
    0.949252836831E+00 0.164281250000E+03 0.242709128488E+01-0.807962226298E-08
   -0.500735143343E-09 0.000000000000E+00 0.970000000000E+03 0.000000000000E+00
    0.700000000000E+01 0.000000000000E+00 0.139698386192E-08 0.490000000000E+02
    0.000000000000E+00 0.000000000000E+00 0.000000000000E+00 0.000000000000E+00
14 98  8 10 10  0  0.0 0.203074887395E-05 0.454747350886E-12 0.000000000000E+00
    0.211000000000E+03-0.357812500000E+02 0.463876465174E-08-0.262483243533E+01
   -0.193715095520E-05 0.978215131909E-03 0.207871198654E-05 0.515355139542E+04
    0.122400000000E+06 0.931322574615E-08 0.213284925682E+01-0.316649675369E-07
    0.973010543052E+00 0.344906250000E+03 0.274217995702E+01-0.844642325600E-08
   -0.191079387795E-09 0.000000000000E+00 0.970000000000E+03 0.000000000000E+00
    0.700000000000E+01 0.000000000000E+00-0.232830643654E-08 0.211000000000E+03
    0.000000000000E+00 0.000000000000E+00 0.000000000000E+00 0.000000000000E+00
 1 98  8 10 10  0  0.0 0.555436126888E-04 0.102318153949E-11 0.000000000000E+00
    0.101000000000E+03-0.979062500000E+02 0.420053211188E-08 0.254137419946E+01
   -0.500492751598E-05 0.418056303170E-02 0.107102096081E-04 0.515369767189E+04
    0.122400000000E+06 0.130385160446E-07-0.312308706904E+01 0.204890966415E-07
    0.956627398091E+00 0.170437500000E+03-0.166203027947E+01-0.785997025645E-08
   -0.135005623526E-09 0.000000000000E+00 0.970000000000E+03 0.000000000000E+00
    0.700000000000E+01 0.000000000000E+00 0.465661287308E-09 0.101000000000E+03
    0.000000000000E+00 0.000000000000E+00 0.000000000000E+00 0.000000000000E+00
```

A3 Example of a GLONASS RINEX Ephemeris File

```
1                GLONASS NAV DATA                                RINEX VERSION / TYPE
□
ASRINEXG V1.0.2 LH  IESSG                 19-AUG-98 12:29      PGM / RUN BY / DATE
□
  1998     8    10   -0.350177288055E-06                        CORR TO SYSTEM TIME

                                                                END OF HEADER
10 98  8 10  8 45  0.0 0.124635174870E-03-0.909494701773E-12 0.429900000000E+05
   -0.890328564453E+04-0.655364990234E-02 0.186264514923E-08 0.000000000000E+00
    0.131827343750E+05-0.273383140564E+01 0.279396772385E-08 0.900000000000E+01
    0.199670195313E+05 0.179383277893E+01-0.931322574615E-09 0.000000000000E+00
17 98  8 10  8 45  0.0-0.104973092675E-03 0.454747350886E-11 0.430200000000E+05
    0.163298457031E+05 0.241644096375E+01 0.000000000000E+00 0.000000000000E+00
   -0.229946289063E+04 0.112297153473E+01 0.186264514923E-08 0.240000000000E+02
    0.194455610352E+05-0.189955902100E+01-0.186264514923E-08 0.000000000000E+00
18 98  8 10  8 45  0.0 0.118834897876E-03 0.909494701773E-12 0.430500000000E+05
   -0.134800732422E+04 0.269815349579E+01 0.000000000000E+00 0.000000000000E+00
   -0.125823339844E+05 0.138913822174E+01-0.931322574615E-09 0.100000000000E+02
    0.221184326172E+05 0.957643508911E+00-0.279396772385E-08 0.000000000000E+00
 3 98  8 10  8 45  0.0 0.198665075004E-03-0.272848410532E-11 0.431100000000E+05
    0.215547553711E+05-0.763931274414E-01-0.279396772385E-08 0.000000000000E+00
   -0.137658984375E+05-0.218620300293E+00 0.000000000000E+00 0.210000000000E+02
   -0.375233886719E+03 0.358474349976E+01 0.000000000000E+00 0.100000000000E+01
 3 98  8 10  9 15  0.0 0.198670662940E-03-0.272848410532E-11 0.432000000000E+05
    0.207658666992E+05-0.770552635193E+00-0.186264514923E-08 0.000000000000E+00
   -0.136690112305E+05 0.356215476990E+00 0.931322574615E-09 0.210000000000E+02
    0.600899365234E+04 0.346314430237E+01 0.000000000000E+00 0.100000000000E+01
 9 98  8 10  9 15  0.0 0.134703703225E-03-0.909494701773E-12 0.432300000000E+05
   -0.113914291992E+05-0.546720504761E+00 0.000000000000E+00 0.000000000000E+00
   -0.113296083984E+05-0.265840244293E+01-0.186264514923E-08 0.600000000000E+01
    0.198046899414E+05-0.183880043030E+01-0.279396772385E-08 0.000000000000E+00
10 98  8 10  9 15  0.0 0.124637037516E-03-0.909494701773E-12 0.432300000000E+05
   -0.931904736328E+04-0.465956687927E+00 0.186264514923E-08 0.000000000000E+00
    0.795137207031E+04-0.302939891815E+01 0.931322574615E-09 0.900000000000E+01
    0.223840258789E+05 0.874116897583E+00-0.186264514923E-08 0.000000000000E+00
17 98  8 10  9 15  0.0-0.104981474578E-03 0.454747350886E-11 0.432300000000E+05
    0.203632280273E+05 0.201863765717E+01 0.000000000000E+00 0.000000000000E+00
   -0.771365722656E+03 0.583773612976E+00 0.279396772385E-08 0.240000000000E+02
    0.153177792969E+05-0.265710735321E+01-0.931322574615E-09 0.000000000000E+00
18 98  8 10  9 15  0.0 0.118833035231E-03 0.909494701773E-12 0.432300000000E+05
    0.380123779297E+04 0.297817420959E+01 0.000000000000E+00 0.000000000000E+00
   -0.103881997070E+05 0.102406787872E+01 0.000000000000E+00 0.100000000000E+02
    0.229625688477E+05-0.257072448730E-01-0.279396772385E-08 0.000000000000E+00
11 98  8 10  9 15  0.0 0.151597894728E-03-0.181898940355E-11 0.445200000000E+05
   -0.205064501953E+04-0.121964454651E+00 0.279396772385E-08 0.000000000000E+00
    0.223467329102E+05-0.168075847626E+01 0.372529029846E-08 0.400000000000E+01
    0.122576889648E+05 0.302210044861E+01 0.000000000000E+00 0.000000000000E+00
 3 98  8 10  9 45  0.0 0.198676250875E-03-0.272848410532E-11 0.450000000000E+05
    0.189106953125E+05-0.124942493439E+01-0.931322574615E-09 0.000000000000E+00
   -0.124027514648E+05 0.106477642059E+01 0.186264514923E-08 0.210000000000E+02
    0.119321938477E+05 0.307572841644E+01-0.931322574615E-09 0.100000000000E+01
11 98  8 10  9 45  0.0 0.151600688696E-03-0.909494701773E-12 0.450000000000E+05
   -0.265360498047E+04-0.570971488953E+00 0.279396772385E-08 0.000000000000E+00
    0.187448740234E+05-0.228185558319E+01 0.279396772385E-08 0.400000000000E+01
    0.171567875977E+05 0.238596057892E+01-0.931322574615E-09 0.000000000000E+00
10 98  8 10  9 45  0.0 0.124637968838E-03-0.909494701773E-12 0.450000000000E+05
   -0.105861787109E+05-0.934312820435E+00 0.931322574615E-09 0.000000000000E+00
    0.246105371094E+04-0.301961135864E+01 0.000000000000E+00 0.900000000000E+01
    0.230724199219E+05-0.114442825317E+00-0.279396772385E-08 0.000000000000E+00
17 98  8 10  9 45  0.0-0.104989856482E-03 0.454747350886E-11 0.450000000000E+05
    0.234450092773E+05 0.136897754669E+01 0.000000000000E+00 0.000000000000E+00
   -0.135736816406E+03 0.147413253784E+00 0.372529029846E-08 0.240000000000E+02
    0.100035878906E+05-0.320916748047E+01 0.000000000000E+00 0.000000000000E+00
18 98  8 10  9 45  0.0 0.118832103908E-03 0.909494701773E-12 0.450000000000E+05
    0.919837500000E+04 0.296794319153E+01 0.000000000000E+00 0.000000000000E+00
   -0.895490576172E+04 0.560797691345E+00 0.931322574615E-09 0.100000000000E+02
    0.220275307617E+05-0.100633144379E+01-0.186264514923E-08 0.000000000000E+00
 3 98  8 10 10 15  0.0 0.198680907488E-03-0.272848410532E-11 0.468000000000E+05
    0.164278735352E+05-0.146325778961E+01 0.000000000000E+00 0.000000000000E+00
```

A4 Example of a Mixed .NOT Observation File

```
IESSG, University of Nottingham.  GPS ANALYSIS SOFTWARE (GAS)  GPS Data File
□
 ------------------------------------------------------------------------

     2                                                    NOTTM DATA FORMAT
 ------------------------------------------------------------------------
 R213                                                     STATION NAME
 'R213'                                                   STATION ID CHAR*4
                                                          COMMENT 1
 BIT 2 OF LLI (+4) FLAGS DATA COLLECTED UNDER "AS" CONDITION COMMENT 2
 MIXED OBS                                                SAT. TYPE
 ASHTECH GG24         GG00                                RECEIVER TYPE
   52 56 26.53305    -1 11 32.22511   116.841             APX COORDS PLH
     3851184.1705     -80151.9954    5066662.7374         APX COORDS XYZ
      6             FILTER pseudorange solution           COORDS QUALITY
   0.0000           Vertical to phase centre              ANTENNA HEIGHT
      0                                                   WAVELENGTH FACTOR
      2                                                   OBSERVATION TYPE
     1.00                                                 DATA INTERVAL
   1998    8  10         10   0    0.999000               DATE/TIME  1st OBS
    970    122400.999000                                  WEEK/SEC   1st OBS
   1998    8  10         11  59   59.997000               DATE/TIME LAST OBS
    970    129599.997000                                  WEEK/SEC  LAST OBS
     16    1  2  3  4  7  8 14 15 16 21 25 29 31 35 36 42  SATELLITES SEEN
      6   43 44 45 49 50 52                                SATELLITES SEEN
 ------------------------------------------------------------------------
  970  122400.9990000  0  -0.99999000   13    1  2  3 14 15 21 29 31 35 42 43
49
  50
   22245506.466   3   116900925.749
   23050373.858   3   121130532.598
   23848554.916   3   125325001.996
   22698319.575   3   119280474.486
   19743351.120   3   103752010.635
   22735385.719   3   119475258.464
   22087169.883   3   116068861.289
   21015550.447   3   110437463.243
   19707470.137   3   106087263.672
   22948399.448   3   123016810.794
   22471007.300   3   120246899.350
   20328845.933   3   109546620.693
   19184809.689   3   102877770.380
  970  122401.9990000  0  -0.99999000   13    1  2  3 14 15 21 29 31 35 42 43
49
  50
   22245326.096   0   116899977.853
   23050195.093   0   121129593.146
   23849206.184   0   125328424.381
   22697583.152   0   119276604.603
   19743036.787   0   103750358.784
   22735870.924   0   119477808.230
   22086723.925   0   116066517.732
   21015989.312   0   110439769.475
   19706964.069   0   106084539.503
   22948631.856   0   123018056.643
   22470614.289   0   120244796.316
   20329424.634   0   109549739.260
   19184568.853   0   102876478.791
  970  122402.9990000  0  -0.99999000   13    1  2  3 14 15 21 29 31 35 42 43
49
  50
   22245145.835   0   116899030.660
   23050016.448   0   121128654.359
   23849857.497   0   125331846.997
   22696846.808   0   119272735.039
   19742722.554   0   103748707.419
   22736356.192   0   119480358.307
   22086278.076   0   116064174.730
   21016428.261   0   110442076.163
   19706458.145   0   106081816.065
```

A5 Example of a GPS .SP3 Ephemeris File

```
#  1998  8 10  1 44  0.00000000  -99999 BREPH WGS84 FIT  BRD
##  970  92684.00000000   900.00000000   222 0.0727314814815
+   17     1  2  3  4  5  7  8  9 14 15 16 18 21 23 25 29 31
+          0  0  0  0  0  0  0  0  0  0  0  0  0  0  0  0  0
+          0  0  0  0  0  0  0  0  0  0  0  0  0  0  0  0  0
+          0  0  0  0  0  0  0  0  0  0  0  0  0  0  0  0  0
+          0  0  0  0  0  0  0  0  0  0  0  0  0  0  0  0  0
++         0  0  0  0  0  0  0  0  0  0  0  0  0  0  0  0  0
++         0  0  0  0  0  0  0  0  0  0  0  0  0  0  0  0  0
++         0  0  0  0  0  0  0  0  0  0  0  0  0  0  0  0  0
++         0  0  0  0  0  0  0  0  0  0  0  0  0  0  0  0  0
++         0  0  0  0  0  0  0  0  0  0  0  0  0  0  0  0  0
%c cc cc ccc ccc cccc cccc cccc cccc ccccc ccccc ccccc ccccc
%c cc cc ccc ccc cccc cccc cccc cccc ccccc ccccc ccccc ccccc
%f  0.0000000  0.000000000  0.00000000000  0.000000000000000
%f  0.0000000  0.000000000  0.00000000000  0.000000000000000
%i    0    0    0    0       0       0       0       0           0
%i    0    0    0    0       0       0       0       0           0
/*cccccccccccccccccccccccccccccccccccccccccccccccccccccccccccc
/*cccccccccccccccccccccccccccccccccccccccccccccccccccccccccccc
/*cccccccccccccccccccccccccccccccccccccccccccccccccccccccccccc
/*cccccccccccccccccccccccccccccccccccccccccccccccccccccccccccc
*  1998  8 10  1 44 44.00000000  0
*  1998  8 10  1 59 44.00000000  0
*  1998  8 10  2 14 44.00000000  0
*  1998  8 10  2 29 44.00000000  0
*  1998  8 10  2 44 44.00000000  0
*  1998  8 10  2 59 44.00000000  0
*  1998  8 10  3 14 44.00000000  0
*  1998  8 10  3 29 44.00000000  0
*  1998  8 10  3 44 44.00000000  0
*  1998  8 10  3 59 44.00000000  0
*  1998  8 10  4 14 44.00000000  0
*  1998  8 10  4 29 44.00000000  0
*  1998  8 10  4 44 44.00000000  0
*  1998  8 10  4 59 44.00000000  0
*  1998  8 10  5 14 44.00000000  2
P  2 -23360.716961  -9831.533386  -8369.702677   -518.626481
P  3  13216.071087 -17985.800603  14408.937861     37.051284
*  1998  8 10  5 29 44.00000000  2
P  2 -23905.094400 -10541.287821  -5748.756195   -518.628455
P  3  13201.465171 -16206.122404  16386.741862     37.054589
*  1998  8 10  5 44 44.00000000 10
P  1  14484.853609   6679.818405 -21104.977550     55.525033
P  2 -24229.936170 -11061.498721  -3030.911895   -518.629782
P  3  13263.688947 -14220.071379  18082.542737     37.057824
P  9  -8844.994960  18538.452415 -16732.516252     -5.759117
P 14  -3986.733419 -18345.478827 -18780.956525      2.021568
P 15   8477.900536 -17369.786668 -18451.194439    586.900914
P 21  24046.828958  10179.850871  -6314.498441     52.478050
P 23  19955.630465  17343.407215   4179.270957      2.607285
P 29  15120.057782  -3730.150235 -21316.550481    496.652042
P 31   6534.763772 -24135.674616   8337.991189      5.706888
*  1998  8 10  5 59 44.00000000 10
P  1  14334.037999   9074.453430 -20305.817719     55.524781
P  2 -24310.447933 -11417.278435   -262.278221   -518.630507
P  3  13426.471073 -12064.820393  19466.953619     37.060991
P  9 -10520.456458  19252.933823 -14806.048291     -5.761351
P 14  -2066.075554 -17224.942152 -20109.313625      2.021954
P 15  10288.660741 -18139.306319 -16683.174195    586.906330
P 21  24444.706385  10631.358478  -3557.820414     52.483048
P 23  19355.108359  17189.142165   6943.900558      2.610199
P 29  15182.928364  -1234.967056 -21569.661422    496.638916
P 31   6799.974054 -23003.912717  10904.324596      5.704741
*  1998  8 10  6 14 44.00000000 10
P  1  14302.857065  11361.981398 -19153.281483     55.524599
P  2 -24128.332881 -11638.613507   2510.764503   -518.630686
P  3  13707.028263  -9782.471107  20515.917896     37.064090
P  9 -11967.179377  19920.253890 -12622.138494     -5.763859
P 14     25.896954 -16145.420230 -21091.577639      2.022378
```

A6 Example of a GLONASS .SP3 Ephemeris File

```
#  1998  8 10  9  0 13.00000000    14400      U IER85 FIT  BRD
□
##  970 118813.00000000      1.00000000   222 0.3751504629630
□
+   10    35 36 41 42 43 44 45 49 50 52  0  0  0  0  0  0  0
+          0  0  0  0  0  0  0  0  0  0  0  0  0  0  0  0  0
+          0  0  0  0  0  0  0  0  0  0  0  0  0  0  0  0  0
+          0  0  0  0  0  0  0  0  0  0  0  0  0  0  0  0  0
+          0  0  0  0  0  0  0  0  0  0  0  0  0  0  0  0  0
++         0  0  0  0  0  0  0  0  0  0  0  0  0  0  0  0  0
++         0  0  0  0  0  0  0  0  0  0  0  0  0  0  0  0  0
++         0  0  0  0  0  0  0  0  0  0  0  0  0  0  0  0  0
++         0  0  0  0  0  0  0  0  0  0  0  0  0  0  0  0  0
++         0  0  0  0  0  0  0  0  0  0  0  0  0  0  0  0  0
%c cc cc ccc ccc cccc cccc cccc cccc ccccc ccccc ccccc ccccc
%c cc cc ccc ccc cccc cccc cccc cccc ccccc ccccc ccccc ccccc
%f  0.0000000  0.000000000  0.00000000000  0.000000000000000
%f  0.0000000  0.000000000  0.00000000000  0.000000000000000
%i    0    0    0    0       0       0       0       0           0
%i    0    0    0    0       0       0       0       0           0
/*cccccccccccccccccccccccccccccccccccccccccccccccccccccccccccc
/*cccccccccccccccccccccccccccccccccccccccccccccccccccccccccccc
/*cccccccccccccccccccccccccccccccccccccccccccccccccccccccccccc
/*cccccccccccccccccccccccccccccccccccccccccccccccccccccccccccc
*  1998  8 10  9  0 13.00000000  6
V 35  21316.491466 -13847.082499   2847.841902    198.668210
V 41 -10976.453024  -8831.296427  21260.416406    134.702886
V 42  -9007.553567  10630.786455  21384.139645    124.636220
V 43  -2017.702843  23690.726250   9431.645555    151.596259
V 49  18438.477180  -1412.713259  17550.097036   -104.977386
V 50   1166.243351 -11401.458028  22762.586709    118.833853
*  1998  8 10  9  0 14.00000000  6
V 35  21316.045198 -13847.035695   2851.400028    198.668213
V 41 -10976.823349  -8834.185057  21259.021623    134.702886
V 42  -9007.782280  10627.867523  21385.486064    124.636221
V 43  -2017.662523  23689.424010   9434.900291    151.596261
V 49  18440.729249  -1411.866987  17547.795742   -104.977391
V 50   1169.115560 -11400.233175  22763.056350    118.833852
*  1998  8 10  9  0 15.00000000  6
V 35  21315.598543 -13846.988571   2854.958085    198.668215
V 41 -10977.193890  -8837.073469  21257.626328    134.702887
V 42  -9008.011251  10624.948427  21386.831971    124.636222
V 43  -2017.622356  23688.121326   9438.154803    151.596263
V 49  18442.981096  -1411.021017  17545.494027   -104.977395
V 50   1171.987926 -11399.008526  22763.525443    118.833851
*  1998  8 10  9  0 16.00000000  6
V 35  21315.151500 -13846.941125   2858.516075    198.668218
V 41 -10977.564647  -8839.961661  21256.230523    134.702888
V 42  -9008.240480  10622.029166  21388.177365    124.636223
V 43  -2017.582341  23686.818197   9441.409089    151.596265
V 49  18445.232721  -1410.175348  17543.191889   -104.977400
V 50   1174.860448 -11397.784083  22763.993987    118.833850
*  1998  8 10  9  0 17.00000000  6
V 35  21314.704069 -13846.893357   2862.073996    198.668221
V 41 -10977.935619  -8842.849633  21254.834207    134.702889
V 42  -9008.469967  10619.109741  21389.522245    124.636224
V 43  -2017.542479  23685.514625   9444.663150    151.596267
V 49  18447.484124  -1409.329982  17540.889329   -104.977405
V 50   1177.733127 -11396.559845  22764.461984    118.833849
*  1998  8 10  9  0 18.00000000  6
V 35  21314.256251 -13846.845268   2865.631849    198.668224
V 41 -10978.306808  -8845.737386  21253.437381    134.702890
V 42  -9008.699711  10616.190151  21390.866614    124.636224
V 43  -2017.502770  23684.210609   9447.916987    151.596269
V 49  18449.735304  -1408.484918  17538.586347   -104.977409
V 50   1180.605963 -11395.335812  22764.929432    118.833848
*  1998  8 10  9  0 19.00000000  6
V 35  21313.808046 -13846.796858   2869.189634    198.668226
V 41 -10978.678212  -8848.624920  21252.040044    134.702891
```

A7 Example of a .NOT File

```
19   2   1    38    19
  1  2  4  7  8 14 15 16 18 25 29 31 35 36 44 45 49 50 52
    3851174.4740     -80152.8750    5066646.9150
    3851174.4740     -80152.8750    5066646.9150
 'R212' 'R213'


    586782020.0000000
  1  1  0  1  1  1  1  1  0  0  1  1  1  1  1  0  1  1  1  1  1  0  1  1  1  1
  1  0  0  1  1  1  1  1  0  1  1  1
 970 126019.991000 970 126019.998000
  20416505.523  21169643.987         0.000  20357477.863  22081079.788
  18458856.544  17211842.493  21435470.445         0.000         0.000
  19217502.809  21062043.602  16585257.761  19425549.206  19666689.942
         0.000  20949207.513  17426184.116  21445803.711  22423897.656
  23177036.041         0.000  22364869.796  24088471.724  20466248.486
  19219234.612  23442862.305         0.000         0.000  21224894.883
  23069435.937  18592650.730  21432943.536  21674083.729         0.000
  22956601.708  19433578.593  23453196.494
         0.000         0.000         0.000         0.000         0.000
         0.000         0.000         0.000         0.000         0.000
         0.000         0.000         0.000         0.000         0.000
         0.000         0.000         0.000         0.000         0.000
         0.000         0.000         0.000         0.000         0.000
         0.000         0.000         0.000         0.000         0.000
         0.000         0.000         0.000         0.000         0.000
         0.000         0.000         0.000
  107289460.752  111247229.118         0.000  106979269.018  116036857.320
   97001946.659   90448843.640  112644157.430         0.000         0.000
  100988658.834  110681785.249   89280085.477  104241622.720  105904641.726
         0.000  112889580.393   93447212.275  114640111.697  117838377.954
  121796145.265         0.000  117528184.821  126585773.900  107550862.667
  100997759.463  123193073.006         0.000         0.000  111537575.592
  121230703.093  100086080.336  115013726.454  116714407.455         0.000
  123706882.189  104211783.769  125370776.962
         0.000         0.000         0.000         0.000         0.000
         0.000         0.000         0.000         0.000         0.000
         0.000         0.000         0.000         0.000         0.000
         0.000         0.000         0.000         0.000         0.000
         0.000         0.000         0.000         0.000         0.000
         0.000         0.000         0.000         0.000         0.000
         0.000         0.000         0.000         0.000         0.000
         0.000         0.000         0.000
    378822.9446   15766578.3301  21508653.3546
   7593725.6224  -22456306.5698  11848712.4483
         0.0000         0.0000         0.0000
   -621650.0181  -15725193.8391  21685085.9733
 -12470843.5482   10091482.1277  20879604.9095
  21477566.7492   -8428234.0443  13181871.3732
  15244302.9560    2325590.8941  21392020.0798
  19379547.0333  -18025618.8312    739006.2692
         0.0000         0.0000         0.0000
         0.0000         0.0000         0.0000
  10550571.8698   15797851.1639  18791723.4752
  25963003.0565    6274572.0676   -740995.0050
  12578488.4865   -3622696.3156  21923302.1749
  13338348.8057  -19694875.4359   9202626.0684
   5519557.3673   19780421.8606  15134987.8787
         0.0000         0.0000         0.0000
  24849343.3476    -444511.7246  -5660883.8973
  20324585.7476   -8776603.7838  12687671.3683
 -12873942.5851   -8302544.9575  20411655.4569
    378822.1463   15766578.1374  21508653.5103
   7593725.9847  -22456306.8449  11848711.6469
         0.0000         0.0000         0.0000
   -621649.2176  -15725193.6715  21685086.1107
 -12470843.7873   10091481.3351  20879605.1430
  21477566.4263   -8428233.6473  13181872.1512
  15244303.1378    2325591.7152  21392019.8632
  19379547.0688  -18025618.7523    739007.2430
         0.0000         0.0000         0.0000
         0.0000         0.0000         0.0000
  10550571.1633   15797851.0573  18791723.9626
  25963003.0177    6274572.1419   -740995.9625
  12578488.0951   -3622695.4912  21923302.5321
  13338348.5955  -19694875.1093   9202627.0717
   5519557.0301   19780421.3261  15134988.6989
         0.0000         0.0000         0.0000
```

```
  24849343.1084   -444511.7365  -5660884.9478
  20324586.2673  -8776603.8883  12687670.4662
 -12873941.7401  -8302545.0405  20411655.9553
   0.48802   0.34229   0.00000   0.48111   0.10693   0.95146   1.43285
0.25683
   0.00000   0.00000   0.73600   0.37125   1.33044   0.43086   0.40464
0.00000
   0.17455   0.92852   0.09423   0.48802   0.34229   0.00000   0.48111
0.10693
   0.95146   1.43285   0.25683   0.00000   0.00000   0.73600   0.37125
1.33044
   0.43086   0.40464   0.00000   0.17455   0.92852   0.09423
  23097958.5849  23679006.6550        0.0000  23258245.4721  24898194.1410
  21124323.2283  20052650.4149  24122573.9979        0.0000        0.0000
  22031129.4379  23728552.3585  19309646.5647  22177694.6841  22329295.1091
        0.0000  23582531.0504  20126637.8492  24141386.8564  23097958.6836
  23679006.7427        0.0000  23258245.3035  24898194.1222  21124323.1009
  20052650.4404  24122573.7873        0.0000        0.0000  22031129.4499
  23728552.5766  19309646.5483  22177694.4924  22329294.9783        0.0000
  23582531.3154  20126637.9782  24141386.6161
    4.8377    6.7224    0.0000    4.9009   19.6340    2.7970    2.3017
8.8154
    0.0000    0.0000    3.3891    6.2289    2.3470    5.4229    5.7480
0.0000
   12.6584    2.8441   21.8461    4.8377    6.7224    0.0000    4.9009
19.6340
    2.7970    2.3017    8.8154    0.0000    0.0000    3.3891    6.2289
2.3470
    5.4229    5.7480    0.0000   12.6584    2.8441   21.8461
```

APPENDIX B

Search Statistics

B1 Search Statistics for GPS Only Observations at Epoch 3

```
EPOCH    3  GPS TIME : 970 126023.0
-----------------------------------

EPOCH    3 PR L1    3851174.5701    -80152.8567   5066647.0627
         Sigma :          1.6411         1.5923         2.7922

EPOCH    3 PHI L1   3851174.5725    -80152.8491   5066647.0417
         Sigma :          1.5154         1.4671         2.7100

  INTEGER SEARCH STATISTICS FOR L1 FREQUENCY
 ------------------------------------------

 SATELLITES PRESENT THIS EPOCH :

 1  2  7  8 14 15 16

 BASELINE NUMBER  1
-------------------

Number of Satellites Present on this Baseline is  7
Redundancy Level Used This Epoch     :     9
Ambiguity Combinations Passing Tests :   2889

Top three ambiguity sets for this epoch
   0.00    1.00    0.00    0.00    1.00    0.00    0.00    0.00
   2.00    0.00    0.00   -3.00    2.00    1.00    0.00    3.00
  -4.00   -3.00    0.00   -4.00   -3.00   -4.00   -4.00   -4.00
Integer Ambiguity Sigma Values
 5.8691  5.8969  6.4737  7.0556  7.1839  7.3582  8.0148********
Corresponding vTWv
            0.0637322986              1.1921193738              1.2143900491
Corresponding Estimated a Posteriori Sigma (cycles)
            0.0841508556              0.3639473976              0.3673312234

F-Test Ratio, Fixed Ratio values required :
FTest Ratio              :    5.402     Fixed Ratio :    5.000
Computed Ratios: F-Test  :   18.705     Fixed       :   19.338

    Top 3 Ambiguity Combinations
    ----------------------------------------------------------
                    Ambiguity      1st       2nd       3rd
    ----------------------------------------------------------
    increase in vTWv, dvTWv       0.0615    1.1899    1.2122
    new vTWv                      0.0637    1.1921    1.2144
    F ratio vTWv / vTWV(1st)                18.71     19.05
    ----------------------------------------------------------
    SV  1                          0.0       2.0      -4.0
    SV  2                          1.0       0.0      -3.0
    SV  4                          0.0       0.0       0.0
    SV  7                          0.0      -3.0      -4.0
    SV  8                          1.0       2.0      -3.0
    SV 14                          0.0       1.0      -4.0
    SV 15                          0.0       0.0      -4.0
    SV 16                          0.0       3.0      -4.0
    ----------------------------------------------------------
    Redundancy (obs - unknowns)     =              9
    F-Test Ratio Tolerance          =           5.40
    Number of Possible Combinations =       19487171.
    Number Passing Cut-Off Test     =           2889
    Best Combination F-Test Ratio   =          18.71     PASS
    ----------------------------------------------------------


 AMBIGUITIES FIXED AND APPLIED DURING RUN
-----------------------------------------

L1 FREQUENCY, BASELINE No.:   1
SATELLITE ID No.       FIXED INTEGER VALUE       INTEGER SD

        14                     0.0                  0.0010
         2                     1.0                  0.0010
         1                     0.0                  0.0010
        15                     0.0                  0.0010
         8                     1.0                  0.0010
         7                     0.0                  0.0010
        16                     0.0                  0.0010
```

```
EPOCH    3  FIXED     3851174.6530     -80152.8794    5066647.1537
          Sigma :           0.0083          0.0081          0.0149
```

B2 Search Statistics for Mixed Observations at Epoch 17

```
EPOCH   17  GPS TIME : 970 126037.0
------------------------------------

EPOCH   17 PR L1     3851174.5343    -80152.8696   5066647.0963
         Sigma :            1.0637         1.0235         1.3493

EPOCH   17 PHI L1    3851174.5442    -80152.8625   5066647.0851
         Sigma :            0.6143         0.5747         0.9705

 INTEGER SEARCH STATISTICS FOR L1 FREQUENCY
 ------------------------------------------

 SATELLITES PRESENT THIS EPOCH :

 1  2  7  8 14 15 16 35 36 44
49 50 52

 BASELINE NUMBER  1
 ------------------

 Number of Satellites Present on this Baseline is 13
 Redundancy Level Used This Epoch     :   136
 Ambiguity Combinations Passing Tests :   1977

 Top three ambiguity sets for this epoch
    0.00    1.00    0.00    0.00    1.00    0.00    0.00    0.00    0.00
0.00    5.00   -4.00    0.00   -3.00    5.00
   -1.00    0.00    0.00   -1.00    0.00   -1.00   -1.00   -1.00    0.00
0.00    5.00   -4.00    0.00   -3.00    5.00
    1.00    2.00    0.00    1.00    2.00    1.00    1.00    1.00    0.00
0.00    5.00   -4.00    0.00   -3.00    5.00
 Integer Ambiguity Sigma Values
  2.4188  2.4359  2.6709  2.8013  2.8574  2.9433  3.0629  8.1520  8.1925
8.5084  8.5135  8.6943**************************
 Corresponding vTWv
        0.3381858593            0.5112743171        1.1226855797
 Corresponding Estimated a Posteriori Sigma (cycles)
        0.0498664289            0.0613137014        0.0908572563

F-Test Ratio, Fixed Ratio values required :
FTest Ratio              :    1.494     Fixed Ratio :    5.000
Computed Ratios: F-Test :    1.512     Fixed       :    1.546

    Top 3 Ambiguity Combinations
    ----------------------------------------------------------
                     Ambiguity     1st      2nd      3rd
    ----------------------------------------------------------
    increase in vTWv, dvTWv      0.3168   0.4899   1.1013
    new vTWv                     0.3382   0.5113   1.1227
    F ratio vTWv / vTWV(1st)                1.51     3.32
    ----------------------------------------------------------
    SV  1                          0.0     -1.0      1.0
    SV  2                          1.0      0.0      2.0
    SV  4                          0.0      0.0      0.0
    SV  7                          0.0     -1.0      1.0
    SV  8                          1.0      0.0      2.0
    SV 14                          0.0     -1.0      1.0
    SV 15                          0.0     -1.0      1.0
    SV 16                          0.0     -1.0      1.0
    SV 35                          5.0      5.0      5.0
    SV 36                         -4.0     -4.0     -4.0
    SV 44                          0.0      0.0      0.0
    SV 49                          0.0      0.0      0.0
    SV 50                         -3.0     -3.0     -3.0
    SV 52                          5.0      5.0      5.0
    ----------------------------------------------------------
    Redundancy (obs - unknowns)      =          136
    F-Test Ratio Tolerance           =         1.49
    Number of Possible Combinations  =  3138428376721.
    Number Passing Cut-Off Test      =         1977
    Best Combination F-Test Ratio    =         1.51     PASS
    ----------------------------------------------------------


 AMBIGUITIES FIXED AND APPLIED DURING RUN
 ----------------------------------------
```

```
L1 FREQUENCY, BASELINE No.:   1
SATELLITE ID No.        FIXED INTEGER VALUE        INTEGER SD

        14                      0.0                   0.0010
         2                      1.0                   0.0010
         1                      0.0                   0.0010
        15                      0.0                   0.0010
         7                      0.0                   0.0010
         8                      1.0                   0.0010
        16                      0.0                   0.0010
        50                     -3.0                   0.0010
        36                     -4.0                   0.0010
        44                      0.0                   0.0010
        35                      5.0                   0.0010
        52                      5.0                   0.0010

EPOCH  17  FIXED    3851174.6520    -80152.8778   5066647.1523
          Sigma :          0.0079         0.0073         0.0133
```

APPENDIX C

Satellite Availabilities

C1 Satellite Availability during Software Validation

GPS

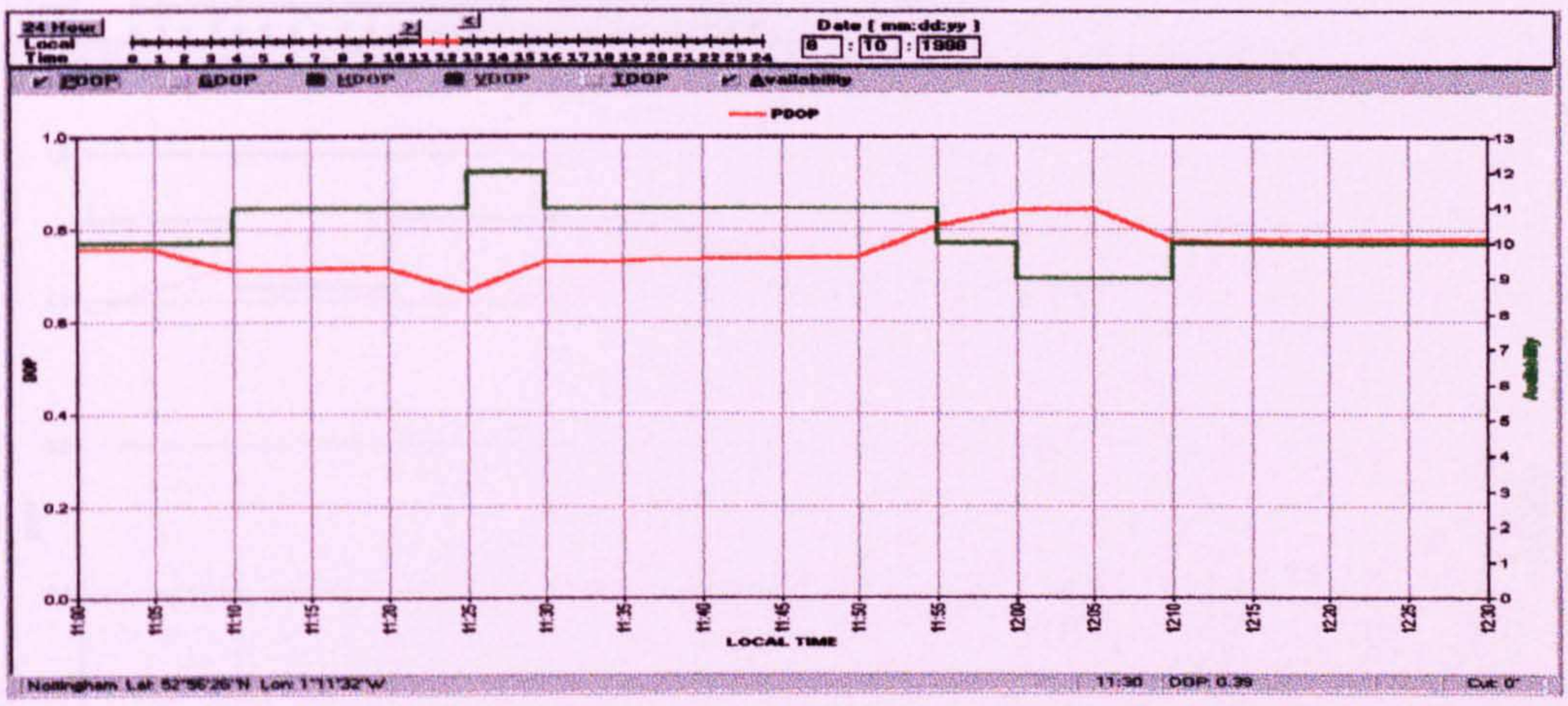

GLONASS

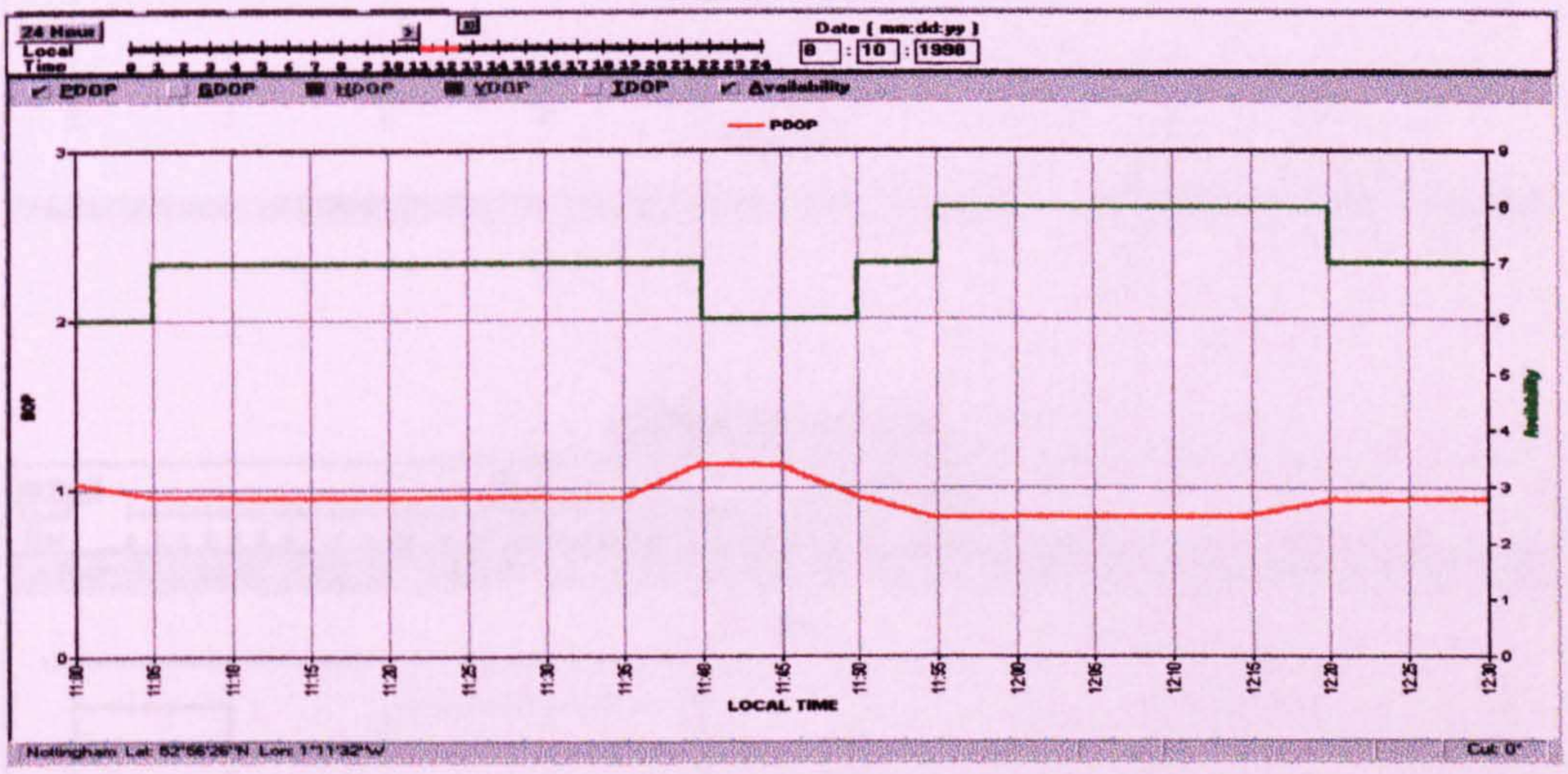

GPS/GLONASS

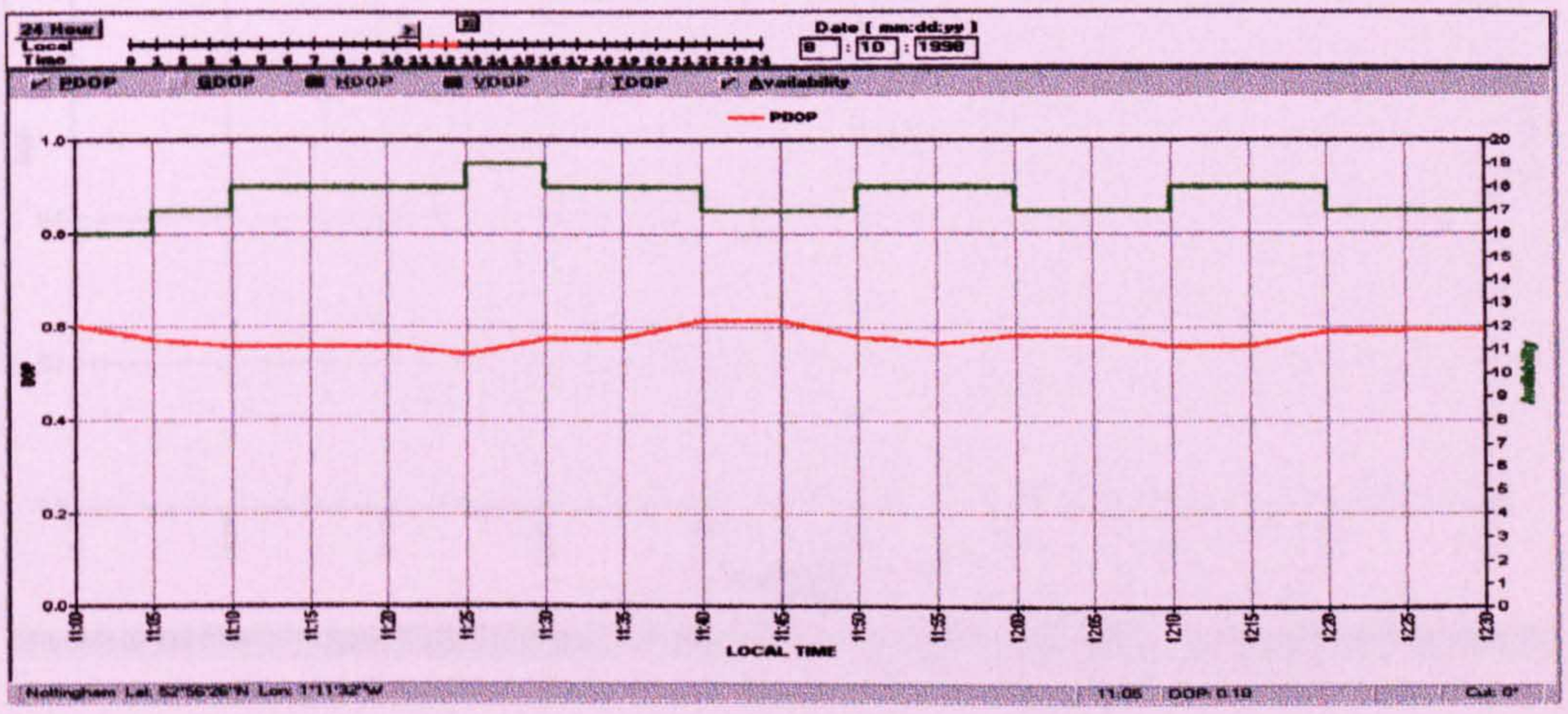

C2 Satellite Availability during the Mini-Bus Trial

GPS

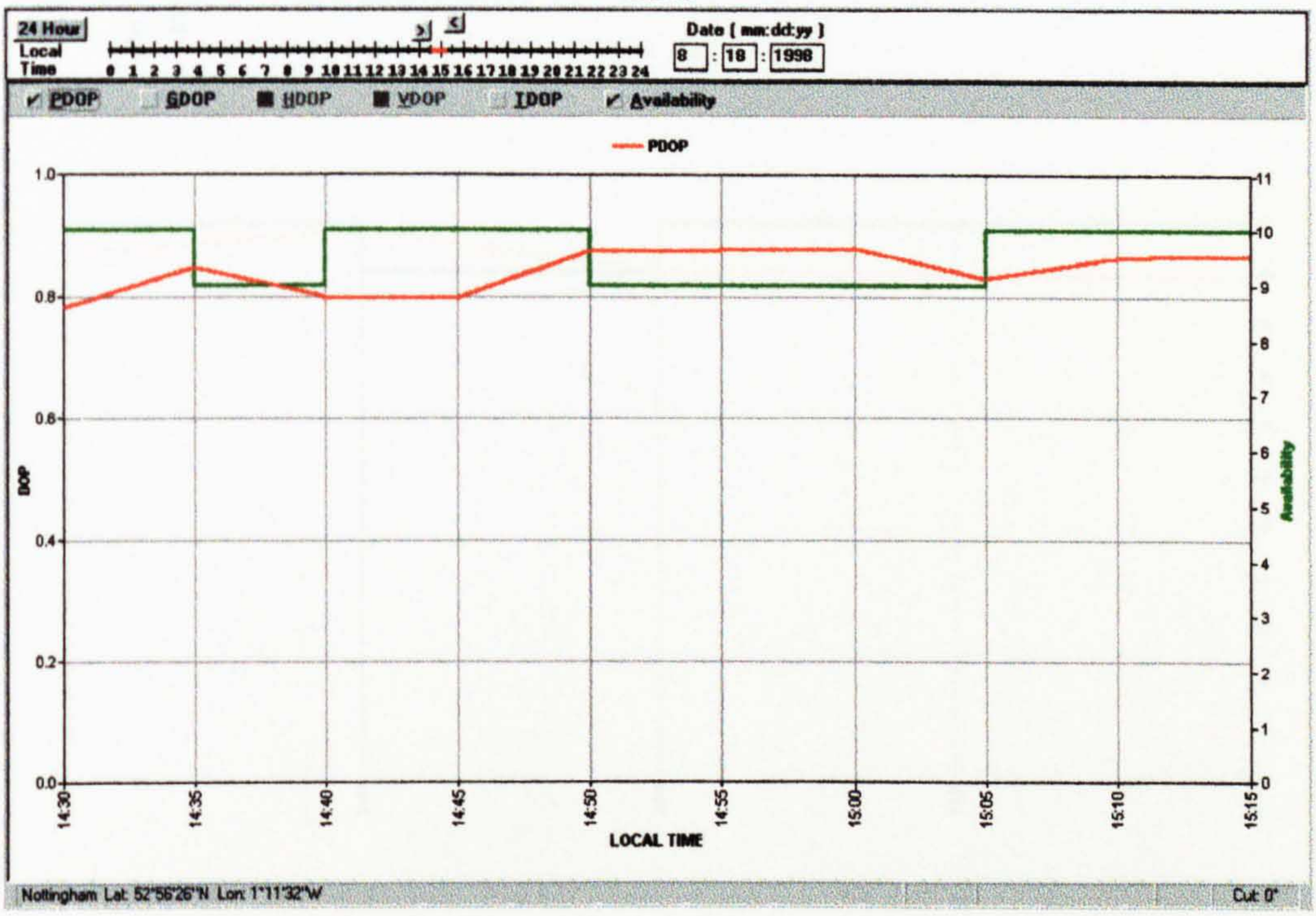

GPS/GLONASS

C3 Satellite Availability during Deck Deflection Monitoring

GPS

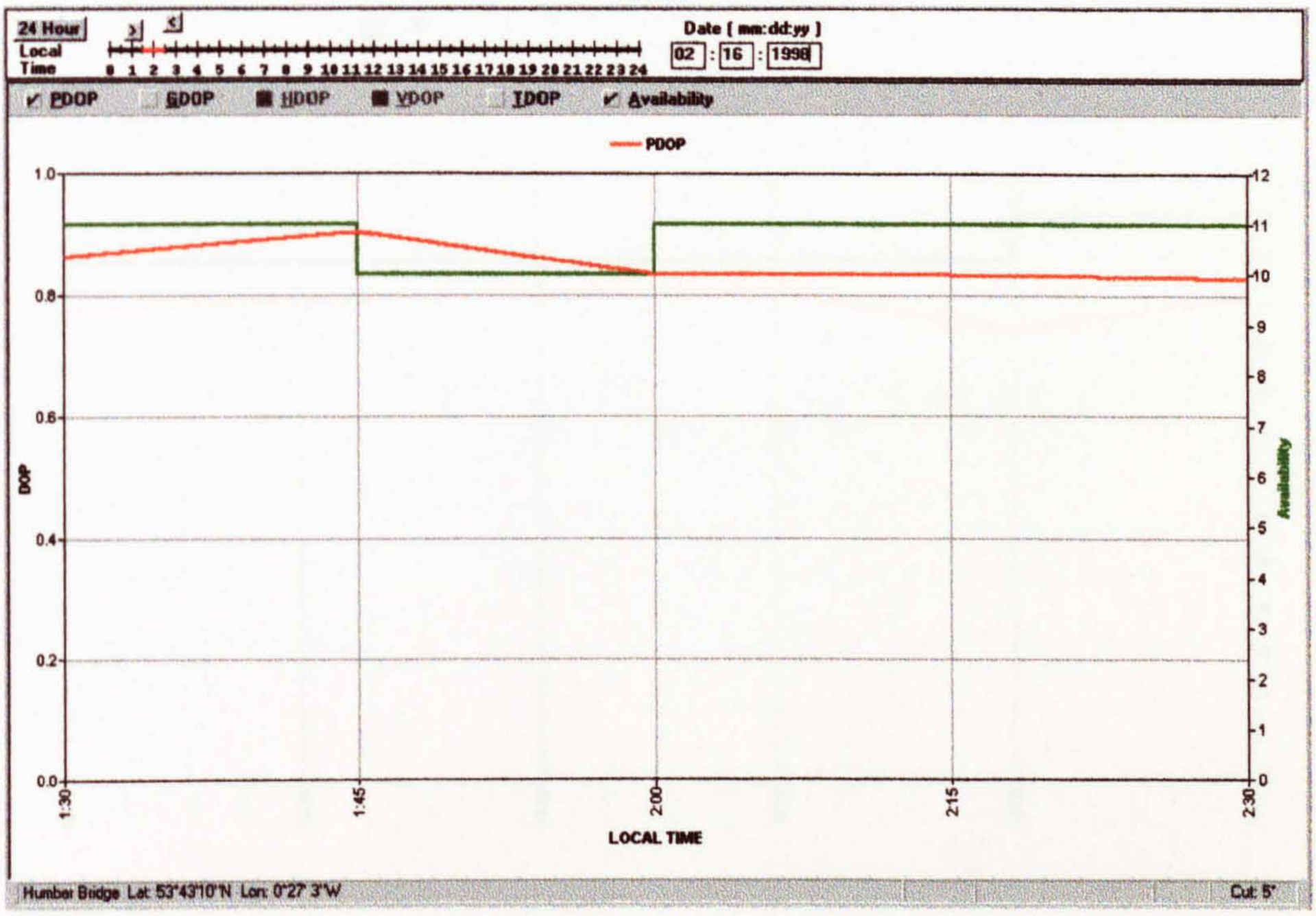

GPS/GLONASS

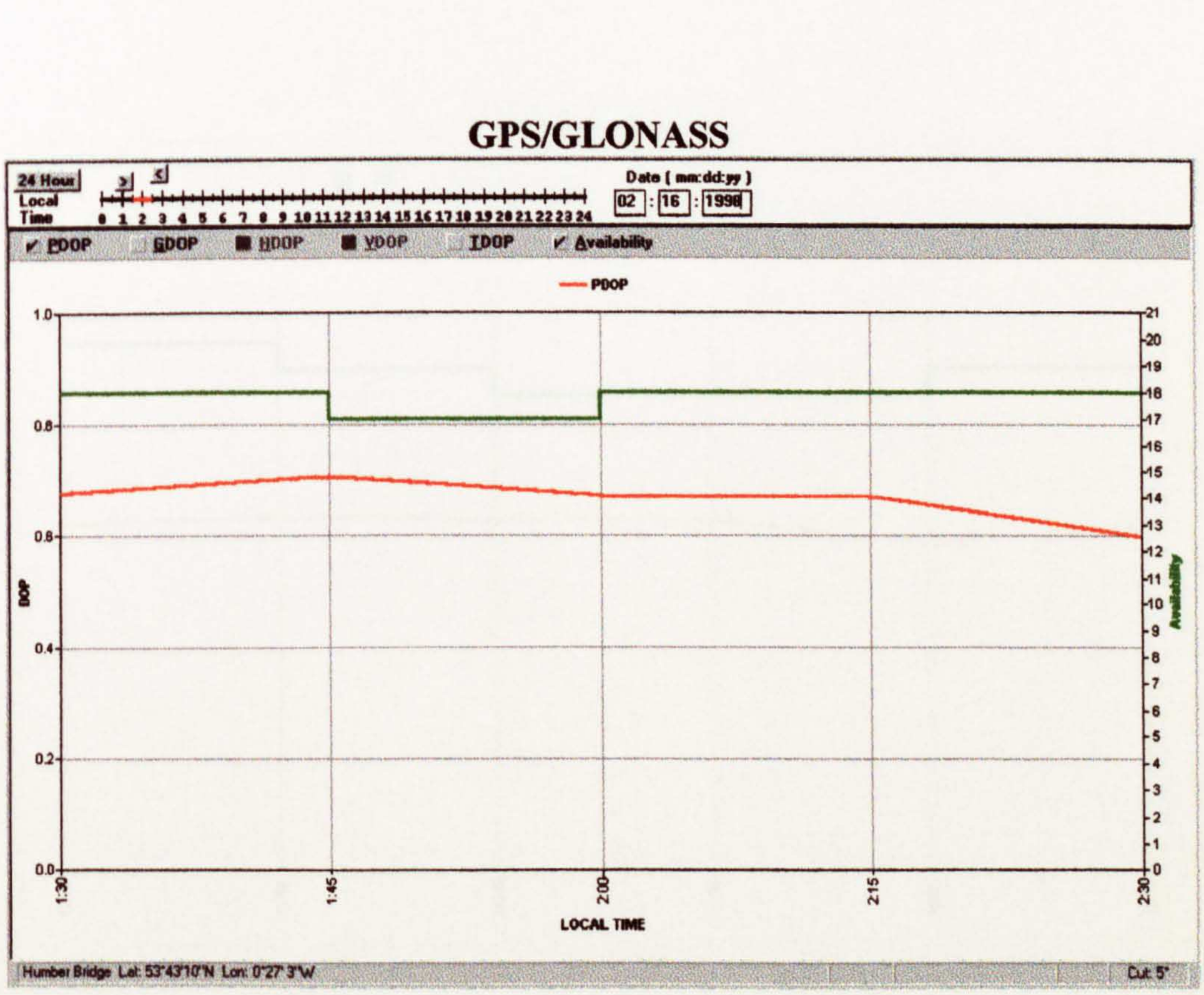

C4 Satellite Availability during Tower Deflection Monitoring

GPS

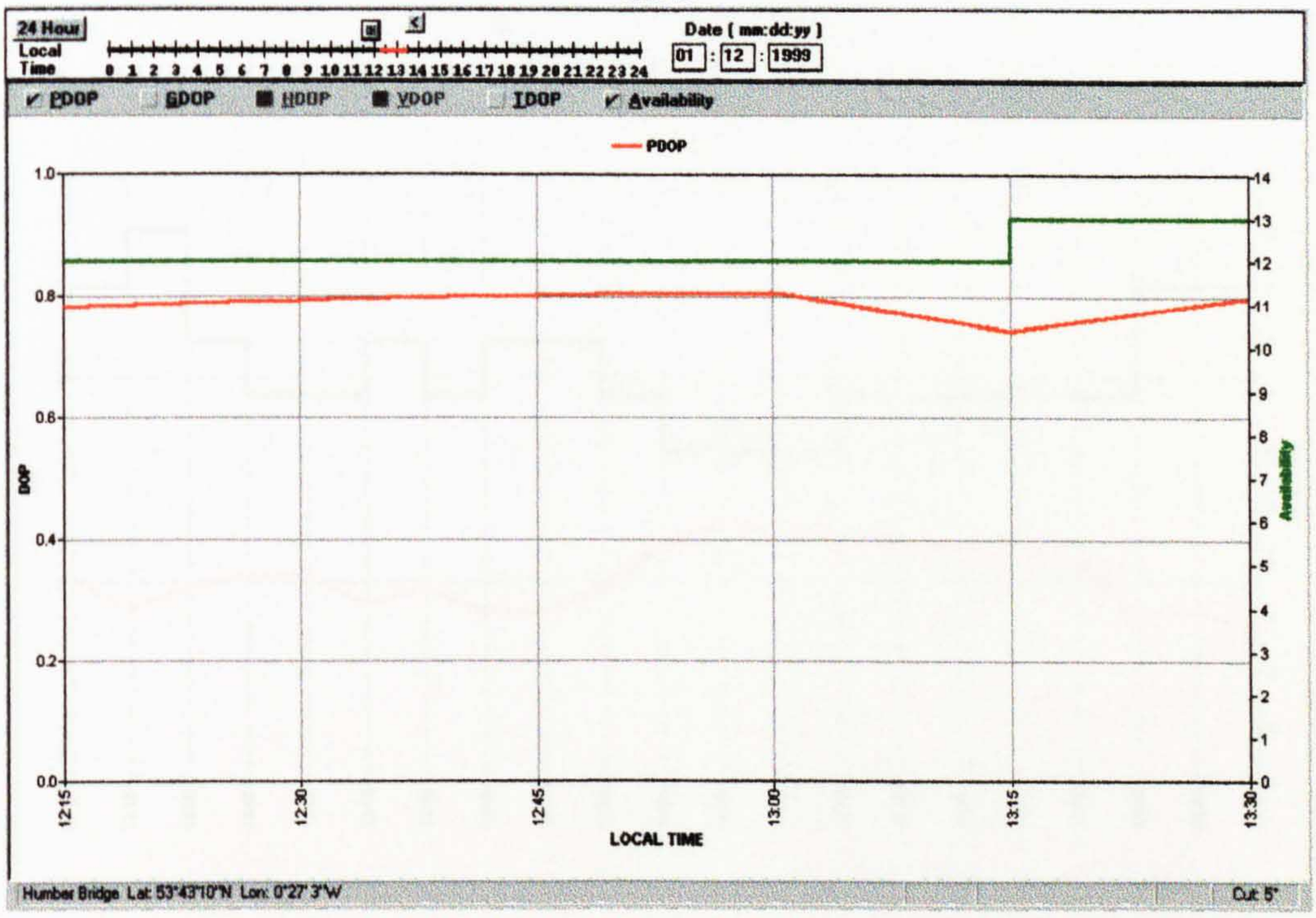

GPS/GLONASS

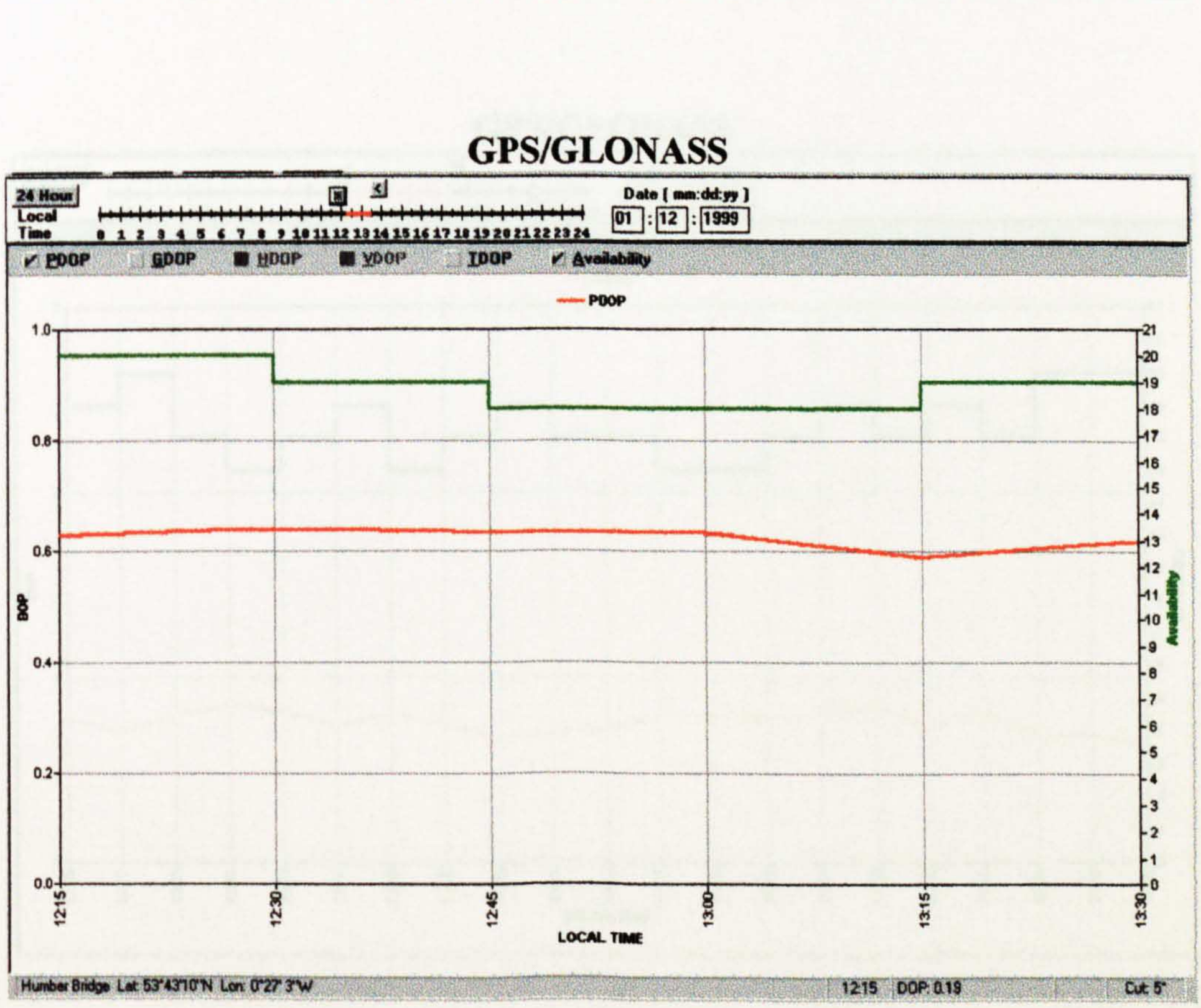

C5 Satellite Availability During Setting-Out Trial

GPS

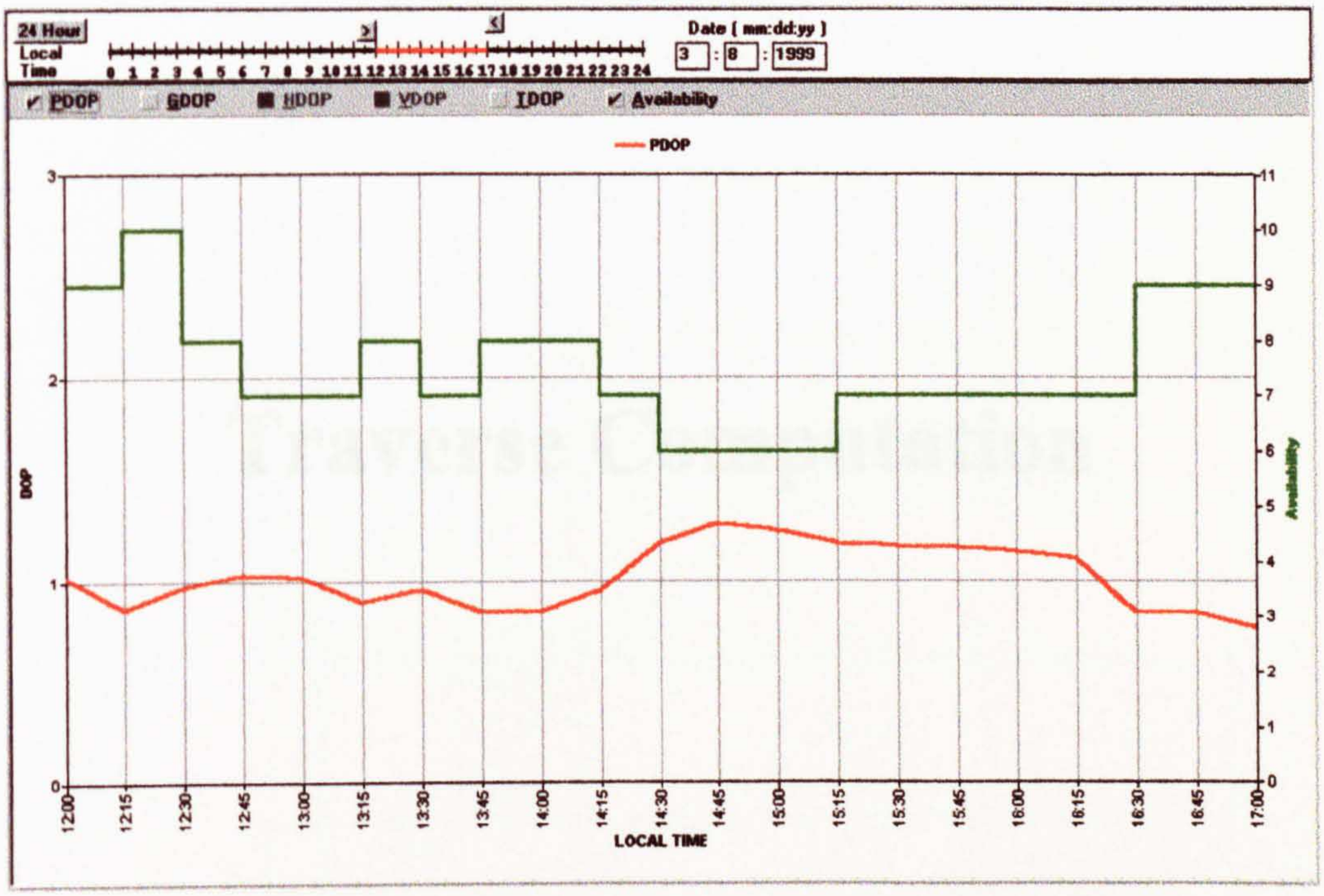

GPS/GLONASS

APPENDIX D

Traverse Computation

UNIVERSITY OF NOTTINGHAM — **LEVEL SHEET** — DEPT OF CIVIL ENGINEERING

OBSERVER ...John Swanwick.....

REDUCED .....

CHECKED .....

DATE ..17/2/77.....

TITLE ...LOOP 1 (ARDWICK BUILDING).....

POINT NO.	BACKSIGHT	FORESIGHT	INT. SIGHT	RISE	FALL	REDUCED LEVEL	ADJUSTMENT	COMPD LEVEL	REMARKS
B.M.	1·308					36·296			
	3·150	1·263		0·055		36·351	+0·000	36·351	
1	2·125	0·327		2·823		39·174	0·001	39·175	
2	2·090	2·132			0·007	39·167	0·001	39·168	
3	0·759	2·092			0·002	39·165	0·002	39·167	
	0·427	3·106			2·347	36·818	0·002	36·820	
4	1·629	1·108			0·681	36·137	0·003	36·140	
	1·468	1·499		0·030		36·167	0·003	36·170	
B.M.		1·343		0·125		36·292	0·004	36·296	
	12·856	12·860		3·033	3·037				

UNIVERSITY OF NOTTINGHAM

LEVEL SHEET

DEPT OF CIVIL ENGINEERING

OBSERVER ...John Scaw.....

DATE ...17/2/99.....

REDUCED .....

CHECKED .....

TITLE ...Loop 2.....

POINT NO.	BACKSIGHT	FORESIGHT	INT. SIGHT	RISE	FALL	REDUCED LEVEL	ADJUSTMENT	COMPD LEVEL	REMARKS
B.M.	1·262					36·296			
	3·151	0·768		0·604		36·800	-0·000	36·800	
INIT	1·264	1·264		1·887		38·687	-0·001	38·686	
	0·778	3·161			1·887	36·800	-0·001	36·799	
B.M.		1·280			0·602	36·298	-0·002	36·296	
	6·456	6·463		2·391	2·389				

UNIVERSITY OF NOTTINGHAM — LEVEL SHEET — DEPT OF CIVIL ENGINEERING

OBSERVER ...John Sumn.....

REDUCED .....

CHECKED .....

DATE ..17/4/92.....

TITLE ..Loop 3.....

POINT NO.	BACKSIGHT	FORESIGHT	INT. SIGHT	RISE	FALL	REDUCED LEVEL	ADJUSTMENT	COMPD LEVEL	REMARKS
INIT	2.952					38.686		38.686	
	3.586	0.867		2.085		40.771	-0.001	40.770	
	3.762	0.178		3.408		44.179	0.001	44.178	
	3.925	0.621		3.141		47.320	0.002	47.318	
	3.121	0.248		3.677		50.997	0.002	50.995	
		0.668		2.463		53.450	0.003	53.447	
5	1.462		0.575	2.546		53.543	0.003	53.540	INTERMEDIATE
6	1.664	2.604			1.142	52.308	0.004	52.304	
7	2.470	1.687			0.033	52.275	0.004	52.271	
	1.088	1.546		0.925		53.200	0.005	53.195	
	2.428	2.282			1.194	52.006	0.005	52.001	
	0.764	2.590			0.162	51.844	0.006	51.838	
8	0.106	2.678			1.814	50.030	0.007	50.023	
	0.139	3.834			3.728	46.302	0.007	46.295	
	1.416	3.479			3.340	42.962	0.008	42.954	
9	2.680	0.739		0.677		43.639	0.008	43.631	
	0.558	3.209			0.529	43.110	0.009	43.101	
	1.142	1.772			1.214	41.896	0.010	41.886	
	0.622	2.721			1.579	40.317	0.010	40.307	
INIT		2.242			1.620	38.697	0.011	38.686	
	55.875	55.864							

D4 Traverse Sheets

UNIVERSITY OF NOTTINGHAM — DEPT OF CIVIL ENGINEERING

TRAVERSE SHEET

STATION AT ..... JNIT.....
THEODOLITE HEIGHT .....
EDM INST. HEIGHT .....
EDM INST. TYPE .....
GROUP No. .....

R.O. EEE TOWER

OBSERVER ..ADN.....
BOOKER ....JWS.....
REDUCED .....
CHECKED .....
DATE ...4/3/99....

STATION TO	HORIZONTAL ANGLES FIRST ROUND FL	FR	MEAN	~~Angle~~ REDUCED
EEE TOWER	293 06 39	10 06 39	293 06 39	
TRAV PT 2	98 27 45	278 27 35	98 27 40	165 21 01

	SECOND ROUND FL	FR	MEAN	REDUCED
RTK1	75 10 38	255 11 57	75 11 17	
RTK4	38 21 09	218 30 55	38 21 02	

OBSERVING DIAGRAM

STATION TO	TARGET HEIGHT	VERTICAL ANGLES FL	FR	REDUCED	MEAN VERTICAL ANGLES
EEE TOWER		88 32 52	279 27 51		
TRAV 2		271 47 54	88 12 38	271 47 38	1 47 38
RTK4		265 21 26	94 28 54	265 31 16	4 28 44
RTK1		271 46 59	88 13 21	271 46 49	1 46 49

STATION TO	MEAN HORIZONTAL ANGLES

STATION TO	OBSERVED SLOPE DISTANCE 1	2	3	4	MEAN SLOPE DISTANCE	~~REFLECTOR TYPE~~ HORIZ DIST	REFLECTOR HEIGHT
EEE TOWER	282.718	282.718	282.719	282.719	282.719	278.876	
TRAV 2	64.613	64.612	64.613	64.618	64.618	64.581	
RTK4	32.742	32.742	32.743	32.743	32.743	32.645	
RTK1	16.118	16.118	16.118	16.118	16.118	16.110	

SHEET REFERENCE No. TRAV.1..... EDM REDUCTION SHEET REFERENCE No. .....

D5

UNIVERSITY OF NOTTINGHAM — DEPT OF CIVIL ENGINEERING

TRAVERSE SHEET

STATION AT ..TRAV PT 2..... R.O. ..... OBSERVER ..ADN.....
THEODOLITE HEIGHT ..... BOOKER ...JWS.....
EDM INST. HEIGHT ..... REDUCED .....
EDM INST. TYPE ..... CHECKED .....
GROUP No. ..... DATE ..4/3/92.....

STATION TO	HORIZONTAL ANGLES			
	FIRST ROUND			
	FL	FR	MEAN	~~ANGLES~~ REDUCED
TRN PT3	266 04 40	86 04 59	266 04 50	
INT	13 24 18	193 24 31	13 24 24	107 19 34
	SECOND ROUND			
	FL	FR	MEAN	REDUCED
RTK PT2	32 08 48	212 08 20	32 08 32	
RTK PT3	72 20 06	252 21 24	72 20 44	

OBSERVING DIAGRAM

STATION TO	TARGET HEIGHT	VERTICAL ANGLES			MEAN VERTICAL ANGLES
		FL	FR	REDUCED	
TRN PT3		82 51 53	277 08 44	82 51 35	7 8 25
INT		91 48 04	268 12 24		
RTK PT2		97 26 17	262 34 03	97 26 08	7 26 08
RTK PT3		95 36 21	264 24 04	95 36 09	7 36 09

STATION TO	MEAN HORIZONTAL ANGLES

STATION TO	OBSERVED SLOPE DISTANCE				MEAN SLOPE DISTANCE	~~HORIZ REFLECTOR~~ DIST ~~TYPE~~	REFLECTOR HEIGHT
	1	2	3	4			
RTK 2	12.061	12.059	12.058	12.057	12.058	11.957	
RTK 3	16.002	16.001	16.000	16.000	16.001	15.925	
INT	64.625	64.625	64.624	64.624	64.624	64.581	
TRN 3	70.753	70.753	70.759	70.762	70.751	70.202	

SHEET REFERENCE No. ..TRN 2..... EDM REDUCTION SHEET REFERENCE No. .....

D6

UNIVERSITY OF NOTTINGHAM — DEPT OF CIVIL ENGINEERING

TRAVERSE SHEET

STATION AT TRAV 3 — R.O. ..... — OBSERVER ADN
THEODOLITE HEIGHT ..... — BOOKER JWS
EDM INST. HEIGHT ..... — REDUCED .....
EDM INST. TYPE ..... — CHECKED .....
GROUP No. ..... — DATE 4/3/99

STATION TO	HORIZONTAL ANGLES FIRST ROUND FL	FR	MEAN	~~REDUCED~~
TRAV 2	231 47 57	51 48 18	51 48 08	
RTK 5	65 46 46	245 46 56	155 46 51	166 01 17

	SECOND ROUND FL	FR	MEAN	REDUCED

OBSERVING DIAGRAM

STATION TO	TARGET HEIGHT	VERTICAL ANGLES FL	FR	REDUCED	MEAN VERTICAL ANGLES
TRAV 2		97 08 41	262 51 42	7 08 30	
RTK 5		86 56 35	273 03 49	3 02 55	

STATION TO	MEAN HORIZONTAL ANGLES

STATION TO	OBSERVED SLOPE DISTANCE 1	2	3	4	MEAN SLOPE DISTANCE	~~REFLECTOR~~ HORIZ DIST ~~TYPE~~	REFLECTOR HEIGHT
TRAV 2	70.744	70.746	70.745	70.748	70.751	70.202	
RTK 5	77.161	77.162	77.161	77.161	77.161	77.050	

SHEET REFERENCE No. TRAV 3 — EDM REDUCTION SHEET REFERENCE No. .....

D7

UNIVERSITY OF NOTTINGHAM — DEPT OF CIVIL ENGINEERING

TRAVERSE SHEET

STATION AT ....RTK5..... R.O. ..... OBSERVER ...ADN.....
THEODOLITE HEIGHT ..... BOOKER ....JWS.....
EDM INST. HEIGHT ..... REDUCED .....
EDM INST. TYPE ..... CHECKED .....
GROUP No. ..... DATE ...4/3/91.....

STATION TO	HORIZONTAL ANGLES			
	FIRST ROUND			
	FL	FR	MEAN	~~ANGLE~~ REDUCED
TRAV 5	52 58 27	232 68 42	52 58 35	
TRAV 3	64 41 35	244 41 55	64 41 45	11 43 10
	SECOND ROUND			
	FL	FR	MEAN	REDUCED
RTK6	314 21 30	134 21 40	314 21 35	
RTK7	316 28 [illegible]	136 30 08	316 30 [illegible]	

OBSERVING DIAGRAM

STATION TO	TARGET HEIGHT	VERTICAL ANGLES			MEAN VERTICAL ANGLES
		FL	FR	REDUCED	
TRAV 5		93 14 29	266 46 07	93 13 58	03 13 58
TRAV 3		93 04 05	266 56 28		
RTK 6		91 05 12	268 55 07	91 05 03	01 05 03
RTK 7		90 54 39	269 05 53	90 54 22	00 54 22

STATION TO	MEAN HORIZONTAL ANGLES

STATION TO	OBSERVED SLOPE DISTANCE				MEAN SLOPE DISTANCE	~~REFLECTOR~~ HORIZ DIST ~~TYPE~~	REFLECTOR HEIGHT
	1	2	3	4			
TRAV 5	63.732	63.730	63.732	63.735	63.733	63.632	
TRAV 3	77.157	77.157	77.157	77.159	77.159		
RTK 6	42.650	42.649	42.649	42.648	42.649	42.641	
RTK 7	54.125	54.124	54.125	54.126	54 125	54.118	

SHEET REFERENCE No. ...TRAV 4..... EDM REDUCTION SHEET REFERENCE No. .....

D8

UNIVERSITY OF NOTTINGHAM — DEPT OF CIVIL ENGINEERING

TRAVERSE SHEET

STATION AT TRAV 5 — R.O. ..... — OBSERVER JWS
THEODOLITE HEIGHT ..... — BOOKER KGT
EDM INST. HEIGHT ..... — REDUCED .....
EDM INST. TYPE ..... — CHECKED .....
GROUP No. ..... — DATE 4/3/99

STATION TO	HORIZONTAL ANGLES			
	FIRST ROUND			Angle
	FL	FR	MEAN	~~REDUCED~~
TRAV 6	343 00 56	163 01 02	343 00 54	
RTK 5	265 31 52	85 32 03	265 31 57	282 31 03
	SECOND ROUND			
	FL	FR	MEAN	REDUCED

OBSERVING DIAGRAM

STATION TO	TARGET HEIGHT	VERTICAL ANGLES			MEAN VERTICAL ANGLES
		FL	FR	REDUCED	
TRAV 6		90 32 22	269 28 23	90 32 00	00 32 00
RTK 5		86 46 33	273 14 04	86 46 15	

STATION TO	MEAN HORIZONTAL ANGLES

STATION TO	OBSERVED SLOPE DISTANCE				MEAN SLOPE DISTANCE	~~REFLECTOR~~ HORIZ DIST ~~TYPE~~	REFLECTOR HEIGHT
	1	2	3	4			
TRAV 6	175.150	175.150	175.158	175.151	175.1534	175.146	
RTK 5	63.733	63.737	63.734	63.734	63.734		

SHEET REFERENCE No. TRAV 5 — EDM REDUCTION SHEET REFERENCE No. .....

D9

UNIVERSITY OF NOTTINGHAM — DEPT OF CIVIL ENGINEERING

TRAVERSE SHEET

STATION AT ...TRAV 6... R.O. ..... OBSERVER ...JWS...
THEODOLITE HEIGHT ..... BOOKER ...KG...
EDM INST. HEIGHT ..... REDUCED .....
EDM INST. TYPE ..... CHECKED .....
GROUP No. ..... DATE ...4/3/77...

STATION TO	HORIZONTAL ANGLES			
	FIRST ROUND			ANGLE
	FL	FR	MEAN	~~REDUCED~~
RTK 8	338 31 02	158 31 16	338 31 10	
TRAV 5	235 28 16	55 28 34	235 28 25	256 57 15
	SECOND ROUND			
	FL	FR	MEAN	REDUCED

OBSERVING DIAGRAM

STATION TO	TARGET HEIGHT	VERTICAL ANGLES			MEAN VERTICAL ANGLES
		FL	FR	REDUCED	
RTK 8		89 10 29	270 50 05	89 10 01	00 49 59
TRAV 5		89 28 38	270 32 02	89 28 10	

STATION TO	MEAN HORIZONTAL ANGLES

STATION TO	OBSERVED SLOPE DISTANCE				MEAN SLOPE DISTANCE	~~REFLECTOR~~ HORIZ DIST ~~TYPE~~	REFLECTOR HEIGHT
	1	2	3	4			
RTK 8	114.007	114.008	114.008	114.008	114.008	113.796	
TRAV 5	175.157	175.157	175.157	175.157			

SHEET REFERENCE No. ...TRAV 6... EDM REDUCTION SHEET REFERENCE No. .....

D10

UNIVERSITY OF NOTTINGHAM — DEPT OF CIVIL ENGINEERING

TRAVERSE SHEET

STATION AT ...RTK 8... R.O. ..... OBSERVER ...ADN...
THEODOLITE HEIGHT ..... BOOKER ...SWS...
EDM INST. HEIGHT ..... REDUCED .....
EDM INST. TYPE ..... CHECKED .....
GROUP No. ..... DATE ...4/3/99...

STATION TO	HORIZONTAL ANGLES			
	FIRST ROUND			Mode ~~REDUCED~~
	FL	FR	MEAN	
RTK9	230 28 54	50 27 16	230 29 05	
TRAV 6	244 31 43	64 31 57	244 31 50	14 02 45
	SECOND ROUND			
	FL	FR	MEAN	REDUCED

OBSERVING DIAGRAM

STATION TO	TARGET HEIGHT	VERTICAL ANGLES			MEAN VERTICAL ANGLES
		FL	FR	REDUCED	
RTK9		92 40 22	267 20 13	22 39 57	2 39 57
TRAV 6		90 50 30	269 09 14	90 50 08	

STATION TO	MEAN HORIZONTAL ANGLES

STATION TO	OBSERVED SLOPE DISTANCE				MEAN SLOPE DISTANCE	~~REFLECTOR~~ Horiz AST TYPE	REFLECTOR HEIGHT
	1	2	3	4			
RTK9	136.432	136.432	136.432	136.432	136.432	136.282	
TRAV6	114.008	114.008	114.008	114.008	114.008		

SHEET REFERENCE No. ...TRAV 7... EDM REDUCTION SHEET REFERENCE No. .....

D11

UNIVERSITY OF NOTTINGHAM — DEPT OF CIVIL ENGINEERING

TRAVERSE SHEET

STATION AT RTK 9 — R.O. ..... — OBSERVER AOW
THEODOLITE HEIGHT ..... — BOOKER JWS
EDM INST. HEIGHT ..... — REDUCED .....
EDM INST. TYPE ..... — CHECKED .....
GROUP No. ..... — DATE 4/3/79

STATION TO	HORIZONTAL ANGLES			
	FIRST ROUND			ANGLE
	FL	FR	MEAN	~~REDUCED~~
TRAV 7	101 03 06	281 03 07	101 03 06	
RTK8	172 12 11	352 12 24	172 12 20	71 09 14
	SECOND ROUND			
	FL	FR	MEAN	REDUCED

OBSERVING DIAGRAM

STATION TO	TARGET HEIGHT	VERTICAL ANGLES			MEAN VERTICAL ANGLES
		FL	FR	REDUCED	
TRAV 7		84 15 18	275 45 46	84 14 46	5 45 14
RTK8		87 20 24	272 40 12	87 20 42	

STATION TO	MEAN HORIZONTAL ANGLES

STATION TO	OBSERVED SLOPE DISTANCE				MEAN SLOPE DISTANCE	~~REFLECTOR~~ HORIZ DIST ~~TYPE~~	REFLECTOR HEIGHT
	1	2	3	4			
TRAV 7	39.786	39.787	39.787	39.787	39.789	39.588	
RTK8	136.427	136.428	136.428	136.428	136.430		

SHEET REFERENCE No. TRAV 8 — EDM REDUCTION SHEET REFERENCE No. .....

D12

UNIVERSITY OF NOTTINGHAM — DEPT OF CIVIL ENGINEERING

TRAVERSE SHEET

STATION AT ...TRAV 7..... R.O. ..... OBSERVER ..ADW.....
THEODOLITE HEIGHT ..... BOOKER ....JWS.....
EDM INST. HEIGHT ..... REDUCED .....
EDM INST. TYPE ..... CHECKED .....
GROUP No. ..... DATE ...4/3/97.....

STATION TO	HORIZONTAL ANGLES			
	FIRST ROUND			ANGLE
	FL	FR	MEAN	~~REDUCED~~
INIT	344 05 18	164 05 37	344 05 27	
RTK9	216 04 24	X 04 34	216 04 29	231 57 02
	SECOND ROUND			
	FL	FR	MEAN	REDUCED

OBSERVING DIAGRAM

STATION TO	TARGET HEIGHT	VERTICAL ANGLES			MEAN VERTICAL ANGLES
		FL	FR	REDUCED	
INIT		93 05 25	266 54 55	93 05 15	03 05 13
RTK9		95 45 46	264 14 48		

STATION TO	MEAN HORIZONTAL ANGLES

STATION TO	OBSERVED SLOPE DISTANCE				MEAN SLOPE DISTANCE	~~REFLECTOR~~ HOriz DIST ~~TYPE~~	REFLECTOR HEIGHT
	1	2	3	4			
INIT	167.842	167.842	167.842	167.842	167.846	167.602	
RTK9	39.792	39.792	39.792	39.792			

SHEET REFERENCE No. ..TRAV 9..... EDM REDUCTION SHEET REFERENCE No. .....

D13

UNIVERSITY OF NOTTINGHAM — DEPT OF CIVIL ENGINEERING

TRAVERSE SHEET

STATION AT ...INIT..... R.O. ..... OBSERVER ..ADN.....
THEODOLITE HEIGHT ..... BOOKER ....JWS.....
EDM INST. HEIGHT ..... REDUCED .....
EDM INST. TYPE ..... CHECKED .....
GROUP No. ..... DATE ....4/3/99.....

STATION TO	HORIZONTAL ANGLES			
	FIRST ROUND			
	FL	FR	MEAN	REDUCED
~~TRAV 7~~	198 37 38	198 37 48	198 37 43	
TRAV 7	122 13 49	302 14 00	122 13 56	76 23 57
	SECOND ROUND			
	FL	FR	MEAN	REDUCED

OBSERVING DIAGRAM

→ 118 15 06 (INT ANGLE)

STATION TO	TARGET HEIGHT	VERTICAL ANGLES			MEAN VERTICAL ANGLES
		FL	FR	REDUCED	
TRAV 7		86 55 06	273 05 21		

STATION TO	MEAN HORIZONTAL ANGLES

STATION TO	OBSERVED SLOPE DISTANCE				MEAN SLOPE DISTANCE	REFLECTOR TYPE	REFLECTOR HEIGHT
	1	2	3	4			
TRAV 7	167.849	167.849	167.849	167.849	167.846		

SHEET REFERENCE No. .TRN...16.... EDM REDUCTION SHEET REFERENCE No. .....

						C	D	E			
station	angle	side	distance	bearing	latitude	departure	distance	L*L/S	L*D/S	D*D/S
INIT	118 15 16				L(Cos)	D (Sin)	S			
		64.581		223 11 29	-47.085	-44.200	64.581	34.329	32.226	30.251
TRAV 2	107 19 45									
		70.202		293 51 39	30.621	-63.172	70.202	13.356	-27.555	56.846
TRAV 3	166 01 27									
		77.050		309 50 12	49.359	-59.165	77.050	31.619	-37.901	45.452
RTK 5	11 43 21									
		63.632		118 06 51	-29.985	56.124	63.632	14.130	-26.447	49.502
TRAV 5	282 31 15									
		175.146		15 35 38	168.699	47.082	175.146	162.481	45.349	12.656
TRAV 6	256 57 26									
		113.996		298 38 12	54.633	-100.052	113.996	26.183	-47.950	87.814
RTK 8	14 02 55									
		136.282		104 35 17	-34.325	131.888	136.282	8.645	-33.218	127.636
RTK 9	71 09 25									
		39.588		213 25 52	-33.038	-21.80	39.588	27.572	18.209	12.016
TRAV 7	231 59 12									
		167.602		161 26 40	-158.889	53.335	167.602	150.629	-50.562	16.972
INIT										
			✓	223 11 19	A	B		C	D	E
					Σ li =	Σ di =		Σ L*L/S =	Σ L*D/S =	Σ D*D/S =
					-0.011	0.030		468.952	-127.857	439.125

$\lambda_2 = 0.00006679$

$\lambda_1 = -0.000005247$

$A = \lambda_1 C + \lambda_2 D$

$B = \lambda_1 D + \lambda_2 E$

$\frac{A - \lambda_2 \cdot D}{C} = \lambda_1$ $\quad \lambda_2 = \frac{(C \cdot B - D \cdot A)}{(C \cdot E - D^2)}$

$\therefore CB = D(A - \lambda_2 \cdot D) + \lambda_2 \cdot EC$

D15 Traverse Computations

What follows are the calculations that were necessary to arrive at the final plan coordinate values presented in Table 7.1

Angular Misclosure

Summation of internal angles give a misclosure of –94 seconds which has been evenly distributed about the angles in Table D.1

Table D.1 Angular Misclosure Distribution

POINT	MEASURED	CORRECTION	ADJUSTED
INIT	118 15' 06"	+10"	118 15' 16"
TRAV 2	107 19' 34"	+11"	107 19' 45"
TRAV 3	166 01' 17"	+10"	166 01' 27"
RTK 5	011 43' 10"	+11"	011 43' 21"
TRAV 5	282 31' 03"	+10"	282 31' 13"
TRAV 6	256 57' 15"	+11"	256 57' 26"
RTK 8	014 02' 45"	+10"	014 02' 55"
RTK 9	071 09' 14"	+11"	071 09' 25"
TRAV 7	231 59' 02"	+10"	231 59' 12"
SUM =	1259 58' 26"	+94"	1260 00' 00"

Traverse Orientation

Coordinates of EEE Tower are:
52 56 31.99962 N 1 11 18.99705 W 133.796 Ht WGS-84
Conversion through WinCoda to OGGBNG gives
454623.358 E 338621.038 N 86.388 Ht

Coordinates of point 'INIT' are:
52 56 27.28414 N 1 11 31.72793 W 087.288 Ht WGS-84
Conversion through WinCoda to OSGBNG gives
454387.360 E 338472.651 N 39.877 Ht

Resultant Bearing from 'INIT' to Tower is therefore Inv. Tan.
Inv. Tan. (454623.358-454387.360) / (338621.038-338472.651)
= 57 50' 23".

Thus bearing of 1st Traverse leg ('INIT' to 'TRAV2')
= 57 50' 23" + 165 21' 01"
= 223 11' 24"

D16

Traverse Adjustment

The above calculations allow the adjusted bearing of each traverse leg to be calculated. With this information, and the horizontal distance between each leg, the difference in Eastings and Northings between each subsequent point can be calculated (D15). As the traverse closes back onto its-self a vector misclosure can also be calculated and this error can be distributed around each point by means of a Least Squares Adjustment, to give final coordinate values for each point (Table D.2).

Table D.2 Least Squares Adjustments, Delta Eastings/Northings and Final Coordinate Values

POINT	ADJ. DE	ADJ. DN	FINAL DE	FINAL DN	E'ING	N'ING
INIT					**454387.360**	**338472.651**
	+0.002	+0.002	-44.202	-47.087		
TRAV 2					454343.158	338425.564
	-0.002	+0.004	-63.176	+30.623		
TRAV 3					454279.982	338456.187
	-0.003	+0.003	-59.168	+49.361		
RTK 5					**454220.814**	**338505.548**
	-0.002	+0.003	+56.121	-29.983		
TRAV 5					454276.935	338475.565
	+0.002	+0.001	+47.081	+168.697		
TRAV 6					454324.016	338644.262
	-0.003	+0.006	-100.058	+54.636		
RTK 8					**454223.958**	**338698.898**
	-0.002	+0.009	+131.879	-34.323		
RTK 9					**454355.837**	**338664.575**
	+0.001	+0.001	-21.811	-33.039		
TRAV 7					454334.026	338631.536
	-0.004	+0.001	+53.334	-158.885		
INIT					**454387.360**	**338472.651**
SUM	-0.011	+0.030	0.000	0.000		

D17

Coordinates of Offset Points

At Points 'INIT', 'TRAV2' and 'RTK5' additional angular and distance measurements were taken to the remainder of the RTK survey points. The absolute bearing from the appropriate traverse leg had first to be calculated before final coordinates could be derived.

At point 'INIT'
Calculated bearing to 'TRAV2' = 223 11' 24''
Circle reading to 'TRAV2' = 098 27' 40''

Thus circle bearing adjustment = 124 43' 44''

Thus Bearing of 'RTK1' from 'INIT' = 199 55' 01''
Bearing of 'RTK4' from 'INIT' = 163 14' 46''

Thus coordinates are

'RTK1'	**454381.872** E	**338457.504** N
'RTK4'	**454396.770** E	**338441.394** N

At point 'TRAV2'
Calculated bearing to 'TRAV3' = 295 51' 39''
Circle reading to 'TRAV3' = 266 04' 50''
Thus circle bearing adjustment = 029 46' 49''

Thus bearing of 'RTK2' from 'TRAV2' = 062 42' 10''
Thus bearing of 'RTK3' from 'TRAV2' = 102 06' 55''

Thus coordinates are

'RTK2'	**454353.708** E	**338431.192** N
'RTK3'	**454358.728** E	**338422.190** N

At point 'RTK5'
Calculated bearing to 'TRAV5' = 118 06' 51''
Circle reading to 'TRAV5' = 052 58' 35''
Thus circle bearing adjustment = 065 08' 16''

Thus bearing of 'RTK6' from 'RTK5' = 019 29' 51''
Thus bearing of 'RTK7' from 'RTK5' = 021 38' 16''

Thus coordinates are

'RTK6'	**454235.045** E	**338545.744** N
'RTK7'	**454240.769** E	**338555.852** N